Visible-Light-Driven C–S Bond Formation

A dissertation submitted in partial fulfillment for the degree of

Doctor of Philosophy

Submitted By

Ashish Kumar Sahoo

Roll No. 176122106

Under the supervision of

Prof. Bhisma Kumar Patel

Department of Chemistry

Indian Institute of Technology Guwahati

Guwahati-781039, Assam, India

January, 2023

भारतीय प्रौद्योगिकी संस्थान गुवाहाटी
Indian Institute of Technology Guwahati

DEDICATED WITH LOVE

To my parents and family, for their endless love, support, and encouragement

My supervisor

Prof. Bhisma K. Patel

भारतीय प्रौद्योगिकी संस्थान गुवाहाटी
Indian Institute of Technology Guwahati

INDIAN INSTITUTE OF TECHNOLOGY GUWAHATI

Department of Chemistry

STATEMENT

I do hereby declare that the matter embodied in this thesis is the result of investigations carried out by me in the Department of Chemistry, Indian Institute of Technology Guwahati, India, under the guidance of *Prof. Bhisma K. Patel*.

In keeping with the general practice of reporting scientific observations, due acknowledgements have been made wherever the work described is based on the findings of other investigators.

January, 2023

IIT Guwahati ***Ashish Kumar Sahoo***

भारतीय प्रौद्योगिकी संस्थान गुवाहाटी
Indian Institute of Technology Guwahati

INDIAN INSTITUTE OF TECHNOLOGY GUWAHATI

Department of Chemistry

CERTIFICATE

This is to certify that *Ashish Kumar Sahoo* has been working under my supervision since December 2017 as a regular registered Ph.D. student. His thesis entitled "***Visible-Light-Driven C–S Bond Formation***" is an authentic record of the results obtained from the research work in the Department of Chemistry, Indian Institute of Technology Guwahati, Assam, India. I am forwarding his thesis to submit for the Ph.D. (Science) degree from this institute. I certify that he has fulfilled all the requirements according to the rules of this institute regarding the investigations embodied in his thesis and this work has not been submitted elsewhere for a degree.

January, 2023
IIT Guwahati

Prof. Bhisma K. Patel
(Thesis Supervisor)
Department of Chemistry

भारतीय प्रौद्योगिकी संस्थान गुवाहाटी
Indian Institute of Technology Guwahati

ACKNOWLEDGEMENT

As the highest academic qualification, a Ph.D. degree can not be completed alone. So, standing at the final stage of a truly unforgettable journey, I would like to acknowledge and thank the people who supported me, believed in me, and encouraged me to complete the journey.

First and foremost, I want to express my deepest respect and profound gratitude to my supervisor Prof. Bhisma K. Patel for providing me the opportunity to work under his guidance. His continuous support, and inspiration through creative and unique scientific ideas helped me to explore the domain of my work assembled in this thesis. I feel blessed to have him as my mentor who gave me moral support and full freedom during the whole journey.

I would also like to extend my heartiest thanks to the doctoral committee members, Prof. Subhas Chandra Pan, Prof. Nitin Chaudhary, and Dr. Dipankar Srimani for their timely evaluation of my Ph.D. work, encouragement, and precious suggestions.

My honest regards to all the faculty and staff members of the Department of Chemistry, IIT Guwahati for their cooperative nature. I would like to thank Babulal da for single-crystal XRD, Imdadul da for NMR, Aniruddha da for HRMS, and Diganta da, Basab da, Tapu, and Michel for various official work and support in the Department of Chemistry.

I wish to express sincere gratitude to MHRD for financial support and to IIT Guwahati for all the facilities that were made available to me for learning several analytical instruments required during my research work. I would also like to especially thank the Department of Chemistry, IIT Guwahati for providing me the opportunity to become an operator of the NMR (500 MHz) instrument. I am grateful to the central Instruments Facility (CIF) for the 600 MHz NMR and single-crystal XRD facilities, MHRD for the 400 MHz NMR facility under the COE-FAST program, DST for the 500 MHz NMR facility under the DST-FIST program, NECBH, IIT Guwahati, and DBT, Govt. of India for the 400 MHz NMR and single-crystal XRD facilities.

I would like to express my gratitude and a big thanks to all the operators inside, and outside IIT Guwahati for successfully carrying out all the instrumental experiments required during my research work. Further, I am extremely thankful to all the co-authors, editors, associate editors, and reviewers for their valuable comments and suggestion.

The credit for successfully completing the most memorable journey of academia must go to all the BKP warriors whom I know personally. I would like to express my deepest gratitude to my Ph.D. senior Dr. Ahalya Behera for her guidance during my earlier stage in the lab. But the most unforgettable journey of academia can not be completed with a single guru so I would also like to thank Dr. Anjali Dahiya not only for the overall training but also for all kinds of support during the difficult stage of this journey. I would also like to express my deepest gratitude to Dr. Amitava Rakshit who helped me a lot throughout the journey. For me, he is not only a cooperative lab senior but also a good friend cum tea partner.

I would like to thank wonderful lab seniors Subendhu bhai, Prakash bhai, Dr. Wajid Ali, Dr. Anju Modi, Dr. Suresh Rajamanickam, Dr. Bilal Ahmed Mir, Dr. Prasenjit Sau, for their help, precious suggestions, and encouragement. I would like to thank postdoctoral lab seniors Dr.Gaurav Shukla, Dr. Ritush Kumar, Dr. Pakiza Begum, Dr. Gongutri Borah, Dr. Bhaskar Deka, Dr. Binoyargha Dam, and Dr. Kamal Krishna Rajbongshi for their help, and support. Especially, Kamal bhai and Binoy bhai, are very supportive and friendly to me.

I also feel lucky to have Tipu, and Nikita as batchmates for their enormous support and encouragement. Probably, I can not forget all the healthy discussions, picnics, and parties, that I had with them during the whole journey. Throughout the journey, all the fights and love between us is obvious because fight and love are like head and tail in a coin of friendship. I want to heartily appreciate all my talented juniors Bubul, Hiru, Tamanna, Pritishree, Raju, and Dinabandhu, for their hard work, and diligence, and for maintaining a friendly environment in the lab. I have lived the most happiest and memorable moments of my life with these fellow warriors. I also had the opportunity to work with some dedicated summer and M.Sc. trainees like Priyabrta, Prashant, Poonam, Garima, Rani, Arihant, Kunika, Sreyashi, Pankaj, Abhishek, Akshar, Abhishek, Angshu, Sourasish, Gaurav, Kaustav, and Pratip.

I would like to express my heartiest thanks to my M.Sc. seniors Ashish bhai, Sandip bhai, Madhual bhai, Manoj bhai, Rakesh bhai, Chandu bhai, Manmath bhai Sumanta bhai for their outstanding contribution before the journey started. Especially, I would like to express my gratitude to Ashish bhai, Manoj bhai, and Sandip bhai for their motivation, encouragement, and all kinds of support during the initial preparation for this journey.

I would like to express millions of gratitude from the bottom of my heart to my best friends Bipin, and Chandrakant for their help, support, and for staying by my side to make good times even better, and the hard times a whole lot easier. All the healthy gossip with them throughout the journey is really unforgettable. Thank you for motivating me at every stage of this journey.

I would also like to thank my Ph.D. friends, seniors, and juniors here at IITG, Subhamoy, Amit, Sonbidya, Arup, Sayanta, Santa, Sourav, Sudip, Surya, Pallav, Vinoy, Araghni, Bitan, Avijeet, Rana, Umesh bhai, Jagnyesh, Paresh, Jitendra, Manmath bhai, Ketan bhai, Shiva bhai, Dr. Nimisha Bania, Dr. Archana Kmari Sahoo, Dr. Tushar Kanta Sahoo, Dr. Sitakanta Panda, Dr. Biswajit Nayak, Dr. Dillip Kumar Sahu, Sandip bhai, Rupkumar, Subhankar, Dipankar, Ram, Prabhat, for making the journey a lot better, easier and entertaining.

I would like to express a big thanks to my M.Sc. friends Dr, Bapun Barik, Debasish (Bhai) Jilu Chand, Anil, Sankha, Niranjan, Sagar, Tapan, Tapas, Deeptikanta (Sakha), Madhushree, Reema, Somya, Arpita, Rupa, and Subhashree for various kinds of support.

No words would suffice to express my feelings toward my teachers to whom I owe my obligations for their great teachings and philosophy to be a good human; Prof. Jayanta Kumar Sahoo, Prof. Rakesh K. Singh, Prof. Pramod Kumar Satpathy, Dr. Lingaraj Behera, Dr. Amar Kumar Dora, Dr. Ashish K. Jena, and the entire fraternity from my school, N.C College (Utkal University), and North Orissa University.

Lastly, and most importantly, my Ph.D. endeavour could not have been completed without the endless love, unending support, tolerance, and blessings from my family. I am very much grateful to my Maa, Bapa, and Bhai for their unconditional support, affection, and deep concern for my career. I would like to express my deepest gratitude to my parents whose unconditional love in every stage of my life motivated me to overcome all the challenges and I owe my entire life to them. Dedicating this thesis to them is a minor recognition for their love, support, and encouragement.

Last but not the least; I am thankful to Almighty for continuous blessing during my research carrier to accomplish this remarkable journey.

Ashish Kumar Sahoo

SYNOPSIS

The contents embodied in this thesis are divided into four chapters including one introductory chapter based on experimental results obtained during the research period. The introductory chapter represents an overview of Visible-light-mediated C–S bond formations. This includes a brief discussion about the visible-light mediated C–S bond formation via difunctionalization of alkynes, C–H functionalization, and radical cyclization reaction. Since most of the chapters leading to the formation of C–S bonds under photocatalytic conditions so C–S bond formations will be more focused.

Chapter II demonstrates a metal-free route for the synthesis of (Z)-*β*-carboxy vinyl sulfones *via* difunctionalization of alkynes. Sodium sulfinates were used as the *S*–centered radical source under photocatalytic conditions.

Chapter III describes a visible-light-induced synthesis of thio-functionalized pyrroles using *β*-ketodintriles and thiophenols. under metal-free conditions. The reaction proceeds via the attack of thiyl radical to one of the nitriles followed by an imine amine tautomerization, nucleophilic attack of the amino group to the carbonyl, and loss of water molecule.

Chapter IV describes a visible-light/solar-light-driven synthesis of thio-funcionalized pyridines using γ-ketodintriles and thiophenols. The reaction proceeds *via* thiyl radical intermediacy.

Each of these chapters comprises seven subsections which include an introduction, previous work, present work, experimental section, references, spectral data, and a few representative spectra.

CHAPTER I. Visible-Light-Driven C–S Bond Formation

The past decades have witnessed rapid progress in radical-mediated carbon−heteroatom bond formations which have been established as powerful tools to access various organic frameworks. In spite of several existing methods in C–X bond formations, there is always a need to develop newer methodologies in this direction. In this regard, visible-light-mediated C–X bond formations have gained immense popularity due to their operational simplicity, minimalization of by-product, easy handling, mild reaction condition, etc. Besides offering a sustainable way to synthesize molecules, photochemistry has the potential to unlock reaction manifolds that are unavailable to conventional thermal pathways. Since the pioneering work from the group of MacMillan, Yoon, and others, photocatalysis has experienced renascence over the past decades. This field is mainly categorized based on the catalytic systems involved. (1) The use of photocatalyst (transition metal complexes or organic dyes) which in its excited state activates the organic molecules via either single electron transfer (SET) energy transfer (EnT), (Figure I.1). (2) Synergistic combination of photocatalyst as well as transition metal catalyst. (3) The use of only transition metal complexes in combination with visible light which plays a dual role first by harnessing photon energy as a photocatalyst and then by catalyzing the bond-breaking and making process. Mostly the use of visible-light irradiation, in combination with photosensitizer (transition metal complexes or organic dyes), has been well-established to be an ideal reaction promoter for many organic transformations. In this direction, transition metal complexes have gained enough popularity due to their outstanding reactivities and selectivity in various photochemical reactions. In spite of their excellent photophysical properties, their high cost, and sometimes toxicity issues have limited their use to some extent in modern organic synthesis. In this context, the use of organic dyes has become an attractive alternative to transition metal complexes in visible-light mediated C–X bond formations due to their low cost, less toxicity, and operational simplicity. In particular, eosin Y has come into focus in many visible-light-mediated transformations. Most of these photochemical reaction proceeds through a single-electron transfer (SET) process from the excited photocatalyst to the organic substrate or reagent which usually involves two pathway oxidative quenching and reductive quenching (Figure I.1).

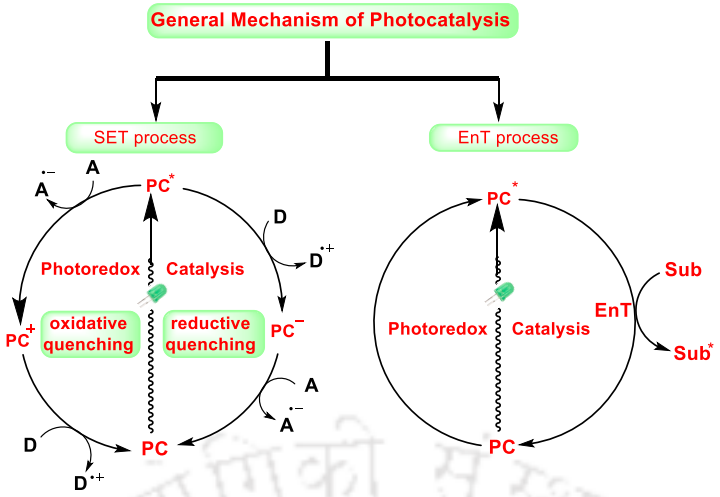

Figure I.1. *General mechanism of visible-light-induced transformations.*

Among various C–heteroatom bond formations, the C–S bond formation reactions have gained tremendous importance due to their widespread applications in pharmaceuticals as well as industries. For instance, Cysteine (**I**) and Methionine (**II**) are two sulfur-containing amino acids, which help in promoting antioxidant activity and. body development (Figure I.2). Garlic is not only a food flavoring but a kind of traditional medicine, enriched with biologically active compounds that have been shown to decrease rates of cancer. Ajoene (**III**) and Allicin (**IV**) are two biological active compounds that were isolated from garlic and were reported to have antibacterial activities. In the pharmaceutical field, organic sulfur compounds are found to have widespread applications. For example, sulfamethoxazole (**V**) and its derivatives are used to produce antibiotic or antiprotozoal drugs such as Bactrim. Organosulfur compounds are also very popular in material science; one such important example is the thiophene-based conjugated polymers, such as poly(1,3-dithienylisothianaphthene) (PDTITN), (**VI**) that have promising applications in organic electronics and photonics (Figure I.2). Owing to the importance of organosulfur compounds development of synthetic methods to form C–S bond is always deemed worthy of investigations

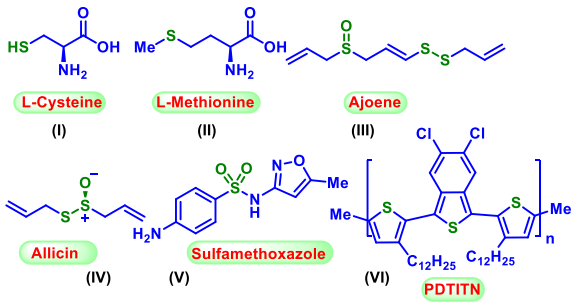

Figure I.2. *Biologically active sulfur compounds.*

To date, significant progress has been achieved in the construction of new C−S bonds, which mainly involves addition and substitution strategies (Figure I.3). The addition of various sulfur nucleophiles to carbon−carbon double and triple bonds, thiolysis of epoxides, aziridines, anhydride, cross-coupling reaction with aryl halides represent the most convenient route for the formation of new C−S bonds (Figure I.3).

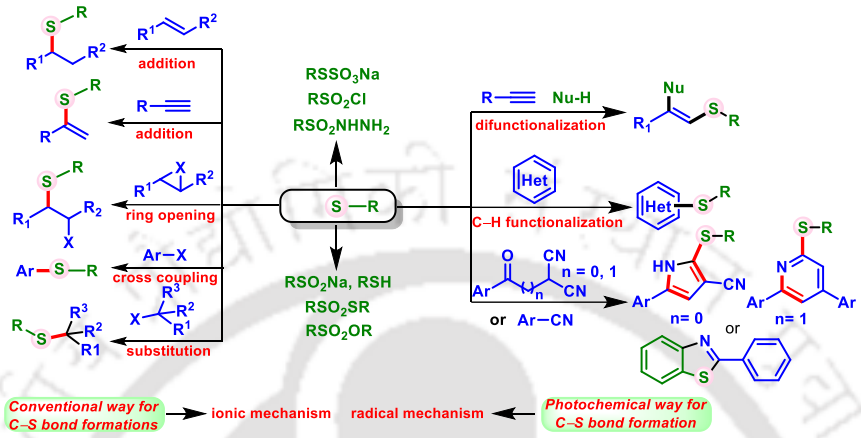

Figure I.3. *Traditional/Photochemical generation of C–S bond formations.*

However, these traditional methods mostly involved an ionic pathway rather than a radical pathway. In spite of these existing conventional methods the C–S bond formation via photocatalysis has gained immense popularity which converts the S–nucleophiles to S–radicals via single electron transfer and triggers the reaction. This mainly includes radical addition to the alkenes and alkyne (mainly difunctionalization strategy), C–H bond functionalization, and S-radical-triggered cyclization reactions, etc. Since all the chapters deal with visible-light-mediated C–S bond formation under metal-free conditions so only metal-free C–S bond-forming reactions are more focused.

I.1. C–S Bond Formaion via Difunctionalization

In recent years, C–S bond formation via difunctionalization of alkenes or alkynes has gained much reputation, in which simultaneous introduction of two functional groups can be possible in a single step. In this endeavor development of newer methodologies in the direction of difunctionalization of alkene/alkynes remains an important topic of research in organic synthesis. For instance, recently, the Maity group demonstrated a visible-light organophotoredox-catalyzed sulfurization of alkenes and alkynes with aromatic and heteroaromatic thiols using eco-friendly air (O_2) as the sole oxidant. The established method provides a metal-free route for the difunctionalization of alkenes and alkynes using Eosin Y as the photosensitizer (Scheme I.1.1).

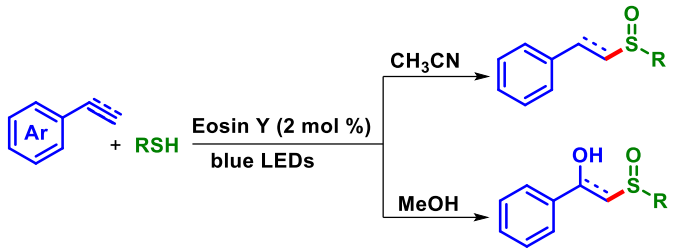

Scheme I.1.1. *Visible-light-mediated sulfurization of alkenes and alkynes.*

In 2021, Singh *et al*. reported a difunctionalization of styrene for the C–S bond formation in the presence of CS_2 and amines providing β-keto dithiocarbamates (Scheme I.1.2).

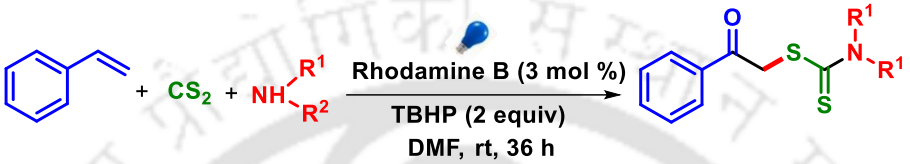

Scheme I.1.2. *Visible-light-mediated difunctionalization of alkenes.*

Recently, another highly efficient visible-light-induced oxysulfonylation of alkynes has been reported by the Zhang group using arylsulfonate phenol esters as the sulfur precursors. The reaction proceeds smoothly in the absence of any photosensitizer and the mechanism proceeds via an electron donor-acceptor complex-mediated radical process (Scheme I.1.3).

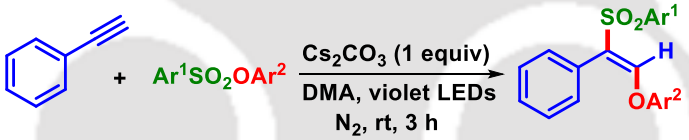

Scheme I.1.3. *EDA complex mediated difunctionalization of alkynes.*

I.2. C–S bond Formation via C–H Bond Functionalization

C–H bond functionalization has attracted much attention in the construction of various organic frameworks leading to the formation of functionalized molecules. The field of catalytic C–H functionalization has attracted much attention over the past four decades. Mostly, the catalytic strategies involving transition metals, metal/metal-free photochemical, and electrochemical have all been utilized for the selective functionalization of C–H bonds. Among several approaches to C–S bond formation, the photocatalytic metal-free approach has been well-established in constructing various sulfur-containing frameworks. In this context, He *et al.* reported a visible-light-induced deoxygenative C2-sulfonylation of quinoline *N*-oxides with sulfinic acids in the presence of eosin Y as the catalyst under mild conditions (Scheme I.2.1).

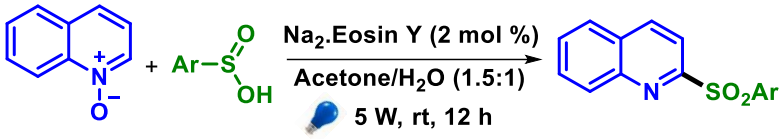

Scheme I.2.1. *Sulfonylation of quinoline N-oxides.*

The Sun group reported an efficient dehydrogenative sulfonylation of tertiary amines with thiosulfonates under visible-light irradiation. This protocol allows for the construction of a variety of cyclic and acyclic *β*-sulfonyl enamines under transition-metal-free, external oxidant-free, and photosensitizer-free conditions (Scheme I.2.2).

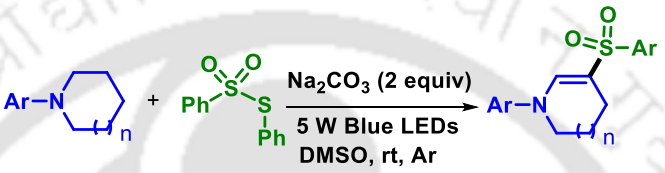

Scheme I.2.2. *Visible-light-mediated sulfonylation of cyclic amines.*

I.3. C–S bond formation via Cyclization

The Visible-light-induced radical cyclization processes have been successfully used for the construction of *N*-heterocycles because of their simplicity, efficiency, and unique activation. In this context construction of C–C, C–S, and C–N bonds using photoredox catalysis has grabbed significant attention giving prominence not only to nitrile functionality but also to other functionality such as alkene, alkyne isonitrile etc. In 2022, a cyclization reaction reported by Zhu *et al*. for the construction of quinolin-2(1H)-ones via Markovnikov-type sulfonylation followed by *6-endo-trig* cyclization and selective C(O)–CF_3 bond cleavage starting from *N*-alkyl *N*-(2-ethynylphenyl)-2,2,2-trifluoroacetamides and sulfinic acids (Scheme I.3.1).

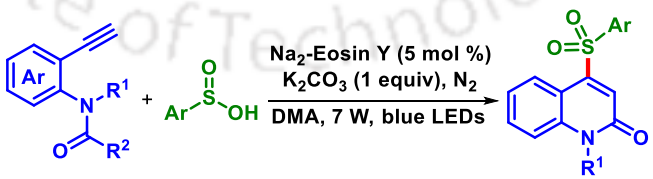

Scheme I.3.1. *Visible-light-mediated synthesis of quinolin-2(1H)-ones.*

Further, Yu *et al*. demonstrated a photosensitizer-free synthesis of pyrrolo[1,2-a]indolediones via persulfate promoted radical cyclization. In this method aryl sulfonyl hydrazide, and ammonium thiocyanate were used as the *S*-cenetered radical source (Scheme I.3.2).

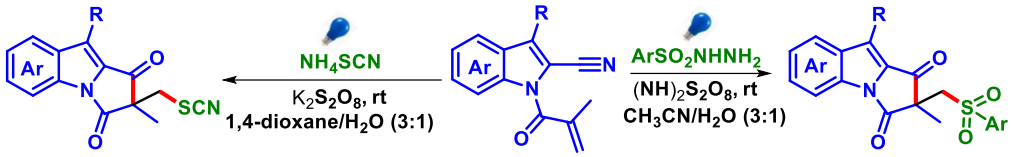

Scheme I.3.2. *Visible-light-mediated synthesis of pyrrolo[1,2-a]indolediones.*

In summary, the use of visible light in metal-free C–S bond formation has bought a tremendous progress in contemporary organic chemistry. In spite of existing traditional methodologies in the direction of C–S bond formations, visible-light-induced synthesis of sulfur-containing framework still attracts considerable attention of chemists. Further improvement in this field may open up new avenues to straightforward and efficient synthesis of various molecular frameworks that may find applications not only in pharmaceuticals but also in other industries.

CHAPTER II: Visible-Light-Mediated Difunctionalization of Alkynes: Synthesis of *β*-Substituted Vinylsulfones using *O*–, and *S*–Centered Nucleophiles

This chapter demonstrates a green-light-induced, regioselective difunctionalization of terminal alkyne using sodium *p-tolyl*sulfinate, and carboxylic acids or NH_4SCN in presence of eosin Y as a photocatalyst. In this protocol, *Z-β*-substituted vinylsulfones are obtained exclusively covering a broad range of alkynes and nucleophiles which are often unaddressed.

Alkenes and alkynes are well-established building blocks in organic synthesis which are useful due to their efficient transformation into other functionalities. In recent years, direct difunctionalization of alkenes and alkynes has grabbed the attention of chemists, in which simultaneous introduction of two functional groups is possible giving rise to functionalized molecules. Alkenes having multiple substituents are prevalent in many bioactive molecules, natural products, and pharmaceuticals *viz*. tamoxifen, doxepin, etc. In this context, the development of a newer methodology for their synthesis is still in demand and chemists always dreamed to develop efficient and suitable methods for their synthesis.

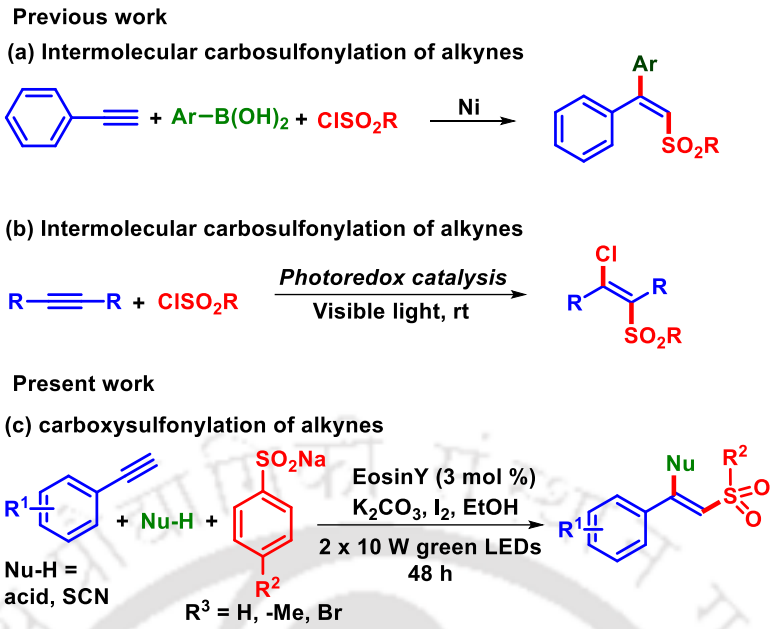

Scheme II.1 *Difunctionalization of alkyne.*

Previously, in 2017, Nevado *et al*. reported an elegant method for the carbosulfonylation of alkynes via a multi-component approach giving tri-substituted alkenes (Scheme II.1a). Further, Han *et al* reported a visible-light mediated halosulfonylation of alkynes in the presence of Ir photocatalyst. Taking cues from the above-mentioned work, herein a visible-light-mediated, metal-free, multi-component approach is articulated for the difunctionalization of terminal alkynes (Scheme II.1).

To reach the suitable conditions for the synthesis of *Z*-*β*-substituted vinylsulfones, various solvents, photocatalysts, light source, oxidants, were screened. The use of eosin Y, green LEDs, I_2, and ethanol as solvent was found to be optimal for the desired protocol. With the optimized condition in hand, this protocol was subsequently applied for the synthesis of various *Z*-*β*-substituted vinylsulfones. It was observed that the reaction underwent smooth reaction in the variation of both electron-withdrawing as well as electron-donating groups in either of the coupling partners. But carboxylic acids with EDGs showed better reactivity than with EWGs this is due to the increased nucleophilicity. Besides this, a variety of long-chain aliphatic carboxylic acids were also underwent very smooth reaction giving the desired *Z*-*β*-substituted vinylsulfones. Next to ascertain the mechanistic path various control experiments were performed and CV and SV measurements were taken. As per the CV value radical anion of eosin Y can able to give an electron to the RSO_2I species. From the SV measurements, It was confirmed that sulfonyl radical generated from the sulfonyl iodide not directly from the sodium sulfinate.

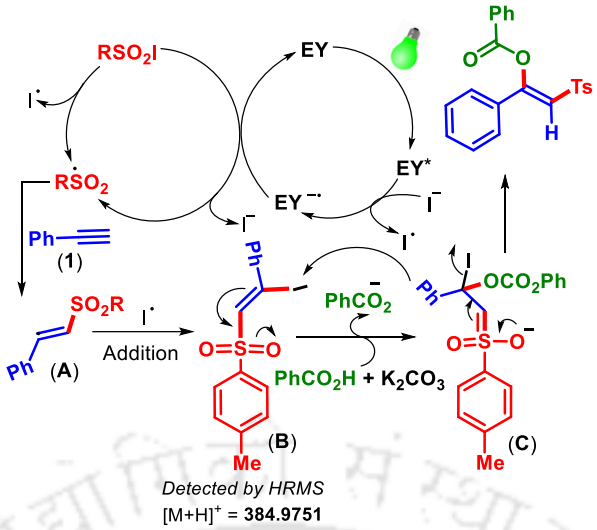

Scheme II.2. *Plausible mechanism for the synthesis of Z-1-phenyl-2-tosylvinyl benzoate*

Based on this a tentative mechanism has been proposed. In the presence of green LEDs, Eosin Y (EY) is first photo-excited, which is reductively quenched by iodine and sodium *p*-tolylsulfinate to sulfonyl radical, iodine radical, and sodium iodide. This is followed by the addition of sulfonyl radical to terminal alkyne (**1**) giving a vinyl sulfone radical intermediate (**A**). Next, the radical addition of iodine to intermediate (**A**) generates β-iodo sulfone intermediate (**B**). A base-promoted nucleophilic attack of the carboxylate ion provides an intermediate (**C**). Subsequently, the corresponding Z-1-phenyl-2-tosylvinyl benzoate (**1az**) is obtained from the intermediate (**C**) via an addition-elimination process (Scheme II.2).

In summary, an elegant visible light-mediated method for the difunctionalization of terminal alkynes is established using sodium *p*-toluenesufinate and *O*–, *S*–centered nucleophiles as the reacting partners. This methodology allows the useful synthesis of many valuable *Z*-*β*-substituted vinylsulfones via a multi-component approach, covering a wide range of substrate scope. In this protocol, C–O, and C–S bonds are assembled at the same time with the introduction of important functional groups *viz*. ester, thiocyanate, and sulfone.

CHAPTER III: Visible-Light-Mediated Synthesis of Thio-Functionalized Pyrroles

This chapter demonstrates a green-light-induced synthesis of thio-functionalized pyrroles using *β*-ketodinitriles and thiophenols as the reacting partners and eosin Y as the photocatalyst. This photochemical strategy involves a photo-induced thiyl radical addition to one of the nitriles of *β*-ketodinitriles leading to the formation of nitrogen centre radical followed by imine amine tautomerization and intramolecular nucleophilic addition of the

amine to the ketone giving the thio-funcionalized pyrroles. Among various five-membered heterocyclic compounds, pyrroles are abundant in many natural products and pharmaceuticals, possessing biological activities such as antifungal, antiviral, antihyperlipidemic, and anti-cancer. In particular, atorvastatin (**I**), the cholesterol-lowering drug, tolmetin (**II**) the nonsteroidal anti-inflammatory drug (NSAIDs), sunitinib (**III**) the multitargeted antitumor, and pyrvinium (**IV**) used for the treatment of pinworm infestation all possess pyrrole unit.

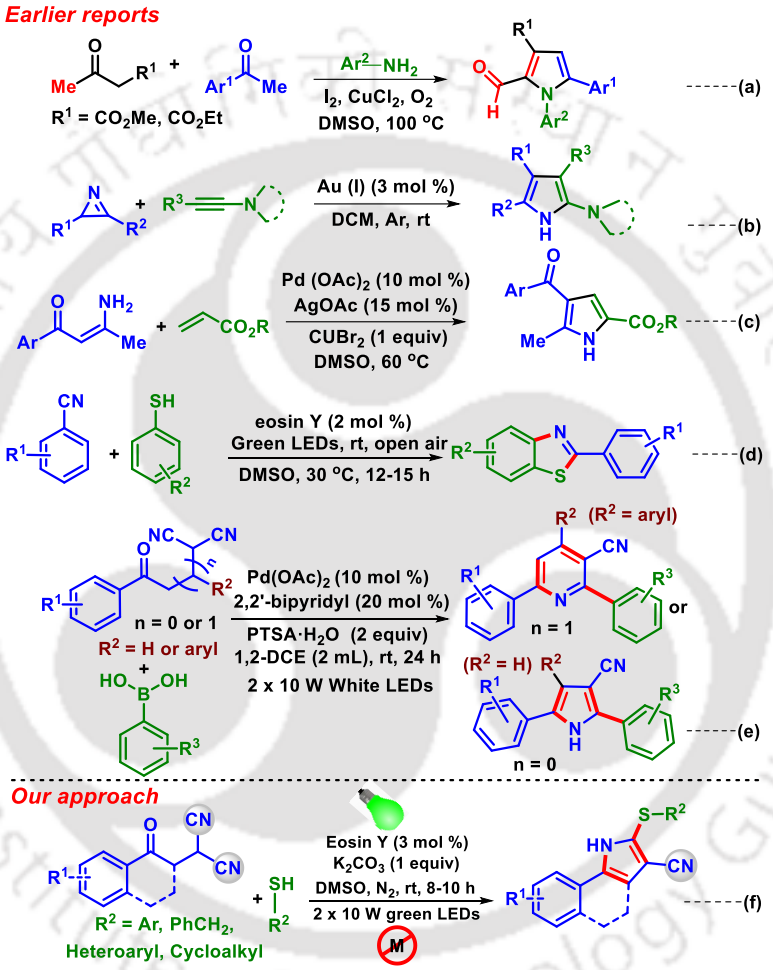

Scheme III.1. *Synthetic approach to substituted pyrroles and photochemical reactivity of functionalized nitriles.*

Owing to their diverse applications, the synthesis of substituted pyrroles has been an impressive area of research for the scientific community. Previously, Natarajan *et al.* developed a visible-light-induced synthesis of 2-substituted benzothiazoles using thiophenols and nitriles. Previously, our group established a Pd-catalyzed nitrile-triggered protocol for the synthesis of 3-cyano pyrrole using boronic acid as the reacting partner under visible light (Scheme III.1). Taking cues from this, we articulated that a photo-induced thiyl radical

addition might be possible with *β*-ketodinitriles as the radical acceptors leading to a pyrrole skeleton *via* the formation of nitrogen centre radical followed by imine amine tautomerization and intramolecular nucleophilic addition of the amine to the ketone. Thus a photochemical metal-free synthesis of thio-functionalized pyrroles has been reported taking thiophenol as the reacting partner and eosin Y as the photocatalyst (Scheme III.1).

In pursuit to accomplish an appropriate reaction condition for this photochemical transformation, other reaction parameters such as solvents light source, and catalyst were screened. After screening of several parameters, the optimal condition for this transformation was found to be the use of **1** (0.25 mmol), **a** (0.50 mmol, 2 equiv), K_2CO_3 (0.25 mmol, 2 equiv), eosin Y (3 mol %), in DMSO (1 mL) under 2 x 10 W green LEDs. Encouraged by this photochemical metal-free protocol scope of the thio-functionalized pyrroles were studied using various *β*-ketodinitriles as well as thiophenols. It was observed that the presence of electron-withdrawing as well as electron-donating gropus on either of the coupling partners showed almost similar reactivity in giving the thio-functionalized pyrroles. Besides this, heteroaromatic and aliphatic variation in either of the coupling partners were also underwent smooth reaction giving the desired thio-functionalized pyrroles. Next, a couple of control experiments, CV and SV measurements were done to decipher the mechanism. The CV, and SV measurements confirm the generation thiyl radical obtained from the thiophenol not from the thiolate anion.

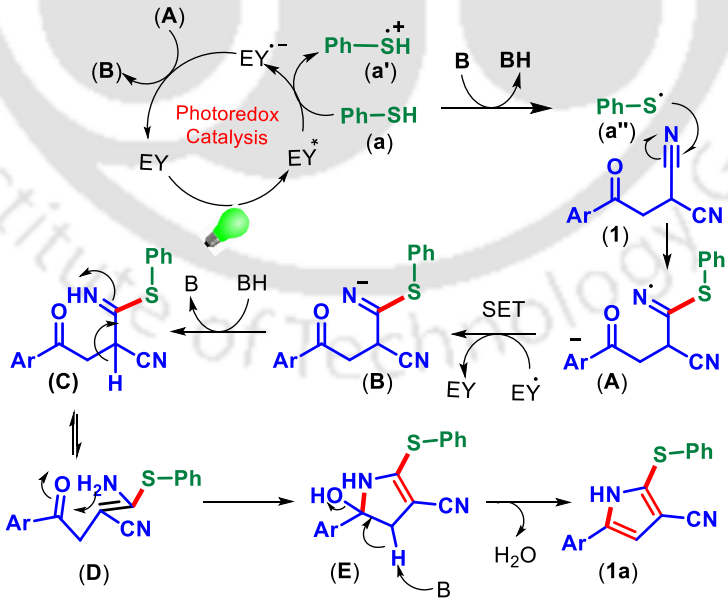

Scheme III.2. *Mechanism for the formation of thio-functionalized pyrroles.*

Based on the control experiments a tentative mechanism has been proposed. In the presence of green LEDs, eosin Y (EY) is photoexcited to EY^* which is reductively quenched by the thiophenol (**a**) to give (**a′**) and radical anion of eosin Y ($EY^{\cdot-}$). Next, the base abstracts a proton from the radical cation intermediate (**a′**) and generates a thiyl radical (**a′′**). The thiyl radical (**a′′**) adds to one of the nitrile groups of *β*-ketodinitrile (**1**) generating intermediate (**A**). Subsequently, intermediate **A** is reduced by $EY^{\cdot-}$ to an anionic intermediate (**B**), thereby completing the catalytic cycle. On protonation, the intermediate (**B**) generates an imine intermediate (**C**). The tautomerization of intermediate (**C**) to (**D**) followed by the attack of the amine nucleophile to the carbonyl group gives intermediate (**E**). Finally, the product (**1a**) is obtained *via* the loss of a water molecule from intermediate (**E**) (Scheme III.2).

In summary, a visible-light-mediated synthesis of thio-functionalized pyrroles is established using thiols, *β*-ketodinitriles and eosin Y as the photocatalyst. In this protocol, C–N, C–S, and C=C bonds are constructed simultaneously. The synthetic utility is demonstrated by a few useful transformations and scale-up experiments.

CHAPTER IV: Visible/Solar-Light-Driven Thiyl-Radical-Triggered Synthesis of Multi-Substituted Pyridines

This chapter focuses on the visible-light mediated synthesis of thio-functionalized pyridines using thiophenols and *γ*-ketodinitrile as the reacting partners. The reaction proceeds via the selective attack at one of the cyano groups by an *in situ* generated thiyl radical. The reaction also proceeds with near equal efficiency using direct sunlight. To show the practical usefulness of the protocol a few useful synthetic transformations of the substituted pyridines are also performed.

The photochemical transformations by harnessing visible light have grabbed significant attention due to their sustainability, unique reactivity, and operational simplicity. Usually, a photochemical reaction is triggered by visible light in combination with a suitable photocatalyst which facilitates the SET process. Though the transition-metal complexes are better for the excitation of organic molecules, the employment of organic dyes has also been useful in many photochemical transformations. In particular, eosin Y has become a competitor to metal catalysts in various reactions due to its cost-effectiveness. Owing to the prevalence of pyridine frameworks in various natural products, and pharmaceuticals, they have found applications in the fields of biology, medicinal sciences, and advanced materials

etc. Considering the multi-faceted applications of substituted pyridines, synthetic chemists are vying for alternative methods to pyridine core. Previously, our group reported a nitrile-triggered synthesis of thio-substituted pyrroles with β-ketodinitriles as an acceptor and thiophenol as the radical donor (Scheme IV.1d). Our interest in nitrile-based precursors we hypothesized that a reaction is feasible with γ-ketodinitriles as the radical acceptors. To confirm our hypothesis, CV of γ-ketodinitrile (**1**) and thiophenol (**a**) were measured. The estimated $E_{1/2oxd}$ of benzene thiol (+0.25 V vs the SCE) is lower compared to $E_{1/2oxd}$ of γ-ketodinitriles (+2.13 V, +0.38 V vs the SCE), enabling them as suitable radical donor and acceptor pairs. Thus a visible-light mediated metal-free synthesis of thio-functionalized pyridines has been reported using thiphenols and γ-ketodinitriles as the reacting partners in the presence of eosin Y as the photocatalyst (Scheme IV.1).

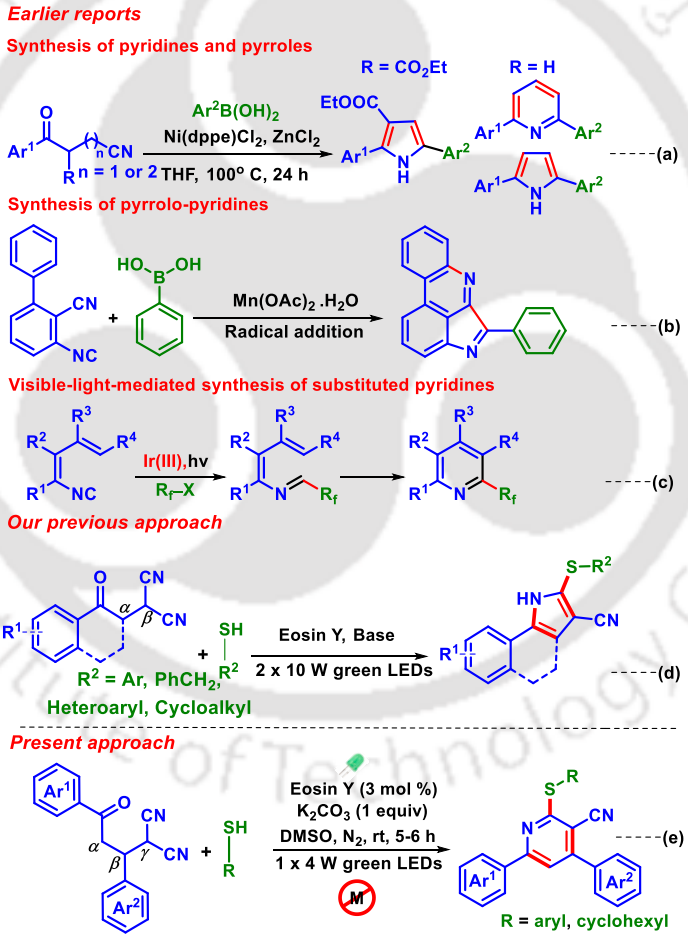

Scheme IV.1. Nitrile-Triggered Synthesis of Substituted Pyridines

To find out an appropriate reaction condition for this photochemical transformation, other reaction parameters such as solvents light source, and catalyst were screened. After screening of several parameters, the optimal condition for this transformation was found to

be the use of β-ketodinitrile(1) (0.25 mmol), thiophenol (0.50 mmol, 2 equiv), K_2CO_3 (0.25 mmol, 2 equiv), eosin Y (3 mol %), in DMSO (1 mL) under 4 x 1 W green LED at N_2 atmosphere. Inspired by this protocol, the scope of the thio-functionalized pyridines was studied using a diverse range of γ-ketodinitriles as well as thiophenols. It was observed that the presence of electron-withdrawing as well as electron-donating gropus on either of the coupling partners showed almost similar reactivity in giving the thio-functionalized pyridines. Besides this, the use of aliphatic thiol such as cyclohexane thiol also worked well in the present protocol. whereas the use of alkyl thiols failed to give the desired thio-functionalized pyridines. Further a mechanistic path has been proposed based on control experiments and literature reports.

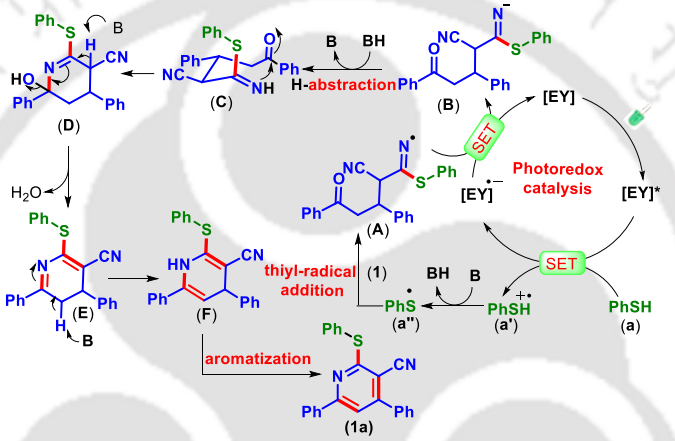

Scheme IV.2. Mechanism for the Formation of Thio-Functionalized Pyridines

Initially, green LEDs, excited the eosin Y (EY) to EY*, which oxidizes the thiophenol (**a**) to a radical cation (**a**′). Next, the thiyl radical (**a**′′) is obtained via deprotonation from the radical cation (**a**′). The thiyl radical (**a**′′) undergoes addition to one of the nitrile groups of γ-ketodinitrile (**1**), generating intermediate **A**. Subsequently, intermediate (**A**) is converted to an anionic intermediate (**B**) via a reductive quenching. The intermediate (**B**) upon protonation generates an imine intermediate (**C**). The nucleophilic attack of imine (**C**) to the carbonyl group provided the intermediate **D**. Finally, the loss of a water molecule from the intermediate **D** gives intermediate **E**, which upon a base promoted tautomerization followed by aromatization gives the desired pyridine **1a** (Scheme IV.2).

In summary, a thiyl radical-triggered synthesis of multi-substituted pyridines is demonstrated using γ-ketodinitriles, thiols, in the presence of eosin Y under metal-free conditions. This protocol simultaneously constructs C–N, C–S, and C=C bonds. This methodology can tolerate different substituents in both coupling partners. A few post-

translational modifications and a scale-up reaction are illustrated to show the practical utility of the present protocol. The reaction also underwent flawlessly employing sunlight as a sustainable energy source.

CONTENTS

CHAPTER I

Visible-Light-Driven C–S Bond Formation

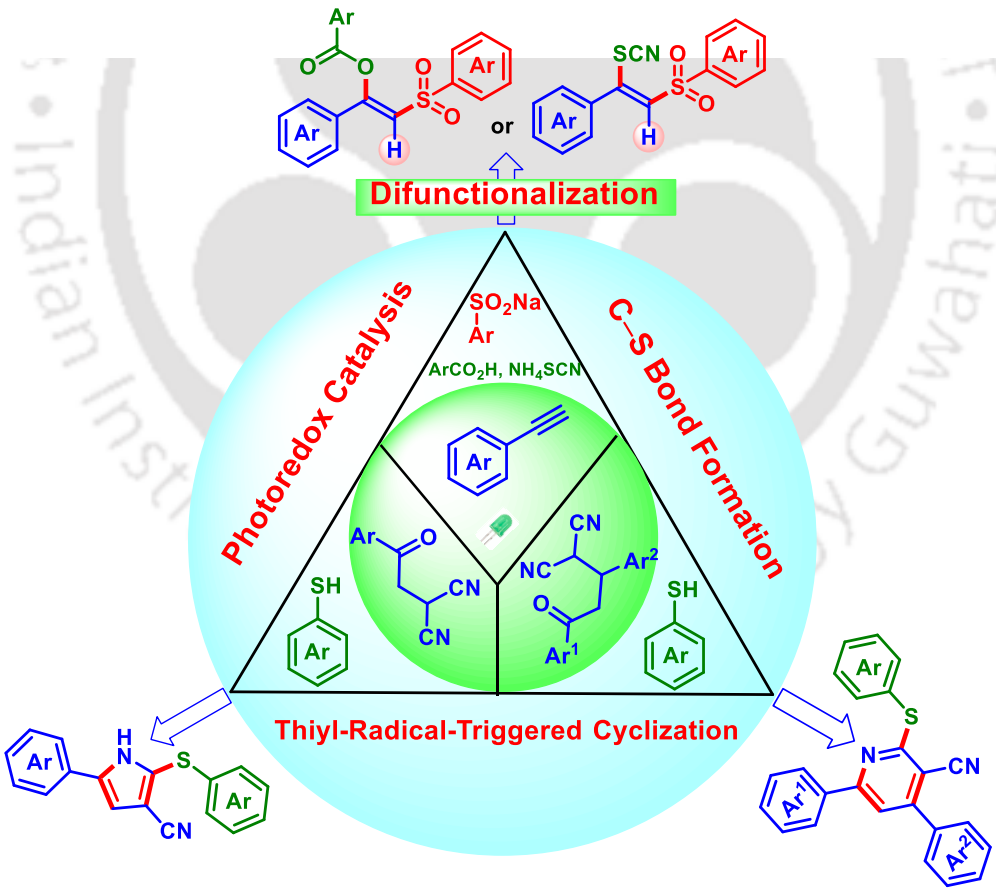

CHAPTER I

Visible-Light-Driven C–S Bond Formation

I.1. Introduction:

The development of radical mediated chemistry in organic synthesis over the past decade has renewed interest in the field of photochemistry. The ongoing interest in radical chemistry has come into focus owing to the reactivity and also the selectivity that can be accessed via the radical intermediacy that is otherwise difficult to attain by other approaches.[1] The past decades have witnessed rapid progress in radical-mediated carbon−heteroatom bond formations which have been established as powerful tools to access various organic frameworks. In spite of several existing methods in C–X bond formations, there is always a need to develop newer methodologies in this direction. In this context, photoredox catalysis has become a rapidly developing areas of radical chemistry.[2] This area of research has come into the limelight of many scientists ranging from biomedical to materials science. Moreover, visible light-mediated C–X bond formations have gained immense popularity due to their operational simplicity, minimization of by-product, easy handling, mild reaction condition, etc.[3,4] Photochemistry not only provides a sustainable way to synthesize complex molecules, but it also has the ability to overcome many challenges which are difficult to attain by conventional thermal pathways. Since the pioneering work from the group of MacMillan, Yoon, and others, photocatalysis has experienced renascence over the past decades.[5] Based on the catalytic systems involved this field are mainly categorized into three types such as: (i) The use of photocatalyst (organic dyes or transition metal complexes) which upon excited in the presence of LEDs activates the organic molecules either via a single electron transfer (SET) or energy transfer (EnT), (Figure I.1). (ii) Synergistic combination of photocatalyst as well as transition metal catalyst. (iii) The use of only transition metal complexes in combination with visible light which acts as a light-absorbing species and initiates the reaction and thereby catalyzes the bond-breaking and making process.[6] Mostly the use of photosensitizer (transition metal complexes or organic dyes), under visible-light irradiation, has been well-established as a reaction promoter for many photocatalytic transformations. In this direction, transition metal complexes have gained enough popularity due to their outstanding reactivities, and selectivity in various photochemical reactions.[7,8] In spite of

their excellent photophysical properties, their high cost, and sometimes toxicity issues has limited their use to some extent in modern organic synthesis. In this context, the use of organic dyes has not lagged far behind as compared to that transition metal complexes. The frequent use of organic dyes in many photochemical transformations is only due to their less toxicity, low cost, and operational simplicity.[9]

I.2. The Beginnings of Organic Photochemistry

From the beginning of life in the universe light-induced reactions are there so it is not much new on this planet or it can be said that they are significantly older than life itself. Long back, sunlight-mediated photochemistry started as soon as living beings began to settle on the earth.[10] For instance, the generation of a protective ozone layer is the result of the photolysis of oxygen which saves human and animal life from the harmful UV radiation of the solar spectrum.[11] All these photoreactions have been occurring for billions of years without human interruption or, without being noticed. The idea, that the interaction of light with the materials not only affects their physical properties but it could also change their chemical properties encourages the chemists to take a deep insight into photochemical reactions. Being focused on the chemical changes occurring due to the interaction of light with the matter three types of changes can be emphasized to make a chemist more curious. The first one is color changes, (photochromism), the second one is the development of gas bubbles in a liquid, and the third one is the precipitation of the product upon photo reaction that is less soluble than its precursor. The color changes induced in a photochromic dye should have been considered as the earliest photochemical reactions.[12] Almost several years back, people made an attempt to utilize the energy of the sun in many directions. Based on the heat capacity of the materials (glass, cast iron or marble) John French showed two setups "to rectify spirits" in which collection and accumulation of solar radiation were possible.[13] Libavius employed the use of lenses, and mirrors, and tried to focus sunlight on a selected area by means of different methods which provide the basic principles of optics.[14]

Joseph Priestley: Photochemistry in the Eighteenth Century: Following Libavius's experiment, Joseph Priestley used a lens (12 inches) to focus the sunlight on a sample of mercury present in a closed vessel.[15a] He observed the appearance of mercury to a red solid form with a slight increase in its weight. Later, this pioneering experiment was corrected by Lavoisier in which he used a combination of mercury with oxygen, i.e. as an oxidation and he concluded

the conversion to be a result of a thermal reaction obtained from sunlight.[15b] Being curious about his experiment, Priestley was further successful in two different fields: inorganic chemistry and photosynthesis in which light has the actual role. In the experiment, he exposed the spirit of nitre (nitric acid) to sunlight and observed the appearance of reddish color in the liquid phase. Later, in his follow-up experiments, he ruled out the possibility of a thermal reaction and confirmed that the reddish product (nitrogen dioxide) was formed in the vapor phase and then dissolved in the liquid.[15c] Finally, he concluded that the color change was due to the action of light upon the vapour of the spirit of nitre. This has been considered the first photochemical reaction in the gas phase.[15c]

J. W. Dobereiner and the Light-Induced Reduction of Metal Ions: J. W. Dobereiner in 1831, was the first who introduced the concept of metal ion reduction upon light exposure. In his experiment, an aqueous solution of iron(III) oxide and oxalic acid were exposed to sunlight in a small glass tube. He observed the development of some gas bubbles and he identified these bubbles as CO_2 and a basic iron(II) oxide, humboldtite, precipitated.[16a] The modified version of this reaction has become the basis for ferrioxalate actinometry.[16b] Further, a similar type of reductions for Ag, Pt, and Ir, salts were observed by him and he performed some control experiments and ruled out the possible dark reactions. However, he skipped out on the first photoreaction of a ruthenium compound, as a result of which so many photochemical studies were not discovered until 1844. Dobereiner's contribution to photoreduction of metal salts provides new avenues for solid state photochemistry.

Trommsdorff, Sestini, Cannizzaro: The Photochemistry of Santonin: Trommsdorff was always investigating whether the light-induced reactions depended upon the wavelength or not. He proved the wavelength dependency of light with the help of a prism. He assumed that santonin exists in two isomeric forms.[17a] Based on the elemental analyses, Heldt argued that yellow and white santonin are identical in their composition, but different in their structural arrangements.[17b] The early workers, of course, were unable to predict the structures of santonin or its photoproduct. The credit for the wavelength dependence of an organic photoreaction belongs to this study which brings a marginal shift in the development of photochemistry. Next, Sestini started investigating the structure of santonin. He got the photosantonin upon irradiating 65% aqueous ethanol which he later identified as a diethyl ester that could be further converted into a photosantonic acid (lactone/acid). However, the photosantonic acid was directly prepared

by irradiating santonin in 80% acetic acid. When Sestini came to Rome, he introduced Cannizzaro to the problems associated with the structure of santonin and its photoproducts. They combinely published one paper and at a later stage, they pursued the problems independently.[17c] Further, Cannizzaro *et al*. were successful in confirming the formation of photosantonic acid and disclosed a new photo and stereochemical complexity of santonin. However, the structure of photosantonic acid was elucidated only in 1958 but the intermediates were not confirmed until 1963 (Scheme I.1).[17d] Being an investigator of santonin and its photoproduct for 20 years, Sestini always got the credit for the discovery of photosantonic acid from Cannizzaro. Sestini's contribution to the history of photochemistry was really useful and he was the only one who deserves the credit for being an introducer of Cannizzaro to light chemistry and, through him, Ciamician, and Silber.[18a,b]

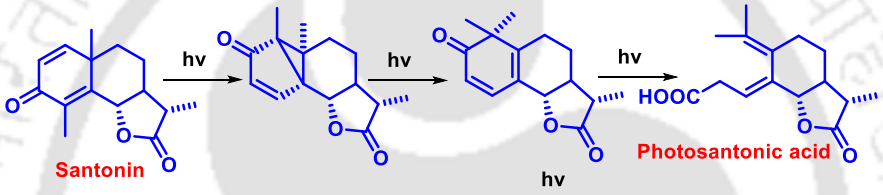

Scheme I.1. *Formation of photosantonic acid.*

Early Photodimerization Contributions by Fritzsche: Among the various photoreactions, the photodimerization product obtained by the precipitation and it was less soluble as compared to their starting precursors. The photodimerization of anthracene, was observed by Fritzsche in Petersburg in 1867 and that has been considered as the earliest laboratory photodimerization.[19]

Geometric Isomerization of Olefins: W H. Perkin as a Photochemist: Among various photo reactions of olefins, geometric isomerization is one of the most common reactions that was first observed by Perkin in 1881. He was investigating the conversion of several "α-isomers" into their "*β*-isomers" of 2-alkoxycinnamic acids (obtained from coumarin) upon exposure to sunlight.[20a] Perkin not only described cis-trans isomerization upon light exposure but also studied the effects of wavelength on various photochemical reactions. To confirm, which range of light caused the actual chemical change he used different colored solutions as filters, such as ammoniacal copper sulphate solution, and sulfate of quinine. Finally, he concluded that the color change is mainly due to the action of the violet and ultraviolet rays.[20b] This led to the frequent use of UV lamp in photochemistry.

Photoinduced Halogenation: With the development of halogen-induced geometric isomerizations of olefins, the light-induced halogenation of aromatic hydrocarbons has come into the limelight in the field of photochemistry. These reactions were between 1884 and 1888 by Julian Schramm.[21a] Initially, as early as 1874, the isolated *p*-bromobenzyl bromide in the light-induced bromination of toluene was not identified.[21b] Later, Paul Jannasch, tried to improve the poor yield of a dibromo derivative obtained from toluene and got the crystal, which Schramm demonstrated as *p*-bromobenzyl bromide (Scheme 1.2).[21b]

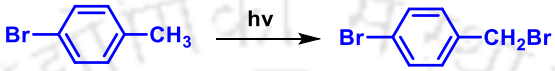

Scheme I.2. *Formation of p-bromobenzyl bromide.*

Photochemistry of Carbonyl Compounds: Among the pioneers of photochemistry, Klinger is the only one who started working on the photoreactions of carbonyl compounds. After conducting several experiments, he got the crystals of a molecular complex of two moles of benzil upon exposure to sunlight and confirmed that benzil dissolved in wet ether undergo reduction upon exposure to sunlight (Scheme I.3).[22a]

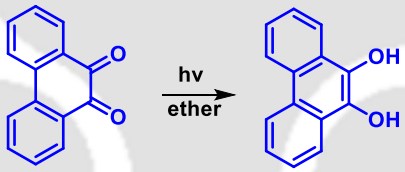

Scheme I.3. *Photochemical reduction of benzil.*

The modified version of the same reaction was extended to a series of aldehydes and ketones and also with different quinones. The reaction of benzoquinone with benzaldehyde provided 2-benzoylhydroquinone or 2,5-dihydroxybenzophenone (Scheme 1.4).[22b] Klinger found a correlation between these reactions with the photosynthesis of the living plants.[22c]

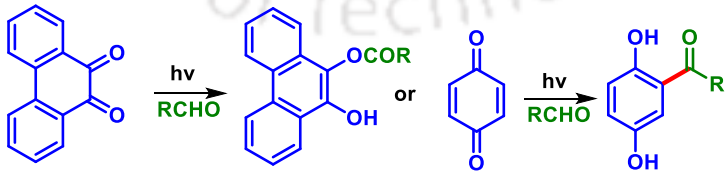

Scheme I.4. *Photochemical reaction of quinones with benzaldehyde.*

Photochemistry of Diazonium Compounds: Peter Griess in 1858, introduced the photochemistry of diazonium compounds. At the very initial stage, when their sensitivity to light was first observed, the chemistry was not very clear. Later, several attempts to utilize them

for further purposes were documented as early as 1889. After the exposure of the film containing diazonium sulfonate the unreacted part of it could be removed by repeated washing (Scheme 1 5).[23]

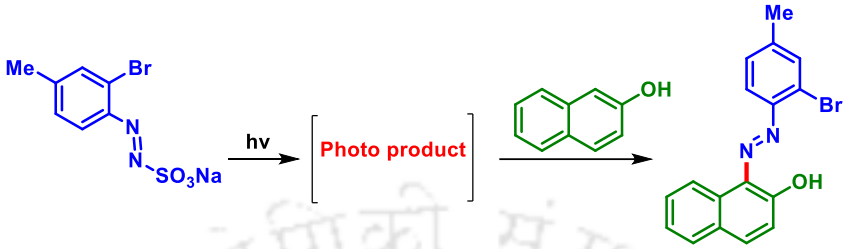

Scheme I.5. *Photochemical reaction of diazonium sulfonate with benzaldehyde.*

At the end of the nineteenth-century, photochemistry was not much explored and has been applied to a limited number of reactions. In those reactions, sun was the frequently used light source which was not focused light. Only Liebermann started working with different light sources, a gas burner with a metal oxide mantle, an arc lamp, and a magnesium flame etc.[24a] Trommsdorff studied the wavelength dependence of a photoreaction with the help of a prism.[24b] Perkin[24c] and Klinger[24d] used a filter solution. The previous effort made by different scientists provides the source to modern photocatalysis.

I.3. Importance of Photoredox Catalysis

Photocatalysis mainly deals with the interaction of light with the molecules or catalyst or any additives present leading to their excitation that enables the chemical reaction to occur. In this context, the use of LEDs of different wavelengths can excite the reacting component that corresponds to the wavelength of that region. Hence different selectivity can be attained which are not usual in most of the conventional approach.[8] In this direction, ruthenium and iridium, photocatalysts have been established as a powerful tools for achieving different molecular frameworks. In spite of their excellent photophysical properties and their high cost, and toxicity issues have limited their scope in many directions. Though the transition metal complexes are well-established in photocatalysis the organic dyes has also shown efficient reactivity in many photochemical tansformation.[9] Besides the switching selective it offers an exciting mechanistic approach that makes the field of photocatalysis more popular day by day. The choice of LEDs has a very crucial role in attaining different selective which particularly deals with the absorbance maximum for the lowest energy absorption (λ_{max}). Based on the absorption maxima, a light source is selected for a particular photoredox catalyst. The most important requirement is

that at least there should be some overlap between absorption of the molecule and emission of the lamp which enables the photochemical reaction to occur. In this regard, the use of LEDs of different wavelengths has come into focus in the field of photoredox catalysis, owing to their relatively narrow emission band which can do selective excitation of the chromophore. Ultimately, the λ_{max} value gives the preliminary idea regarding the energy required for a photo-induced electron transfer.[25]

I.4. General Mechanistic Schemes for Photoredox Catalysis

The mechanism of photocatalysis mainly involves two processes one is energy transfer and the other is the electron transfer process (Figure I.1).

1) Energy Transfer
2) Electron Transfer

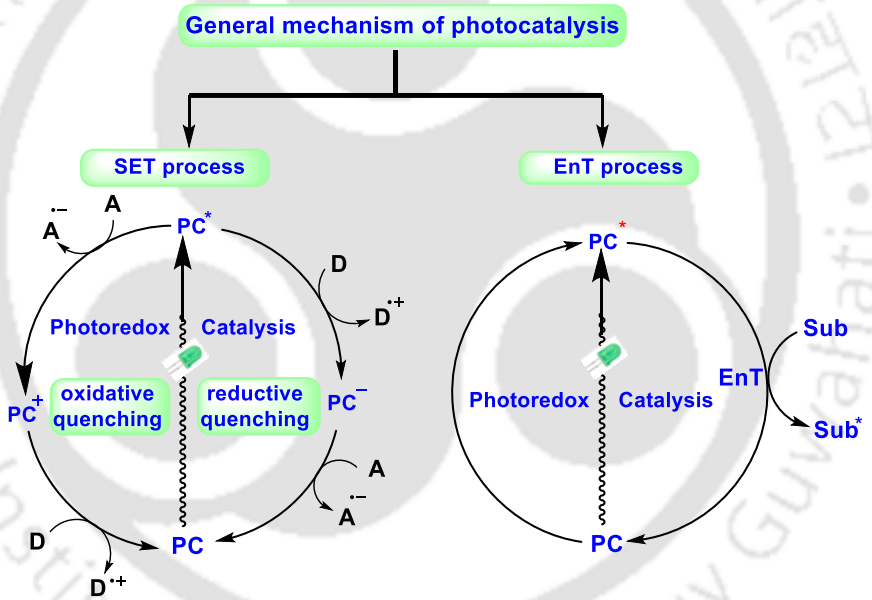

Figure I.1. *General mechanism for energy and electron transfer.*

I.4.1. Energy Transfer: In energy transfer reactions the photosensitizers (at their excited states) transfer their energy to the substrate and initiate the reaction. Photosensitizers such as benzophenone, rose bengal, and methylene blue, can be better used as triplet sensitizers owing to their long lifetimes in their triplet state as compared to their singlet state. One of the most well-known applications of triplet sensitization is the photo-sensitization of the ground state triplet dioxygen ($^3O_2$) to generate their singlet dioxygen ($^1O_2$).

Usually, intramolecular cyclization, [2+2] cycloaddition reactions involve the energy transfer pathway.[26]

I.4.2. Electron Transfer: Although the outcome of energy transfer processes is distinct and recognizable in select cases (for instance, the Schenck-Ene reactivity of olefins and $^1O_2$), electron transfer and energy transfer cannot be readily distinguishable in other systems. For triplet sensitization, the organic molecules used as substrates must have high triplet energies which usually exceed 60 kcal mol^{-1} (2.6 eV). Hence in an electron transfer reaction, the catalysts remain redox neutral in their ground state at the initial stage but at the excited state, they either accept or lose one of its electrons to the substrate thereby acting either as an oxidizing or a reducing agent. Most of the photochemical reaction mechanism involves the electron transfer process which are of different types (a) Oxidative and Reductive Quenching (b) Proton Coupled Electron Transfer (PCET) (c) Proton Transfer followed by Electron Transfer (PT/ET) (d) Electron-Donor-Acceptor Complexes (EDA Complex), and Exciplex etc.[27]

I.4.2.1. Oxidative and Reductive Quenching

In an oxidative quenching cycle, the quenching of excited state photocatalyst PC* happens via the donation of an electron either to substrate or an oxidant [ox] present in the reaction whereas in a reductive quenching cycle, an excited state of the photocatalyst PC* accepts an electron from substrate or a reductant [red]. In the oxidative cycle, the catalytic turnover is maintained via the reduction of the oxidized $[PC]^{\bullet+}$ whereas in the reductive cycle oxidation of the reduced $[PC]^{\bullet-}$ happens to maintain the catalytic turnover. Any of the used substrates, an intermediate, or the external redox-active reagent (light absorbing species) are mainly responsible for catalyst turnover.[28]

I.4.2.2. Proton-Coupled-Electron Transfer

Proton-coupled electron transfer (PCET) involves the exchange of electrons and protons in a concerted manner and found to have applications in recent inorganic technologies for small molecular activation and numerous important biological redox processes. The activation of a wide variety of organic functional groups (that are energetically unfavorable) using usual molecular H atom transfer catalysts is the main application of this kind of mechanistic approach. The basic requirement for PCET is the formation of hydrogen bond between the substrate and a proton donor/acceptor prior to the charge transfer. Usually, PCET mechanisms are of two types such as reductive PCET and oxidative PCET. The ketyl radical mainly involves the reductive

PCET whereas the generation of amidyl radical involves the oxidative PCET pathway (Figure I.2).[29a]

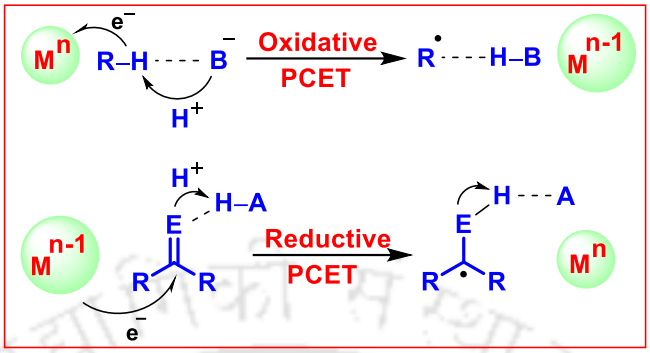

Figure I.2. *General mechanism for oxidative and reductive PCET.*

I.4.2.3. Proton Transfer Followed by Electron Transfer (PT/ET)

The electron transfer process which involves the first deprotonation followed by a single-electron process is known as PT/ET Process. In this case, both the proton transfer and electron transfer do not happen in a concerted manner (Figure I.3).[29b]

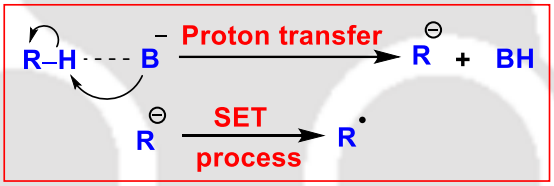

Figure I.3. *General mechanism for PT/ET.*

I.4.2.4. Electron Donor-Acceptor Complexes

In spite of the frequent use of transition metal complexes or organic dyes, in photocatalysis, there are some photocatalytic transformations that can happen without using any photocatalyst.[30a] In such cases, the reacting partners are unable to absorb the light independently corresponding to the wavelength range of irradiation. However, the reacting components show a color change upon mixing which indicates the formation of an electron donor−acceptor (EDA) complex (charge-transfer complex).[30b] The mechanistic insight and the reactivity pattern of these species were well explained by Kochi[30c] and has been clearly described by Melchiorre[30d] and others to attain catalyst-free visible-light-mediated transformations. Moreover, the reacting components combinely able to absorb the light and undergo a red shift than the individual reactant which is an indication of the EDA complexation between them (Figure I.4). The exciplexes, which are excited-state complexes are different from that the ground state EDA

complexes and cooperatively emit a photon. Usually, an exciplex operates when an excited state electron-deficient photocatalyst, such as a cyanoarene, encounters an electron-rich substrate. The red shifting of the fluorescence spectra relative to the maximum of the uncomplexed fluorescence confirms the formation of an exciplex.[30e]

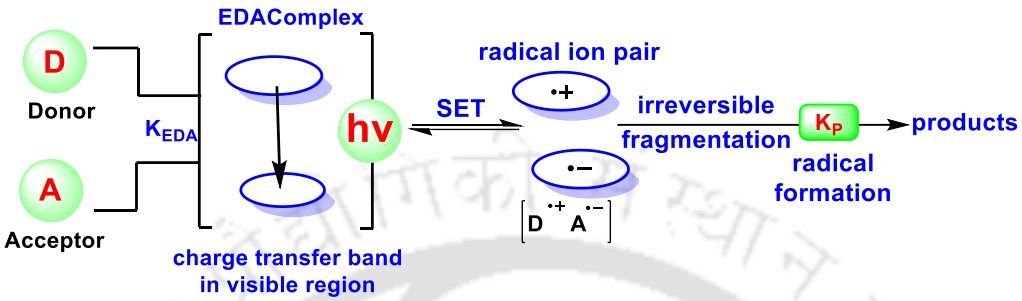

Figure I.4. *General mechanism for EDA complex formation.*

Owing to the switching selectivity and different mechanistic aspects photocatalysis has been frequently used in various directions to synthesize different organic molecular frameworks via the C–heteroatom bond formation. But owing to the biological importance of organosulfur compounds C–S bond–forming reactions have become an important area of research.[31]

I.5. Importance of C–S Bond Formation

Among different bond formations, the C–S bond formation reactions have gathered immense popularity due to their frequent applications in pharmaceuticals as well as industries. For instance, Cysteine (**I**) and Methionine (**II**) are two sulfur-containing amino acids, which help in promoting antioxidant activity and body development (Figure I.5). Garlic which is considered to be one of the home remedies, is associated with biologically active compounds that have been reported to reduce rates of cancer. Ajoene (**III**) and Allicin (**IV**) were isolated from garlic and were found to act as antibacterial agent.[32] Organic sulfur compounds are found to have numerous applications in pharmaceuticals. For instance, antibiotic or antiprotozoal drugs such as Bactrim were obtained from sulfamethoxazole (**V**) and its derivatives.[33a] Besides their medicinal importance, organosulfur compounds are also very popular in material science. A thiophene based conjugated polymer such as poly(1,3-dithienylisothianaphthene) (PDTITN) (**VI**) has shown application in organic electronics and photonics (Figure I.5).[33b] Owing to the importance of organosulfur compounds the development of synthetic methods to form C–S bond is always deemed worthy of investigations.[31]

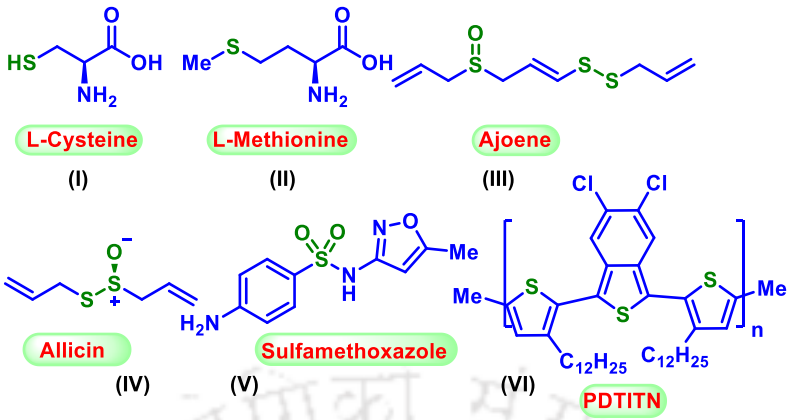

Figure I.5. *Biologically active sulfur compounds.*

To date, tremendous progress has been achieved in the construction of new C−S bonds, which mainly involves addition and substitution reactions (Scheme I.6). The addition of various sulfur nucleophiles to carbon−carbon double and triple bonds, thiolysis of epoxides, aziridines, anhydride, cross-coupling reaction with aryl halides is the traditional way of C−S bond formation (Scheme I.6).[34a]

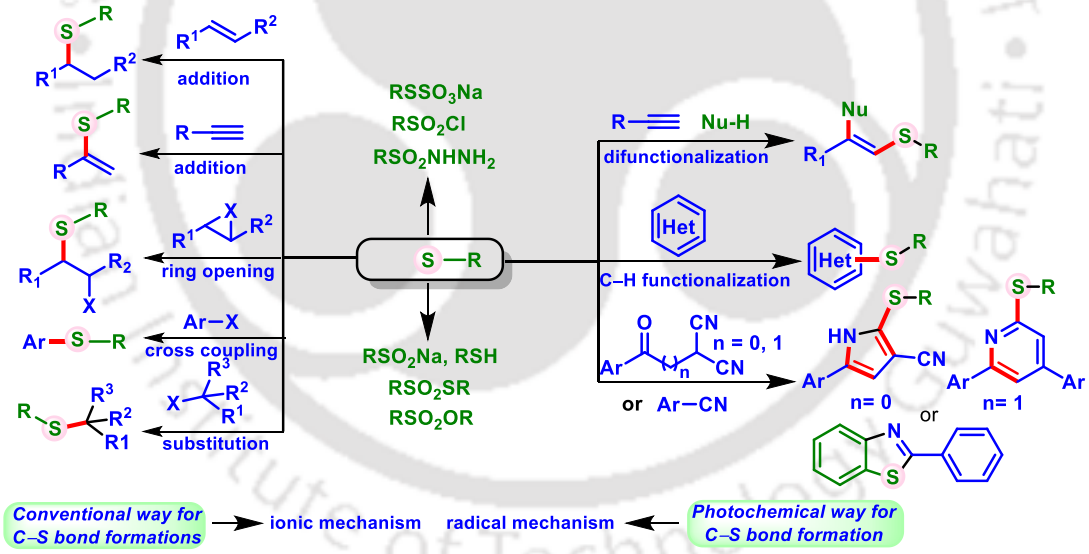

Scheme I.6. *Traditional/Photochemical generation of C–S bond formations.*

However, these traditional methods mostly involved an ionic pathway rather than a radical pathway. In spite of these existing conventional methods, the C–S bond formation via photocatalysis has gained immense popularity which converts the *S*–nucleophiles to *S*–radicals via single electron transfer and triggers the reaction.[34b] This mainly includes radical addition to the alkenes and alkyne following difunctionalization strategy, C–H bond functionalization, S-radical-triggered cyclization reactions, etc. Since all the chapters deal with visible-light-

mediated C–S bond formation under metal-free conditions so only metal-free C–S bond-forming reactions are focused.

I.6. Strategies for Visible-Light-Mediated C–S Bond Formation

There are several strategies involved in the C–S bond formation under visible-light irradiation which involves the following.

1) Difunctionalization Strategy
   a) Difunctionalization of Alkenes
   b) Difunctionalization of Alkynes
2) C–H Bond Functionalization
   a) C–H Functionalization Involving Sulfonylation/Sulfenylation
   b) C–H Functionalization Involving thiolation
3) Radical Cyclization Reactions

I.6.1. Difunctionalization Strategy

The difunctionalization approach has gained much importance in modern organic synthesis due to its excellent regioselectivity thereby providing complex molecules in a simple manner. Two functional groups can be installed simultaneously onto a carbon−carbon double or carbon-carbon triple bond which offers an excellent way for achieving complex molecular framework.[35]

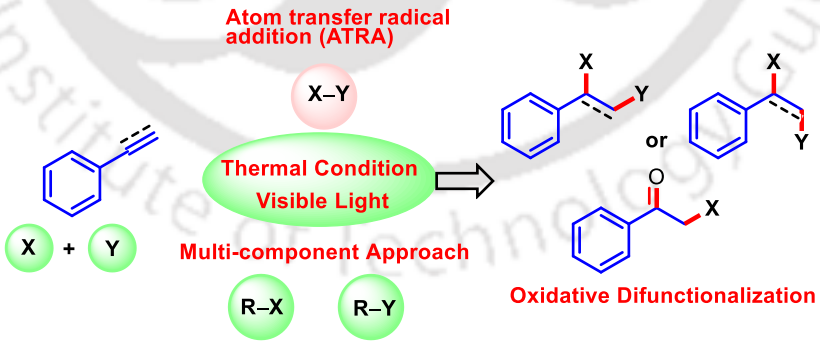

Figure I.6. *Different difunctionalization strategies.*

Usually, difunctionalization can be done by different approaches *viz*. atom transfer radical addition, and multi-component approach. In the atom transfer radical addition approach both the coupling partner comes from a single radical precursor whereas in the multi-component approach both the coupling partners come from different radical precursors. However, in multi-

component approach, if one of the radicals is trapped by the O_2 or moisture then this type difucntionalization is called oxidative difunctionalization. In this regard, tremendous progress has been achieved in difucntionalization of alkenes and alkynes under thermal and photochemical approach to construct diverse frameworks (Figure I.6). Mainly the difunctionalization reaction via photochemical approaches has gained much reputation in recent days for the construction of C–S bonds.[36] The mechanism of the difunctionalization mainly involves the initial attack of one of the radical precursors to the alkenes or alkynes generating a vinyl radical intermediate. This radical is either directly trapped by another radical partner or undergo a SET process to give a carbocation intermediate and is further trapped by a nucleophilic partner and provides the desired difunctionlized product (Figure I.7).

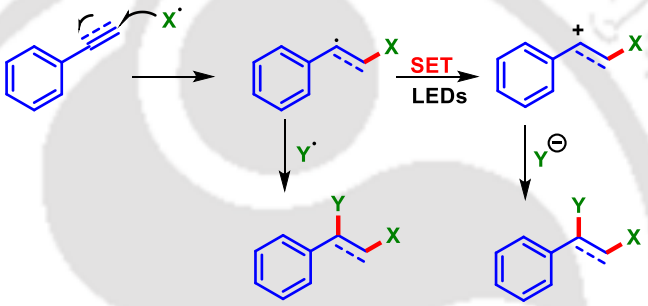

Figure I.7. *General mechanism for the difunctionalization of alkenes and alkynes.*

I.6.1.1. Difunctionalization of Alkenes

The difunctionalization of alkene has come into the focus of chemists as a complex molecular framework can be attained via the simultaneous installation of two functional groups onto a carbon−carbon double bond.[37a] In particular, styrenes have been frequently used as an important and commercially available building block of many pharmaceuticals, natural products, and materials. In this context, styrene difunctionalization via visible light irradiation has gained importance in modern organic synthesis. In 2021, Singh *et al*. reported a difunctionalization of styrene using CS_2 and amines as the reacting partners and provided a diverse range of *β*-keto dithiocarbamates (Scheme I.7). This protocol demonstrated an excellent way for the oxidative difucntionalization of styrene under metal-free conditions.[37b]

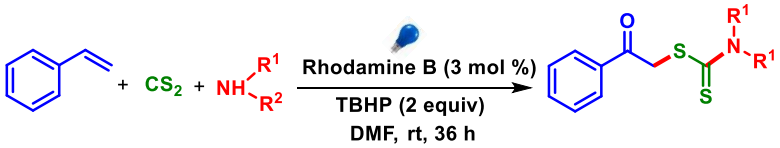

Scheme I.7. *Visible-light-mediated difunctionalization of alkenes.*

Recently, the Maity group demonstrated a visible-light-promoted sulfurization of alkenes and alkynes with thiols using air as the oxidant. The present method provided a route for the difunctionalization of alkenes and alkynes using eosin Y as the photosensitizer under metal-free conditions (Scheme I.8).[37c]

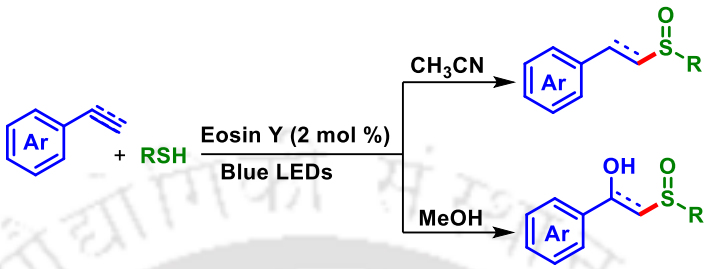

Scheme I.8. *Visible-light-mediated sulfurization of alkenes and alkynes.*

In 2022 Li *et al*. accomplished a pyridylthioesterification of styrenes under blue LEDs irradiation via the unusual cleavage of C(nonacyl)–S bond rather than the C (acyl)–S bond (Scheme I.9).[37d]

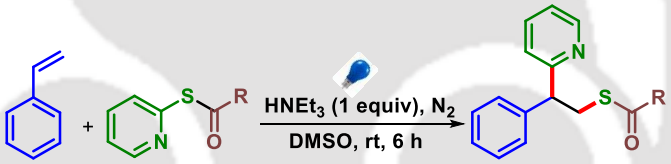

Scheme I.9. *Visible-light-mediated pyridylthioesterification of styrenes.*

In 2016, Wang *et al*. demonstrated a visible light-driven oxysulfonylation of alkenes with aryl sulfinic acids as the sulfonyl precursors. The developed protocol occurs at room temperature under transition-metal-free conditions. In this oxysulfonylation, the moisture is the source of oxygen rather than the atmospheric O_2 (Scheme I.10).[37e]

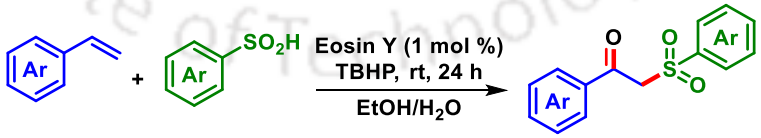

Scheme I.10. *Visible-light-mediated oxysulfonylation of styrenes.*

In 2018, trifluoromethylthiolation of styrenes has been reported by the Singh group in which they employed CF_3SO_2Na as the CF_3 source and CS_2 as a sulfur source. A terminal, as well as internal alkenes were well tolerated in this protocol. Cyclic alkenes also worked well and provided the desired trifluoromethylthiolated product (Scheme I.11).[38a]

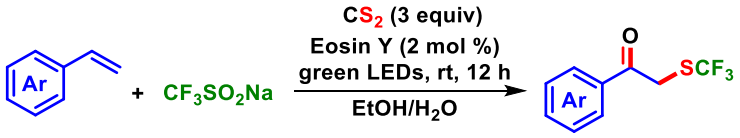

Scheme I.11. *Green-light-induced trifluoromethylthiolation of styrenes.*

In 2019, Zhu *et al*. disclosed the synthesis of *β*-keto/hydroxyl sulfones under blue light irradiation using alkene and sulfonyl hydrazides as the reacting partners. In this protocol, sulfonyl radicals are generated via the visible-light-induced oxidation of sulfonyl hydrazides which undergo oxidative addition with the alkenes. Notably, the present protocol employed O_2 as the oxidant without requiring any additional oxidants (Scheme I.12).[38b]

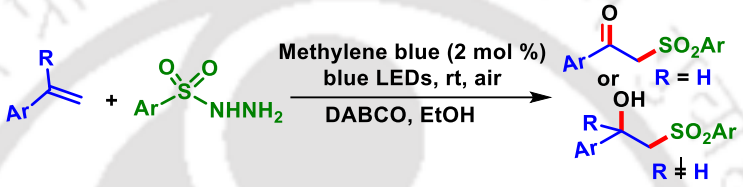

Scheme I.12. *Blue-light-induced synthesis of β-keto/hydroxyl sulfones.*

Recently, Akondi *et al*. reported a trifluoromethyl-thiocyanation of alkenes using Umemoto reagent as the CF_3 source and ammonium thiocyanate as the thiocyanating agent under visible light irradiation. The protocol avoids the use of transition metals, photosensitizers, and additives. This protocol is compatible with different alkene systems such as styrenes, unactivated alkenes, and acrylates and produces a variety of trifluoromethyl-thiocyanates in good to excellent yields (Scheme I.13).[38c]

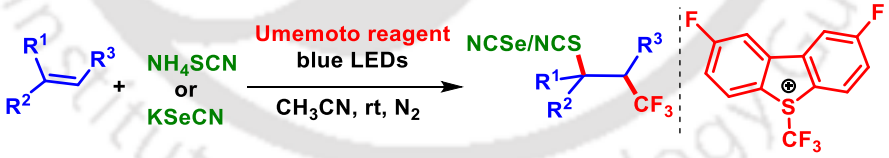

Scheme I.13. *Visible-light-induced trifluoromethyl-thiocyanation of alkenes.*

In 2022, the Liu group accomplished the hydroxysulfenylation of styrenes using air as the oxygen source and thiols as the thioaryl source. The reaction proceeds through the formation electron donor–acceptor (EDA) complex between the reacting species. The protocol tolerates a wide range of functional groups on either of the reacting partners (Scheme I.14).[38d]

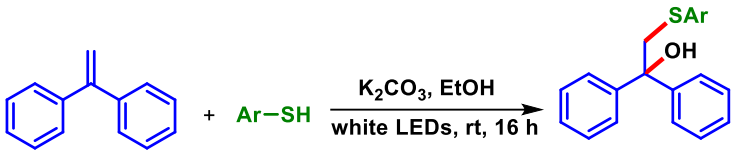

Scheme I.14. *Visible-light-induced hydroxysulfenylation of alkenes.*

I.6.1.2. Difunctionalization of Alkynes

Alkynes are important building blocks in organic synthesis that can be efficiently transformed into other functionalities. In this regard, poly-substituted alkenes can be obtained via difunctionalization of alkynes which enables the simultaneous introduction of two functional groups into the same molecule.[39] Muti-functionalized alkenes are ubiquitous in many natural products, bioactive molecules, and pharmaceuticals *viz*., doxepin, tamoxifen, etc.[40a,b] In this context, chemists are always in search for the development of suitable methods for their synthesis. Although there are well-established transition metal-catalyzed methodologies available for the difunctionalization of alkynes the metal-free process is always demanding.[40c] In this regard, visible-light mediated difucntionalization has come into the limelight due to the operational simplicity and switching selectivity. Owing to the importance of sulfur-containing compounds, this strategy has been found to have widespread applications in the synthesis of organosulfur compounds.[31]

Recently, in 2022 a visible-light-induced oxysulfonylation of alkynes has been reported by the Zhang group using arylsulfonate phenol esters as the *S*–centered radical source. The reaction proceeds smoothly in the absence of any photosensitizer and the mechanism proceeds via an electron donor-acceptor complex-mediated radical process (Scheme I.15).[41a]

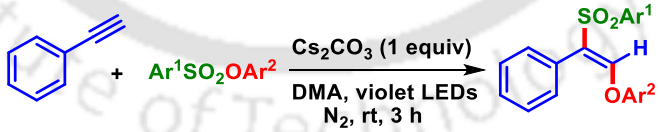

Scheme I.15. *Visible-light-induced oxysulfonylation of alkynes.*

Recently, in 2022, the patel group reported a visible-light-induced oxidative difunctionalization of alkynes using g-C_3N_4 as the recyclable photocatalyst. Both terminals, as well as internal alkynes underwent smooth reactions in this protocol (Scheme I.16).[41b] The present protocol demonstrated green chemistry metrics calculation which shows the greener aspects of the present methodology.

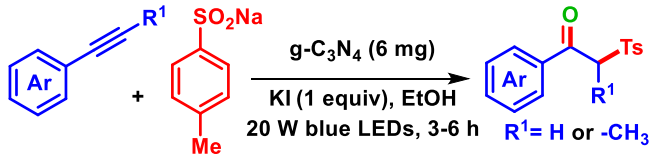

Scheme I.16. *Blue-light-induced oxidative difunctionalization of alkynes.*

In 2021, Li, and co-workers reported a visible-light-induced iodosulfonylation of alkynes using sulfonyl chlorides as the aryl sulfonyl radical source. In this protocol, both terminal and internal alkynes well reacted with sulfonyl chlorides in the presence of NaI in micellar media in water, giving their difunctionalized product good to excellent yields (Scheme I.17).[41c]

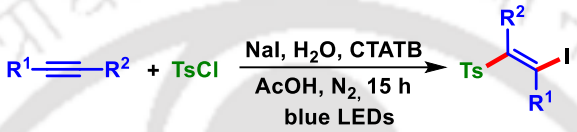

Scheme I.17. *Blue-light-induced iodosulfonylation of alkynes.*

Niu *et al*. in 2020 reported a hydrosulfonylation of alkynes with the simultaneous incorporation of sulfur dioxide under aerobic conditions leading to *β*-keto sulfones. In this protocol p-g-C_3N_4 has been used as the photocatalyst. The source of oxygen comes from H_2O, not from the O_2. They also performed the recyclability of the metal-free heterogeneous semiconductor up to 6 consecutive cycles which showed no significant reduction in its catalytic activity. The present protocol is also efficient in the presence of sunlight (Scheme I.18).[41d]

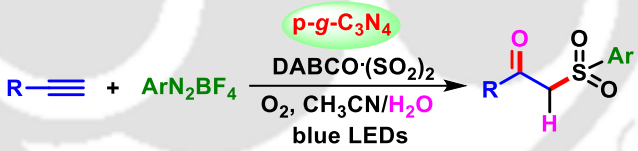

Scheme I.18. *Oxysulfonylation of alkynes using DABSO as SO_2 surrogate.*

Ananikov *et al*. in 2016, accomplished a metal-free thiol–yne click reaction using eosin Y as the photocatalyst. In this protocol, C–S coupling products were obtained in high yields, and excellent selectivity (Scheme I.19).[41e]

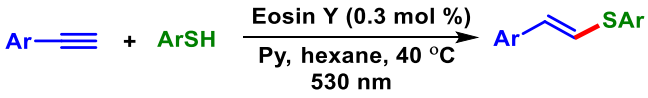

Scheme I.19. *Eosin Y catalyzed hydrosulfenylation of alkynes.*

I.6.2. C–H Bond Functionalization

C–H bond functionalization has gained enormous importance in the construction of various organic frameworks leading to the formation of functionalized molecules. The field of catalytic C−H functionalization has gathered tremendous progress over the past four decades. Mostly, the catalytic strategies involving transition metals, photochemical, and electrochemical have all been employed for the functionalization of C−H bonds.[42] These strategies have been widely applied in the selective functionalization of natural products, petroleum feedstock's, functionalization of heterocycles, functionalization of pharmaceutical derivatives, and polymers.[43] Particularly, photocatalysis has become a trending area of research and covers vast areas of organic synthesis. This includes applications for renewable energy and natural product synthesis, new reaction development, chemical feedstocks, materials, and biological applications. Moreover, photocatalysis has been frequently employed in many synthetic transformations which involve C–H functionalization leading to the construction of C–C, C–N, C–O, C–S, and C–P bond formations.[44] Usually, organic photocatalysts operate via their excited singlet states(S_1) rather than their triplet (T_1) states. In spite of their shorter lifetimes (10−50 ns), this provides a larger redox window available to these catalysts. The organic photoredox catalysts are more efficient for carrying out single electron transfer reactions. Overall, organic photoredox catalysts have become an impressive area of research in C−H functionalization. Particularly, the C–S bond formation via C–H functionalization has gained much importance owing to the easy introduction of sulfur-containing group to any heterocycles or others. Usually, the C–S bond formation can be frequently achieved either via sulfonylation or sulfenylation.[45]

1.6.2.1. C–H Functionalization Involving Sulfonylation/Sulfenylation

The introduction of a sulfonyl group into any molecular frameworks (heterocycles and others) can tremendously increase their biological importance for which the sulfonylation reaction is on demand.[46] Being a good leaving group sulfones are found to show unique chemical reactivity enabling many organic transformations. Owing to their leaving tendency it has been described as a chemical chameleon by Trost.[47a] In this context, the development of efficient methods for the synthesis of molecules with sulfone backbone is always the need of the hour. In this context, He *et al*. reported a deoxygenated C2-sulfonylation of quinoline *N*-oxides

with sulfinic acids in the presence of eosin Y as the photocatalyst under visible light irradiation (Scheme I.20).[47b]

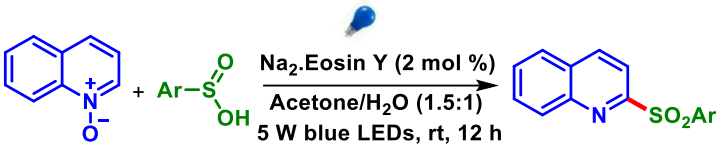

Scheme I.20. *Sulfonylation of quinoline N-oxides.*

The Sun group reported an efficient method for the sulfonylation of tertiary amines with thiosulfonates under visible-light irradiation. This protocol provided a wide variety of cyclic and acyclic *β*-sulfonyl enamines under metal, oxidant, and photosensitizer-free conditions (Scheme I.21).[47c]

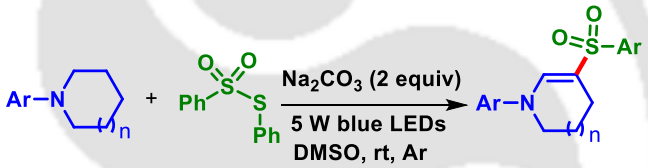

Scheme I.21. *Visible-light-promoted sulfonylation of cyclic amines.*

Xuan *et al*. in 2019 accomplished a visible-light-promoted decarboxylative sulfonylation of cinnamic acids with aryl sulfonate phenol esters as the sulfonyl precursors. The decarboxylative sulfonylation involved an electron donor−acceptor complex formation between the DMA and the sulfonate phenol ester. The method provided a mild route for the synthesis of vinyl sulfones without requiring any photosensitizer, oxidant, etc (Scheme I.22).[47d]

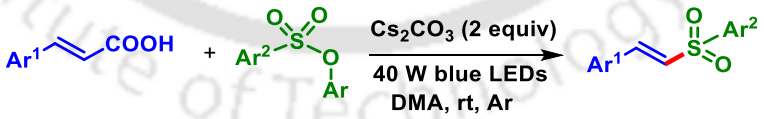

Scheme I.22. *Visible-light-driven decarboxylative sulfonylation of cinnamic acids.*

In 2017, Wu and co-workers disclosed a photosensitizer-free sulfonylative coupling of aryl/alkyl halides, using DABSO (1,4-diazabicyclo[2.2.2]octane-sulfur dioxide), as the sulfonyl surrogate, and silyl enolates as the reacting partners. This transformation provided a broad range of *β*-ketosulfones at room temperature along with good functional group tolerance. Both aryl iodides and aryl bromides worked well in this protocol (Scheme I.23).[47e]

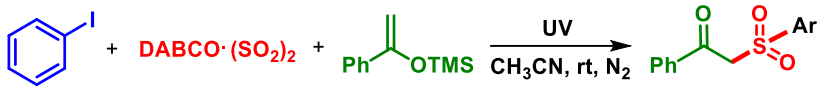

Scheme I.23. *Synthesis of β-ketosulfone using DABSO as SO_2 surrogate.*

In 2017, Manolikakes *et al*. demonstrated a photochemical synthesis of sulfonamide using diaryldiazonium salt as the aryl precursors, sodium metabisulfite as the SO_2 surrogate, and hydrazines as the aminating source. In this reaction, perylene dye (PDI) was used as the photocatalyst. Both aromatic, as well as aliphatic hydrazines, worked well in the present protocol (Scheme I.24).[47f]

Scheme I.24. *Synthesis of sulfonamide using PDI as photoredox catalysts.*

Konig *et al*. reported a persulfate-mediated synthesis of heteroaromatic sulfoxides under visible light irradiation. Electron-rich heteroarenes, such as pyrroles and indoles were efficiently sulfenylated in the present protocol. The mechanism involves an electrophilic sulfinamide intermediacy and provided the sulfenyated product (Scheme I.25).[47g]

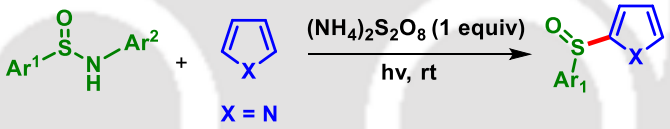

Scheme I.25. *Visible-light- mediated sulfenylation of heteroaromatics.*

1.6.2.2 C–H Functionalization Involving Thiolation

Sulfur-containing organic scaffolds, particularly thioarylated compounds are found to have widespread applications in pharmaceuticals as well as in biologically relevant molecules including thymitaq, nelfinavir, and axitinib [48a-c] The diaryl sulfides serves as the backbones of many natural products and also found to have applications in material sciences.[48d,e] Owing to the biological importance of thioarylated organic framework development of newer methodology for the thiolation of various heterocycles, aromatic compounds is always the need of the hour. In this context, an efficient tris(pentafluorophenyl)borane $B(C_6F_5)_3$-catalyzed oxidative C−S cross-coupling reaction of thiophenol with indoles was established by Tang *et al*. providing a diverse range of diaryl sulfides in good yields. The proposed mechanism suggests an EDA complex formation between $B(C_6F_5)_3$ and indoles thereby facilitating the single electron transfer (SET)

from indole to the $B(C_6F_5)_3$ catalyst. The protocol used the $B(C_6F_5)_3$ catalyst as a single-electron oxidant (Scheme I.26).[49a]

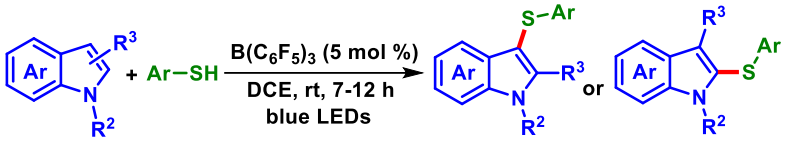

Scheme I.26. *Visible-light-mediated sulfenylation of indoles.*

In 2019, Liao and co-workers developed a visible-light-promoted deaminating thioesterification of amino acid-derived Katritzky salts with thiobenzoic acid as the thioaroylating agent. This protocol provides a new route for the synthesis of α-mercapto acid derivatives under photochemical conditions. The proposed mechanism suggests an EDA complex formation between the thiobenzoic acid anion and the Katritzky salt (Scheme I.27).[49 b]

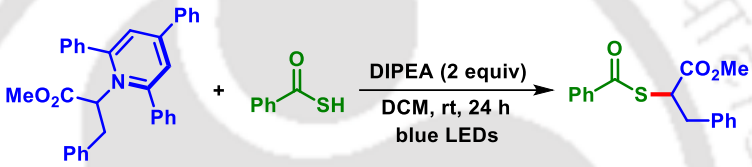

Scheme I.27. *Deaminative thioesterification of amino acid-derived Katritzky salts.*

In 2018, Hajra and co-workers reported an elegant method for the oxidative coupling between thiophenols and arylhydrazines to afford diaryl sulfides under blue LEDs irradiation. A wide variety of unsymmetrical diarylsulfides were synthesized in good yields at room temperature. The present methodology worked well with benzo[d]thiazole-2-thiols, 1H-benzo[d]imidazole-2-thiols, benzo[d]oxazole-2-thiol, and 1H-imidazole-2-thiol (Scheme I.28).[49c]

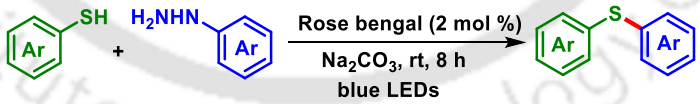

Scheme I.28. *Visible-light-mediated synthesis of unsymmetrical diaryl sulphides.*

Similarly, Miyake *et al*. disclosed a visible-light-driven cross-coupling reaction between thiols and aryl halides in the absence of any photosensitizer. The mechanism involves the formation of an EDA complex between thiolate anion, and aryl halide which is confirmed from the UV−vis spectroscopy. A wide range of aryl halides and thiophenols were well reacted in this protocol proving a diverse range of diaryl sulfides (Scheme I.29).[49d]

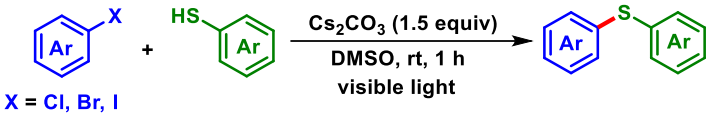

Scheme I.29. *Visible-light-mediated C−S cross-coupling of thiophenol with aryl halides.*

Akiyama *et al*. in 2021 reported a photochemical synthesis of aryl sulfides using alkanes and thiols as the reacting partners. This reaction proceeds via the excitation of an EDA complex between a thiolate and an aryl halide, followed by the hydrogen atom transfer from an alkane to the generated aryl radical (Scheme I.30).[49e]

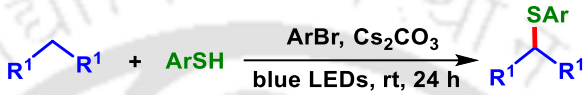

Scheme I.30. *Visible-light-promoted thio-arylation of alkanes.*

In 2019, Wu and co-workers demonstrated an efficient method for the synthesis of *S*-aryl thiosulfonates via a three-component reaction of aryldiazonium tetrafluoroborates sodium metabisulfite, and thiourea under photochemical conditions. A diverse range of aryldiazonium tetrafluoroborates worked well in this transformation. However, the present protocol was unsuccessful for *S*-alkyl thiosulfonates due to the lesser stability of alkyl diazonium salts (Scheme I.31).[49f]

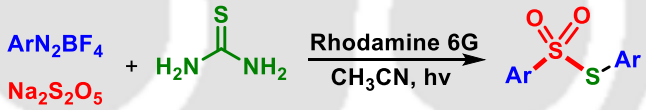

Scheme I.31. *Photochemical synthesis of S-aryl thiosulfonates.*

A similar kind of photochemical synthesis of thiosulfonates was reported by He *et al*. using aryldiazonium salts thiols, and sodium metabisulfite under metal-free conditions. The present protocol used Rhodamine 6G as the photocatalyst to provide a diverse range of unsymmetrical thiosulfonates (Scheme I.32).[49g]

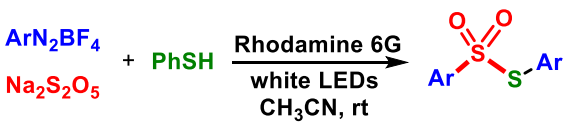

Scheme I.32. *Visible-light-driven synthsesis of S-aryl thiosulfonates.*

Yang *et al*. disclosed an elegant method for the synthesis of *S*–aryl dithiocarbamates under visible light irradiation. The protocol avoids the use of transition metal catalysts, ligands,

or photocatalysts, and provided the easiest way to synthesize *S*–aryl dithiocarbamates (Scheme I.33).[49h]

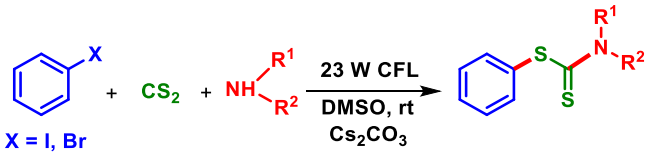

Scheme I.33. *Visible-light driven synthesis of S–aryl thiocarbamates.*

I.6.3. Radical Cyclization Reactions

Radical cyclization has proven to be an efficient method for the construction of carbo- and heterocycles due to its high atom- and step-economy.[50] Heterocyclic synthesis is mainly based on the design of the starting precursors in combination with matching reacting partners. A suitable radical acceptor can undergo cyclization to give any carbo and heterocycles upon reacting with a suitable radical donor. Porter and coauthors reported an unsaturated peroxy radical cyclization to construct prostaglandin analogs which have been considered to be a pioneering reaction in radical cascade cyclization.[51a,b] Despite the significant advances, in the field of radical chemistry the construction of carbo and heterocycles with existing radical acceptors is still challenging for chemists. In this regard, alkenes, alkynes, nitriles, and isonitriles, have been well-established as radical acceptors for many radical cyclization reactions.[51c,d] Therefore, the development of newer methodologies for accessing functionalized carbo and heterocycles via radical cyclization is always the need of the hour. Usually, cascade radical cyclization mainly involves four phases: (i) generation of radical: radical species is formed via a single-electron transfer (SET) process; (ii) radical addition: radical addition to an unsaturated bond generates a carbon radical intermediate; (iii) radical cyclization: carbon radical undergo cyclization and a carbon-carbon/heteroatom bond is formed; (iv) radical quenching: the quenching of carbon radical intermediate occurs via the hydrogen abstraction or another radical donor coupling to construct a carbo- and heterocyclic molecule (SchemeI.34).

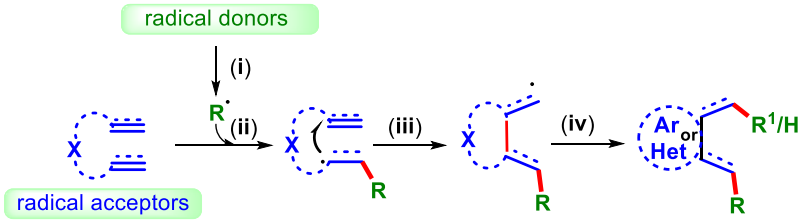

Scheme I.34. *General pathway for the cascade radical cyclization.*

Recently, visible light-induced radical cyclization has brought a paradigm shift in radial chemistry for the synthesis of the different molecular frameworks. In particular, the *S*–centered radical triggered cyclization reactions have gained much reputation in modern organic chemistry owing to the biological importance of sulfur-containing compounds.[31] In this direction, visible light-induced radical cyclization has come into the limelight of many photochemists. In this context, Chen *et al*. in 2021, reported a photochemical synthesis of thioarylated dibenzofurans via a radical cascade reaction of 2-vinyloxy arylalkynes with thiosulfonates. The present protocol utilized diaryl disulfide as an additive which plays the role of hydrogen abstraction in the aromatization process to provide the desired product. This protocol provides a new route for the construction of polycyclic oxygen heterocycles (Scheme I.35).[52a]

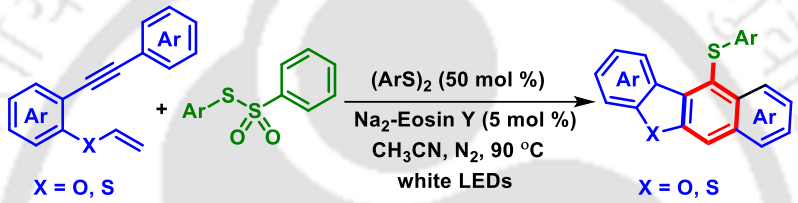

Scheme I.35. *Visible-light-mediated synthesis of dibenzofuran derivatives.*

Li *et al*. disclosed a photocatalytic synthesis of 2-aryl benzothiazoles via radical cyclization of ortho-halothiobenzanilides under metal-free conditions. Visible light enables the substrates to undergo dehalogenative cyclization to provide a diverse array of 2–aryl benzothiazoles (Scheme I.36).[52b]

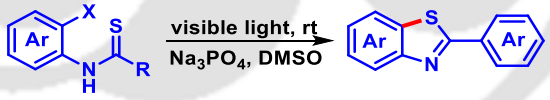

Scheme I.36. *Photochemical synthesis of 2–aryl benzothiazole.*

Similarly, kind of metal-free synthesis of 2–aryl benzothiazoles has been reported by the Zhou *et al*. using g-C_3N_4 as the photocatalyst. This protocol provided a wide variety of 2-substituted benzothiazoles at room temperature without the addition of a strong base or organic oxidizing reagents. The reusability of the catalyst is one of the salient features of this protocol (Scheme I.37).[52c]

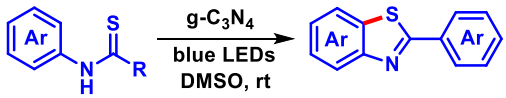

Scheme I.37. *Graphitic carbon nitride catalyzed synthesis of 2-aryl benzothiazole.*

Zhang *et al*. reported a photochemical synthesis of pyrido[1,2-*a*]indoles and indolizines using sulfonyl chloride as the aryl sulfonyl precursors. The present protocol avoids the use of any photocatalysts and oxidants. The mechanistic investigation showed the role of pyrrole and indole as the pre-photocatalysts to facilitate the sulfonylation followed by cyclization (Scheme I.38).[52d]

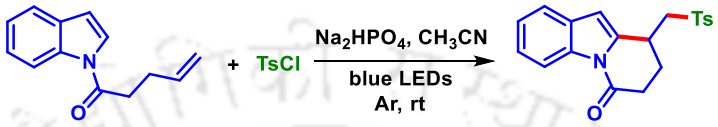

Scheme I.38. *Photochemical synthesis of pyrido indoles.*

An efficient multi-component iodosulfonylative cyclization of enynes has been reported by Zhu *et al*. in which the sulfonyl radical is generated via visible-light irradiation of iodoform with sulfinates. The sulfonyl radical triggers the radical addition, followed by cyclization, and provided a variety of vinyl iodide-containing sulfone groups (Scheme I.39).[52e]

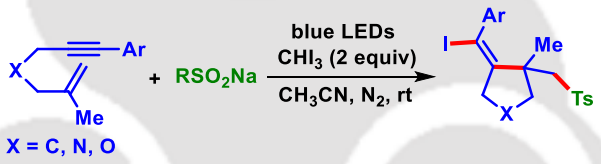

Scheme I.39. *Iodosulfonylative cyclization of enynes.*

Recently, in 2022 Yu *et al*. demonstrated a persulfate-promoted synthesis of pyrrolo[1,2-*a*]indolediones via radical cyclization in the absence of any photosensitizer. In this protocol, aryl sulfonyl hydrazide and ammonium thiocyanate were used as the *S*–centered radical source (Scheme I.40).[53a]

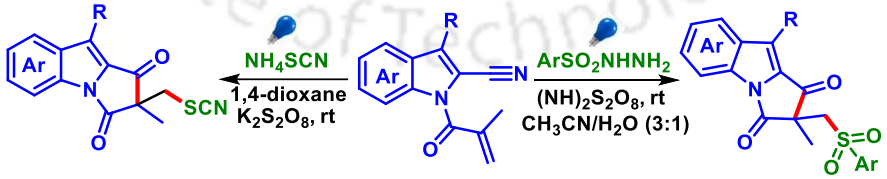

Scheme I.40. *Visible-light-mediated synthesis of pyrrolo[1,2- a]indolediones.*

In 2022, Zhu and co-workers reported a photochemical synthesis of quinolin-2(1*H*)-ones via Markovnikov-type sulfonylation followed by *6-endo-trig* cyclization and selective C(O)–

CF_3 bond cleavage starting from *N*–alkyl *N*–(2-ethynylphenyl)-2,2,2-trifluoroacetamides and sulfinic acids (Scheme I. 41).[53b]

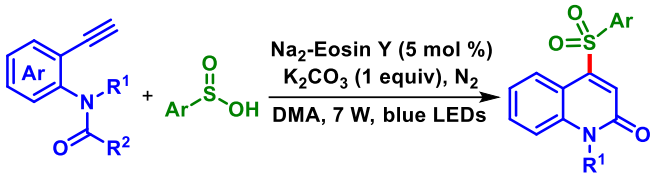

Scheme I.41. *Photochemical synthesis of quinolin-2(1H)-ones.*

Recently, Wei and co-workers reported a blue-light or sunlight-mediated synthesis of sulfonylfunctionalized dihydro benzofurans via tandem radical addition/1,5-hydrogen atom transfer/cyclization cascade of 2-alkynylarylethers with sulfonyl chlorides in 2-methyl tetrahydrofuran. This protocol experienced a unique energy transfer pathway to generate sulfonyl radicals for the synthesis of a wide variety of sulfonylated benzofuran derivatives (Scheme I. 42).[53c]

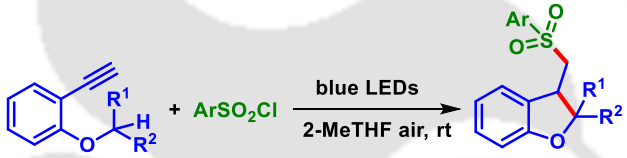

Scheme I.42. *Synthesis of sulfonyl functionalized dihydro benzofurans.*

Singh *et al*. in 2022 demonstrated a visible-light-promoted cascade radical cyclization for the synthesis of sulfonylated benzimidazo/indolo[2,1-*a*]iso-quinolin-6(5*H*)-ones under metal-free conditions. The present protocol has utilized the sodium metabisulfite as the SO_2 surrogate (Scheme I. 43).[53d]

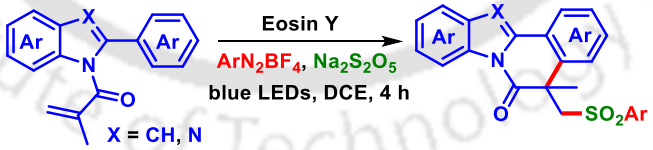

Scheme I.43. *Synthesis of sulfonylated benzimidazo/indolo[2,1-a]iso-quinolin-6(5H)-ones.*

Li and coworkers disclosed an efficient method for the photocatalytic synthesis of sulfonated chromanes and sulfonated 1,2,3,4-tetrahydroquinolines via a radical cascade cyclization of 1-(arylethynyl)-2-(vinyloxy)benzenes and *N*–allyl-2–(aryl ethynyl) anilines with

sulfinic acids as the sulfonyl source, eosin Y as the photocatalyst, and TBHP as an oxidant (Scheme I. 44).[53e]

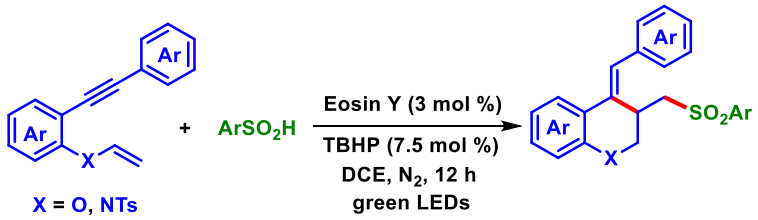

Scheme I.44. *Synthesis of sulfonated chromanes and sulfonated 1,2,3,4-tetrahydroquinolines.*

A visible-light-initiated oxidative cyclization of phenyl propiolates with sulfinic acids has been developed by Wang and co-workers. The present protocol provides a wide range of coumarin derivatives with good functional group tolerance and high regioselectivity. The mechanism involves an oxidative quenching pathway for the formation of coumarin derivatives (Scheme I. 45).[53f]

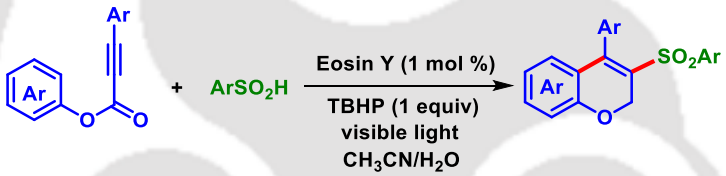

Scheme I.45. *Visible-light mediated synthesis of coumarin derivatives.*

In 2017, Pan and coworkers developed an efficient photocatalytic oxidative/reductive cyclization reaction of *N*–cyanamide alkenes with aryl sulfinic acids or arylsulfonyl chlorides, which proceeds through C–S, C–C, and C–N bond formations. This photocatalytic strategy provided a wide variety of sulfonated quinazolinones (Scheme I. 46).[53g]

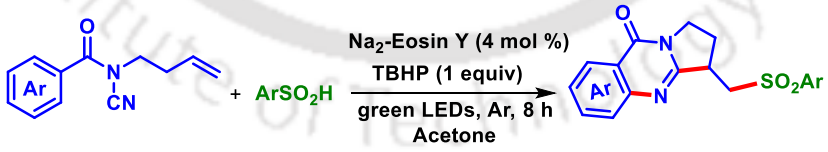

Scheme I.46. *Visible-light mediated synthesis of sulfonated quinazolinones.*

Fan *et al*. in 2018, disclosed a photochemical synthesis of 2–imino thiazolidine–4–ones via a multi-component tandem annulation of amines, α-bromoesters, and aryl/alkyl isothiocyanates, in the absence of any photosensitizer. This cyclization strategy involves the formation of an EDA complex between the *in-situ* generated thiourea and the α-bromoesters.

Broad substrate scope, mild reaction conditions, good functional group tolerance, and operational simplicity, are some of the outstanding features of this protocol (Scheme I. 47).[54a]

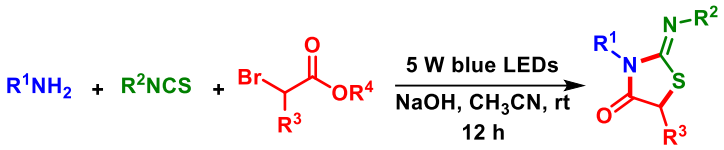

Scheme I.47. *Visible-light mediated synthesis of 2–imino thiazolidin–4–ones.*

The same group in 2019, reported a three-component coupling annulation strategy for the synthesis of 2–iminothiazolidin–4–ones from amines, isothiocyanates, and alkyl acetylene dicarboxylates under visible-light irradiation. The *in situ* formed electron donor−acceptor (EDA) complexes act as the light absorber and facilitate the reaction and provided the corresponding 2-imino thiazolidin–4–ones (Scheme I. 48).[54b]

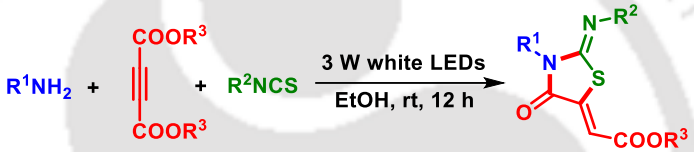

Scheme I.48. *EDA complex enabled synthesis of 2–iminothiazolidin–4–ones.*

In 2020, Sharma, and co-workers reported an EDA complex-mediated synthesis of benzothiazoles via decarboxylative cross-coupling between 2-aminothiophenols and α-keto acids under blue LED irradiation. The protocol experienced a photosensitizer-free photochemical reaction and provided a diverse array of 2–aryl benzothiazoles in good yields. The formation of benzothiazole is driven by the EDA (electron donor-acceptor) complex formed between α-keto acid and 2-amino thiophenols (Scheme I. 49).[54c]

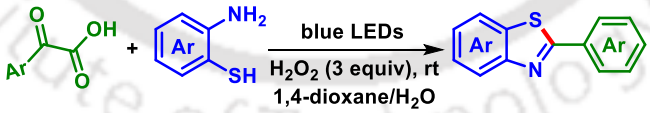

Scheme I.49. *EDA complex enabled synthesis of benzothiazole.*

In summary, the above-mentioned literature gives the idea that how *S*-centered radicals can be generated under visible-light irradiation and can trigger the radical cascade reaction leading to heterocycles, and other functionalized molecular frameworks. Taking cues from the above literatures the difunctionalization strategy, and the thiyl-radical triggered synthesis of heterocycles have been designed.

I.7. References:

[1] (a) Yi, H.; Zhang, G.; Wang, H.; Huang, Z.; Wang, J.; Singh, A. K.; Lei, A. *Chem. Rev.* **2017**, *117*, 9016−9085. (b) Togo, H. Advanced Free Radical Reactions for Organic Synthesis, 1st ed.; Elsevier: Amsterdam, Boston, **2004**. (c) Fontecave, M.; Ollagnier-de-Choudens, S.; Mulliez, E. *Chem. Rev.* **2003**, *103*, 2149−2166.

[2] (a) Holmberg-Douglas, N.; Nicewicz, D. A. *Chem. Rev.* **2022**, *122*, 1925−2016. (b) Zeitler, K. *Angew. Chem., Int. Ed.* **2009**, *48*, 9785−9789. (c) Narayanam, J. M. R.; Stephenson, C. R. J. *Chem. Soc. Rev.* **2011**, *40*, 102−113. (c) Shi, L.; Xia, W. *Chem. Soc. Rev.* **2012**, *41*, 7687−7697.

[3] (a) Nicewicz, D. A.; Nguyen, T. M. *ACS Catal.* **2014**, *4*, 355−360. (b) Zhang, G.; Bian, C.; Lei, A. *Chin. J. Catal.* **2015**, *36*, 1428−1439. (c) Angnes, R. A.; Li, Z.; Correia, C. R. D.; Hammond, G. B. *Org. Biomol. Chem.* **2015**, *13*, 9152−9167.

[4] (a) Romero, N. A.; Nicewicz, D. A. *Chem. Rev.* **2016**, *116*, 10075−10166. (b) Tóth, B. L.; Tischler, O.; Novák, Z. *Tetrahedron Lett.* **2016**, *57*, 4505−4513. (c) Siddiqui, R.; Ali, R. *Beilstein J. Org. Chem.* **2020**, *16*, 248−280. (d) Amos, S. G. E.; Garreau, M.; Buzzetti, L.; Waser, J. *Beilstein J. Org. Chem.* **2020**, *16*, 1163−1187.

[5] (a) Prier, C. K.; Rankic, D. A.; MacMillan, D. W. C. *Chem. Rev.* **2013**, *113*, 5322−5363. (b) Yoon, T. P.; Ischay, M. A.; Du, J. *Nat. Chem.* **2010**, *2*, 527−532. (c) Hopkinson, M. N.; Sahoo, B.; Li, J.-L.; Glorius, F. *Chem. Eur. J.* **2014**, *20*, 3874−3886.

[6] (a) Koike, T.; Akita, M. *Inorg. Chem. Front.* **2014**, *1*, 562−576. (b) Skubi, K. L.; Blum, T. R.; Yoon, T. P. *Chem. Rev.* **2016**, *116*, 10035−10074. (c) Levin, M. D.; Kim, S.; Toste, F. D. *ACS Cent. Sci.* **2016**, *2*, 293−301.

[7] (a) Teply, F. *Chem. Commun.* **2011**, *76*, 859−917. (b) Xuan, J.; Xiao, W.-J. *Angew. Chem., Int. Ed.* **2012**, *51*, 6828−6838. (c) Brachet, E.; Ghosh, T.; Ghosh, I.; König, B. *Chem. Sci.* **2015**, *6*, 987−992. (d) Chen, J.-R.; Hu, X.-Q.; Lu, L.-Q.; Xiao, W.-J. *Chem. Soc. Rev.* **2016**, *45*, 2044−2056.

[8] (a) Karkas, M. D. *ACS Catal*. **2017**, *7*, 4999−5022. (b) Zhao, Y.; Xia, W. *Chem*. *Soc*. *Rev*. **2018**, *47*, 2591−2608. (c) Jiang, H.; Studer, A. *Angew*. *Chem*., *Int*. *Ed*. **2017**, *56*, 12273−12276.

[9] Penzkofer, A.; Beidoun, A.; Daiber, M. *J*. *Lumin*. **1992**, *51*, 297−314. (b) Majek, M.; Filace, F.; von Wangelin, A. J. *Beilstein J*. *Org*. *Chem*. **2014**, *10*, 981−989. (c) Timpe, H.-J.; Neuenfeld, S. *J*. *Chem*. *Soc*. *Faraday Trans*. **1992**, *88*, 2329−2336. (d) Yoshioka, E.; Kohtani, S.; Jichu, T.; Fukazawa, T.; Nagai, T.; Takemoto, Y.; Miyabe, H. *Synlett* **2015**, *26*, 265−270.

[10] Canuto, V. M.; Levine, J. S.; Augustsson, T. R.; Imhoff, C. L.; Giam-papa, M. S. *Nature* **1983**, *305*, 281–286.

[11] (a) Blake, A. J.; Carver, J. H.; *J*. *Atmos*. *Sci*. **1977**, *34*,720–728. (b) Levine, J. S.; Hays, P. B.; Walker, J. C. G. *Icarus* **1979**, *39* 295–309.

[12] Beatty, J. M.; Winds, T. *Adv*. *Phorochem*. **1963**, *1*, 275–321.

[13] J. French: The Art of Distillation, Williams, T. London **1653**, 42.

[14] A. Libavius: Alchymra. 1608, reprinted in D. Diderot: Encyclopedie, **1766**; cf. Gmelin-Institut (Ed.): Die Alchemie des Andreas Libavius, VCH Verlagsgesellschaft. Weinheim **1985**.

[15] (a) Priestley, J. quoted by Lavoisier, A. 520–521. (b) Lavoisier, A. *Traite Elementaim de Chimie*, **1789**. 2nd. edition, translated by Edinburgh, R. K. **1793**. (c) Priestley, J.: Experiments and Observations on Different Kinds of Air, Pearson, T. Birmingham **1790.**

[16] (a) Dohereiner, J. F. Schweigger J. 62 (Jahr) 8 90-96; see *Pharm*. *Centralbl*. **1831,** *2*, 383–385. (b) Parker, C. A.; *Proc*. *R*. *SOC*. (London) A220 **1953** 104–116.

[17] (a) Trommsdorff, H. *Ann*. *Chem*. *Pharm*. **1834**, *11*, 190–208. (b) Heldt, W. *Ann*. *Chem*. *Pharm*. 1847, *63*, 10–47. (c) Cannizzaro, S. Sestini, F. *Gazz*. *Chim*. *Ital*. **1873**, *3*, 241–251. (d) Chapman, O. L.; Englert, L. F.; *J*. *Am*. *Chem*. *Soc*. **1963**, *85*, 3028–3029.

(18) Sestini, F.; *Gazz*. *Chim*. *Ital*. **1876**, *6*, 357–369. (b) Sestini, E. *Repert*. *Iial*. *Chim*. *Pharm*. **1865**.

[19] Fritzsche, J. *Ann*. *Chem*. *Pharm*. **1859**, *104*, 247–250.

[20] (a) Perkin, W. H. *J. Chem. Soc*. **1881**, *39*, 409–452. (b) Perkin, W H. *J Chem. Soc*. **1882**, *41*, 330.

[21] (a) Schramm, J. *Ber. Dtsch. Chem. Ges*. **1884**, *17*, 2922–2925. (b) Jannasch, P. *Justus Liebtgs Ann. Chem*. **1875**, *176*, 283–290.

[22] (a) Klinger, H. *Ber. Dtsch. Chem. Ges*. **1886**, *19*, 1862–1870. (b) Klinger, H. Standke, O. *Ber. Dfsch. Chem. Ges*. **1891**, 24, 1340–1346. (c) Klinger, H. *Justus Liebigs Ann. Chem*. **1911**,*382*, 211–221.

[23] Griess, P. *Justus Liebigs Ann. Chem*. **1858**, *106*, 123–125.

[24] (a) Liebermann, C. *Ber. Dtsch. Chem. Ges*. **1895**, *28*, 143-1448. (b) Trommsdorff, H. *Ann. Chem. Pharm.* **1834,** 190–208. (c) Perkin, W. H. *J. Chem. Soc*. **1881**, *39*, 409–452. (d) Klinger, H. *Justus Liebigs Ann. Chem*. **1888**, *249* 137–146.

[25] (a) Akasaki, I. *Rev. Mod. Phys*. **2015**, *87*, 1119−1131. (b) Nakamura, S. Nobel Lecture: *Rev. Mod. Phys*. **2015**, *87*, 1139−1151.

[26] (a) Clennan, E. L.; Pace, A. *Tetrahedron* **2005**, *61*, 6665−6691. (b) Gorman, A. A.; Rodgers, M. A. J. *Chem. Soc. Rev*. **1981**, *10*, 205−231. (c) Ohloff, G. *Pure Appl. Chem*. **1975**, *43*, 481−502. (d) Tanielian, C.; Wolff, C. *J. Phys. Chem*. **1995**, *99*, 9831−9837.

[27] Ni, T.; Caldwell, R. A.; Melton, L. A. *J. Am. Chem. Soc*. **1989**, *111*, 457−464.

[28] (a) Mangion, D.; Kendall, J.; Arnold, D. R. *Org. Lett*. **2001**, *3*, 45−48. (b) Griesbeck, A. G.; Hundertmark, T.; Steinwascher, J. *Tetrahedron Lett*. **1996**, *37*, 8367−8370. (c) Davies, J.; Booth, S. G.; Essafi, S.; Dryfe, R. A. W.; Leonori, D. *Angew. Chem*. **2015**, *127*, 14223−14227. (d) Yang, D.-T.; Meng, Q.-Y.; Zhong, J.-J.; Xiang, M.; Liu, Q.; Wu, L.-Z. *Eur. J. Org. Chem*. **2013**, *2013*, 7528−7532.

[29] (a) Gentry, E. C.; Knowles, R. R. *Acc. Chem. Res*. **2016**, *49*, 1546−1556. (b) Dahiya, A.; Das, B.; Sahoo, A. K.; Patel, B. K. *Adv. Synth.Catal*. **2022**,*364*, 966–973.

[30] (a) Rosokha, S. V.; Kochi, J. K. *Acc. Chem. Res*. **2008**, *41*, 641−653. (b) Rosokha, S. V.; Kochi, J. K. *J. Am. Chem. Soc*. **2007**, *129*, 3683−3697. (c) Kochi, J. K. *Pure Appl. Chem*. **1991**, *63*, 255−264. (d) Silvi, M.; Arceo, E.; Jurberg, I. D.; Cassani, C.; Melchiorre, P. *J. Am. Chem.*

Soc. **2015**, *137*, 6120−6123. (e) Wozniak,́ Ł.; Murphy, J. J.; Melchiorre, P. *J*. *Am*. *Chem*. *Soc*. **2015**, *137*, 5678−568.

[31] (a) Shen, C.; Zhang, P.; Sun, Q.; Bai, S.; Andy Hor. T. S.; Liu, X. *Chem*. *Soc*. *Rev*. **2015**, *44*, 291−314. (b) Xia, C.; Wei, Z.; Shen, C.; Xu, J.; Yang, Y.; Su W.; Zhang, P. *RSC Adv*. **2015**, *65*, 52588. (c) Lu, Q. Zhang, J. Wei, F. Qi, Y. Wang, H. Liu, Z. Lei, A. *Angew*. *Chem*., *Int*. *Ed*. **2013**, *52*, 7156−7159.

[32] (a) Ledezma, E.; Apitz-Castro, R. *Rev Iberoam Micol* **2006**, *23*, 75–80. (b) Lazem, J. S.; AL kelabe, A. H. *J*. *Phys*. *Conf*. *Ser*. **2019**, *1294*, 092039.

[33] (a) Lavanya R.; Sudhakar Rao, Ch.; Swaroop B.; Akhila P.; Vineetha P.; Kiran, M. e-ISSN:2322-0066. (b) Vangeneugden D. L.; Vanderzande, D. J. M. *J*. *Phys*. *Chem*. *B*. **2001**, *105*, 11106−11113.

[34] (a) Lyons, T. W.; Sanford. *Chem. Rev*. 2010, 110, 1147. (b) Uchikura, T.; Hara, Y.; Tsubono, K.; Akiyama, T. *ACS Org*. *Inorg*. *Au*. **2021**, *1*, 23−28.

[35] (a) Patel, M.; Saunthwal, R. K.; Verma, A. K. *Acc*. *Chem. Res*. **2017**, *50*, 240−254. (b) Wille, U. *Chem*. *Rev*. **2013**, *113*, 813−853. (c) Yue, H.; Zhu, C.; Kancherla, R.; Liu, F.; Rueping, M. *Angew*. *Chem*., *Int*. *Ed*. **2020**, *59*, 5738−5746. (d) Huang, L.; Rudolph, M.; Rominger, F.; Hashmi, A. S. K. *Angew*. *Chem*., *Int*. *Ed*. **2016**, *55*, 4808−4813. (e) Xu, T.; Cheung, C. W.; Hu, X. *Angew*. *Chem*., *Int*. *Ed*. **2014**, *53*, 4910−4914.

[36] (a) Li, Z.; Wang, S.; Huo, Y.; Wang, B.; Yan J.; Guo, Q. *Org*. *Chem*. *Front*. **2021**, *8*, 3076–3081. (b) Hossain, A.; Engl, S.; Lutsker, E.; Reiser, O. *ACS Catal*. **2019**, *9*, 1103–1109. (c) Lei, W.-L.; Wang, T.; Feng, K.-W.; Wu, L.-Z.; Liu, Q. *ACS Catal*. **2017**, *7*, 7941–7945. (d) Reddy, M. B.; Anandhan, R. *Chem*. *Commun*. **2020**, *56*, 3781–3784. (e) Shi, P.; Tu, Y.; Zhang, D.; Wang, C.; Truong, K.-N.; Rissanen K.; Bolm, C. Adv. Synth. Catal. 2021, 363, 2552–2556.

[37] (a) Lee, K.; Lee, S.; Kim, N.; Kim, S.; Hong, S. *Angew*. *Chem*. *Int*. *Ed*. **2020**, *59*, 2–8. (b) Vishwakarma, R. K.; Kumar, S.; Singh, K. Nand. *Org*. *Lett*. **2021**, *23*, 4147−4151. (c) Rahaman, R.; Hoque, M. T.; Maiti, D. K. *Org*. *Lett*. **2022**, *24*, 6885−6890. (d) Wu, Q.; Zhao,Y-H.; Lu, C.L.; Li, H-Y.; Li, H-X. *Org*. *Chem*. *Front*. **2022**, *9*, 2977–2985. (e) Yang, D.; Huang, B.; Wei, W.; Li, J.; Lin, G.; Liu, Y.; Ding, J.; Sun P.; Wang, H. *Green Chem.* **2016**, *18*, 5630–5634.

[38] (a) Yadav, A. K.; Singh, K. N. *Chem*. *Commun*. **2018**, *54*, 1976–1979. (b) Wu, J.; Zhang, Y.; Gong, X.; Meng, Y.; Zhu, C. *Org*. *Biomol*. *Chem*. **2019**, *17*, 3507–3513. (c) Nadiveedhi, M.

R.; Cirandur, S. R.; Akondi, S. M. *Green Chem*. **2020**, *22*, 5589–5593. (d) Chen, Z.; Xue, F.; Liu, T.; Wang, B.; Zhang, Y.; Jin, W.; Xia, Y.; Liu, C. *Green Chem*. **2022**, *24*, 3250–3256.

[39] (a) Flynn, A. B.; Ogilvie, W. W. *Chem. Rev*. **2007**, *107*, 4698− 4745. (b) Song, Z.-Q.; Liu, Z.; Gan, Q.-C.; Lei, T.; Tung, C.-H.; Wu, L.-Z. *Org*. *Lett*. **2020**, *22*, 832−836.

[40] (a) Ganapathy, D.; Sekar, G. *Org. Lett*. **2014**, *16*, 3856− 3859. (b) McKinley, N. F.; O'Shea, D. F. *J. Org*. *Chem*. **2006**, *71*, 9552−9555. (c) Wang, H.; Li, Y.; Tang, Z.; Wang, S.; Zhang, H.; Cong, H.; Lei, A. *ACS Catal*. **2018**, *8*, 10599−10605.

[41] (a) Xie, W.; Ma, P.; Zhang, Y.; Xi, L.; Qiu, S.; Huang, X.; Yang, B.; Gao, Y.; Zhang, J. *Org*. *Lett*. **2022**, *24*, 6099−6104. (b) Dam, B.; Sahoo, A. K.; Patel, B. K. *Green Chem*. **2022**, *24*, 7122-7130. (c) Lin, L.; Yang, Z.; Liu, J.; Wang, J.; Zheng, J.; Li, J-L.; Zhang, X.; Liu, X-W.; Jiang, H.; Li, J. *Green Chem*. **2021**, *23*, 5467–5473. (d) Ni, B.; Zhang, B.; Han, J.; Peng, B.; Shan, Y.; Niu, T. *Org*. *Lett*. **2020**, *22*, 670−674. (e) Zalesskiy, S. S.; Shlapakov, N. S.; Ananikov, V. P.; *Chem*. *Sci*. **2016**, *7*, 6740–6745.

[42] (a) Alberico, D.; Scott, M. E.; Lautens, M. *Chem*. *Rev*. **2007**, *107*, 174−238. (b) Davies, H. M. L.; Manning, J. R. *Nature* **2008**, *451*, 417−424. (c) Colby, D. A.; Bergman, R. G.; Ellman, J. A. *Chem*. *Rev*. **2010**, *110*, 624−655. (d) Mkhalid, I. A. I.; Barnard, J. H.; Marder, T. B.; Murphy, J. M.; Hartwig, J. F. *Chem*. *Rev*. **2010**, *110*, 890−931. (e) Yamaguchi, J.; Yamaguchi, A. D.; Itami, K. *Angew*. *Chem*., *Int*. *Ed*. **2012**, *51*, 8960−9009. (f) Davies, H. M. L.; Morton, D. *ACS Cent*. *Sci*. **2017**, *3*, 936−943.

[43] (a) Yang, Y.; Nishiura, M.; Wang, H.; Hou, Z. *Chem*. *Rev*. **2018**, *376*, 506−532. (b) Williamson, J. B.; Lewis, S. E.; Johnson, R. R.; Manning, I. M.; Leibfarth, F. A. *Angew*. *Chem*., *Int*. *Ed*. **2019**, *58*, 8654−8668.

[44] (a) Wang, C−S.; Dixneuf, P. H.; Soulé, J.-F. *Chem*. *Rev*. **2018**, *118*, 7532−7585. (b) Banerjee, A.; Lei, Z.; Ngai, M.-Y. *Synthesis* **2019**, *51*, 303−333. (c) Uygur, M.; Garcia Mancheño, O. *Org*. *Biomol*. *Chem*. **2019**, *17*, 5475−5489.

[45] (a) Liua, J.; Zhenga, L. *Adv*. *Synth*. *Catal*. **2019**, *361*, 1710–1732. (b) Iwasaki, M.; Fujii, T.; Nakajima, K.; Nishihara, Y. *Angew*. *Chem*. *Int*. *Ed*. **2014**, *53*, 13880 –13884.

[46] (a) Wolf, W. M. *J. Mol. Struct*. **1999**, *474*, 113–124. (b) Doherty, G. A.; Kamenecka, T.; McCauley, E. G.; Riper, V.; Mumford, R. A.; Tong, S.; Hagmann, W. K.; *Bioorg. Med. Chem. Lett*. **2002**, *12*, 729–731. (c) Hartz, R. A. A.; Arvanitis, G.; Arnold, C.; Rescinito, J. P.; Hung, K. L.; Zhang, G.; Wong, H.; Langley, D. R; Gilligan P. J.; Trainor, G. L. *Bioorg. Med. Chem. Lett.* **2006**, *16*, 934–937.

[47] (a) Trost, B. M.; Kalnmals, C. A. *Chem. Eur. J.* **2019**, *25*, 11193−11213. (b) Xie, L-Y.; Fang, T-G.; Tan, J-X.; Zhang, B.; Cao, Z.; Yanga, L-H.; He, W-M. *Green Chem.* **2019**, *21*, 3858–3863. (c) Tong, J.; Li, H.; Zhu, Y.; Liu P.; Sun, P. *Green Chem*. **2022**, *24*, 1995–1999. (d) Ge, Q-Q.; Qian, J-S.; Xuan, J. *J. Org. Chem*. **2019**, *84*, 8691−8701. (e) Li, Y.; Wu, J. *Chem. Lett*. **2020**, *49*, 1066-1070. (f) Liu, N.-W.; Liang S.; Manolikakes, G. *Adv. Synth. Catal*. **2017**, *359*, 1308–1319. (g) Meyer, A. U.; Wimmer, A.; Konig, B. *Angew. Chem. Int. Ed*. **2017**, *56*, 409–412.

[48] (a) Feng, M.; Tang, B.; Liang, S.; Jiang, X. *Curr. Top. Med. Chem*. **2016**, *16*, 1200. (b) Patani, G. A.; LaVoie, E. J. *Chem. Rev*. **1996**, *96*, 3147–3176. (c) Ilardi, E. A.; Vitaku, E.; Njardarson, J. T. *J. Med. Chem*. **2014**, *57*, 2832–2842. (d) Boyd, D. A. *Angew. Chem., Int. Ed*. **2016**, *55*, 15486–15502. (e) Rahate, A. S.; Nemade, K. R.; Waghuley, S. A. *Rev. Chem. Eng*. **2013**, *29*, 471–489.

[49] (a) Yuan, W.; Huang, J.; Xu, X.; Wang, L.; Tang, X-Y. *Org. Lett*. **2021**, *23*, 7139−7143.(b) Yang, M.; Cao, T.; Xu, T.; Lao, S. *Org. Lett*. **2019**, *21*, 8673–8678. (c) Kibriya, G.; Mondal, S.; Hajra, A. *Org. Lett*. **2018**, *20*, 7740–7743. (d) Liu, B.;Lim, C-H.; Miyake, G. M. *J. Am. Chem. Soc*. **2017**, *139*, 13616–13619. (e) Uchikura, T.; Hara, Y.; Tsubono, K.; Akiyama, T. *Acs. Org. Inorg. Au*. **2021**, *1*, 23-28. (f) Gong, X.; Li, X.; Xie, W.; Wu, J.; Ye, S. *Org. Chem. Front*. **2019**, *6*, 1863–1867. (g) Lv, Y.; Luo, J.; Ma, Y.; Dong, Q.; He, L. *Org. Chem. Front*. **2021**, *8*, 2461–2467. (h) Li, G.; Yan, Q.; Gan, Z.; Li, Q.; Dou, X.; Yang, D. *Org. Lett*. **2019**, *21*, 7938-7942.

[50] (a) Yi, H.; Zhang, G.; Wang, H.; Huang, Z.; Wang, J.; Singh A. K.; Lei, A. *Chem. Rev*. **2017**, *117*, 9016–9085. (b) Xuan, J. Studer, A.; *Chem. Soc. Rev*. **2017**, *46*, 4329–4346. (c) Huang, H.-M.; Garduño-Castro, M. H.; Morrill, C.; Procter, D. J. *Chem. Soc. Rev*. **2019**, *48*,

4626–4638. (e) Zhang, Y.; Sun, K.; Lv, Q.; Chen, X.; Qu, L.; Yu, B. *Chin. Chem. Lett.* **2019**, *30*, 1361–1398.

[51] (a) Funk, M. O.; Isaac R.; N. Porter, A.; *J. Am. Chem. Soc.* **1975**, *97*, 12814; (b) Porter, N. A.; Funk, M. O.; *J. Org. Chem.* **1975**, *40*, 3614. (c) Sun, K.; Lv, Q.-Y.; Lin, Y.-W.; Yu, B.; He, W.-M. *Org. Chem. Front.* **2021**, *8*, 445–465. (d) Liao, J.; Yang, X.; Ouyang, L.; Lai, Y.; Huang, J.; Luo, R. *Org. Chem. Front.* **2021**, *8*, 1345–1363.

[52] (a) Chen, H.; Yan, Y.; Zhang, N.; Mo, Z.; Xu, Y.; Chen, Y. *Org. Lett.* **2021**, *23*, 376–381. (b) Wang, H.; Wu, Q.; Zhang, J-D.; Li, H-Y.; Li, H-X. *Org. Lett.* **2021**, *23*, 2078−2083. (c) Bai, J.; Yan, S.; Zhang, Z.; Guo, Z.; Zhou, C-Y. *Org. Lett.* **2021**, *23*, 4843−4848. (d) Yang, R.; Yi, D.; Shen, K.; Fu, Q.; Wei, J.; Lu, J.; Yang, L.; Wang, L.; Wei, S.; Zhang, Z. *Org. Lett.* **2022**, *24*, 2014−2019. (e) Cheng, Q.; Zhang, F.; Chen, X.; Han, Y.; Yan, C.; Shi, Y.; Hou, H.; Zhu, S. *Org. Lett.* **2022**, *24*, 2515−2519.

[53] (a) Huang, A-X.; Zhu, H-L.; Zeng, F-L.; Chen, X-L.; Huang, X-Q.; Qu, L-B.; Yu, B. *Org. Lett.* **2022**, *24*, 3014−3018. (b) Zhai, Y-L.; Zhou, H.; Liu, Q-Q.; Leng, B-R.; Zhang, Z.; Li, J-Z.; Wang, D-C.; Zhu, Y-L. *Chem. Commun.* **2022**, *58*, 5112–5115. (c) Li, L.; Li, J-Z.; Sun, Y-B.; Luo, C-M.; Qiu, H.; Tang, K.; Liu, H.; Wei, W-T. *Org. Lett.* **2022**, *24*, 4704−4709. (d) Upreti, G. C.; Singh, T.; Ranjan, S.; Gupta, R. K.; Singh, A. *ACS Omega* **2022**, *7*, 29728−29733. (e) Liu, Q.; Mei, Y.; Wang, L.; Ma, Y.; Li, P.; *Adv. Synth. Catal.* **2020**, *362*, 5669–5680. (f) Yang, W.; Yang, S.; Li, P.; Wang, L. *Chem. Commun.* **2015**, *51*, 7520—7523. (g) Qian, P.; Deng, Y.; Mei, H.; Han, J.; Zhou, J.; Pan, Y. *Org. Lett.* **2017**, *19*, 4798−4801.

[54] (a) Guo, W.; Zhao, M.; Tan, W.; Zheng, L.; Tao, K.; Liu, L.; Wang, X.; Chen, D.; Fan, X. *J. Org. Chem.* **2018**, *83*, 1402−1413. (b) Guo, W.; Tao, K.; Zheng, L.; Zhao, M.; Tan, W.; Cai, L.; Xie, Z.; Chen, D.; Fan, X. *J. Org. Chem.* **2019**, *84*, 6448−6458. (c) Monga, A.; Bagchi, S.; Soni, R. K.; Sharma, A. *Adv. Synth. Catal.* **2020**, *362*, 2232–2237.

CHAPTER-II

Visible-Light-Mediated Difunctionalization of Alkynes: Synthesis of *β*-Substituted Vinylsulfones Using *O*–and *S*–Centered Nucleophiles

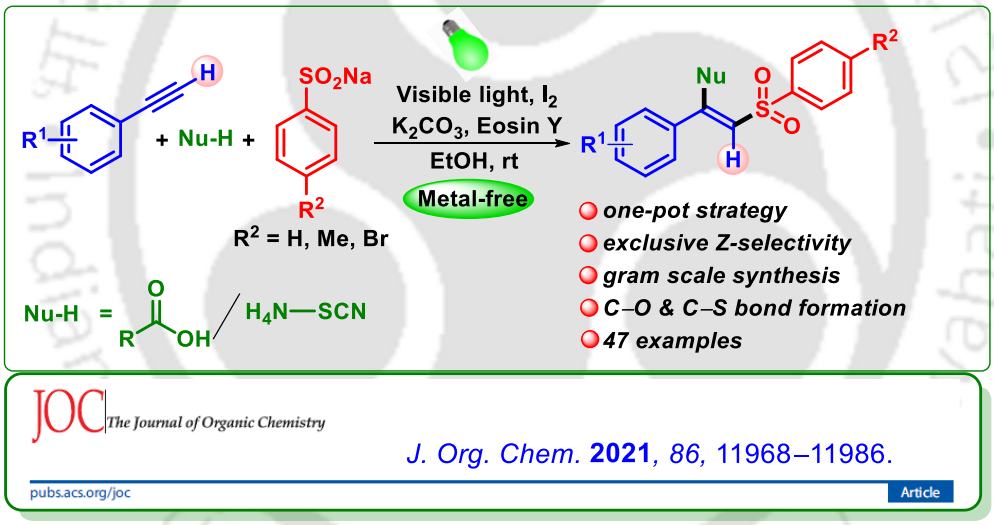

Abstract: *An inimitable illustration of a green-light-induced, regioselective difunctionalization of terminal alkyne has been disclosed using sodium arylsulfinates and carboxylic acids in the presence of eosin Y as the photocatalyst. The present methodology is further demonstrated by employing NH_4SCN as S–centered nucleophile instead of carboxylic acid.*

भारतीय प्रौद्योगिकी संस्थान गुवाहाटी
Indian Institute of Technology Guwahati

CHAPTER II

Visible-Light-Mediated Difunctionalization of Alkynes: Synthesis of *β*-Substituted Vinylsulfones Using *O*– and *S*–Centered Nucleophiles

II.1. Introduction:

Alkynes are well-established building blocks in organic synthesis which are useful due to their efficient transformation into other functionalities.[1] In recent years, direct di-functionalization of alkynes has grabbed the attention of chemists, in which simultaneous introduction of two functional groups provides either a tri- or a tetra-substituted alkene depending on whether the alkyne is terminal or internal.[2] Alkenes having multiple substituents are prevalent in many bioactive molecules, natural products, and pharmaceuticals, *viz*. tamoxifen, doxepin, etc. Hence, the development of a newer methodology for their synthesis is still in demand and chemists always dreamed of developing efficient and suitable methods for their synthesis.[3] Multi-component reactions (MCRs) are popular because they allow the construction of multifaceted structures starting from simple substrates. In this context, MCR has been recognized as a transformative tool, which not only increases efficiency and productivity but also reduces the cost and environmental impact.[4] Unlike alkenes, the application of MCRs to the difunctionalization of alkynes is not well explored. Moreover, alternative approaches require the use of organometallic species and multistep transformations. Therefore, it is desirable to develop a general, efficient and practical method for the difunctionalization of terminal alkynes.[5] Mechanistically, a general reaction pathway is suggested, in which the reaction proceeds via the radical addition to an alkyne to form a vinylic radical, which is then coupled with another radical partner to form a substituted alkene. Generally, the vinyl radical is much more reactive, so it is prone to hydrofunctionalization via a H-atom abstraction, causing serious problems in developing radical-based alkyne difunctionalization.[6] However, difunctionalization can be achieved under a condition that suppresses the H-abstraction capturing the other radical partners.[7] Due to the high reactivity of radicals they are not always as selective as initially designed.[8a,b] Due to the importance of *Z*-alkenes there are well-

established methods for their synthesis *viz*. Wittig reaction,[8c] catalytic alkynes hydrogenation,[8d] and Negishi coupling.[8e] Normally, a transition metal is essential to attain selectivity in difunctionlization protocol. Hence, the synthetic approach to *Z*-alkenes via a radical addition under a transition metal-free condition is very intriguing.[9] Nowadays, sulfonylation has gained a unique reputation as the sulfur-containing compounds have remarkable biological activity, pharmaceutical importance, and synthetic utility. For instance, K11777 (I) is a well-known cysteine protease inhibitor, and sulfone (II) is a Nrf activator, which has the potential for curing Parkinson's disease. There is a class of anti-HIV reverse transcriptase inhibitors (III) having both indole moiety and sulfonyl group (Figure II.1).[10]

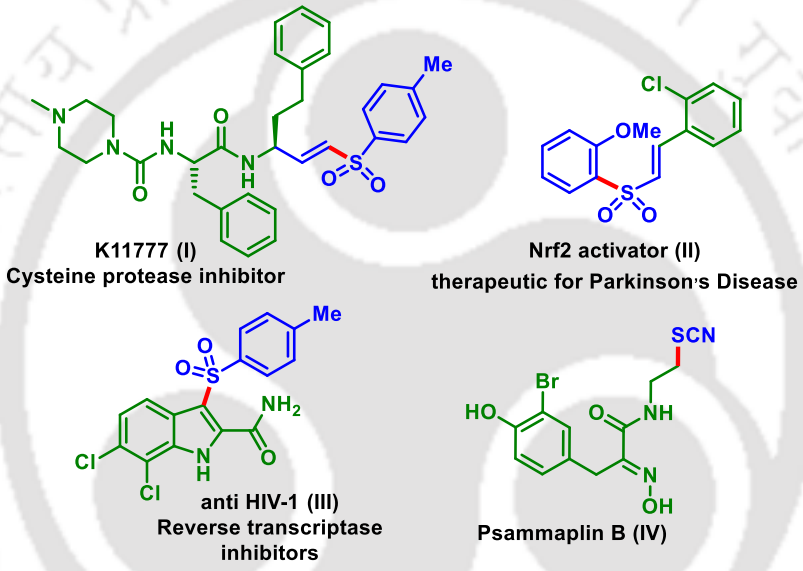

Figure II.1. *Bioactive compounds containing vinyl sulfones and thiocyanate group.*

Vinyl sulfones are utilized as expedient synthons in many reactions. Besides this, sulfones are good leaving groups that often show unique chemical reactivity.[11] Thus, a variety of organic transformations are possible using the sulfonyl group, so aptly described as a chemical chameleon by Trost.[11c] In this context, the development of a newer methodology for the synthesis of such molecules is deemed worthy of investigation.[12] Recently, visible-light-mediated functionalizations have emerged as a significant tool in contemporary organic chemistry. Much of the potential of visible-light photoredox catalysis focuses on its ability to accomplish exotic bond formations that are not possible using conventional approaches. However, most organic compounds do not absorb visible light efficiently, which has limited the application of photochemical synthesis. Therefore, photocatalysts, usually transition-

metal complexes of Ir, Ru and organic dyes, are often utilized to sensitize organic molecules.[13,14] The employment of organic dyes such as Rose Bengal, eosin Y, and eosin B as photo-catalysts has proven to be a practical, greener, and better alternative due to their low cost, less toxicity and at times superior reactivity compared to transition metal-based photoredox catalysts. In particular, eosin Y is used as a photoredox catalyst in several radical-based organic transformations.[14]

II.2. Ideas Toward the Synthesis of *β*-Substituted Vinylsulfones

Owing to the omnipresence of sulfones in both biological and pharmaceuticals, several methods have been implemented for the difunctionalization of alkynes. Some of the strategies are demonstrated below. In this context, Nakamura *et al*. in 2011 established an elegant method in which terminal alkynes react with aromatic sulfonyl chlorides in the presence of an iron(II) catalyst and a phosphine ligand to give (*E*)-*β*-chlorovinylsulfones with 100% regio- and stereoselectivity. Various functional groups, such as chloride, bromide, iodide, nitro, ketone, and aldehyde, were well tolerated under these reaction conditions (Scheme II.1).[15a]

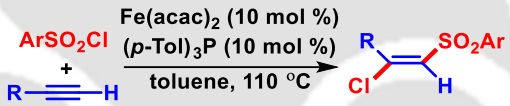

Scheme II.1. *Iron-catalyzed synthesis of (E)-β-chlorovinylsulfones.*

Jiang *et al*. in 2014 developed an efficient NBS-promoted method for the synthesis of (*E*)-*β*-halo vinyl sulfones via a multi-component approach. The present metal-free protocol achieved the halosulfonylation of terminal alkynes with high selectivity in an environmentally friendly manner which makes it noteworthy over other difunctionalization strategies (Scheme II.2).[15b]

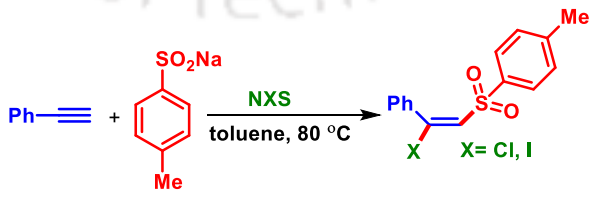

Scheme II.2. *NXS-promoted synthesis of (E)-β-halovinylsulfones.*

Bi *et al*. in 2017 reported a silver-catalyzed intermolecular aminosulfonylation of terminal alkynes with sodium sulfinates and $TMSN_3$ through a sequential hydroazidation of the terminal alkynes, and the addition of a sulfonyl radical to the resultant vinyl azide. A wide range of arylacetylene-bearing electron-donating, as well as electron-withdrawing groups, were well tolerated in this protocol (Scheme II.3).[15c]

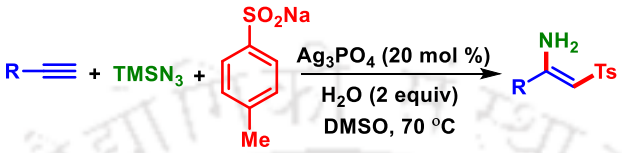

Scheme II.3. *Silver-catalyzed aminosulfonylation of terminal alkynes.*

Recently, Kumar *et al*. demonstrated an elegant method for the stereoselective sulfur-nitrogen difunctionalization (aminosulfonylation) across the alkynes framework in a multi-component fashion using sodium sulfinates and azoles, in the presence of I_2/base. This strategy is applicable to a variety of terminal alkynes, sodium sulfinates, and azoles as the reaction partners, affording the (*Z*)-*β*-amino vinyl sulfones in good yields (Scheme II.4).[15d]

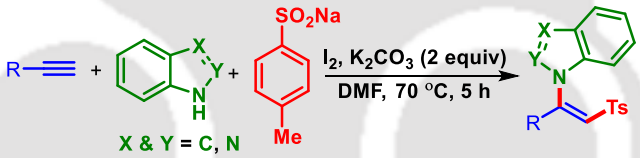

Scheme II.4. *Metal-free aminosulfonylation of terminal alkynes.*

Cai *et al*. reported an efficient method for the synthesis of *β*-ketosulfone using phenylacetylene and sulfonyl hydrazide as the reacting partners in the presence of $Ru(bpy)_3Cl_2$ as the photocatalyst. The protocol has tolerated a broad range of functional groups and provided a wide range of *β*-ketosulfones in good yields (Scheme II.5).[15e]

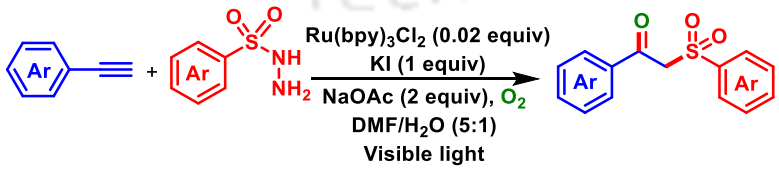

Scheme II.5. *Visible-light-mediated synthesis of β-keto sulfones.*

Cho *et al.* in 2013 demonstrated an elegant method for the controlled trifluoromethylation of terminal alkynes using iodotrifluoromethane as the reacting partner. Notably, excellent *E*/*Z*

stereoselectivity was obtained with the selective formation of the *E*-isomers, especially in reactions of phenylacetylene derivatives. Moreover, phenylacetylenes bearing electron-donating as well as electron-withdrawing groups were well tolerated in this protocol. The choice of the base was vital for this process, as the base acts not only as a reductive quencher of the activated photocatalyst but also as a hydrogen donor (Scheme II.6).[15f]

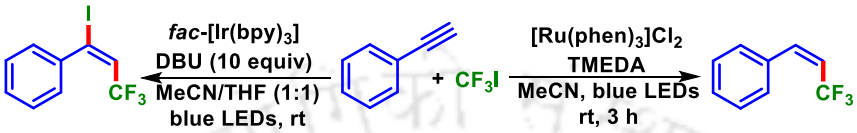

Scheme II.6. *Visible-light-mediated controlled trifluoromethylation of terminal alkynes.*

In 2017, Nevado *et al*. reported a method for the carbosulfonylation of alkynes via a multi-component approach giving tri-substituted alkenes. The present difunctionalization protocol used aryl boronic acid, and aryl sulfonyl chlorides as the reacting partners. The protocol has tolerated a broad range of functional groups (Scheme II.7).[16]

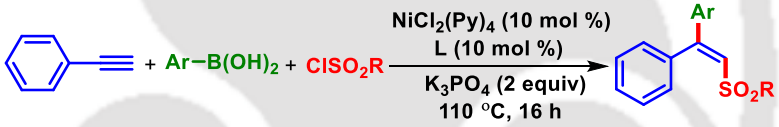

Scheme II.7. *Carbosulfonylation of terminal alkynes.*

In 2018, Han *et al*. demonstrated an elegant visible light-mediated chlorosulfonylation of alkynes in the presence of *fac*-Ir(bpy)$_3$ photoredox catalyst under blue light irradiation. A variety of commercially available aryl sulfonyl chlorides were well-tolerated in this protocol. Both terminal, as well as internal alkynes, underwent a smooth reaction (Scheme II.8).[17]

Scheme II.8. *Visible-light-mediated halo sulfonylation of alkynes.*

The existing literature revealed that sulfonyl radical can be generated both in thermal as well as under photochemical conditions which adds to the alkyne and generates a vinyl sulfone intermediate that could be functionalized to achieve the difunctionalization.

Taking cues from the above-mentioned literature, we anticipated that *β*-iodo sulfonyl intermediate can be generated *in situ* using I_2 under metal-free conditions, and that could be replaced by an appropriate nucleophile to make the difunctionalization strategy successful (Scheme II.9).[18]

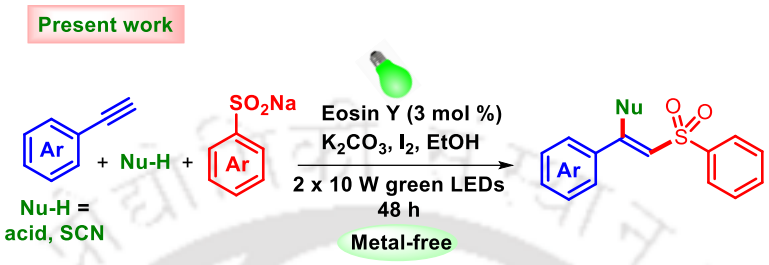

Scheme II.9. *Visible-light-mediated difunctionalization of terminal alkynes.*

II.3. Present Work

To synchronize our assumption, we initiated a reaction between phenylacetylene (**1**, 1 equiv), sodium *p*-tolylsulfinate (**b′**, 1 equiv), and *p*-toluic acid (**b**, 1.5 equiv) in the presence of K_2CO_3 (2 equiv), I_2 (1 equiv), eosin Y (3 mol %), in methanol (2 mL) under the irradiation of 20 W (2 x 10) green LEDs at room temperature. To our delight, a new product containing an ester and a tosyl moiety was isolated in a 30% yield. The spectroscopic analysis (^{1}H and ^{13}C{^{1}H} NMR) revealed the structure of the product to be *Z*-*β*-carboxy vinylsulfone (**1bb′**). Further, the X-ray crystallography of one of its derivatives (**1db′**) re-confirmed its structure and the *Z*-geometry (Figure II.2).

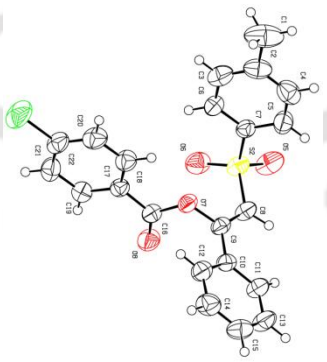

Figure II.2. *ORTEP diagram of (**1db′**) with 40% ellipsoid probability (CCDC 2057146).*

Although phenylacetylene (**1**) got fully consumed, the formation of *β*-keto sulfone, *β*-iodo alkenyl sulfone, and a minor amount of phenylacetylene dimer as the side products reduced the yield of the desired product (**1bb′**). This method has certain merits over existing reports

such as the use of inexpensive organic dye as a photocatalyst, one-pot strategy, and broad substrate scope due to *in situ* replacement of the halo group with appropriate nucleophiles. Usually, transition metal catalysts are required for the difunctionalization of alkynes but herein visible light-mediated, metal-free, the multi-component approach is articulated for the difunctionalization of terminal alkynes. To the best of our knowledge, this is the unique report on the visible light-mediated difunctionalization of alkynes using sodium sulfinate salts as the aryl sulfonyl source, carboxylic acids, and ammonium thiocyanate as the *O*–and *S*–centered nucleophiles (Scheme II.9). [18]

Optimization of Reaction Conditions

Inspired by this metal-free protocol, further operational parameters were screened to maximize the product yield. For this, phenylacetylene (**1**), sodium *p*-tolylsulfinate (**b′**), and *p*-toluic acid (**b**) were chosen as the reacting components. Initially, various inorganic bases were screened and K_2CO_3 was found to be optimal compared to other bases such as Na_2CO_3 (25%), Cs_2CO_3 (20%), KOH (15%), and NaOH (18%) (Table II.1, entries 2–5). The reaction was extremely sluggish in the absence of base and the product (**1bb′**) was isolated in a suppressed yield (< 10%) (Table II.1, entry 6). This suggests that the base is indispensable for the present difunctionalization protocol. The use of fewer than 2 equiv of base resulted in poor conversion, but an excess amount of base led to the formation of *β*-keto sulfone as the side product via a hydrolytic path. Next, different solvents were tested to enhance the product yield. The use of CH_3CN instead of MeOH gave a 25% yield (Table II.1, entry 7), whereas, DMSO (12%), and DMF (15%), gave a comparatively lesser yield of the product (**1bb′**) (Table II.1, entries 8 and 9). Interestingly, an improved yield of 40% was obtained when protic solvent such as EtOH was used (Table II.1, entry 10). Switching the catalytic system from eosin Y to Rose Bengal and transition metal complex $[Ru(bpy)_3]PF_6$, failed to improve the product yield beyond 25% (Table II.1, entries 11 and 12). Therefore, further optimizations were carried out using eosin Y. Other iodine-based reagents were also tested in the hope to get a satisfactory yield. The use of KI (20%) and TBAI (35%) as oxidants gave a lower yield of the product (Table II.1, entries 13 and 14). "*When $K_2S_2O_8$ was used no product formation was observed which confirms the role of iodine as an iodinating agent.*" (Table II.1, entry 15).

Table II.1. *Optimization of the reaction conditions*[a–e]

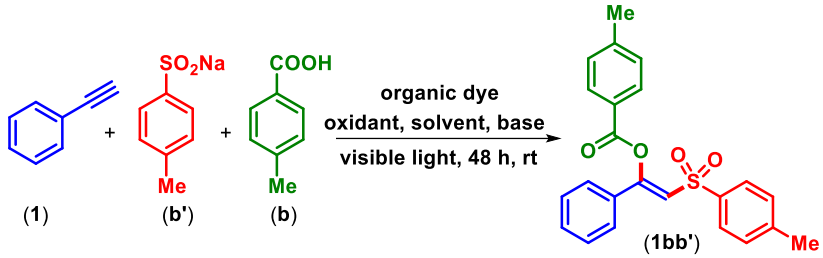

entry	photocatalyst(mol %)	base (equiv)	oxidant (equiv)	solvent	yield[b] (%)
1	Eosin Y (2)	K_2CO_3 (2)	I_2 (1)	MeOH	30
2	Eosin Y (2)	Na_2CO_3 (2)	I_2 (1)	MeOH	25
3	Eosin Y (2)	Cs_2CO_3 (2)	I_2 (1)	MeOH	20
4	Eosin Y (2)	KOH (2)	I_2 (1)	MeOH	15
5	Eosin Y (2)	NaOH (2)	I_2 (1)	MeOH	18
6	Eosin Y (2)	-	I_2 (1)	MeOH	<10
7	Eosin Y (2)	K_2CO_3 (2)	I_2 (1)	CH_3CN	25
8	Eosin Y (2)	K_2CO_3 (2)	I_2 (1)	DMSO	12
9	Eosin Y (2)	K_2CO_3 (2)	I_2 (1)	DMF	15
10	Eosin Y (2)	K_2CO_3 (2)	I_2 (1)	EtOH	40
11	Rose Bengal (2)	K_2CO_3 (2)	I_2 (1)	EtOH	25
12	$[Ru(bpy)_3]PF_6$ (2)	K_2CO_3 (2)	I_2 (1)	EtOH	20
13	Eosin Y (2)	K_2CO_3 (2)	KI (1)	EtOH	20
14	Eosin Y (2)	K_2CO_3 (2)	TBAI (1)	EtOH	35
15	Eosin Y (2)	K_2CO_3 (2)	$K_2S_2O_8$ (1)	EtOH	n.d.[c]
16	Eosin Y (3)	K_2CO_3 (2)	I_2 (1)	EtOH	70
17	Eosin Y (4)	K_2CO_3 (2)	I_2 (1)	EtOH	72
18	Eosin Y (3)	K_2CO_3 (2)	I_2 (0.5)	EtOH	45
19	Eosin Y (3)	K_2CO_3 (2)	I_2 (1.5)	EtOH	69
20	Eosin Y (3)	K_2CO_3 (2)	I_2 (1)	EtOH	35[d]
21	Eosin Y (3)	K_2CO_3 (2)	I_2 (1)	EtOH	30[e]
22	-	K_2CO_3 (2)	I_2 (1)	EtOH	n.d.

23	Eosin Y (3)	K_2CO_3 (2)	-	EtOH	n.d.

[a]Reaction conditions: **1** (0.15 mmol), **b** (1.5 equiv), **b′** (1 equiv), catalyst (mol %), base (equiv), and oxidant (equiv) in 2 mL solvent with a 2 x 10 W green LEDs irradiation at room temperature. [b]Yield of isolated product. [c]n.d. = Not detected. [d]Reaction performed using 10 W (430 nm) blue LEDs light. [e]Reaction performed using 10 W white LEDs light.

To further improve the yield, the loadings of eosin Y and iodine were varied. At 3 mol % eosin Y loading, 70% yield of the desired product was obtained (Table II.1, entry 16). Whereas, further increment (4 mol %) led to no significant change in the yield of the product (Table II.1, entry 17). A satisfactory yield was obtained using 1 equivalent of iodine (Table II.1, entries 18, and 19). Since the iodine is serving as an iodinating agent, so the use of less than one equivalent of iodine led to poor conversion. However, a higher loading of iodine (1.5 equiv) was also not beneficial. The wavelength and intensity of the visible light can affect the rate of photochemical reactions. Thus, the reaction was carried out using (2 x 10 W) blue LEDs (430 nm) and (2 x 10 W) white LEDs (Table II.1, entries 20, and 21). As can be seen, previously used (2 x 10 W) green LEDs (513 nm) provided superior result (Table II.1, entry 16). The intensity of the blue light is indeed higher than the green light. The excitation maxima of eosin Y in a basic ethanolic solution was measured and found to be 542 nm, which perfectly overlaps in the green region (490–570 nm), and the green LED used had a wavelength of 513 nm. Thus, the green light is a better choice for the excitation of eosin Y which also minimalizes the formation of side products by avoiding the decomposition of iodine compared to LEDs of lower wavelength (higher energy). Control experiments suggest that both the catalyst and iodine are essential for this reaction (Table II.1, entry 22 and 23). The eosin Y is indispensable for this reaction as it suppresses the other competing paths such as hydrofunctionalization and reaction with molecular oxygen to produce *β*-keto sulfone product. The surrounding reaction temperature was maintained at room temperature (~28 ^{o}C), by using a fan near the reaction flask thereby confirming the photochemical nature of this protocol (Figure II.3).

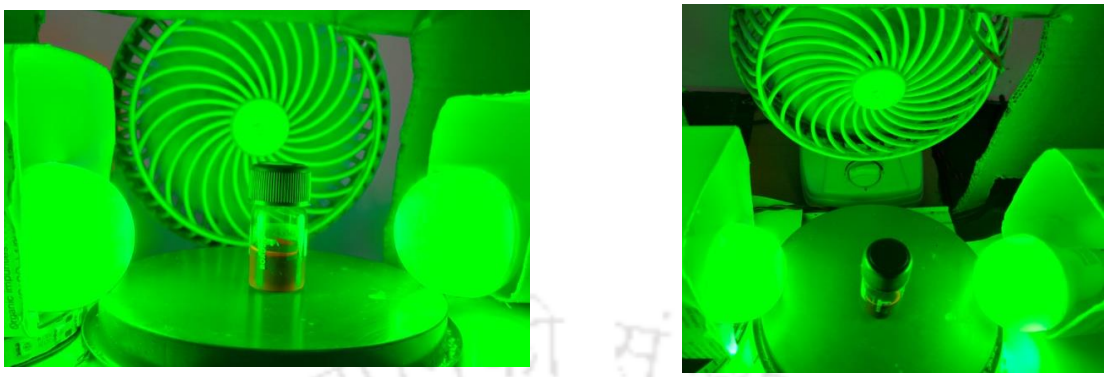

Figure II.3. *Photochemical reaction Set-up (a) Front view (b) Top view*

Substrate Scope for β-Substituted Vinyl Sulfone

With the optimized condition in hand, this protocol was subsequently applied for the difunctionalization of various substituted phenyl acetylenes using substituted benzoic acids and sodium *p*-tolylsulfinate as the reacting partners. At first, the scope of different benzoic acids (**a-u**) was tested with phenylacetylene (**1**) and sodium *p*-tolyl sulfinate (**b′**) (Scheme II.10). As can be seen from Scheme II.10, a range of substituted benzoic acids bearing electron-donating as well as electron-withdrawing groups reacted smoothly with (**1**) and (**b′**) to afford the desired difunctionalized products (**1ab′-1ub′**) in moderate yields (Scheme II.10). Benzoic acid (**a**) and its derivatives bearing electron-donating substituents such as *p*-Me (**b**), *p*-OMe (**c**), reacted smoothly and afforded their corresponding products (**1ab′**, 68%), (**1bb′**, 70%), and (**1cb′**, 74%). The reaction also worked effectively with benzoic acids bearing electron-withdrawing substituents, such as *p*-Cl (**d**), *p*-Br (**e**), and afforded their desired products (**1db′**, 62%), and (**1eb′**, 64%) but in inferior yields compared to substrates having electron-donating substituents. This may be due to the enhanced nucleophilicity of substituted benzoic acids which is driven by the +I and +R effect of the electron-donating groups.

Scheme II.10. *Scope of (Z)-β-carboxy vinylsulfones with different acids*[a,b]

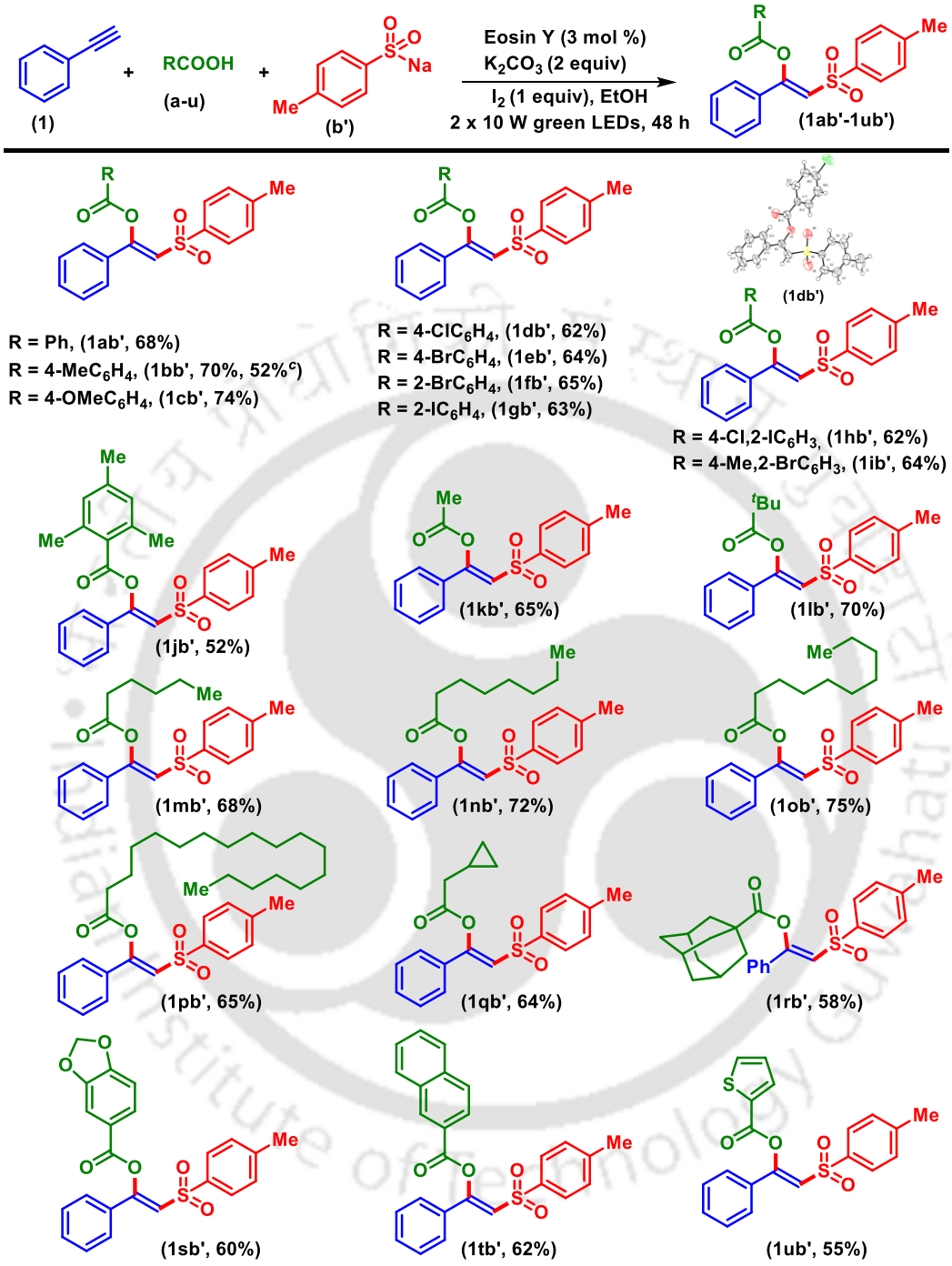

[a]Reaction conditions: **1** (0.5 mmol), **a-u** (0.75 mmol), **b'** (0.5 mmol), I_2 (0.5 mmol), K_2CO_3 (1 mmol), eosin Y (3 mol %) in 2 mL ethanol, 2 x 10 W green LEDs. [b]Isolated yield. [c]10 mmol scale.

The use of *o*-substituted benzoic acids, *viz.*, *o*-Br (**f**), and *o*-I (**g**) afforded their corresponding *Z*-*β*-carboxy vinylsulfones (**1fb′**, 65%) and (**1gb′**, 63%) (Scheme II.10). Apart

from the mono-substituted carboxylic acids, di- and tri-substituted benzoic acids (**h-j**) were also employed and the desired products (**1hb′**, 62%), (**1ib′**, 64%), and (**1jb′**, 52%) were isolated in moderate yields. The aliphatic carboxylic acids such as acetic acid (**k**), pivalic acid (**l**), hexanoic acid (**m**) and saturated fatty acids such as octanoic acid (**n**), capric acid (**o**) and stearic acid (**p**) all reacted efficiently giving their *Z*-*β*-carboxy vinylsulfones (**1kb′**), (**1lb′**), (**1mb′**), (**1nb′**), (**1ob′**) and (**1pb′**) in 65%, 70%, 68%, 72%, 75% and 65% yields, respectively (Scheme II.10). Similarly, cyclopropylacetic acid (**q**) and 1-admantanecarboxylic acid (**r**) gave their expected *Z*-*β*-carboxy vinylsulfones **1qb′** (64%) and **1rb′** (58%). Moderate yields of the products **1sb′** (60%), **1tb′**, 62%), and **1ub′** (55%) were obtained when polyaromatic carboxylic acids *viz*. piperonylic acid (**s**), 2-napthanoic acid (**t**), and heteroaromatic acid such as thiopene 2-carboxylic acid (**u**) were reacted under the optimized conditions.

Scheme II.11. *Scope of (Z)-β-carboxy vinyl sulfones with different alkynes*[a,b,c]

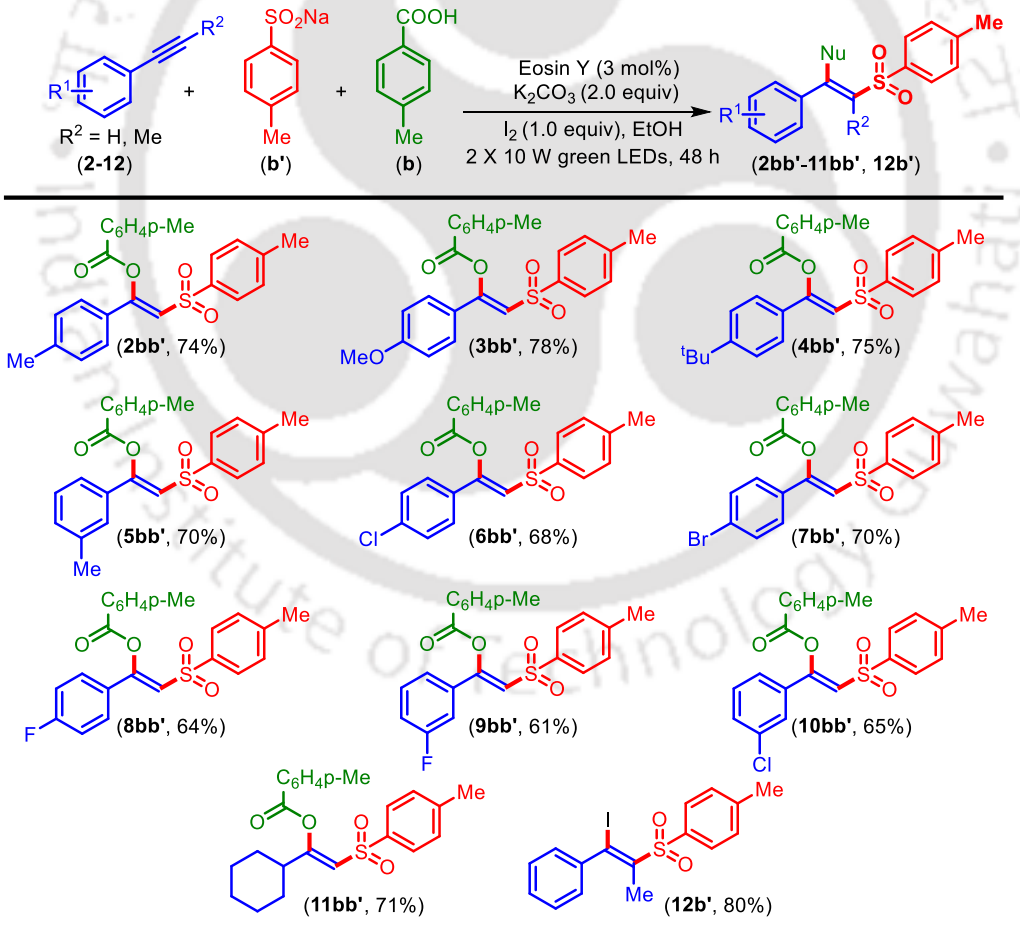

[a]Reaction conditions: **2-12** (0.5 mmol), **b** (0.75 mmol), **b′** (0.5 mmol), I_2 (0.5 mmol), K_2CO_3 (1 mmol), eosin Y (3 mol %), ethanol (2 mL) in 2 x 10 W green LEDs. [b]Isolated yield. [c]Under unoptimized condition.

Next, the scope of this methodology was extended by reacting a variety of terminal alkynes (**2-11**) with *p*-toluic acid (**b**) and sodium *p*-tolylsulfinate (**b′**) and the results are summarized in Scheme II.11. Phenyl acetylenes bearing electron-donating and electron-withdrawing substituent in the phenyl ring (**2-11**) underwent efficient reaction with *p*-toluic acid (**b**) and sodium *p*-tolylsulfinate (**b′**) giving their respective *Z*-*β*-carboxy vinylsulfones (**2bb′-11bb′**) in good to moderate yields (61-78%). Phenyl acetylenes bearing electron-donating substituents such as *p*-Me (**2**), *p*-OMe (**3**), and *p*-^{t}Bu (**4**), *m*-Me (**5**) afforded their corresponding products **2bb′** (74%), **3bb′** (78%), **4bb′** (75%) and **5bb′** (70%) in moderate yields. Next, a series of phenyl acetylenes bearing electron-withdrawing substituents such as *p*-Cl (**6**), *p*-Br (**7**), *p*-F (**8**), *m*-F (**9**), and *m*-Cl (**10**) were reacted and all gave their anticipated products **6bb′** (68%), **7bb′** (70%), **8bb′** (64%), **9bb′** (61%) and **10bb′** (65%) in acceptable yields. Moderate yield of the product **11bb′** (71%) was obtained when cyclohexyl acetylene was reacted under the optimized condition (Scheme II.11). After successfully synthesizing a library of *Z*-*β*-carboxy vinylsulfones using terminal alkynes, we were curious to know the fate of reaction with internal alkyne (**12**). Unlike terminal alkynes, the internal alkyne provided *β*-iodo sulfone (**12b′**, 80%) under the present photochemical condition.

The generality of this method was further extended to various sodium arylsulfinates (**a′, c′-i′**) with terminal alkynes (**1**, **2**, **4**, **7**) and carboxylic acids {*p*-Me (**b**), *p*-OMe (**c**), *p*-Cl (**d**)} having different electronic effects. The electronically neutral sodium benzenesulfinate (**a′**) gave the anticipated *Z*-*β*-carboxy vinylsulfones **2ba′** (70%), **4ba′** (72%), and **7ba′** (68%) in good yields. The reaction also worked effectively with sodium 4-(*tert*-butyl)benzenesulfinate (**c′**) and provided the anticipated product (**1bc′**) in 74% yield. Similarly, sodium arylsulfinates having moderately electron-withdrawing substituents {*p*-Cl (**d′**), *p*-Br (**e′**)} underwent efficient reactions with phenylacetylene (**1**) and carboxylic acids {*p*-Me (**b**), *p*-OMe (**c**), *p*-Cl (**d**)} resulting in the corresponding products **1bd′** (66%), **1be′** (67%), **1ce′** (73%) and **1de′** (62%) in good yields (Scheme II.12). Next, sodium arylsulfinates bearing strong electron-withdrawing substituents such as *p*-NO_2 (**f′**) and 2-Br-4-CF_3 (**g′**) were tested

and the corresponding *Z*-*β*-carboxy vinylsulfones **1bf′** (58%) and **1bg′** (50%) were obtained in acceptable yields (Scheme II.12).

Scheme II.12. *Scope of (Z)-β-carboxy vinylsulfones with different sodium aryl sulfinates*[a,b]

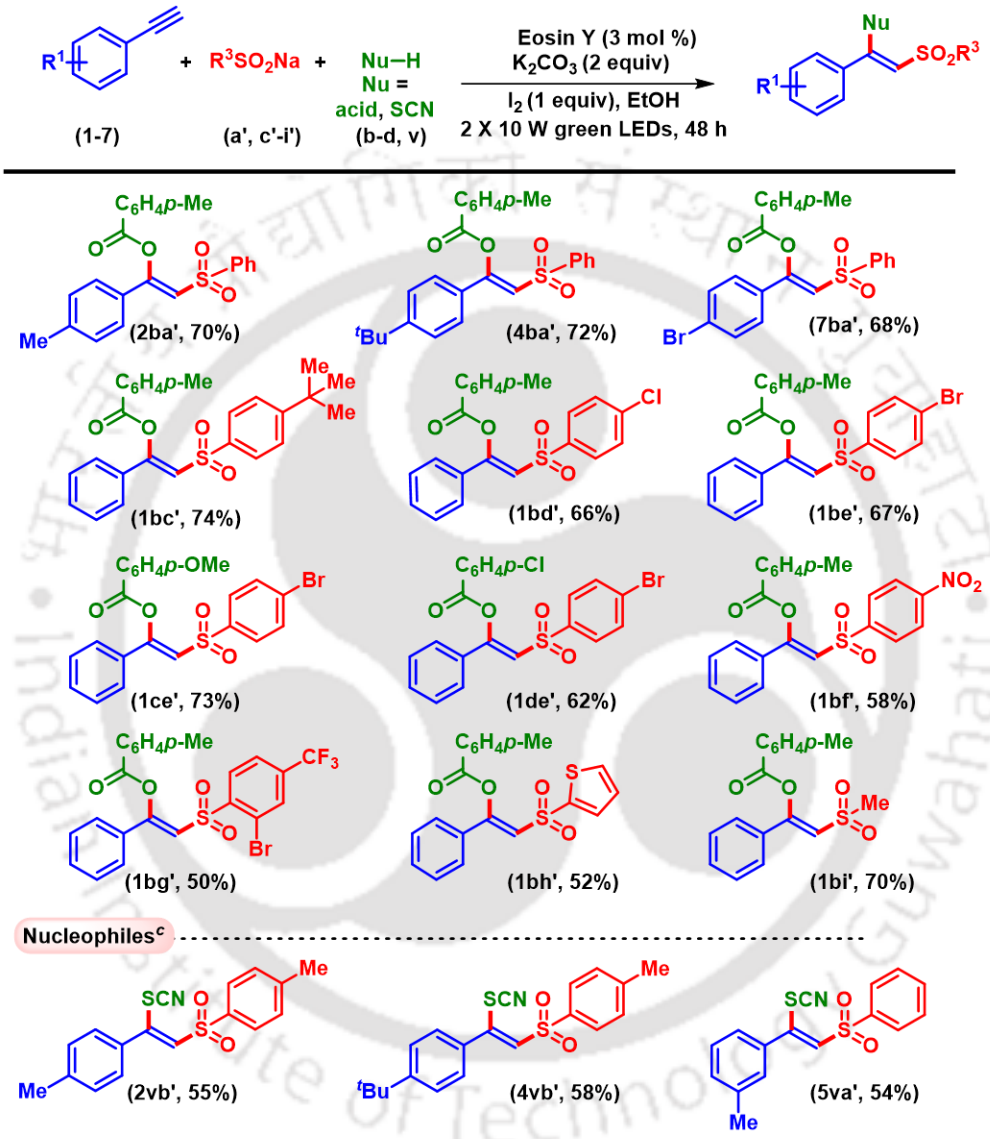

[a]Reaction conditions: **1-7** (0.5 mmol), **b-d, v** (0.75 mmol), **a′, c′-i′** (0.5 mmol), I_2 (0.5 mmol), K_2CO_3 (1 mmol), eosin Y (3 mol %), ethanol (2 mL) in 2 x 10 W green LEDs. [b]isolated yield. [c]Under unoptimized condition.

Apart from aryl substituents, both heteroaryl (**h′**) and sodium alkylsulfinate (**i′**) successfully yielded their anticipated products **1bh′** (52%) and **1bi′** (70%) under present

condition. Organic thiocyanates (RSCN) are potential synthetic intermediates, as the sulfur-containing compounds have remarkable bioactivity and synthetic utility.[10e] Thus, under the established reaction condition for carboxylic acid, NH_4SCN (**v**) was tested as a *S*-centered nucleophile to further expand the utility of the present protocol. Gratifyingly, –SCN was successfully employed and its difunctionalized products **2vb′**, **4vb′**, and **5va′** were obtained in 55%, 58%, and 54% yields, respectively (Scheme II.12).

Mechanistic Investigation

To study the electronic effect of the substituents, present on the phenylacetylene and benzoic acid, a few intermolecular competitive reactions were carried out. In our first experiment, an equimolar mixture of *p*-toluic acid (**b**), and *p*-chlorobenzoic acid (**d**) were reacted with phenylacetylene (**1**) and sodium *p*-tolylsulfinate (**b′**). The yield of the *p*-Me (**b**) substituted product (**1bb′**, 30%) was higher than *p*-Cl (**d**) product (**1db′**, 22%) which is evident from the yield pattern obtained in scheme II.13. The higher electron density at the carboxylate anion for substrate (**b**) having an electron-donating group (due to +I effect) makes it a better nucleophile thus, giving a higher yield of the product {Scheme II.13. (i)}. In the second experiment, an equimolar mixture of 4-ethynyltoluene (**2**), and 1-chloro-4-ethynylbenzene (**6**) were reacted with the *p*-toluic acid (**b**) and sodium *p*-tolylsulfinate (**b′**) under the standard conditions.

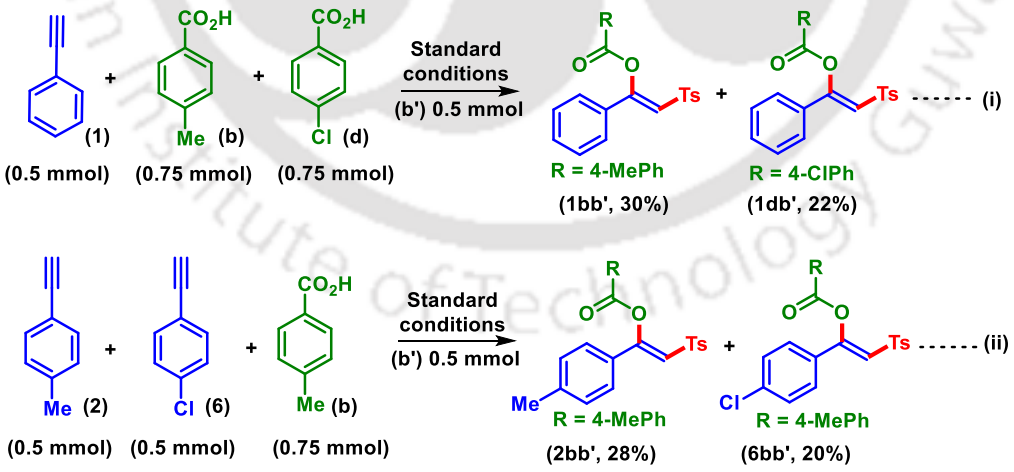

Scheme II.13. *Intermolecular competition experiments.*

It was observed that phenylacetylene having EDG shows better reactivity {Scheme II.13. (ii)}, which is also in agreement with the yield pattern found in Scheme 3. 4-ethynltoluene (**2**)

provided higher yields of the product which is due to the better stabilization of the intermediate vinyl radical formed.

To understand the mechanism of this transformation, systematic investigations were carried out based on some literature precedents.[17] To validate the radical nature of the reaction, two independent reactions were performed, one in the presence of 2,2,6,6-tetramethylpiperidine-1-oxyl (TEMPO, 2 equiv) and the other with 2,6-di-tertbutyl-4-methyl phenol (BHT, 2 equiv). In the case of TEMPO, no product was observed while BHT provided a < 10% yield of the product (**1bb′**), thereby suggesting the radical nature of the reaction {Scheme II. 14. (i)}. The BHT adduct (**M**) with sodium *p*-tolylsulfinate (**b′**) was obtained in 65% yield which was further characterized by NMR and HRMS analysis. The iodo intermediate (**B**) was identified by the HRMS analysis of the reaction mixture. In a control experiment, the reaction of 1-((2-iodo-2-phenylvinyl)sulfonyl)-4-methylbenzene (**B**) with *p*-toluic acid (**b**)/K_2CO_3 {Scheme II.14 (ii)} both in the presence and absence of light yielded the identical product **1bb′**. However, a slight reduction (12%) in the yield was observed in the absence of light, thereby suggesting a positive influence of light for this addition-elimination step, which is possibly due to the facile cleavage of the C–I bond in the presence of light.[19]

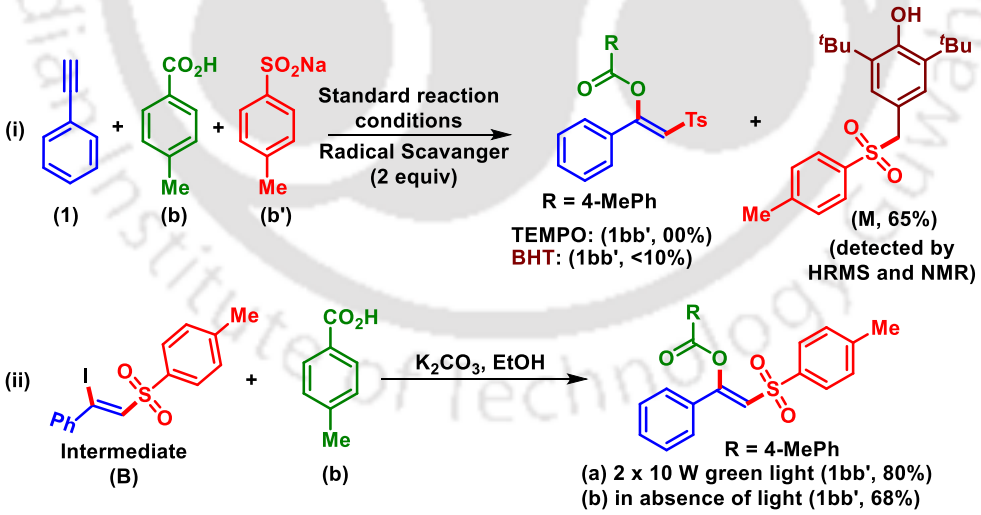

Scheme II.14. *Control experiments.*

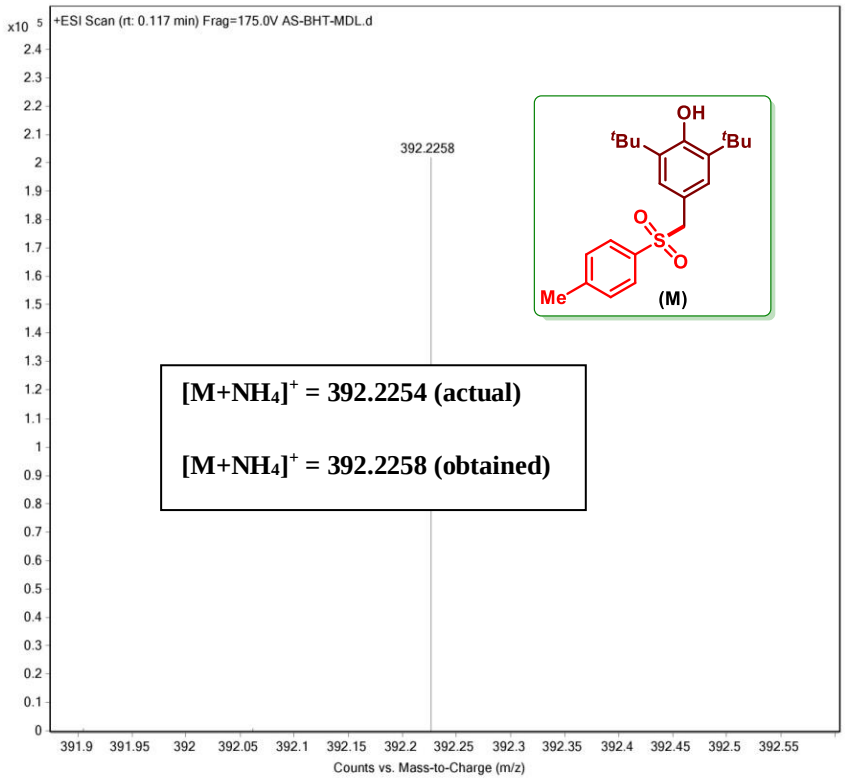

Figure II.4. *HRMS spectra of BHT adduct (**M**).*

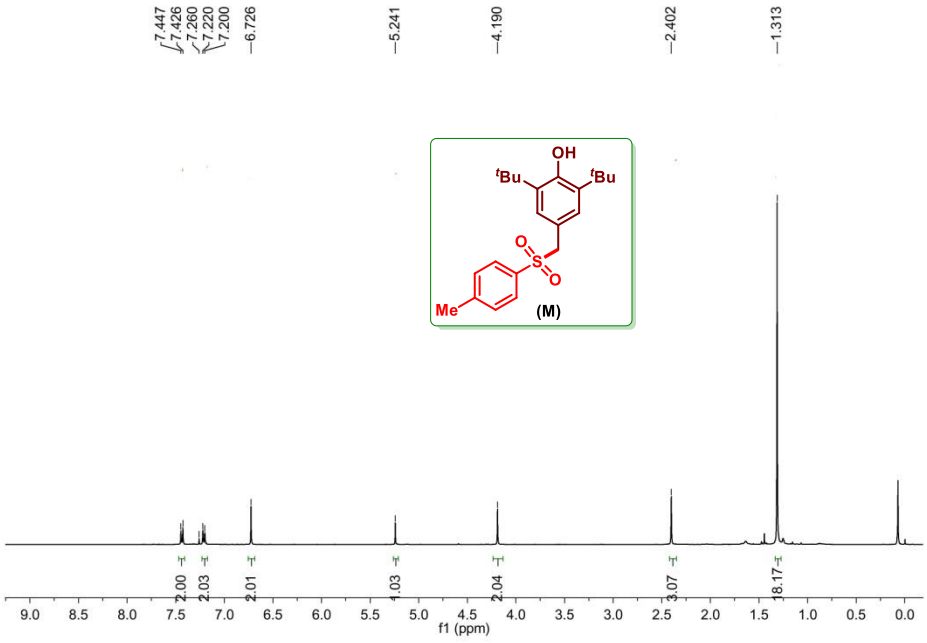

Figure II.5. *^{1}H NMR spectra of BHT adduct (**M**).*

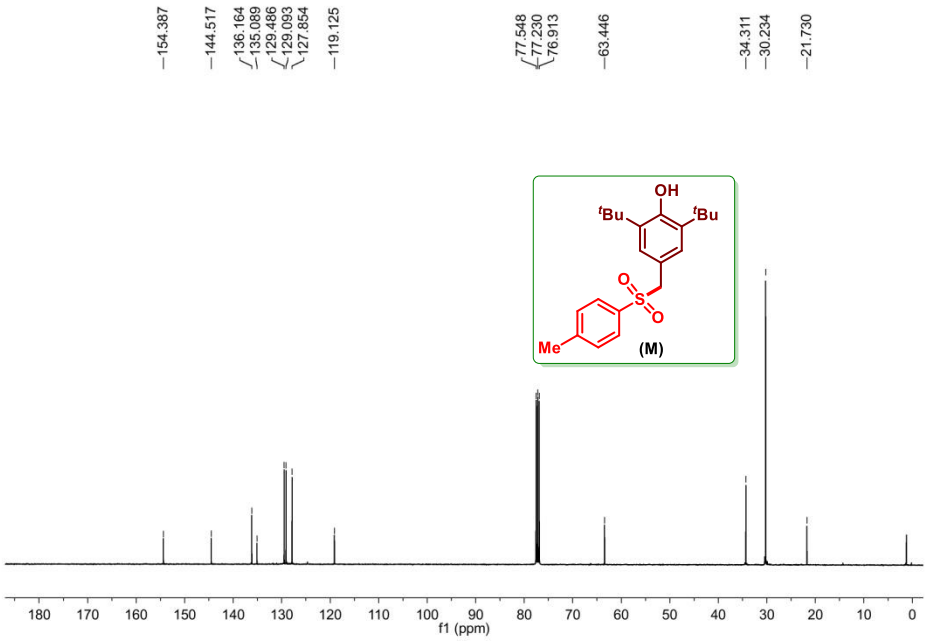

Figure II.6. *$^{13}C\{^{1}H\}$ HRMS spectra of BHT adduct (**M**).*

To further confirm the radical nature of this protocol, the Stern-Volmer fluorescence quenching experiment of eosin Y was performed using sodium *p*-toluene sulfinate (**b′**) as the quencher. Initially, the excitation and emission spectra of eosin Y was examined and fluorescence maximum was obtained at 534 nm when excited at 515 nm (excitation maximum of eosin Y). The peak at 534 nm gradually decreases on increasing the quencher concentration (5-35 mM) (Figure II.7). Similarly, a Stern-Volmer fluorescence quenching experiment was carried out using *in situ* generated RSO_2I obtained by mixing and stirring RSO_2Na and I_2 for 2 h. A better quenching pattern of the eosin Y was observed in the later case which suggests more facile electron transfer between the catalyst and the quencher RSO_2I as compared to that RSO_2Na {Figure II.7. (a, and b)}. With these data, the Stern-Volmer graph for both experiments was plotted using the equation $I_0/I_t = 1+K_{SV}[Q]$ where I_0 and I_t are integrated emission intensity in the absence and presence of quencher and Ksv are quenching constant. A linear quenching was observed in both the cases {Figure II.7. (c and d)}.

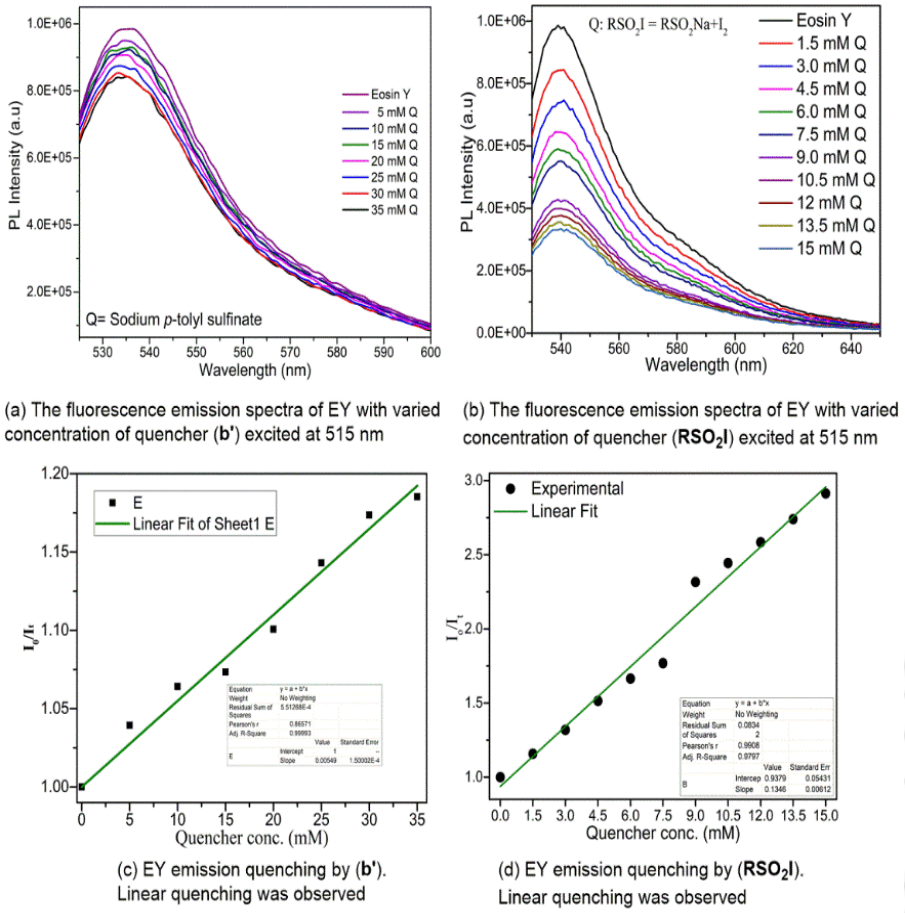

(a) The fluorescence emission spectra of EY with varied concentration of quencher (**b'**) excited at 515 nm

(b) The fluorescence emission spectra of EY with varied concentration of quencher (**RSO_2I**) excited at 515 nm

(c) EY emission quenching by (**b'**). Linear quenching was observed

(d) EY emission quenching by (**RSO_2I**). Linear quenching was observed

Figure II.7. *Stern-Volmer quenching experiments.*

These observations were further supported by redox potential values of the eosin Y and a mixture of sodium *p*-toluene sulfinate and iodine. The observed $E_{½\ red}$ value of RSO_2I species (RSO_2Na+I_2) was found to be -0.376 V vs SCE (-0.42 V vs Ag/AgCl sat. KCl) which is greater than the $E_{½\ oxd}$ value of $EY^{\bullet -}$ (-1.06 V vs SCE).[20a] A closer look at the CV graph of RSO_2I shows a small anodic peak at 0.357 V and a cathodic peak at 0.457 V which closely resembles the literature value of NaI (Figure II.8).[20b] This confirms that the formation of sulfonyl iodide was completed before the electric input started. For better understanding, the CV experiment of RSO_2Na was also recorded {Figure II.8 (b)}. The observed $E_{½\ red}$ value of RSO_2Na species was found to be -1.006 V vs SCE (-1.05 V vs Ag/AgCl sat. KCl) whereas, for RSO_2I species (RSO_2Na+I_2) $E_{½\ red}$ value was found at -0.376 V vs SCE (-0.42 V vs Ag/AgCl sat. KCl).Therefore, the species RSO_2I have a higher tendency to gain an electron from the EY radical anion compared to the RSO_2Na.

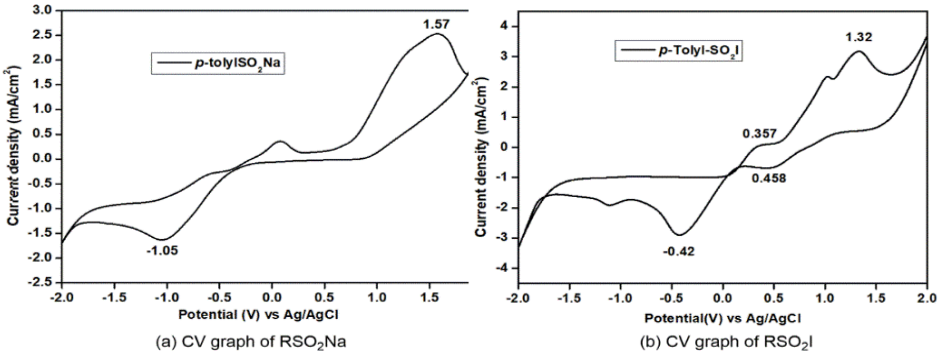

Figure II.8. *Cyclic voltammetry experiments.*

Based on the above experiments and previous reports, a plausible mechanism has been proposed in Scheme II.15.[21] In the presence of green LEDs, eosin Y (EY) is first photo-excited, which is reductively quenched by iodide ion.[21a-d] The reaction of sodium sulfinate and iodine generates sulfonyl iodide which is reduced by EY anion radical to give sulfonyl radical.[21e-g] Next, the addition of sulfonyl radical to terminal alkyne (**1**) gives a vinyl sulfone radical intermediate (**A**). The formation of a vinyl carbocation via SET process and the subsequent attack of carboxylate is completely ruled out, as this reaction does not proceed in the absence of iodine. The radical addition of iodine to intermediate (**A**) generates a *β*-iodo sulfone intermediate (**B**) (detected by HRMS analysis).

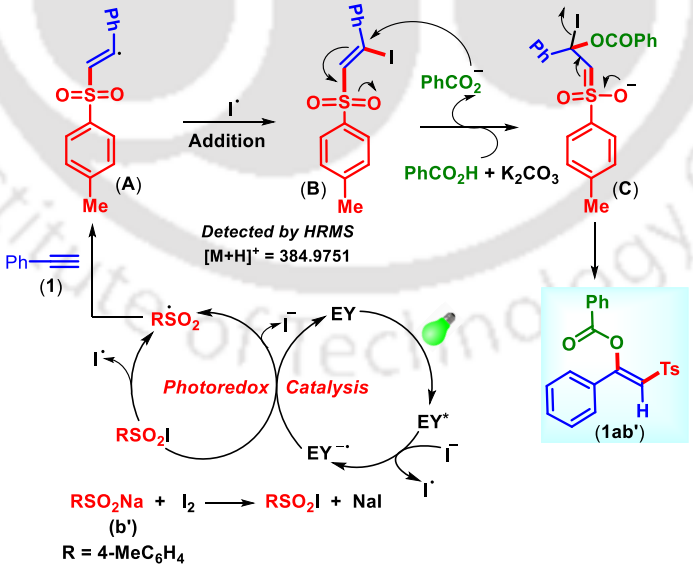

Scheme II.15. *Plausible mechanism for the synthesis of Z-β-carboxy vinylsulfones.*

Subsequently, a base-promoted nucleophilic attack of the carboxylate ion provides an intermediate (**C**) which is followed by an addition-elimination process to give the corresponding *Z*-1-phenyl-2-tosylvinyl benzoate (**1ab′**) (Scheme II.15). Next, (*Z*)-1-phenyl-2-tosylvinyl 4-methylbenzoate (**1bb′**) was subjected to few useful organic transformations as shown in Scheme II.16. Acid hydrolysis of (*Z*)-1-phenyl-2-tosylvinyl 4-methylbenzoate (**1bb′**) furnished 1-phenyl-2-tosylethan-1-one (**X**) in 80% isolated yield. Treatment of (*Z*)-1-phenyl-2-tosylvinyl 4-methylbenzoate (**1bb′**) with butylamine resulted in the formation of 1-phenyl-2-tosylethan-1-one (**X**) and *N*-acylated product (**Y**) {Scheme II.16}.

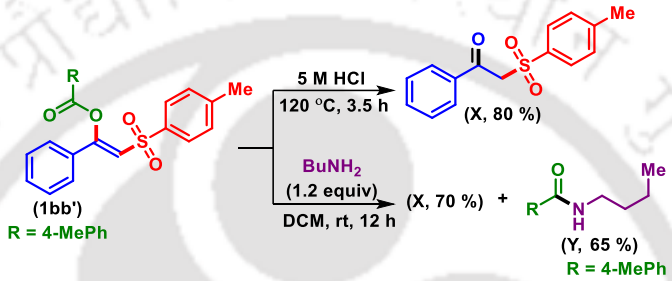

Scheme II.16. *Post-synthetic modification.*

Thus, (*Z*)-1-phenyl-2-tosylvinyl 4-methylbenzoate (**1bb′**) is serving as an efficient acyl-transfer reagent (Scheme II.16). Though *α*-sulfonylated ketones can be accessed via the method reported by Lan *et al* using substituted aryl ketones and sodium *p*-tolylsulfinate, this is yet another path to *α*-sulfonylated ketones with the benefit of concurrent *N*-acylation at ambient temperature.[22]

In summary, an elegant visible light-mediated method for the difunctionalization of terminal alkynes is established using sodium *p*-toluenesufinate and *O*– and *S*–centered nucleophiles as the reacting partners. This methodology allows the useful synthesis of many valuable *Z*-*β*-substituted vinylsulfones via a multi-component approach, covering a wide range of substrate scope. In this protocol, C–O and C–S bonds are constructed simultaneously with the introduction of important functional groups such as ester, thiocyanate, and sulfone.

II.4. Experimental Section

II.4.1. General Information: Starting materials (acetylenes and carboxylic acids) were commercially available (Sigma-Aldrich or Alfa-Aesar or TCI chemicals) and used as

received. Some aryl and alkyl sodium sulfinates were commercially available (**a′-d′**) while other (**e′-i′**) were prepared following the literature procedure.[23] The sodium sulfinates obtained were used as such without further purification. Organic extracts were dried over anhydrous sodium sulfate. Solvents were removed in a rotary evaporator under reduced pressure. Silica gel (60-120 mesh size) was used for the column chromatography. Reactions were monitored by TLC on silica gel 60 F_{254} (0.25 mm). NMR spectra were recorded in $CDCl_3$ as the internal standard for ^1H NMR (400, 500 MHz, and 600 MHz) and $^{13}C\{^1H\}$ NMR (100, 125, and 150 MHz). MS spectra were recorded using ESI mode. IR spectra were recorded in KBr or neat.

Light Information:

Philips 10 W green LEDs (513 nm) were used as a light source for tlight-promotedoted reaction without any filter. Borosilicate glass was used as the reaction vessel. Distance from the light source to the irradiation vessel was approximately ~6–8 cm. Regular fan was used for proper aeration to maintain the temperature 28–30 ^oC (Figure II.3).

II.4.2. Crytallographic Description

Sample preparation: The compound (**1db',** 15 mg) was dissolved in 1 mL of DCM:MeOH (5:1) and kept at room temperature for slow evaporation.

Diffraction data were collected at 292 K with MoKα radiation (λ = 0.71073 Å) using a Bruker Nonius SMART APEX CCD diffractometer equipped with graphite monochromator and Apex CD camera. The SMART software was used for data collection and for indexing the reflections and determining the unit cell parameters. Data reduction and cell refinement were performed using SAINT[24a,b] software and the space groups of these crystals were determined from systematic absences by XPREP and further justified by the refinement results. The structures were solved by direct methods and refined by full-matrix least-squares calculations using SHELXTL-97[24c] software. All the non-H atoms were refined in the anisotropic approximation against F^2 of all reflections.

Crystallographic description of (Z)-1-phenyl-2-tosylvinyl 4-chlorobenzoate (1db'):

M.F. = $C_{22}H_{17}ClO_4S$, crystal dimensions 0.22 x 0.17 x 0.15 mm, M_r = 412.87, monoclinic space, group P 21/n, a = 10.4280 (13), b = 10.2098 (12), c = 18.854 (2) Å, α = 90^o (3), β =

97.004° (4) , γ = 90°, V = 1992.4(4) Å^3, Z = 4, ρ_{calcd} = 1.376 g/cm^3, μ = 0.322 mm^{-1}, F(000) = 856.0, refinement method = full-matrix least-squares on F^2, final R indices [$I > 2\sigma(I)$]: R_1 = 0.0534(3362), wR_2 = 0.1820(4971), goodness of fit = 1.000. CCDC No = 2057146 for (Z)-1-phenyl-2-tosylvinyl 4-chlorobenzoate **(1db′)** contains the supplementary crystallographic data for this paper. These data can be obtained free of charge from The Cambridge Crystallographic Data Centre via www.ccdc.cam.ac.uk/data_request/cif.

II.4.3. General Procedure for the Synthesis of *Z*-*β*-Carboxy Vinylsulfone (1bb′):

To an oven-dried 10 mL borosilicate vial, phenylacetylene (**1**) (0.5 mmol, 51.06 mg) sodium *p*-tolylsulfinate (**b′**) (0.5 mmol, 89.09 mg), and *p*-toluic acid (**b**) (0.75 mmol, 102 mg), eosin Y (3 mol %, 9.7 mg), I_2 (1 equiv, 126 mg) and K_2CO_3 (2 equiv, 138 mg) were taken. After that 2 mL EtOH was added and the reaction mixture was stirred at room temperature for 48 h, tentatively at a distance of ~6-8 cm from two 10 W green LED bulbs. After completion of the reaction (monitored by TLC analysis), the solvent was removed *in vacuo* and the mixture was admixed with 25 mL of ethyl acetate followed by washing with a saturated solution of aqueous $Na_2S_2O_3$ (1 x 10 mL) and aqueous $NaHCO_3$ (1 x 10 mL). The organic layer was dried over anhydrous Na_2SO_4, and the solvent was evaporated under reduced pressure. The crude residue thus obtained was purified by column chromatography over silica gel (60-120 mesh) using hexane and ethyl acetate (9:1) as eluent to afford the *Z*-1-phenyl-2-tosylvinyl 4-methylbenzoate (**1bb′**) in 70% yield. The identity and purity of the product were confirmed by spectroscopic analysis.

II.4.4. General Procedure for 10 mmol Scale Reaction of *Z*-1-Phenyl-2-tosylvinyl 4 methylbenzoate (1bb′):

To an oven-dried 50 mL borosilicate round bottom flask, phenylacetylene (**1**) (10 mmol, 1.021 g) sodium *p*-tolylsulfinate (**b′**) (10 mmol, 1.782 g), and *p*-toluic acid (**b**) (15 mmol, 2.040 g), eosin Y (3 mol %, 0.194 g), I_2 (10 mmol, 2.520 g) and K_2CO_3 (20 mmol, 2.760 g) were taken. After that 30 mL EtOH was added and the reaction mixture was stirred at room temperature for 48 h, tentatively at a distance of ~6-8 cm from two 10 W green LED bulbs. After completion of the reaction (monitored by TLC analysis), the solvent was removed *in vacuo* and the mixture was admixed with 100 mL of ethyl acetate followed by washing with a saturated solution of aqueous $Na_2S_2O_3$ (1 x 30 mL) and aqueous $NaHCO_3$ (1 x 30 ml). The organic layer was dried over anhydrous Na_2SO_4, and the solvent was evaporated under

reduced pressure. The crude residue thus obtained was purified by column chromatography over silica gel (60-120 mesh) using hexane and ethyl acetate (9:1) as eluent to afford the *Z*-1-phenyl-2-tosylvinyl 4-methylbenzoate (**1bb′**) in 52% (2.04 g) yield. The identity and purity of the product were confirmed by spectroscopic analysis.

II.4.5. General Procedure for the Synthesis of 1-Phenyl-2-tosylethan-1-one (X)

To an oven-dried 5 mL round bottom flask, *Z*-1-phenyl-2-tosylvinyl 4-methylbenzoate (**1bb′**) (137 mg, 0.5 mmol) and 1 mL of 5M HCl were taken. The flask was fitted with a condenser and the reaction mixture was stirred in a preheated oil bath at 120 ^{o}C for 4 h. Next, the reaction mixture was cooled to room temperature and admixed with ethyl acetate (20 mL). The organic layer was washed with saturated sodium bicarbonate solution (2 x 5 mL) and dried over Na_2SO_4 and the solvent was removed under reduced pressure. The crude product so obtained was purified over a column of silica gel (hexane:ethyl acetate, 17:3) to afford the 1-phenyl-2-tosylethan-1-one (110 mg, yield 80%) (**X**). The identity and purity of the product were confirmed by spectroscopic analysis.

II.4.6. General Procedure for the Synthesis of *N*-Butyl-4-methylbenzamide (Y)

To an oven-dried 5 mL round bottom flask, *Z*-1-phenyl-2-tosylvinyl 4-methylbenzoate (**1bb′**) (137 mg, 0.5 mmol) and $BuNH_2$ (1.2 equiv) were taken. Next, 2 mL of DCM was added and the reaction mixture was stirred at room temperature for 24 h. After completion of the reaction, the solvent was evaporated and the reaction mixture was admixed with ethyl acetate (20 mL). The organic layer was washed with brine solution (2 x 5 mL) and dried over Na_2SO_4 and the solvent was removed under reduced pressure. The crude product so obtained was purified over a column of silica gel to afford the 1-phenyl-2-tosylethan-1-one (**X**, 55%) and *N*-butyl-4-methylbenzamide (**Y**, 55%). The identity and purity of the product were confirmed by spectroscopic analysis.

II.4.7. General Procedure for Radical Trapping Experiment

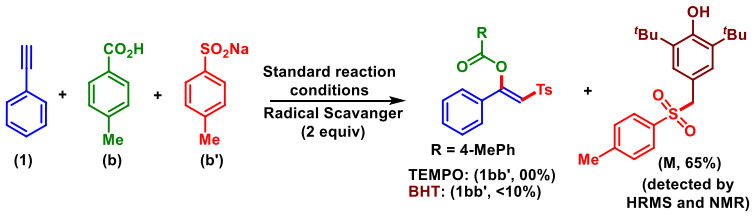

To prove the photocatalytic radical pathway, a standard experiment between (**1**), (**b**), and (**b′**) was carried out in the presence of TEMPO (2 equiv) and BHT (2 equiv) under otherwise identical conditions. While in the former no formation of the desired product (**1bb′**, 0%) was observed but the later radical scavenger provided <10% yield of (**1bb′**). In the case of BHT as a scavenger, tosyl radical was trapped and adduct (**M**) was obtained in 65% yield thereby confirming the radical nature of the present protocol (Scheme 6 and S1). The adduct (**M**) was purified by column chromatography over silica gel (60-120 mesh) using hexane and ethyl acetate (49:1) as eluent to afford the 2,6-di-*tert*-butyl-4-(tosylmethyl)phenol (**M**) in 65% yield. The identity and purity of the product was confirmed by spectroscopic analysis.

II.4.8. HRMS Study for the Detection of Reaction Intermediates:

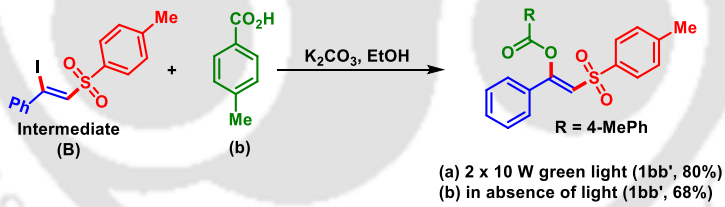

In this study (**1bb′**) was taken as a representative example and a standard experiment between (**1**), (**b**), and (**b′**) was carried out. After 2 h of reaction, a small aliquot was withdrawn from the reaction mixture and subjected to HRMS analysis after diluting it with CH_3CN:H_2O (60:40). The formation of 2-iodo-2-phenylvinyl)sulfonyl)-4-methylbenzene (**B**) intermediate was judged from the appearance of a peak at $[M+H]^+$ = 384.9751. To further confirm the intermediacy of (**B**), a standard experiment was carried out between pre-synthesized (**B**), *p*-toluic acid (**b**) in presence of K_2CO_3 (2 equiv) and ethanol (2 mL) in dark at room temperature. The desired product **1bb′** was obtained in 68% yield thereby suggesting the involvement of this intermediate in the present protocol.

II.4.9. The UV-Visible Spectroscopy and Fluorescence Quenching Experiment (Stern-Volmer Studies)

A 1 mM solution was prepared by mixing eosin Y in water by appropriate dilution of 0.01 M stock solution and taken in quartz UV cuvette of 1 cm path length. The UV-visible spectroscopy showed λ_{max} of 515 nm. For the fluorescence measurement, the sample was excited at 515 nm, and the emission was observed at 534 nm. For each fluorescence quenching experiment, a 10 μL (1 M) solution of sodium *p*-toluene sulfinate was added to eosin Y solution (1 mM) taken in a fluorescence cuvette and fluorescence emission spectra were recorded after each addition (Figure II.7). As evident from Figure II.7, a decrease in emission intensity was observed after each addition of sodium *p*-toluene sulfinate (5 → 35 mM). This confirms the electron transfer between eosin Y and quencher sodium *p*-toluene sulfinate (**b′**). A true fluorescence quenching phenomenon of eosin Y under various concentrations of sodium *p*-toluene sulfinate was demonstrated from Stern-Volmer graph using the equation $I_0/I_t = 1+K_{SV}$ [Q] where I_0 and I_t are integrated emission intensity in the absence and presence of quencher and Ksv is quenching constant. As evident from Figure II.7, a linear quenching was observed which confirmed the electron transfer between eosin Y and quencher sodium *p*-toluene sulfinate (**b′**).

II.4.10. CV Experiments Performed to Determine the Redox Potentials

Cyclic voltammetry (CV) was performed using three-electrode cell configuration comprised a platinum sphere, a platinum plate and Ag(s)/$AgNO_3$ (0.01 M) as the working, auxiliary, and reference electrodes respectively. [Cyclic voltammetry experiment of RSO_2I (RSO_2Na+I_2) taken at a scan rate 100mv/s. Experiment conditions: Init E = 2.0 V, High E = 2.0 V, Low E = -2.0 V, Init P/N = N, Scan Rate = 0.1 V/s, Sample Interval = 0.001 V, Quiet Time = 2s, Sensitivity = $2e^{-4}$ A/V]. The supporting electrolyte used was tetraethylammonium hexafluorophosphate (TEAHFP) $(C_2H_5)_4N(PF_6)$. Samples were prepared with a substrate concentration of 0.01 M in a 0.1 M TEAHFP in an acetonitrile electrolyte solution. From the result, it was found that, E_{red} = -1.06 V vs SCE whereas E^*_{Oxd} (RSO_2I) = -0.37 V vs SHE (experimental value -0.42V vs Ag/AgCl) (Figure II.8).which clearly indicated that the catalyst eosin Y ($EY^{-\bullet}$) can easily donate an electron to the RSO_2I species which provides strong evidence to the catalytic cycle suggested in mechanism (Scheme II.15).

II.5. References

[1] (a) Trost, B. M.; Li, C.-J. Modern Alkyne Chemistry: Catalytic and Atom-Economic Transformations. Wiley-VCH: Weinheim, 2014.

[2] (a) Patel, M.; Saunthwal, R. K.; Verma, A. K. *Acc. Chem. Res.* **2017**, *50*, 240–254. (b) Wille, U. *Chem. Rev*. **2013**, *113*, 813–853. (c) Flynn, A. B.; Ogilvie, W. W. *Chem. Rev*. **2007**, *107*, 4698–4745. (d) Yue, H.; Zhu, C.; Kancherla, R.; Liu, F.; Rueping, M. *Angew. Chem. Int. Ed*. **2020**, *59*, 5738–5746. (e) Song, Z.-Q.; Liu, Z.; Gan, Q.-C.; Lei, T.; Tung, C.-H.; Wu. L.-Z. *Org. Lett*. **2020**, *22*, 832–836. (f) Huang, L.; Rudolph, M.; Rominger, F.; Hashmi, A. S. K. *Angew. Chem. Int. Ed*. **2016**, *55*, 4808–4813. (g) Iqbal, N.; Jung, J.; Park, S.; Cho, E. J. *Angew. Chem. Int. Ed*. **2014**, *53*, 539–542. (h) Xu, T.; Cheung, C. W.; Hu, X. *Angew. Chem. Int. Ed*. **2014**, *53*, 4910–4914.

[3] (a) Ganapathy, D.; Sekar, G. *Org. Lett*. **2014**, *16*, 3856–3859. (b) McKinley, N. F.; O' Shea, D. F. Olefins. *J. Org. Chem*. **2006**, *71*, 9552–9555. (c) Xu, C.; Shen, X.; Hovedya, A. H. *J. Am. Chem. Soc.* **2017**, *139*, 10919–10928. (d) Crossley, S. W. M.; Obradors, C.; Martinez, R. M.; Shenvi, R. A. *Acc. Chem. Res* **2016**, *116*, 8912–9000.

[4] (a) Zhang, Y.; Sun, Y.; Chen, B.; Xu, M.; Li, C.; Zhang, D.; Zhang, G. *Org. Lett*. **2020**, *22*, 1490–1494. (b) Buquoi, J. Q.; Lear, J M.; Gu, X.; Nagib, D. A. *ACS Catal*. **2019**, *9*, 5330–5335. (c) Kuchukulla, R. R.; Li, F.; He, Z.; Zhou, L.; Zeng, Q. *Green Chem*. **2019**, *21*, 5808–5812. (d) Liu, Y.; Zheng, Q. Z.; Li, Y.; Zhang, Q. *J. Org. Chem*. **2017**, *82*, 2269–2275. (e) Ruijter, E.; Scheffelaar, R.; Orru, R. V. A. *Angew. Chem., Int. Ed*. **2011**, *50*, 6234–6246. (f) Ning, Y.; Ji, Q.; Liao, P.; Anderson, E. A.; Bi, X. *Angew. Chem. Int. Ed*. **2017**, *56*, 13805–13808. (g) Xiong, Y.; Sun, Y.; Zhang, G. *Org. Lett*. **2018**, *20*, 6250–6254.

[5] (a) Israr, M.; Xiong, H.; Li, Y.; Bao, H. *Adv. Synth. Catal*. **2020**, *362*, 2211–2215. (b) Cheung, C. W.; Hu, X. *Chem. Eur. J*. **2015**, *21*, 18439–18444. (c) Hopkinson, M. N.; Tlahuext-Aca, A.; Glorius, F. *Acc. Chem. Res*. **2016**, 49, 2261–2272. (d) Ansari, M. Y.; Kumar, N.; Kumar, A. *Org. Lett*. **2019**, *21*, 11, 3931–3936. (e) Ansari, M. Y.; Swarnkar, S.; Kumar, A. *Chem. Commun*. **2020**, *56*, 9561–9564. (f) Mir, B. A.; Singh, S. J.; Kumar, R.; Patel, B. K. *Adv. Synth. Catal*. **2018**, *360*, 3801–3809.

[6] (a) Shimizu, Y.; Kanai, M. *Tetrahedron Lett*. **2014**, *55*, 3727–3737. (b) Liang, H.; Ji, Y.-X.; Wang, R.-H.; Zhang, Z.-H.; Zhang, B. *Org. Lett*. **2019**, *21*, 2750–2754. (c) Chen, T.; Zhao, C.-Q.; Han, L.-B. *J. Am. Chem. Soc*. **2018**, *140*, 3139–3155. (d) Sun, J.; Deng, L. *ACS Catal*. **2016**, *6*, 290–300. (e) Lv, Y.; Pu, W.; Shi, L. *Org. Lett*. **2019**, *21*, 6034–6039. (f) Gao, B.; Huang, H. *Adv. Synth. Catal*. **2016**, *358*, 4075–4084.

[7] (a) Liu, W.; Kong, W. *Org. Chem. Front*. **2020**, *7*, 3941–3955. (b) Ding, W.; Chai, J.; Wang, C.; Wu, J.; Yoshikai, N. *J. Am. Chem. Soc*. **2020**, *142*, 8619–8624. (c) Lee, W.; Lee, Y.; Yoo, M.; Han, S. B.; Kim, H. *Org. Chem. Front*. **2020**, *7*, 3209–3214. (d) Li, W.; Yu, S.; Li, J.; Zhao, Y. *Angew. Chem., Int. Ed*. **2020**, *59*, 14404–14408. (e) Lu, Q.; Zhang, J.; Zhao, G.; Qi, Y.; Wang, H.; Lei, A. *J. Am. Chem. Soc*. **2013**, *135*, 11481–11484.

[8] (a) Dahiya, A.; Sahoo, A. K.; Alam, T.; Patel, B. K. *Chem. Asian. J*. **2019**, *14*, 4454–4492. (b) Majji, G.; Rout, S. K.; Rajamanickam, S.; Guin, S.; Patel, B. K. *Org. Biomol. Chem*. **2016**, *14*, 8178–8211. (c) Dong, D.-J.; Li, H.-H.; Tian, S.-K. *J. Am. Chem. Soc*. **2010**, *132*, 5018–5020. (d) Chen, C.; Huang, Y.; Zhang, Z.; Dong, X.-Q.; Zhang, X. *Chem. Commun*. **2017**, *53*, 4612–4615. (e) Hatakeyama, T.; Nakagawa, N.; Nakamura, M. *Org. Lett*. **2009**, *11*, 4496–4499.

[9] (a) Dutta, U.; Maity, S.; Kancherla, R.; Maiti, D. *Org. Lett*. **2014**, *16*, 6302–6305. (b) Guo, L.; Song, F.; Zhu, S.; Li, H.; Chu, L. *Nat. Commun*. **2018**, *9*, 4543. (c) Wang, H.; Li, Y.; Tang, Z.; Wang, S.; Zheng, H.; Cong, H.; Lie, A. *ACS Catal*. **2018**, *8*, 10599–10605.

[10] (a) Park, J. W.; Kim, Y. S.; Lee, K.-J.; Kim, D. *Bioconjugate Chem*. **2012**, *23*, 350–362. (b) Tang, P.-Y.; Wang, M.; He, C.Y.; Yao, S. Q. *Chem. Commun*. **2012**, *48*, 835–837. (c) Woo, S.Y.; Kim, J. H.; Moon, M. K.; Han, S.-H.; Yeon, S. K.; Choi, J. W.; Jang, B. K.; Song, H. J.; Kang, Y. G.; Kim, J. W.; Lee, J.; Kim, D. J.; Hwang, O.; Park, K. D. *J. Med. Chem*. **2014**, *57*, 1473–1487. (d) Rosenthal, P. P.; Olson, J. E.; Lee, G. K.; Palmer, J. T.; Klaus, J. L.; Rasnick, D. **1996**, *40*, 1600–1603. (e) Castanheiro, T.; Suffert, J.; Donnard, M.; Gulea, M. *Chem. Soc. Rev*. **2016**, *45*, 494–505.

[11] (a) Noshi, M. N.; Ei-awa, A.; Tores, E.; Fuchs, P. L. *J. Am. Chem. Soc*. **2007**, *129*, 11242–11247. (b) Das, J.; Dey, S.; Pathak, T. *J. Org. Chem*. **2019**, *84*, 15437–15447. (c) Trost, B. M.; Kalnmals, C. A. *Chem. Eur. J*. **2019**, *25*, 11193–11213.

[12] (a) Bogonda, G.; Patil, D. V.; Kim, H. Y.; Oh, K. *Org. Lett*. **2019**, *21*, 3774–3779. (b) Kramer, P.; Halaczkiewicz, M.; Sun, Y.; Kelm, H.; Manolikakes, G. *J. Org. Chem.* **2020**, *85*, 3617–3637. (c) Qian, P.; Deng, Y.; Mei, H.; Han, J.; Zhou, J.; Pan, Y. *Org. Lett*. **2017**, *19*, 4798–4801. (d) Hossain, A.; Engl, S.; Lutsker, E.; Reiser, O. *ACS Catal*. **2019**, *9*, 1103–1109. (e) Peng, Z.; Yin, H.; Zhang, H.; Jia, T. *Org. Lett*. **2020**, *22*, 5885–5889. (f) Alkan-Zambada, M.; Hu, X. *J. Org. Chem*. **2019**, *84*, 7, 4525–4533. (g) Reddy, R. J.; Kumar, J. J.; Kumari A. H. *Eur. J. Org. Chem*. **2019**, 3771–3775. (h) Reddy, R. J.; Kumar, J. J.; Kumari A. H.; Krishna, G. R. *Adv. Synth. Catal*. **2020**, *362*, 1317–1322. (i) Sun, Y.; Abdukader, A.; Lu, D.; Zhang, H.; Liu, C. *Green Chem*. **2017**, *19*, 1255–1258.

[13] (a) Lee, J. W.; Lee, K. N.; Ngai, M.-Y. *Angew. Chem. Int. Ed*. **2019**, *58*, 11171–11181. (b) Zhu, J.; Yang, W.-C.; Wang, X.-D.; Wu, L. *Adv. Synth. Catal*. **2018**, *360*, 386–400. (c) Gingipalli, L.; Boerth, J.; Emmons, D.; Grebe, T.; Hatoum-Mokdad, H.; Peng, B.; Sha, L.; Tentarelli, S.; Wang, H.; Wu, Y.; Zheng, X.; Edmondson, S.; Gopalsamy, A. *Org. Lett*. **2020**, *22*, 3418–3422. (d) Kammer, L. M.; Krumb, M.; Spitzbarth, B.; Lipp, B.; Kühlborn, J.; Busold, J.; Mulina, O. M.; Terentev, A. O.; Opatz, T. *Org. Lett*. **2020**, *22*, 3318–3322. (e) Shukla, G.; Dahiya, A.; Alam, T.; Patel, B. K. *Asian J. Org. Chem*. **2019**, *8*, 2243–2248 (f) Courant, T.; Masson, G. *J. Org. Chem.* **2016**, *81*, 6945–6952. (g) Pelliccia, S.; Alfano, A. I.; Luciano, P.; Novellino, E.; Massarotti, A.; Tron, G. C.; Ravelli, D.; Giustiniano, M. *J. Org. Chem*. **2020**, *85*, 1981–1990. (h) Shang, T.; Zhang, J.; Zhang, Y.; Zhang, F.; Li, X.-S.; Zhu, G. *Org. Lett*. **2020**, *22*, 3667–3672.

[14] (a) Srivastava, V.; Singh, P. P. *RSC Adv*. **2017**, *7*, 31377–31392. (b) Hari, D. P.; König, B. *Chem. Commun*. **2014**, *50*, 6688–6699. (c) Majek, M.; Filace, F.; Wangelin, A. J. V. *J. Org. Chem*. **2014**, *10*, 981–989. (d) Alam, T.; Rakshit, A.; Begum, P.; Dahiya, A.; Patel, B. K. *Org. Lett*. **2020**, *22*, 3728–3733. (e) Hou, H.; Xu, Y.; Yang, H.; Chen, X.; Yan, C.; Shi, Y.; Zhu, S. *Org. Lett*. **2020**, *22*, 1748–1753. (f) Ghiazza, C.; Debrauwer, V.; Monnereau, C.; Khrouz, L.; Medebielle, M.; Billard, T.; Tlili, A. *Angew. Chem. Int. Ed*. **2018**, *57*, 11781–11785. (g) Liu, Y.; Wang, Q.-L.; Chen, Z.; Li, H.; Xiong, B.-Q.; Zhang, P.-L.; Tang, K.-W. *Chem. Commun*. **2020**, *56*, 3011–3014. (h) Chand, S.; Pandey, A. K.; Singh, R.; Kumar, S.; Singh, K. N. *Chem. Asian J*. **2019**, *14*, 4712–4716.

[15] (a) Zeng, X.; Ilies, L.; Nakamura, E. *Org. Lett*. **2012**, *14*, 954–956. (b) Gao, Y.; Wu, W.; Huang, Y.; Huang, K.; Jiang, H. *Org. Chem. Front*. **2014**, *1*, 361–364. (c) Ning, Y.; Ji, Q.; Liao, P.; Anderson, E. A.; Bi, X. *Angew. Chem. Int. Ed*. **2017**, *56*, 13805–13808. (d) Ansari, M. Y.; Swarnkar, S.; Kumar, A. *Chem. Commun*. **2020**, *56*, 9561–9564. (e) Cai, S.; Chen, D.; Xu, Y.; Weng, W.; Li, L.; Zhang, R.; Huang, M. *Org. Biomol. Chem*. **2016**, *14*, 4205–4209. (f) Iqbal, N.; Jung, J.; Park, S.; Cho, E. J. *Angew. Chem. Int. Ed*. **2014**, *53*, 539 –542.

[16] Dominguez, A. G.; Müller, S.; Nevado, C. *Angew. Chem. Int. Ed*. **2017**, *56*, 9949–9952.

[17] Chakrasali, P.; Kim, K.; Jung, Y.-S.; Kim, H.; Han, S. B. *Org. Lett*. **2018**, *20*, 7509−7513.

[18] Sahoo, A. K.; Dahiya, A.; Das, B.; Behera, A.; Patel, B. K. *J. Org. Chem*. **2021**, *86*, 11968−11986.

[19] Ding, T,-H.; Qu, J.-P.; Kang, Y.-B. *Org. Lett*. **2020**, *22*, 3084−3088. (b) Li, G.; Yan, Q.; Gan, Z.; Li, Q.; Dou, X.; Yang, D. *Org. Lett.* **2019**, *21*, 7938−7942.

[20] Pavlishchuka, V. V.; Addison A. W. *Inorganica Chim. Acta*. **2000**, *298*, 97–102. (b) Fotouhi, L.; Ganjavi, M.; Nematollahi, D. **2004**, *4*, 170–180.

[21] (a) Matsuzaki, K.; Hiromura, T.; Amii, H.; Shibata, N. *Molecules*, **2017**, *22*, 1130–1142. (b) Koike, T.; Akita, M. *Chem*. **2018**, *4*, 409–437. (c) Meyer, A. U.; Slanina, T.; Yao, C.-J.; König, B. *ACS Catal*. **2016**, *6*, 369–375. (d) Gardner, J. M.; Abrahamsson, M.; B. Farnum, H.; Meyer G. J. *J. Am. Chem. Soc*. **2009**, *131*, 44, 16206–16214. (e) Katrun, P.; Mueangkeaw, C.; Pohmokatr, M.; Reutrakul, V.; Jaipetch, T.; Soorukram, D.; Kuhakarn, C. *J. Org. Chem*. **2014**, *79*, 1778–1785. (f) Xiao, F.; Hui, X.; Chen, S.; Yang, L.; Deng, G.-J. *Org. Lett*. **2014**, *16*, 50–53. (g) Hou, Y.; Zhu, L.; Hu, H.; Chen, S.; Li, Z.; Liu, Y.; Gong, P. *New J. Chem*. **2018**, *42*, 8752–8755. (h) Uwe, M. A.; Jager, S.; Hari, D.; König, B. *Adv. Synth. Catal*. **2015**, *357*, 2050–2054. (i) Storozhenko, O. A.; Festa, A. A.; Detistova, G. I.; Rybakov, V. B.; Varlamov, A. V.; Van der Eycken, E. V.; Voskressensky, L. G. *J. Org. Chem*. **2020**, *85*, 2250–2259.

[22] Lan, X.-W.; Wang, N.-X.; Bai, C.-B.; Zhang, W.; Xing, Y.; Wen, J.-L.; Wang, Y.-J.; Li, Y.-H. *Sci. Rep*. **2015**, *5*, 18391.

[23] Lv, F.; Guo, X.; Wu, H.; Li, H.; Tang, B.; Yu, C.; Hao, E.; Jiao, L. *Chem. Commun.* **2020**, *56*, 15577–15580.

[24] (a) Sheldrick, G. M. SADABS, **1996**, based on the method described in: Blessing, R. H. *Acta Crystallogr.* **1995**, **A51**, 33–38. (b) SMART and SAINT, Siemens Analytical X-ray Instruments Inc., Madison, WI, **1996.** (c) Sheldrick, G. M. *Acta Crystallogr.* **2008**, *A64*, 112–122.

II.6. Spectral Data

(Z)-1-Phenyl-2-tosylvinyl benzoate (1ab'):

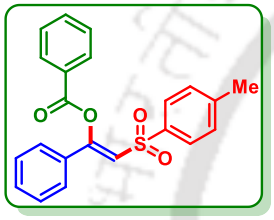

As a white solid (130 mg, 68% yield); mp 120–122 °C; purified over a column of silica gel (8% EtOAc in hexane); ^{1}H NMR ($CDCl_3$, 400 MHz): δ 8.13 (d, 2H, J = 7.2 Hz), 7.81 (d, 2H, J = 8.4 Hz), 7.68 (t, 1H, J = 7.2 Hz), 7.54 (t, 2H, J = 7.8 Hz), 7.50 (d, 2H, J = 7.8 Hz), 7.43 (t, 1H, J = 7.2 Hz), 7.36 (t, 2H, J = 7.8 Hz), 7.24 (d, 2H, J = 7.8 Hz), 6.81 (s, 1H), 2.39 (s, 3H); ^{13}C{^{1}H} NMR ($CDCl_3$, 100 MHz): δ 163.4, 156.7, 144.7, 138.6, 134.4, 132.4, 131.8, 130.7, 129.9, 129.2, 128.9, 128.4, 128.1, 126.2, 118.7, 21.8; IR (KBr, cm^{-1}): 3061, 2925, 2857, 1744, 1616, 1453, 1234, 1061; HRMS (ESI/Q-TOF) (m/z): calcd for $C_{22}H_{18}O_4SNa$, $[M + Na]^+$: 401.0818, found 401.0835.

(Z)-1-Phenyl-2-tosylvinyl 4-methylbenzoate (1bb'):

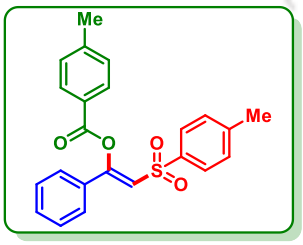

As a brown solid (138 mg, 70% yield); mp 102–104 °C; purified over a column of silica gel (8% EtOAc in hexane); ^{1}H NMR ($CDCl_3$, 400 MHz): δ 7.87 (d, 2H, J = 8.0 Hz), 7.66 (d, 2H, J = 8.0 Hz), 7.35 (t, 2H, J = 7.2 Hz), 7.27 (d, 1H, J = 7.2 Hz), 7.17-7.23 (m, 4H), 7.10 (t, 2H, J = 8.4 Hz), 6.66 (s, 1H), 2.33 (s, 3H), 2.25 (s, 3H); ^{13}C{^{1}H} NMR ($CDCl_3$, 100 MHz): δ 163.4, 156.9, 145.4, 144.6, 138.7, 132.5, 131.7, 130.8, 129.9, 129.6, 129.2, 128.1, 126.2, 125.7, 118.7, 22.0, 21.8; IR (KBr, cm^{-1}): 3066, 2945, 2847, 1740, 1610, 1235, 1062; HRMS (ESI/Q-TOF)

(m/z): calcd for $C_{23}H_{24}O_4SN$, $[M + NH_4]^+$: 410.1421, found 410.1420.

(Z)-1-Phenyl-2-tosylvinyl 4-methoxybenzoate (1cb'):

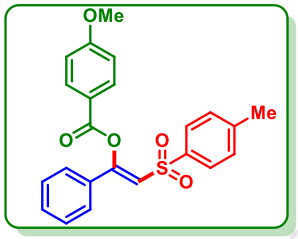

As a brown solid (152 mg, 74% yield); mp 130–132 °C; purified over a column of silica gel (12% EtOAc in hexane); ^{1}H NMR ($CDCl_3$, 400 MHz): δ 8.07 (d, 2H, J = 9.2 Hz), 7.81 (d, 2H, J = 8.4 Hz), 7.49 (t, 2H, J = 4.2 Hz), 7.42 (t, 1H, J = 7.2 Hz), 7.36, (t, 2H, J = 7.4 Hz), 7.23 (d, 2H, J = 8.0 Hz), 7.00 (d, 2H, J = 8.8 Hz), 6.79 (s, 1H), 3.92, (s, 3H), 2.39 (s, 3H); ^{13}C{^{1}H} NMR ($CDCl_3$, 100 MHz): δ 164.6, 163.0, 157.0, 144.6, 138.7, 132.9, 132.6, 131.7, 129.9, 129.2, 128.1, 126.2, 120.7, 118.7, 114.2, 55.8, 21.8; IR (KBr, cm^{-1}): 3066, 2957, 2839, 1741, 1605, 1511, 1242, 1167, 1065; HRMS (ESI/Q-TOF) (m/z): calcd for $C_{23}H_{21}O_5S$, $[M + H]^+$: 409.1104, found 409.1103.

(Z)-1-Phenyl-2-tosylvinyl 4-chlorobenzoate (1db'):

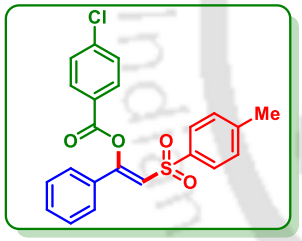

As a white solid (128 mg, 62% yield); mp 89–91 °C; purified over a column of silica gel (12% EtOAc in hexane); ^{1}H NMR ($CDCl_3$, 400 MHz): δ 7.98 (d, 2H, J = 8.4 Hz), 7.71 (d, 2H, J = 8.4 Hz), 7.40–7.43 (m, 3H), 7.39 (t, 1H, J = 3.6 Hz), 7.32–7.35 (m, 1H), 7.28 (t, 2H, J = 7.6 Hz), 7.17 (t, 2H, J = 8.4 Hz), 6.70 (s, 1H), 2.31 (s, 3H); ^{13}C{^{1}H} NMR ($CDCl_3$, 100 MHz): δ 162.7, 156.4, 144.8, 141.0, 138.6, 132.2, 132.1, 131.9, 130.0, 129.34, 129.26, 128.0, 127.0, 126.2, 118.6, 21.8; IR (KBr, cm^{-1}): 3065, 2935, 2845, 1746, 1606, 1234, 1145, 1063; MS (ESI/Q-TOF) (m/z): calcd for $C_{22}H_{18}ClO_4S$, $[M + H]^+$: 413.0609, found 413.2609.

(Z)-1-Phenyl-2-tosylvinyl 4-bromobenzoate (1eb'):

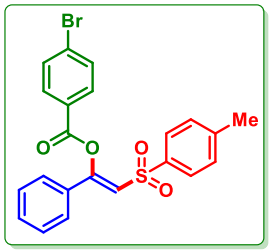

As a white solid (147 mg, 64% yield); mp 116–118 °C; purified over a column of silica gel (12% EtOAc in hexane); ^{1}H NMR ($CDCl_3$, 600 MHz): δ 8.0 (d, 2H, J = 9.0 Hz), 7.80 (d, 2H, J= 8.4 Hz), 7.68 (d, 2H, J = 9.0 Hz), 7.49 (d, 2H, J = 7.2 Hz), 7.44 (t, 1H, J = 7.2 Hz), 7.37 (t, 2H, J = 7.2 Hz), 7.27 (d, 2H, J = 7.2

Hz), 6.80 (s, 1H), 2.41 (s, 3H); $^{13}C\{^{1}H\}$ NMR ($CDCl_3$, 150 MHz): δ 162.9, 156.3, 144.8, 138.5, 132.3, 132.2, 132.1, 131.9, 130.0, 129.7, 129.3, 128.0, 127.4, 126.2, 118.5, 21.8; IR (KBr, cm^{-1}): 3063, 2929, 2853, 1748, 1622, 1242, 1147, 1067; HRMS (ESI/Q-TOF) (m/z): calcd for $C_{22}H_{21}BrO_4SN$, $[M + NH_4]^+$: 457.0104, found 457.0103.

(Z)-1-Phenyl-2-tosylvinyl 2-bromobenzoate (1fb'):

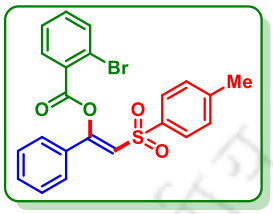

As a white solid (148 mg, 65% yield); mp 105–107 °C; purified over a column of silica gel (8% EtOAc in hexane); ^{1}H NMR ($CDCl_3$, 400 MHz): δ 8.29 (dd, 1H, J_1 = 7.6 Hz, J_2 = 2.0 Hz), 7.83 (d, 2H, J = 7.6 Hz), 7.76 (dd, 1H, J_1 = 7.6 Hz, J_2 = 1.2 Hz), 7.57 (dd, 2H, J_1 = 3.6 Hz, J_2 = 7.2 Hz), 7.52 (dd, 1H, J_1 = 7.2 Hz, J_2 = 7.6 Hz), 7.49 (dd, 1H, J_1 = 4.8 Hz, J_2 = 3.6 Hz), 7.46 (t, 1H, J = 4.0 Hz), 7.43–7.45 (m, 1H), 7.40 (t, 2H, J = 7.6 Hz), 7.28 (d, 1H, J = 2.8 Hz), 6.77 (s, 1H), 2.41 (s, 3H); $^{13}C\{^{1}H\}$ NMR ($CDCl_3$, 100 MHz): δ 162.2, 156.2, 144.9, 138.4, 135.0, 134.0, 133.17, 132.19, 131.8, 130.0, 129.6, 129.2, 127.9, 127.7, 126.4, 123.0, 118.3, 21.8; IR (KBr, cm^{-1}): 3063, 2926, 2850, 1760, 1619, 1228, 1149, 1076; HRMS (ESI/Q-TOF) (m/z): calcd for $C_{22}H_{21}BrO_4SN$, $[M + NH_4]^+$: 474.0369, found 474.0367.

(Z)-1-Phenyl-2-tosylvinyl 2-iodobenzoate (1gb'):

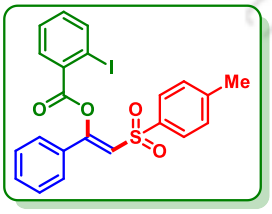

As a white solid (158 mg, 63% yield); mp 115–117 °C; purified over a column of silica gel (12% EtOAc in hexane); ^{1}H NMR ($CDCl_3$, 400 MHz): δ 8.21 (dd, 1H, J_1 = 8.0 Hz, J_2 = 1.6 Hz), 7.99 (d, 1H, J = 8.0 Hz), 7.71 (d, 2H, J = 8.4 Hz), 7.42–7.45 (m, 3H), 7.34 (t, 1H, J = 7.2 Hz), 7.28 (t, 2H, J = 7.2 Hz), 7.15 (dd, 3H, J_1 = 8.0 Hz, J_2 = 6.4 Hz), 6.65 (s, 1H), 2.30 (s, 3H); $^{13}C\{^{1}H\}$ NMR ($CDCl_3$, 100 MHz): δ 162.4, 156.2, 144.9, 142.2, 138.4, 134.1, 132.9, 132.2, 132.1, 131.8, 130.0, 129.2, 128.5, 128.0, 126.4, 118.4, 95.6, 21.9; IR (KBr, cm^{-1}): 3061, 2922, 2839, 1756,

1622, 1227, 1148, 1071; HRMS (ESI/Q-TOF) (m/z): calcd for $C_{22}H_{18}IO_4S$, $[M + H]^+$: 504.9965, found 504.9957.

(Z)-1-Phenyl-2-tosylvinyl 4-chloro-2-iodobenzoate (1hb'):

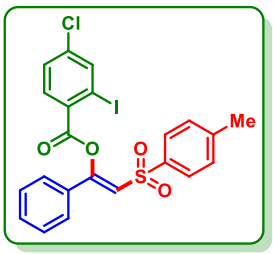

As a brown solid (168 mg, 62% yield); mp 137–139 °C; purified over a column of silica gel (18% EtOAc in hexane);^{1}H NMR ($CDCl_3$, 400 MHz): δ 8.14 (d, 1H, J = 8.4 Hz), 7.99, (d, 1H, J = 2.0 Hz), 7.69 (d, 2H, J = 8.4 Hz), 7.41 (dd, 3H, J_1 = 7.6 Hz, J_2 = 1.2 Hz), 7.32–7.36 (m, 1H), 7.26–7.30 (m, 2H), 7.16 (t, 2H, J = 8.0 Hz), 6.63 (s, 1H), 2.31 (s, 3H); $^{13}C\{^1H\}$ NMR ($CDCl_3$, 100 MHz): δ 161.8, 155.9, 145.0, 141.7, 139.8, 138.3, 133.5, 132.1, 131.9, 130.5, 130.1, 129.3, 128.8, 128.0, 126.4, 118.3, 96.0, 21.9; IR (KBr, cm^{-1}): 3069, 2920, 2844, 1755, 1615, 1573, 1149, 1089; HRMS (ESI/Q-TOF) (m/z): calcd for $C_{22}H_{17}ClIO_4S$, $[M + H]^+$: 538.9575, found 538.9567.

(Z)-1-Phenyl-2-tosylvinyl 2-bromo-4-methylbenzoate (1ib'):

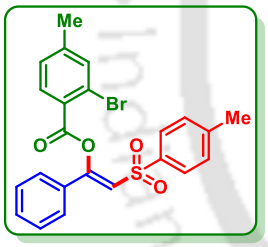

As a white solid (151 mg, 64% yield); mp 139–141 °C; ^{1}H NMR ($CDCl_3$, 400 MHz): δ 8.17 (d, 1H, J = 8.0 Hz), 7.81 (d, 2H, J = 8.0 Hz), 7.58 (s, 1H), 7.54 (d, 2H, J = 7.2 Hz), 7.43 (d, 1H, J = 7.2 Hz), 7.39 (dd, 2H, J_1 = 8.4 Hz, J_2 = 6.8 Hz), 7.29 (dd, 1H, J_1 = 8.0 Hz, J_2 = 0.8 Hz), 7.26 (s, 1H), 7.24 (s, 1H), 6.75 (s, 1H), 2.44 (s, 3H), 2.40 (s, 3H); $^{13}C\{^1H\}$ NMR ($CDCl_3$, 100 MHz): 161.9, 156.4, 145.5, 144.8, 138.4, 135.7, 133.3, 132.4, 131.7, 130.0, 129.2, 128.6, 128.0, 126.4, 126.3, 123.4, 118.5, 21.9, 21.5; IR (KBr, cm^{-1}): 3060, 2912, 2850, 1757, 1601, 1229, 1146, 1076; HRMS (ESI/Q-TOF) (m/z): calcd for $C_{23}H_{20}BrO_4S$, $[M + H]^+$ 471.0260, found 471.0251.

(Z)-1-Phenyl-2-tosylvinyl 2,4,6-trimethylbenzoate (1jb'):

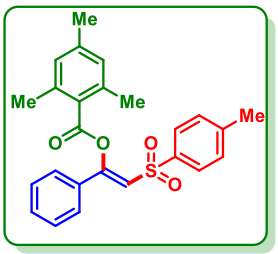

As a white solid (110 mg, 52% yield); mp 128–130 °C; ^{1}H NMR ($CDCl_3$, 600 MHz): δ 7.69 (d, 2H, J = 8.4 Hz), 7.53 (d, 2H, J = 7.8 Hz), 7.44 (t, 1H, J = 7.2 Hz), 7.39 (t, 2H, J = 7.2 Hz), 7.19 (d, 2H, J = 8.4 Hz), 6.96 (s, 2H), 6.70 (s, 1H), 2.50 (s, 6H), 2.40 (s, 3H), 2.35 (s, 3H); $^{13}C\{^1H\}$ NMR ($CDCl_3$, 150 MHz): δ 165.4, 157.4, 144.5, 141.8, 139.6, 138.9, 133.2, 131.5, 130.1, 129.8, 129.1, 128.0, 126.8,

126.6, 119.5, 31.2, 22.2, 21.8, 21.5; IR (KBr, cm^{-1}): 3065, 2924, 1747, 1610, 1225, 1145, 1048; HRMS (ESI/Q-TOF) (m/z): calcd. for $C_{25}H_{28}O_4SN$, $[M + NH_4]^+$: 438.1734, found 438.1732.

***(Z)-1-Phenyl-2-tosylvinyl acetate* (*1kb'*):**

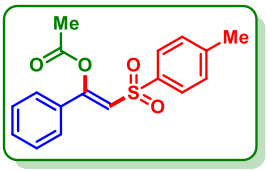

As a gummy (103 mg, 65% yield); purified over a column of silica gel (8% EtOAc in hexane); ^1H NMR ($CDCl_3$, 600 MHz): δ 7.86 (d, 2H, J = 8.4 Hz), 7.45–7.47 (m, 2H), 7.41–7.43 (m, 1H), 7.38 (d, 2H, J = 7.8 Hz), 7.35 (d, 2H, J = 8.4 Hz), 6.64 (s, 1H),), 2.43 (s, 3H), 2.39 (s, 3H); $^{13}C\{^1H\}$ NMR ($CDCl_3$, 150 MHz): δ 168.0, 156.3, 144.9, 138.8, 132.3, 131.8, 130.0, 129.1, 127.7, 126.2, 117.4, 21.8, 21.1; IR (KBr, cm^{-1}): 3063, 2929, 1737, 1620, 1597, 1319, 1144, 1085; HRMS (ESI/Q-TOF) (m/z): calcd for $C_{17}H_{17}O_4S$, $[M + H]^+$: 317.0842, found 317.0858.

(Z)-1-Phenyl-2-tosylvinyl pivalate (1lb'):

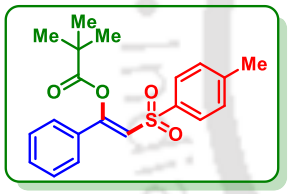

As a brown solid (126 mg, 70% yield); mp 85–87 °C; purified over a column of silica gel (5% EtOAc in hexane); ^1H NMR ($CDCl_3$, 400 MHz): δ 7.86 (d, 2H, J = 8.4 Hz), 7.41–7.46 (m, 3H), 7.39 (s, 1H), 7.33–7.37 (m, 3H), 6.57 (s, 1H), 2.44 (s, 3H), 1.43 (s, 9H); $^{13}C\{^1H\}$ NMR ($CDCl_3$, 100 MHz): δ, 175.4, 156.7, 144.7, 139.0, 133.2, 131.6, 130.0, 129.2, 127.7, 126.2, 117.5, 39.5, 27.5, 21.8; IR (KBr, cm^{-1}): 3063, 2925, 1759, 1622, 1480, 1262, 1150, 1078; HRMS (ESI/Q-TOF) (m/z): calcd for $C_{20}H_{23}O_4S$ $[M + H]^+$: 359.1312, found 359.1309.

(Z)-1-Phenyl-2-tosylvinyl hexanoate (1mb'):

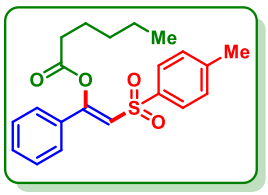

As a gummy (126 mg, 68% yield); purified over a column of silica gel (5% EtOAc in hexane); ^1H NMR ($CDCl_3$, 400 MHz): δ 7.86 (d, 2H, J = 8.0 Hz), 7.46 (s, 1H), 7.41–7.44 (m, 2H), 7.38 (d, 2H, J = 7.6 Hz), 7.35 (d, 2H, J = 8.0 Hz), 6.62 (s, 1H), 2.66 (t, 2H, J = 8.0 Hz), 2.44 (s, 3H), 1.72–1.79 (m, 2H), 1.37–1.41 (m, 4H), 0.93 (t, 3H, J = 7.2 Hz); $^{13}C\{^1H\}$ NMR ($CDCl_3$, 100 MHz): δ 170.8, 156.6, 144.8, 139.0, 132.8, 131.7, 130.0, 129.2, 127.8, 126.3, 117.6,

34.2, 31.4, 24.3, 22.5, 21.9, 14.1; IR (KBr, cm^{-1}): 3065, 2925, 2852, 1765, 1638, 1159, 1075; HRMS (ESI/Q-TOF) (m/z): calcd for $C_{21}H_{24}O_4SK$, $[M + K]^+$: 411.1027, found 411.1022.

(Z)-1-Phenyl-2-tosylvinyl octanoate (1nb'):

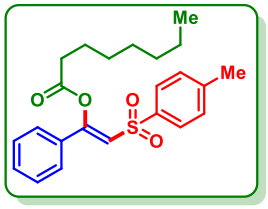

As a gummy (145 mg, 72% yield); purified over a column of silica gel (5% EtOAc in hexane); ^1H NMR ($CDCl_3$, 400 MHz): δ 7.86 (d, 2H, J = 8.0 Hz), 7.45 (d, 1H, J = 4.4 Hz), 7.41–7.44 (m, 2H), 7.38 (d, 2H, J = 7.6 Hz), 7.35 (d, 2H, J = 8.0 Hz), 6.62 (s, 1H), 2.66 (t, 2H, J = 7.6 Hz), 2.44 (s, 3H), 1.71–1.78 (m, 2H), 1.28–1.40 (m, 7H), 1.25 (s, 1H), 0.89 (t, 3H, J = 7.2 Hz); $^{13}C\{^1H\}$ NMR ($CDCl_3$, 100 MHz): δ 170.8, 156.6, 138.9, 134.8, 132.7, 131.7, 130.0, 129.2, 127.8, 126.3, 117.6, 34.2, 31.9, 31.1, 29.1, 24.6, 22.8, 21.9, 14.3; IR (KBr, cm^{-1}): 3065, 2934, 2829, 1770, 1612, 1134, 1077; HRMS (ESI/Q-TOF) (m/z): calcd for $C_{23}H_{32}O_4SN$, $[M + NH_4]^+$: 418.2047, found 418.2045.

(Z)-1-Phenyl-2-tosylvinyl decanoate (1ob'):

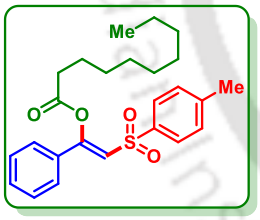

As a gummy (161 mg, 75% yield); purified over a column of silica gel (5% EtOAc in hexane); ^1H NMR ($CDCl_3$, 600 MHz): δ 7.88 (d, 2H, J = 8.4 Hz), 7.44–7.47 (m, 3H), 7.40 (d, 2H, J = 7.8 Hz), 7.37 (d, 2H, J = 7.8 Hz), 6.64 (s, 1H), 2.69 (t, 2H, J = 7.2 Hz), 2.46 (s, 3H), 1.75–1.80 (m, 2H), 1.41–1.44 (m, 2H), 1.28–1.32 (m, 10H), 0.91 (t, 3H, J = 7.2 Hz); $^{13}C\{^1H\}$ NMR ($CDCl_3$, 150 MHz): δ 170.8, 156.6, 144.8, 138.9, 132.7, 131.7, 130.0, 129.1, 127.8, 126.3, 117.6, 34.2, 32.1, 29.6, 29.49, 29.48, 29.3, 24.6, 22.9, 21.9, 14.3; IR (KBr, cm^{-1}): 3063, 2924, 2854, 1772, 1621, 1149, 1081; HRMS (ESI/Q-TOF) (m/z): calcd for $C_{25}H_{33}O_4S$, $[M + H]^+$: 429.2094, found 429.2088.

(Z)-1-Phenyl-2-tosylvinyl stearate (1pb'):

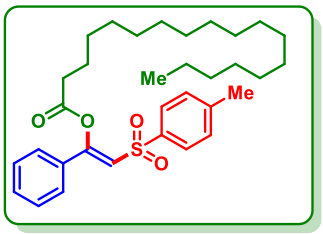

As a gummy (176 mg, 65% yield); purified over a column of silica gel (3% EtOAc in hexane); ^{1}H NMR ($CDCl_3$, 400 MHz): δ 7.86 (d, 2H, J = 8.0 Hz), 7.45 (d, 1H, J = 4.4 Hz), 7.41–7.43 (m, 2H), 7.38 (d, 2H, J = 7.6 Hz), 7.34 (d, 2H, J = 8.0 Hz), 6.62 (s, 1H), 2.66 (t, 2H, J = 7.6 Hz), 2.44 (s, 3H), 2.35 (t, 1H, J = 7.6 Hz), 1.71–1.78 (m, 2H), 1.62 (dd, 2H, J_1 = 14.8 Hz J_2 = 6.8 Hz), 1.25 (m, 25H), 0.87 (t, 3H, J = 6.8 Hz); ^{13}C{^{1}H} NMR ($CDCl_3$, 100 MHz): δ 170.8, 156.6, 144.8, 138.9, 132.7, 131.7, 130.0, 129.2, 127.8, 126.3, 117.6, 34.2, 33.9, 32.1, 29.91, 29.87, 29.8, 29.69, 29.65, 29.6, 29.50, 29.45, 29.31, 29.27, 24.9, 24.6, 22.9, 21.9, 14.3; IR (KBr, cm^{-1}): 3063, 2921, 2851, 1772, 1709, 1619, 1150, 1080; HRMS (ESI/Q-TOF) (m/z): calcd for $C_{33}H_{52}O_4SN$, $[M + NH_4]^+$: 558.3612, found 558.3612.

(Z)-1-Phenyl-2-tosylvinyl 2-cyclopropylacetate (1qb'):

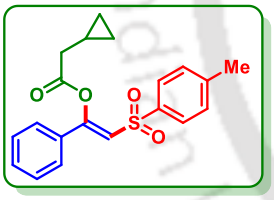

As a white solid (114 mg, 64% yield); mp 125–127 ^{o}C; purified over a column of silica gel (3% EtOAc in hexane); ^{1}H NMR ($CDCl_3$, 600 MHz): δ 7.89 (d, 2H, J = 8.4 Hz), 7.50 (d, 2H, J = 7.2 Hz), 7.46 (t, 1H, J = 7.2 Hz), 7.41 (d, 2H, J = 7.8 Hz), 7.37 (d, 2H, J = 7.8 Hz), 6.66 (s, 1H), 2.60 (d, 2H, J = 7.2 Hz), 2.46 (s, 3H), 1.89–1.24 (m, 1H), 0.68 (q, 2H, J_1 = 13.2 Hz, J_2 = 5.4 Hz), 0.33 (q, 2H, J_1 = 10.2 Hz, J_2 = 4.8 Hz) (a single J value for quartet); ^{13}C{^{1}H} NMR ($CDCl_3$, 150 MHz): δ 170.2, 156.5, 144.8, 138.9, 132.6, 131.7, 130.0, 129.1, 127.8, 126.3, 117.4, 39.4, 21.9, 6.7, 4.8; IR (KBr, cm^{-1}): 3066, 3001, 1772, 1621, 1149, 1080; HRMS (ESI/Q-TOF) (m/z): calcd for $C_{20}H_{24}O_4SN$, $[M + NH_4]^+$: 374.1421, found 374.1422.

(Z)-1-Phenyl-2-tosylvinyl (3r,5r,7r)-adamantane-1-carboxylate (1rb'):

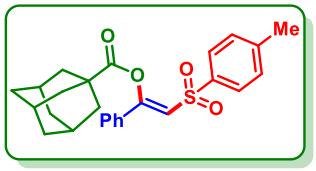

As a white solid (127 mg, 58% yield); mp 156–158 °C; purified over a column of silica gel (3% EtOAc in hexane); ^{1}H NMR ($CDCl_3$, 600 MHz): δ 7.86 (d, 2H, J = 8.4 Hz), 7.44 (t, 2H, J = 9.0 Hz), 7.41 (dd, 1H, J_1 = 7.8 Hz, J_2= 1.2 Hz), 7.37 (d, 2H, J = 7.8 Hz), 7.35 (d, 2H, J = 7.8 Hz), 6.57 (s, 1H), 2.44 (s, 3H), 2.14 (s, 6H), 2.11 (s, 3H), 1.78 (s, 6H); ^{13}C{^{1}H} NMR ($CDCl_3$, 150 MHz): δ 174.5, 156.7, 144.6, 139.0, 133.1, 131.5, 130.0, 129.1, 127.7, 126.2, 117.4, 41.4, 38.9, 36.6, 28.1, 21.9; IR (KBr, cm^{-1}): 3060, 2907, 2852, 1757, 1623, 1176, 1149, 1047; HRMS (ESI/Q-TOF) (m/z): calcd for $C_{26}H_{28}O_4SNa$, $[M + Na]^+$: 459.1601, found 459.1601.

(Z)-1-Phenyl-2-tosylvinyl benzo[d][1,3]dioxole-5-carboxylate (1sb'):

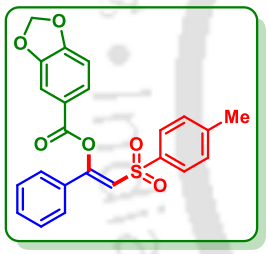

As a brown solid (127 mg, 60% yield); mp 152–154 °C; purified over a column of silica gel (12% EtOAc in hexane); ^{1}H NMR ($CDCl_3$, 600 MHz): δ 7.74 (d, 2H, J = 7.8 Hz), 7.68 (dd, 1H, J_1= 8.4 Hz, J_2 = 1.2 Hz), 7.44 (d, 1H, J = 1.8 Hz), 7.41 (d, 2H, J= 7.2 Hz), 7.35 (d, 1H, J = 7.8 Hz), 7.29 (t, 2H, J = 7.8 Hz), 7.19 (d, 2H, J = 7.8 Hz), 6.85 (d, 1H, J = 8.4 Hz), 6.71 (s, 1H), 6.03 (s, 2H), 2.33 (s, 3H); ^{13}C{^{1}H} NMR ($CDCl_3$, 150 MHz): δ 162.7, 156.8, 152.9, 148.2, 144.7, 138.6, 132.4, 131.7, 129.9, 129.2, 128.0, 127.1, 126.2, 122.2, 118.6, 110.3, 108.5, 102.3, 21.8; IR (KBr, cm^{-1}): 3058, 2929, 1745, 1611, 1482, 1257, 1149, 1063; HRMS (ESI/Q-TOF) (m/z): calcd for $C_{23}H_{18}O_6SNa$, $[M + Na]^+$: 445.0716, found 445.0715.

(Z)-1-Phenyl-2-tosylvinyl 2-naphthoate (1tb'):

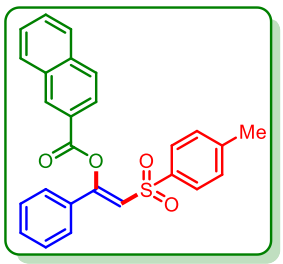

As a white solid (133 mg, 62% yield); mp 90–92 °C; purified over a column of silica gel (12% EtOAc in hexane); ^{1}H NMR ($CDCl_3$, 600 MHz): δ 8.71 (s, 1H), 8.09 (dd, 1H, J_1 = 8.4 Hz, J_2 = 1.8 Hz), 8.01 (d, 1H, J = 7.8 Hz), 7.96 (dd, 2H, J_1 = 12.6 Hz, J_2 = 8.4 Hz), 7.83 (d, 2H, J = 8.4 Hz), 7.66–7.69 (m, 1H), 7.60–7.63 (m,

1H), 7.55 (d, 2H, *J*= 7.8 Hz), 7.44 (t, 1H, *J* = 7.2 Hz), 7.37 (t, 2H, *J* = 7.8 Hz), 7.22 (d, 2H, *J* = 7.8 Hz), 6.87 (s, 1H), 2.37 (s, 3H);$^{13}C\{^{1}H\}$ NMR ($CDCl_3$, 150 MHz): δ 163.5, 156.8, 144.7, 138.6, 136.2, 132.7, 132.6, 132.4, 131.8¸129.9, 129.7, 129.2, 128.8, 128.5, 128.11, 128.09, 127.3, 126.3, 125.6, 125.5, 118.8, 21.8; IR (KBr, cm^{-1}): 3464, 3055, 2931, 1713, 1630, 1280, 1196, 1090; HRMS (ESI/Q-TOF) (m/z): calcd for $C_{26}H_{24}O_4SN$, $[M + NH_4]^+$: 446.1421, found 446.1412.

(Z)-1-Phenyl-2-tosylvinyl thiophene-2-carboxylate (1ub'):

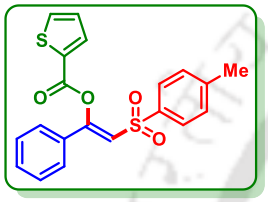

As a white solid (106 mg, 55% yield); mp 122–124 °C; purified over a column of silica gel (15% EtOAc in hexane); ^{1}H NMR ($CDCl_3$, 600 MHz): δ 7.97 (dd, 1H, J_1 = 4.2 Hz, J_2 = 1.2 Hz), 7.86 (d, 2H, *J* = 8.4 Hz), 7.73 (dd, 1H, J_1 = 5.4 Hz, J_2 = 1.2 Hz), 7.51 (d, 2H, *J* = 7.8 Hz), 7.43 (t, 1H, *J*= 7.8 Hz), 7.37 (t, 2H, *J* = 7.2 Hz), 7.28 (d, 2H, *J* = 7.8 Hz), 7.21 (dd, 1H, J_1 = 4.8 Hz, J_2 = 4.2 Hz), 6.80 (s, 1H), 2.41 (s, 3H); $^{13}C\{^{1}H\}$ NMR ($CDCl_3$, 150 MHz): δ 158.7, 156.1, 144.8, 138.6, 135.9, 134.6, 132.3, 131.8, 131.5, 129.9, 129.2, 128.5, 128.1, 126.3, 119.0, 21.9; IR (KBr, cm^{-1}): 3055, 2925, 1735, 1619, 1409, 1238, 1147, 1062; HRMS (ESI/Q-TOF) (m/z): calcd for $C_{20}H_{17}O_4S_2$, $[M + H]^+$: 385.0563, found 385.0565.

(Z)-1-(p-Tolyl)-2-tosylvinyl 4-methylbenzoate (2bb'):

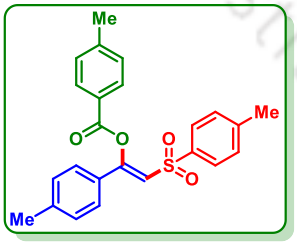

As a brown solid (151 mg, 74% yield); mp 123–125 °C; purified over a column of silica gel (8% EtOAc in hexane); ^{1}H NMR ($CDCl_3$, 400 MHz): δ 8.0 (d, 2H, *J* = 8.0 Hz), 7.80 (d, 2H, *J* = 8.4 Hz), 7.38, (d, 2H, *J* = 8.0 Hz), 7.33 (d, 2H, *J* = 8.0 Hz), 7.23 (d, 2H, *J* = 8.0 Hz), 7.15 (d, 2H, *J* = 8.0 Hz), 6.76 (s, 1H), 2.47 (s, 3H), 2.39 (s, 3H), 2.34 (s, 3H); $^{13}C\{^{1}H\}$ NMR ($CDCl_3$, 100 MHz): δ 163.4, 157.1, 145.3, 144.5, 142.4, 138.8, 130.8, 130.4, 129.9, 129.8, 129.6, 129.4, 128.0, 126.2, 117.6, 22.0, 21.8, 21.6; IR (KBr, cm^{-1}): 3049, 2924, 1746, 1689, 1610, 1148, 1085; HRMS (ESI/Q-TOF) (m/z): calcd for $C_{24}H_{22}O_4SNa$, $[M + Na]^+$: 429.1131, found 429.1135.

(Z)-1-(4-Methoxyphenyl)-2-tosylvinyl 4-methylbenzoate (3bb'):

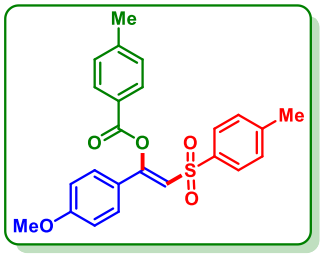

As a brown solid (165 mg, 78% yield); mp 128–130 °C; purified over a column of silica gel (12% EtOAc in hexane); ^{1}H NMR ($CDCl_3$, 600 MHz): δ 8.01 (d, 2H, J = 8.4 Hz), 7.79 (d, 2H, J = 8.4 Hz), 7.43, (d, 2H, J = 9.0 Hz), 7.33 (d, 2H, J = 7.8 Hz), 7.23 (d, 2H, J = 8.4 Hz), 6.85 (d, 2H, J = 8.4 Hz), 6.70 (s, 1H), 3.80 (s, 3H), 2.48 (s, 3H), 2.39 (s, 3H); ^{13}C{^{1}H} NMR ($CDCl_3$, 150 MHz): δ 163.3, 162.3, 156.7, 145.1, 144.2, 138.8, 132.0, 130.6, 129.6, 129.4, 127.8, 125.6, 124.4, 116.2, 114.4, 55.5, 21.9, 21.6; IR (KBr, cm^{-1}): 3066, 2925, 2853, 1745, 1602, 1156, 1087; HRMS (ESI/Q-TOF) (m/z): calcd for $C_{24}H_{26}O_5SN$, $[M + NH_4]^+$: 440.1526, found 440.1524.

(Z)-1-(4-(tert-Butyl)phenyl)-2-tosylvinyl 4-methylbenzoate (4bb'):

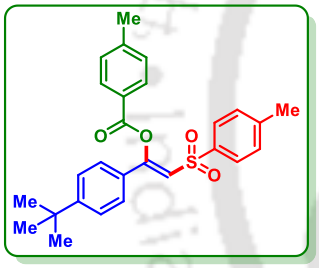

As a brown solid (169 mg, 75% yield); mp 159–161 °C; purified over a column of silica gel (8% EtOAc in hexane); ^{1}H NMR ($CDCl_3$, 400 MHz): δ 8.0 (d, 2H, J = 8.4 Hz), 7.80 (d, 2H, J = 8.4 Hz), 7.43 (d, 2H, J = 8.4 Hz), 7.37 (s, 1H), 7.34 (t, 3H, J = 8.0 Hz), 7.23 (d, 2H, J = 8.0 Hz), 6.79 (s, 1H), 2.48 (s, 3H), 2.39 (s, 3H), 1.27 (s, 9H); ^{13}C{^{1}H} NMR ($CDCl_3$, 100 MHz): δ 163.5, 157.0, 155.4, 145.3, 144.5, 138.9, 130.8, 129.8, 129.6, 129.5, 128.0, 126.2, 126.0, 125.8, 117.8, 35.1, 31.2, 22.0, 21.8; IR (KBr, cm^{-1}): 3052, 2957, 2920, 1746, 1610, 1264, 1177, 1067; HRMS (ESI/Q-TOF) (m/z): calcd for $C_{27}H_{32}O_4SN$, $[M + NH_4]^+$: 466.2047 found 466.2047.

(Z)-1-(m-Tolyl)-2-tosylvinyl 4-methylbenzoate (5bb'):

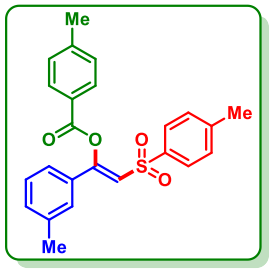

As a gummy (143 mg, 70% yield); purified over a column of silica gel (7% EtOAc in hexane); ^{1}H NMR ($CDCl_3$, 600 MHz): δ 8.01 (d, 2H, J = 7.8 Hz), 7.80 (d, 2H, J = 8.4 Hz), 7.33 (d, 2H, J = 7.8 Hz), 7.28–7.30 (m, 2H), 7.23 (d, 4H, J = 7.2 Hz), 6.79 (s, 1H), 2.48 (s, 3H), 2.39 (s, 3H), 2.31 (s, 3H); ^{13}C{^{1}H} NMR ($CDCl_3$, 150 MHz): δ 163.4, 157.1, 145.3, 144.6, 139.0, 138.7, 132.6, 132.5,

130.8, 129.8, 129.6, 129.1, 128.1, 126.8, 125.7, 123.4, 118.5, 22.0, 21.8, 21.6; IR (KBr, cm^{-1}): 3063, 2920, 1745, 1611, 1235, 1147, 1068; HRMS (ESI/Q-TOF) (m/z): calcd for $C_{24}H_{23}O_4S$, $[M + H]^+$: 407.1312, found 407.1336.

(Z)-1-(4-Chlorophenyl)-2-tosylvinyl 4-methylbenzoate (6bb'):

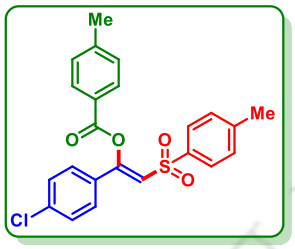

As a white solid (145 mg, 68% yield); mp 115–117 °C; purified over a column of silica gel (12% EtOAc in hexane); ^1H NMR ($CDCl_3$, 600 MHz): δ 8.0 (d, 2H, J = 8.4 Hz), 7.79, (d, 2H, J = 7.8 Hz), 7.42 (d, 2H, J = 9.0 Hz), 7.34 (s, 2H), 7.33 (d, 2H, J = 1.8 Hz), 7.24 (d, 2H, J = 8.4 Hz), 6.78 (s, 1H), 2.48 (s, 3H), 2.39 (s, 3H); $^{13}C\{^1H\}$ NMR ($CDCl_3$, 150 MHz): δ 163.4, 155.7, 145.6, 144.8, 138.4, 137.9, 131.1, 130.8, 129.9, 129.7, 129.5, 128.1, 127.5, 125.4, 119.1, 22.1, 21.9; IR (KBr, cm^{-1}): 3069, 2960, 2923, 1749, 1613, 1172, 1066; HRMS (ESI/Q-TOF) (m/z): calcd for $C_{23}H_{20}ClO_4S$, $[M + H]^+$: 427.0765, found 427.0767.

(Z)-1-(4-Bromophenyl)-2-tosylvinyl 4-methylbenzoate (7bb'):

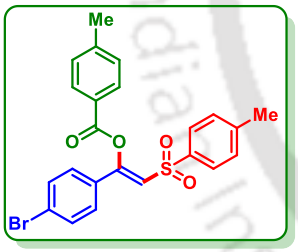

As a white solid (165 mg, 70% yield); mp 162–164 °C; purified over a column of silica gel (12% EtOAc in hexane); ^1H NMR ($CDCl_3$, 600 MHz): δ 8.0 (d, 2H, J = 8.4 Hz), 7.80 (d, 2H, J = 8.4 Hz), 7.48 (d, 2H, J = 8.4 Hz), 7.34 (dd, 4H, J_1 = 10.2 Hz, J_2 = 7.8 Hz), 7.24 (d, 2H, J = 7.8 Hz), 6.80 (s, 1H), 2.47 (s, 3H), 2.39 (s, 3H), $^{13}C\{^1H\}$ NMR ($CDCl_3$, 150 MHz): δ 163.3, 155.7, 145.6, 144.8, 138.3, 132.4, 131.5, 130.7, 129.9, 129.7, 128.1, 127.7, 126.3, 125.3, 119.1, 22.0, 21.8; IR (KBr, cm^{-1}): 3069, 2960, 2923, 1749, 1613; HRMS (ESI/Q-TOF) (m/z): calcd for $C_{23}H_{19}BrO_4SNa$, $[M + Na]^+$: 493.0080, found 493.0040.

(Z)-1-(4-Fluorophenyl)-2-tosylvinyl 4-methylbenzoate (8bb'):

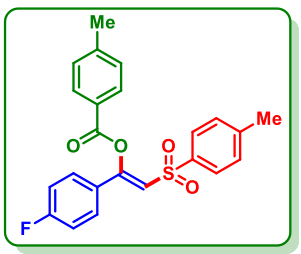

As a white solid (132 mg, 64% yield); mp 142–144 °C; purified over a column of silica gel (12% EtOAc in hexane); ^1H NMR ($CDCl_3$, 600 MHz): δ 8.0 (d, 2H, J = 8.4 Hz), 7.79 (d, 2H, J = 8.4 Hz), 7.47–7.50 (m, 2H), 7.33 (d, 2H, J = 8.4 Hz), 7.24 (d, 2H, J =

7.8 Hz), 7.05 (t, 2H, *J* = 9.0 Hz), 6.74 (s, 1H), 2.48 (s, 3H), 2.39 (s, 3H); $^{13}C\{^{1}H\}$ NMR ($CDCl_3$, 150 MHz): δ 164.8, (d, *J* = 100.8 Hz), 155.8, 144.8, 144.7 (d, *J* = 48.1 Hz), 138.5, 130.8, 129.9, 129.7, 128.7 (d, *J* = 12.6), 128.52, 128.47, 128.1, 125.5, 118.6, 116.5 (d, *J* = 28.2 Hz), 22.1, 21.9; ^{19}F NMR ($CDCl_3$, 564 MHz): δ –107.4; IR (KBr, cm^{-1}): 3063, 2923, 2853, 1745, 1610, 1238, 1147, 1064; HRMS (ESI/Q-TOF) (m/z): calcd for $C_{23}H_{23}FO_4SN$, $[M + NH_4]^+$: 428.1326, found 428.1320.

(Z)-1-(3-Fluorophenyl)-2-tosylvinyl 4-methylbenzoate (9bb'):

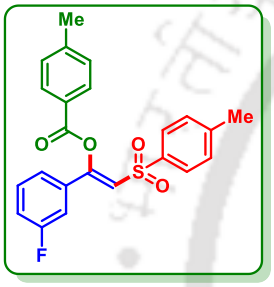

As a white solid (126 mg, 61% yield); mp 121–123 °C; purified over a column of silica gel (12% EtOAc in hexane); ^{1}H NMR ($CDCl_3$, 400 MHz): δ 8.01 (d, 2H, *J* = 8.4 Hz), 7.80 (d, 2H, *J* = 8.4 Hz), 7.33 (d, 3H, *J* = 8.0 Hz), 7.28–7.31 (m, 1H), 7.24 (d, 2H, *J* = 8.0 Hz), 7.15–7.19 (m, 1H), 7.08–7.14 (m, 1H), 6.80 (s, 1H), 2.48 (s, 3H), 2.39 (s, 3H); $^{13}C\{^{1}H\}$ NMR ($CDCl_3$, 100 MHz): δ 163.4, 163.0 (d, *J* = 98.6 Hz), 155.3 (d, *J* = 11.2 Hz), 145.6, 144.9, 138.4, 134.9 (d, *J*= 30.4 Hz), 130.9, 130.8, 129.9, 129.7, 128.1, 125.4, 122.0 (d, *J* = 12.4 Hz), 119.8, 118.6 (d, *J*= 84.4 Hz), 113.3 (d, *J* = 38.3 Hz), 22.0, 21.8; ^{19}F ($CDCl_3$, 376 MHz): δ –111.2; IR (KBr, cm^{-1}): 3066, 2925, 2857, 1736, 1487, 1216, 1100, 1030; HRMS (ESI/Q-TOF) (m/z): calcd for $C_{23}H_{19}FO_4SNa$, $[M + Na]^+$: 433.0880, found 433.0898.

(Z)-1-(3-Chlorophenyl)-2-tosylvinyl 4-methylbenzoate (10bb'):

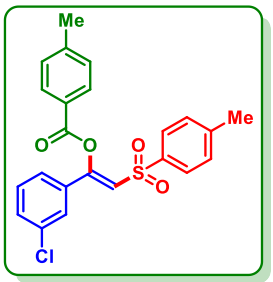

As a white solid (139 mg, 65% yield); mp 122–124 °C; purified over a column of silica gel (10% EtOAc in hexane); ^{1}H NMR ($CDCl_3$, 400 MHz): δ 8.0 (d, 2H, *J* = 8.4 Hz), 7.79 (d, 2H, *J* = 8.0 Hz), 7.44 (t, 1H, *J* = 7.6 Hz), 7.35–7.38 (m, 2H), 7.32 (d, 2H, *J* = 8.0 Hz), 7.29 (d, 1H, *J* = 8.0 Hz), 7.23 (d, 2H, *J* = 8.0 Hz),), 6.78 (s, 1H), 2.46 (s, 3H), 2.38 (s, 3H); $^{13}C\{^{1}H\}$ NMR ($CDCl_3$, 100 MHz): δ 163.2, 155.1, 145.4, 144.7, 138.2, 135.2, 134.4, 131.5, 130.7, 130.3, 129.8, 129.5, 128.0, 126.1, 125.2, 124.3, 119.7, 21.9, 21.7; IR (KBr,

cm^{-1}): 3065, 2925, 2851, 1749, 1613, 1172, 1066; HRMS (ESI/Q-TOF) (m/z): calcd for $C_{23}H_{23}ClO_4SN$, $[M + NH_4]^+$: 444.1031, found 444.1031.

(Z)-1-Cyclohexyl-2-tosylvinyl 4-methylbenzoate (11bb'):

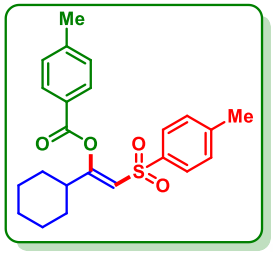

As a gummy (142 mg, 71% yield); purified over a column of silica gel (5% EtOAc in hexane); ^{1}H NMR ($CDCl_3$, 500 MHz): δ 7.93 (d, 2H, J = 7.5 Hz), 7.72 (d, 2H, J = 7.5 Hz), 7.28 (d, 2H, J = 7.5 Hz), 7.23 (d, 2H, J = 7.5 Hz), 6.17 (s, 1H), 2.44 (s, 3H), 2.39 (s, 3H), 1.63–1.67 (m, 2H), 1.59 (s, 4H), 0.90 (t, 3H, J = 11.5 Hz), 0.83 (d, 2H, J = 3.5 Hz); ^{13}C{^{1}H} NMR ($CDCl_3$, 125 MHz): δ 163.6, 162.5, 145.1, 144.3, 138.9, 130.7, 129.8, 129.5, 127.9, 126.0, 116.4, 29.90, 29.87, 22.0, 21.8, 15.9, 7.1; IR (KBr, cm^{-1}): 3058, 2915, 2824, 1748, 1619, 1152, 1035.; HRMS (ESI/Q-TOF) (m/z): calcd for $C_{23}H_{27}O_4S$, $[M + H]^+$: 399.1625, found 399.1680.

(Z)-1-((1-Iodo-1-phenylprop-1-en-2-yl)sulfonyl)-4-methylbenzene (12b'):

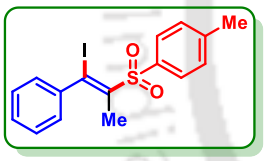

As a brown solid (161 mg, 80% yield); mp 120–122 ^{o}C; purified over a column of silica gel (3% EtOAc in hexane); ^{1}H NMR ($CDCl_3$, 400 MHz): δ 7.39 (d, 2H, J = 8.4 Hz), 7.23 (t, 3H, J = 6.5 Hz), 7.16 (d, 2H, J = 8.0 Hz), 7.09–7.12 (m, 2H), 2.51 (s, 3H), 2.39 (s, 3H); ^{13}C{^{1}H} NMR ($CDCl_3$, 100 MHz): δ 144.3, 144.1, 143.2, 137.5, 129.7, 128.8, 128.0, 127.84, 127.76, 115.9, 27.3. 21.8; IR (KBr, cm^{-1}): 3035, 2928, 2847, 1587, 1442, 1135, 1080; HRMS (ESI/Q-TOF) (m/z): calcd for $C_{16}H_{19}IO_2SN$, $[M + NH_4]^+$: 416.0187, found 416.0183.

(Z)-2-(Phenylsulfonyl)-1-(p-tolyl)vinyl 4-methylbenzoate (2ba'):

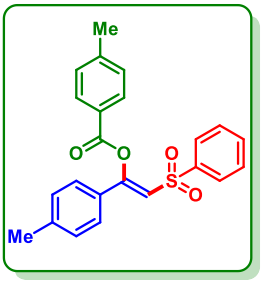

As a brown solid (139 mg, 70% yield); mp 132–134 ^{o}C; purified over a column of silica gel (8% EtOAc in hexane); ^{1}H NMR ($CDCl_3$, 400 MHz): δ 8.0 (d, 2H, J = 8.4 Hz), 7.93 (d, 2H, J = 8.0 Hz), 7.56 (t, 1H, J = 7.6 Hz), 7.44, (t, 2H, J = 8.0 Hz), 7.39 (d, 2H, J = 8.4 Hz), 7.33 (d, 2H, J = 8.4 Hz), 7.16 (d, 2H, J = 8.0 Hz), 6.78 (s, 1H), 2.47 (s, 3H), 2.39 (s, 3H), 2.34 (s, 3H); ^{13}C{^{1}H} NMR ($CDCl_3$, 100

MHz): δ 163.4, 157.6, 145.4, 142.5, 141.8, 133.5, 130.8, 130.0, 129.6, 129.5, 129.2, 128.0, 126.2, 125.7, 117.4, 22.0, 21.6; IR (KBr, cm^{-1}): 3056, 2925, 1744, 1611, 1261, 1055; HRMS (ESI/Q-TOF) (m/z): calcd for $C_{23}H_{24}O_4SN$, $[M + NH_4]^+$: 410.1432, found 410.1431.

***(Z)-1-(4-(tert-Butyl)phenyl)-2-(phenylsulfonyl)vinyl4-methylbenzoate* (*4ba'*):**

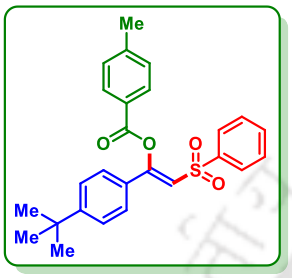

As a brown solid (152 mg, 72% yield); mp 160–162 °C; purified over a column of silica gel (12% EtOAc in hexane); ^{1}H NMR ($CDCl_3$, 500 MHz): δ 8.01, (d, 2H, J = 8.5 Hz), 7.94 (d, 2H, J = 8.0 Hz), 7.55 (t, 1H, J = 7.5 Hz), 7.43–7.46 (m, 4H), 7.37 (d, 2H, J = 8.5 Hz), 7.33 (d, 2H, J = 8.0 Hz), 6.81 (s, 1H), 2.47 (s, 3H), 1.28 (s, 9H); $^{13}C\{^1H\}$ NMR ($CDCl_3$, 125 MHz): δ 163.4, 157.5, 155.5, 145.3, 141.8, 133.5, 130.7, 129.6, 129.4, 129.1, 127.9, 126.2, 126.1, 125.7, 117.5, 35.1, 31.2, 22.0; IR (KBr, cm^{-1}): 3052, 2988, 1745, 1611, 1261, 1065; HRMS (ESI/Q-TOF) (m/z): calcd for $C_{26}H_{30}O_4SN$, $[M + NH_4]^+$: 452.1901, found 452.1898.

***(Z)-1-(4-Bromophenyl)-2-(phenylsulfonyl)vinyl 4-methylbenzoate* (*7ba'*):**

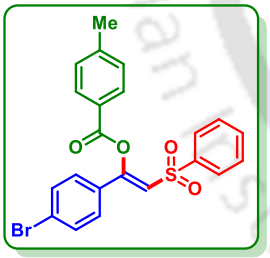

As a brown solid (157 mg, 68% yield); mp 157–159 °C; purified over a column of silica gel (10% EtOAc in hexane); ^{1}H NMR ($CDCl_3$, 500 MHz): δ 7.95 (d, 2H, J = 5.5 Hz), 7.88 (d, 2H, J = 7.0 Hz), 7.50 (d, 1H, J = 7.5 Hz), 7.44 (d, 2H, J = 6.5 Hz),), 7.35–7.40 (m, 3H), 7.29 (t, 2H, J = 8.5 Hz), 7.21 (d, 1H, J = 7.0 Hz), 6.77 (s, 1H), 2.41 (s, 3H); $^{13}C\{^1H\}$ NMR ($CDCl_3$, 125 MHz): δ 163.4, 157.4, 145.4, 141.6, 133.6, 132.4, 131.8, 130.8, 129.7, 129.20, 129.17, 128.0, 126.3, 125.6, 118.4, 22.0; IR (KBr, cm^{-1}): 3065, 2959, 2928, 1745, 1610; HRMS (ESI/Q-TOF) (m/z): calcd for $C_{22}H_{21}BrO_4SN$, $[M + NH_4]^+$: 474.0380, found 474.0358.

***(Z)-2-((4-(tert-butyl)phenyl)sulfonyl)-1-phenylvinyl 4-methylbenzoate* (*1bc'*):**

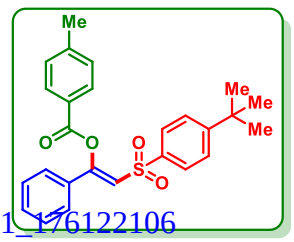

As a gummy (162 mg, 74% yield); purified over a column of silica gel (15% EtOAc in hexane); ^{1}H NMR ($CDCl_3$, 500 MHz): δ

8.0, (d, 2H, *J*= 5.0 Hz), 7.84 (d, 2H, *J* = 8.5 Hz), 7.49 (t, 2H, *J* = 8.0 Hz), 7.43 (t, 3H, *J* = 12.0 Hz), 7.34 (dd, 4H, J_1 = 18.0 Hz, J_2 = 7.5 Hz), 6.82 (s, 1H), 2.48 (s, 3H), 1.30 (s, 9H); $^{13}C\{^1H\}$ NMR ($CDCl_3$, 125 MHz): δ 163.4, 157.5, 156.8, 145.4, 138.5, 132.6, 131.7, 130.8, 129.6, 129.2, 127.9, 126.26, 126.25, 125.7, 118.8, 35.4, 31.2, 22.0; IR (KBr, cm^{-1}): 3064, 2928, 2905, 1745, 1618; HRMS (ESI/Q-TOF) (m/z): calcd for $C_{26}H_{27}O_4S$, $[M + H]^+$: 435.1625, found 435.1611.

***(Z)-2-((4-chlorophenyl)sulfonyl)-1-phenylvinyl 4-methylbenzoate* (*1bd'*):**

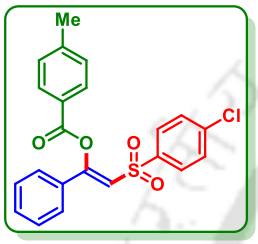

As a white solid (137 mg, 66% yield); mp 142–149 °C; purified over a column of silica gel (10% EtOAc in hexane); ^1H NMR ($CDCl_3$, 400 MHz): δ 7.99 (d, 2H, *J* = 8.0 Hz), 7.85 (d, 2H, *J* = 8.4 Hz), 7.50 (d, 3H, *J* = 7.6 Hz), 7.39 (d, 2H, *J* = 2.8 Hz), 7.35 (t, 4H, *J* = 8.0 Hz), 6.79 (s, 1H), 2.48 (s, 3H); $^{13}C\{^1H\}$ NMR ($CDCl_3$, 125 MHz): δ 163.4, 157.8, 145.7, 140.4, 140.1, 132.3, 132.0, 130.8, 129.8, 129.6, 129.3, 129.2, 126.4, 125.5, 118.1, 22.1; IR (KBr, cm^{-1}): 3062, 2929, 2908, 1744, 1618; HRMS (ESI/Q-TOF) (m/z): calcd for $C_{22}H_{21}ClO_4SN$, $[M + NH_4]^+$: 430.0874, found 430.0854.

***(Z)-2-((4-Bromophenyl)sulfonyl)-1-phenylvinyl 4-methylbenzoate* (*1be'*):**

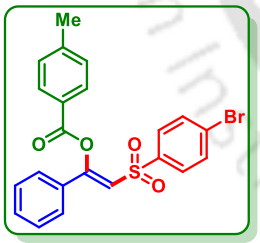

As a white solid (154 mg, 67% yield); mp 120–122 °C; purified over a column of silica gel (15% EtOAc in hexane); ^1H NMR ($CDCl_3$, 400 MHz): δ 7.99 (d, 2H, *J* = 8.0 Hz), 7.78 (d, 2H, *J* = 8.8 Hz), 7.57 (d, 2H, *J* = 8.8 Hz), 7.50, (d, 2H, *J* = 7.6 Hz), 7.44 (t, 1H, *J* = 7.2 Hz), 7.38 (d, 2H, *J* = 7.6 Hz), 7.34 (d, 2H, *J* = 7.6 Hz), 6.79 (s, 1H), 2.48 (s, 3H); $^{13}C\{^1H\}$ NMR ($CDCl_3$, 125 MHz): δ 163.3, 157.8, 145.7, 140.6, 132.6, 132.3, 132.0, 130.8, 129.8, 129.6, 129.3, 128.9, 126.3, 125.5, 118.0, 22.1; IR (KBr, cm^{-1}): 3068, 2965, 2923, 1745, 1610; HRMS (ESI/Q-TOF) (m/z): calcd for $C_{22}H_{17}BrO_4SK$, $[M +K]^+$: 494.9673, found 494.9663.

***(Z)-1-(4-Bromophenyl)-2-(phenylsulfonyl)vinyl 4-methoxy benzoate* (*1ce'*):**

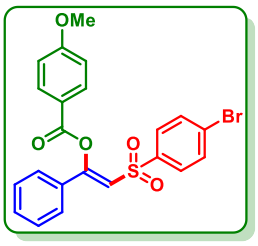

As a white solid (173 mg, 73% yield); mp 138–140 °C; purified over a column of silica gel (15% EtOAc in hexane); ^{1}H NMR ($CDCl_3$, 400 MHz): δ 8.05 (d, 2H, J = 8.8 Hz), 7.78 (d, 2H, J = 8.4 Hz), 7.57 (d, 2H, J = 8.4 Hz), 7.50, (d, 2H, J = 7.6 Hz), 7.43 (d, 1H, J = 7.6 Hz), 7.36 (t, 2H, J = 7.2 Hz), 7.01 (d, 2H, J = 8.8 Hz), 6.79 (s, 1H), 3.92 (s, 3H); ^{13}C{^{1}H} NMR ($CDCl_3$, 125 MHz): δ 164.7, 162.9, 157.8, 140.6, 132.9, 132.5, 132.3, 131.9, 129.6, 129.2, 128.9, 126.3, 120.4, 118.0, 114.4, 55.8; IR (KBr, cm^{-1}): 3069, 2948, 2925, 1747, 1628; HRMS (ESI/Q-TOF) (m/z): calcd for $C_{22}H_{21}BrO_5SN$, [M + NH_4]$^{+}$: 490.0329, found 490.0310.

***(Z)-1-(4-Bromophenyl)-2-(phenylsulfonyl)vinyl 4-chlorobenzoate* (*1de'*):**

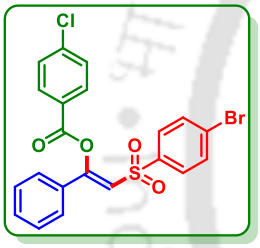

As a white solid (150 mg, 62% yield); mp 125–127 °C; purified over a column of silica gel (12% EtOAc in hexane); ^{1}H NMR ($CDCl_3$, 400 MHz): δ 8.06 (d, 2H, J = 8.5 Hz), 7.78 (d, 2H, J = 8.5 Hz), 7.61 (d, 2H, J = 8.5 Hz), 7.53 (d, 2H, J = 8.0 Hz), 7.50 (d, 2H, J = 7.5 Hz), 7.45 (d, 1H, J = 7.0 Hz), 7.39 (t, 2H, J = 7.5 Hz), 6.78 (s, 1H), ^{13}C{^{1}H} NMR ($CDCl_3$, 100 MHz): δ 162.6, 157.2, 141.3, 140.5, 132.7, 132.2, 132.04, 132.01, 129.50, 129.47, 129.4, 129.1, 126.8, 126.3, 117.8; IR (KBr, cm^{-1}): 3058, 2925, 2912, 1742, 1628, 1158, 1050; HRMS (ESI/Q-TOF) (m/z): calcd for $C_{21}H_{18}BrClO_4SN$, [M + NH_4]$^{+}$: 493.9834, found 493.9834.

***(Z)-2-((4-nitrophenyl)sulfonyl)-1-phenylvinyl 4-methylbenzoate* (*1bf'*):**

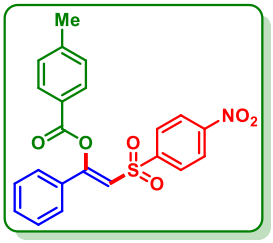

As a white solid (139 mg, 58% yield); mp 145–147 °C; purified over a column of silica gel (15% EtOAc in hexane); ^{1}H NMR ($CDCl_3$, 400 MHz): δ 7.91, (dd, 1H, J_1 = 8.0 Hz, J_2 = 1.2 Hz), 7.75 (d, 2H, J = 8.0 Hz), 7.64 (d, 1H, J = 8.0 Hz), 7.45, (d, 2H, J= 7.6 Hz), 7.36 (d, 1H, J = 7.2 Hz), 7.31 (d, 2H, J = 7.6 Hz), 7. 27 (dd, 1H, J_1 = 7.6 Hz, J_2 = 1.2 Hz),), 7.19 (d, 2H, J_1 = 7.6 Hz), 7.10 (t, 1H, J = 7.6 Hz), 7.04 (s, 1H), 2.38 (s, 3H); ^{13}C{^{1}H} NMR ($CDCl_3$, 100 MHz): δ 162.7, 158.2, 145.5, 141.0, 135.4, 134.4, 131.4, 130.7,

129.6, 129.3, 127.5, 126.4, 121.2, 118.0; 22.0; IR (KBr, cm^{-1}): 3065, 2938, 2935, 1744, 1610; HRMS (ESI/Q-TOF) (m/z): calcd for $C_{22}H_{17}NO_6SNa$, $[M + Na]^+$: 446.0669, found 446.2684.

(Z)-2-((2-bromo-4-(trifluoromethyl)phenyl)sulfonyl)-1-phenylvinyl4-methylbenzoate (1bg'):

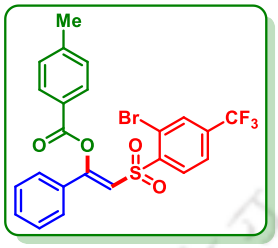

As a white solid (131 mg, 50% yield); mp 132–135 °C; purified over a column of silica gel (15% EtOAc in hexane); ^1H NMR ($CDCl_3$, 400 MHz): δ 8.08 (d, 1H, J = 8.0 Hz), 7.96, (s, 1H), 7.77 (d, 2H, J = 8.4 Hz), 7.53 (d, 2H, J = 7.6 Hz), 7.46 (d, 1H, J = 7.6 Hz), 7.35–7.42 (m, 3H), 7.28 (s, 1H),), 7.26 (s, 1H), 7.10 (s, 1H), 2.47 (s, 3H); $^{13}C\{^1H\}$ NMR ($CDCl_3$, 100 MHz): δ 162.6, 159.1, 145.9, 144.3, 136.1, 135.8, 132.4 (q, J = 30.4 Hz), 132.3, 132.1, 132.0, 130.6, 129.7, 129.4, 126.5, 125.0, 124.5 (q, J = 29.6 Hz), 122.0, 117.2, 22.1; ^{19}F NMR ($CDCl_3$, 376 MHz): δ –63.30; IR (KBr, cm^{-1}): 3064, 2928, 2915, 1743, 1625; HRMS (ESI/Q-TOF) (m/z): calcd for $C_{23}H_{20}BrF_3O_4SN$, $[M + NH_4]^+$: 542.0243, found 542.0230.

(Z)-1-phenyl-2-(thiophen-2-ylsulfonyl)vinyl 4-methylbenzoate (1bh'):

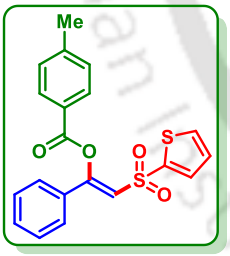

As a brown solid (100 mg, 52% yield); mp 158–160 °C; purified over a column of silica gel (15% EtOAc in hexane); ^1H NMR ($CDCl_3$, 500 MHz): δ 8.08 (d, 2H, J = 8.0 Hz), 7.69 (d, 1H, J = 4.0 Hz), 7.65 (d, 1H, J = 5.0 Hz), 7.53 (d, 2H, J = 7.5 Hz), 7.44 (t, 1H, J = 12.0 Hz), 7. 38 (d, 2H, J = 7.5 Hz), 7.34 (d, 2H, J = 9.5 Hz), 7.06 (t, 1H, J = 9.0 Hz), 6.86 (s, 1H), 2.47 (s, 3H); $^{13}C\{^1H\}$ NMR ($CDCl_3$, 125 MHz): δ 163.5, 157.5, 145.5, 143.1, 134.04, 134.0, 132.5, 131.9, 130.9, 129.7, 129.3, 127.9, 126.4, 125.7, 118.6, 22.0; IR (KBr, cm^{-1}): 3059, 2928, 2915, 1742, 1625; HRMS (ESI/Q-TOF) (m/z): calcd for $C_{20}H_{17}O_4S_2$, $[M + H]^+$: 385.0563, found 385.0562.

(Z)-2-(methylsulfonyl)-1-phenylvinyl 4-methylbenzoate (1bi'):

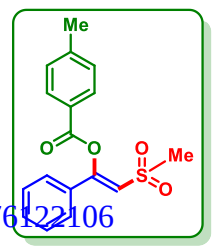

As a gummy (111 mg, 70% yield); purified over a column of silica gel (9% EtOAc in hexane); ^1H NMR ($CDCl_3$, 500 MHz): δ 8.08 (d, 2H, J = 7.5 Hz), 7.58 (d, 2H, J = 8.0 Hz), 7.42 (t, 2H, J = 7.5

Hz), 7.33 (d, 2H, J = 7.5 Hz), 6.72 (s, 1H), 3.11 (s, 3H), 2.46 (s, 3H); $^{13}C\{^1H\}$ NMR ($CDCl_3$, 125 MHz): δ 163.8, 158.1, 145.6, 132.4, 132.0, 130.8, 129.8, 129.3, 126.4, 125.6, 117.0, 43.8, 22.0; IR (KBr, cm^{-1}): 3059, 2924, 2912, 1744; HRMS (ESI/Q-TOF) (m/z): calcd for $C_{17}H_{16}O_4SNa$, $[M + Na]^+$: 339.0662, found 339.0688.

***(Z)-1-Methyl-4-((2-thiocyanato-2-(p-tolyl)vinyl)sulfonyl)benzene* (*2vb′*):**

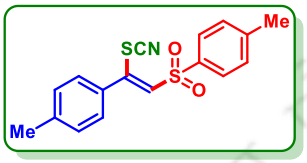

As a brown solid (91 mg, 55% yield); mp 136–138 °C; purified over a column of silica gel (8% EtOAc in hexane); ^1H NMR ($CDCl_3$, 500 MHz): δ 7.89 (d, 2H, J = 8.0 Hz), 7.40 (d, 2H, J = 8.0 Hz), 7.24 (dd, 4H, J_1 = 16.5 Hz, J_2 = 8.0 Hz), 6.64 (s, 1H), 2.48 (s, 3H), 2.37 (s, 3H); $^{13}C\{^1H\}$ NMR ($CDCl_3$, 125 MHz): δ 145.9, 145.6, 142.3, 137.0, 132.6, 130.4, 130.1, 129.9, 128.3, 127.8, 108.5, 21.9, 21.6; IR (KBr, cm^{-1}): 3388, 2948, 2257, 1637, 1436; HRMS (ESI/Q-TOF) (m/z): calcd for $C_{17}H_{15}NO_2S_2K$, $[M + K]^+$: 368.0187, found 368.0176.

***(Z)-1-(tert-Butyl)-4-(1-thiocyanato-2-tosylvinyl)benzene* (*4vb′*):**

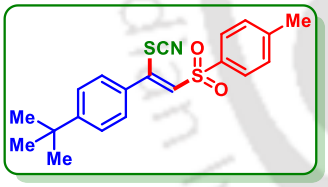

As a brown solid (109 mg, 58% yield); mp 142–144 °C; purified over a column of silica gel (8% EtOAc in hexane); ^1H NMR ($CDCl_3$, 500 MHz): δ 7.90, (d, 2H, J = 8.0 Hz), 7.44 (t, 2H, J = 8.5 Hz), 7.41 (d, 2H, J = 8.0 Hz), 7.35 (dd, 2H, J_1 = 6.5 Hz, J_2 = 2.0 Hz), 6.65 (s, 1H), 2.49 (s, 3H), 1.31 (s, 9H); $^{13}C\{^1H\}$ NMR ($CDCl_3$, 125 MHz): δ 155.5, 145.9, 145.4, 137.1, 132.6, 130.5, 130.3, 128.2, 127.9, 126.2, 108.5, 35.2, 31.3, 22.0; IR (KBr, cm^{-1}): 3368, 2975, 2265, 1686, 1484 HRMS (ESI/Q-TOF) (m/z): calcd for $C_{20}H_{21}NO_2S_2K$, $[M + K]^+$: 410.0656, found 410.0655.

***(Z)-1-Methyl-3-(2-(phenylsulfonyl)-1-thiocyanatovinyl)benzene* (*5va′*):**

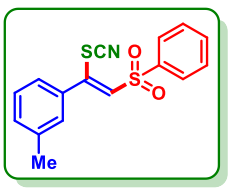

As a gummy (90 mg, 54% yield); purified over a column of silica gel (8% EtOAc in hexane); ^1H NMR ($CDCl_3$, 400 MHz): δ 7.55 (t, 2H, J = 8.0 Hz), 7.95, (d, 2H, J = 8.0 Hz), 7.65 (t, 1H, J = 7.2 Hz), 7.24 (t, 2H, J = 5.6 Hz), 7.10 (d, 2H, J = 11.2 Hz),), 6.58 (s, 1H),

2.30 (s, 3H); $^{13}C\{^{1}H\}$ NMR ($CDCl_3$, 100 MHz): δ 146.4, 140.0, 139.3, 135.4, 134.7, 132.5, 130.0, 129.9, 129.1, 128.8, 127.8, 125.5, 108.3, 21.5; IR (KBr, cm^{-1}): 3387, 2946, 2257, 1637, 1435; HRMS (ESI/Q-TOF) (m/z): calcd for $C_{16}H_{13}NO_2S_2Na$, $[M + Na]^+$: 333.0737, found 333.0710.

(Z)-1-((2-Iodo-2-phenylvinyl)sulfonyl)-4-methylbenzene (B):

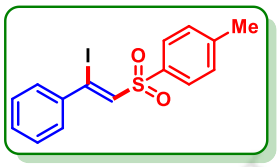

As a brown solid (2 mmol scale, 560 mg, 74%); mp 80–82 °C; purified over a column of silica gel (5% EtOAc in hexane); ^{1}H NMR ($CDCl_3$, 400 MHz): δ 7.38 (d, 2H, J = 8.4 Hz), 7.29 (s, 1H), 7.22 (dd, 3H, J_1 = 15.6 Hz, J_2 = 8.0 Hz), 7.15 (d, 2H, J = 6.4 Hz), 7.11 (d, 2H, J = 8.0 Hz), 2.32 (s, 3H); $^{13}C\{^{1}H\}$ NMR ($CDCl_3$, 100 MHz): δ 144.8, 141.4, 139.8, 137.5, 130.0, 129.9, 128.1, 128.0, 127.9, 114.4, 21.8; IR (KBr, cm^{-1}): 3038, 2923, 2847, 1585, 1443, 1149, 1084; HRMS (ESI/Q-TOF) (m/z): calcd for $C_{15}H_{14}IO_2S$, $[M + H]^+$ 384.9754, found 384.9751.

2,6-di-tert-Butyl-4-(tosylmethyl)phenol (M):

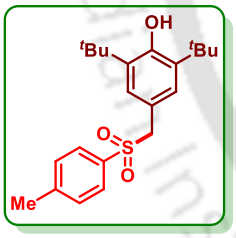

As a white solid (122 mg, 65% yield); mp 102–104 °C; purified over a column of silica gel (3% EtOAc in hexane); ^{1}H NMR ($CDCl_3$, 400 MHz): δ 7.44 (d, 2H, J = 8.4 Hz), 7.21 (d, 2H, J = 8.0 Hz), 6.73 (s, 2H), 5.24 (s, 1H), 4.19 (s, 2H), 2.40 (s, 3H), 1.31 (s, 18H); $^{13}C\{^{1}H\}$ NMR ($CDCl_3$, 100 MHz): δ 154.4, 144.5, 136.2, 135.1, 129.5, 129.1, 127.9, 119.1, 63.4, 34.3, 30.2, 21.7; IR (KBr, cm^{-1}): 3631, 3585, 2957, 1597, 1435, 1316, 1299, 1148, 1086; HRMS (ESI/Q-TOF) (m/z): calcd for $C_{22}H_{34}O_3SN$, $[M + NH_4]^+$: 392.2254, found 392.2258.

1-Phenyl-2-tosylethan-1-one (X):

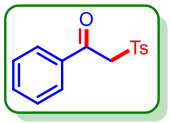

As a brown solid (110 mg, 80% yield); mp 110–112 °C; purified over a column of silica gel (15% EtOAc in hexane); ^{1}H NMR ($CDCl_3$, 600 MHz): δ 7.95 (d, 2H, J = 7.2 Hz), 7.76 (d, 2H, J = 8.4 Hz), 7.62 (t, 1H, J = 7.2 Hz), 7.48 (t, 2H, J = 7.8 Hz), 7.34 (d, 2H, J = 7.8 Hz), 4.72 (s, 2H), 2.44 (s, 3H); $^{13}C\{^{1}H\}$ NMR ($CDCl_3$, 150 MHz): δ 188.4,

145.6, 135.93, 135.88, 134.6, 130.0, 129.6, 129.1, 128.8, 63.8, 21.9; IR (KBr, cm^{-1}): 3052, 1679, 1597, 1445, 1323, 1158, 1087; HRMS (ESI/Q-TOF) (m/z): calcd for $C_{15}H_{15}O_3S$, $[M + H]^+$ 275.0736, found 275.0730.

N-Butyl-4-methylbenzamide (Y):

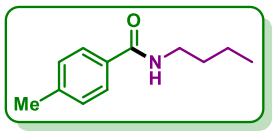

As a gummy (62 mg, 65% yield); purified over a column of silica gel (8% EtOAc in hexane); ^1H NMR ($CDCl_3$, 400 MHz): δ 7.65 (d, 2H, J = 8.4 Hz), 7.22 (d, 2H, J = 8.0 Hz), 6.1 (s, 1H), 3.44 (dd, 2H, J_1 = 9.6 Hz, J_2 = 7.2 Hz), 2.38 (s, 3H), 1.55–1.63 (m, 2H), 1.36–1.45 (m, 2H), 0.95 (t, 3H, J = 7.6 Hz); $^{13}C\{^1H\}$ NMR ($CDCl_3$, 100 MHz): δ 167.7, 141.9, 132.2, 129.4, 127.0, 39.9, 32.0, 21.6, 20.4, 14.0; IR (KBr, cm^{-1}): 3314, 2957, 2929, 1631, 1543, 1305, 1153; HRMS (ESI/Q-TOF) (m/z): calcd for $C_{12}H_{18}NO$, $[M + H]^+$: 192.1383, found 192.1383.

Sodium 4-nitrobenzenesulfinate (f'):

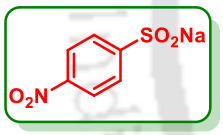

As white solid (2 mmol scale, 384 mg, 92%); ^1H NMR (D_2O, 500 MHz): δ 7.81 (d, 1H, J = 6.5 Hz), 7.62 (t, 2H, J = 7.0 Hz), 7.41 (s, 1H); $^{13}C\{^1H\}$ NMR (D_2O, 125 MHz): δ 133.2, 132.2, 128.6, 123.7.

Sodium 2-bromo-4-(trifluoromethyl)benzenesulfinate (g'):

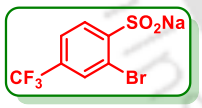

As white solid (2 mmol scale, 547 mg, 88%); ^1H NMR (D_2O, 500 MHz): δ 8.08 (s, 1H), 7.95 (q, 2H, J = 8.5 Hz); $^{13}C\{^1H\}$ NMR (D_2O, 125 MHz): δ 130.3, 130.2, 125.5 (q, J = 11.5 Hz), 124.41, 124.36, 120.9, 120.6; ^{19}F NMR (D_2O, 470 MHz): δ –62.5.

Sodium thiophene-2-sulfinate (h'):

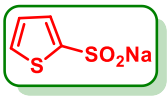

As brown solid (2 mmol scale, 316 mg, 93%); ^1H NMR (D_2O, 500 MHz): δ 7.70 (d, 1H, J = 4.5 Hz), 7.43 (d, 1H, J = 3.5 Hz) 7.23 (t, 1H, J = 4.5 Hz); $^{13}C\{^1H\}$ NMR (D_2O, 125 MHz): δ 158.6, 128.7, 127.8, 126.5.

Sodium methanesulfinate (i'):

As white solid (2 mmol scale, 196 mg, 96%); ^1H NMR (D_2O, 500 MHz): δ 2.45 (s, 1H); $^{13}C\{^1H\}$ NMR (D_2O, 125 MHz): δ 48.1.

II.7. Representative Spectra

(Z)-1-Phenyl-2-tosylvinyl benzoate (1az): **^{1}H NMR ($CDCl_3$, 600 MHz)**

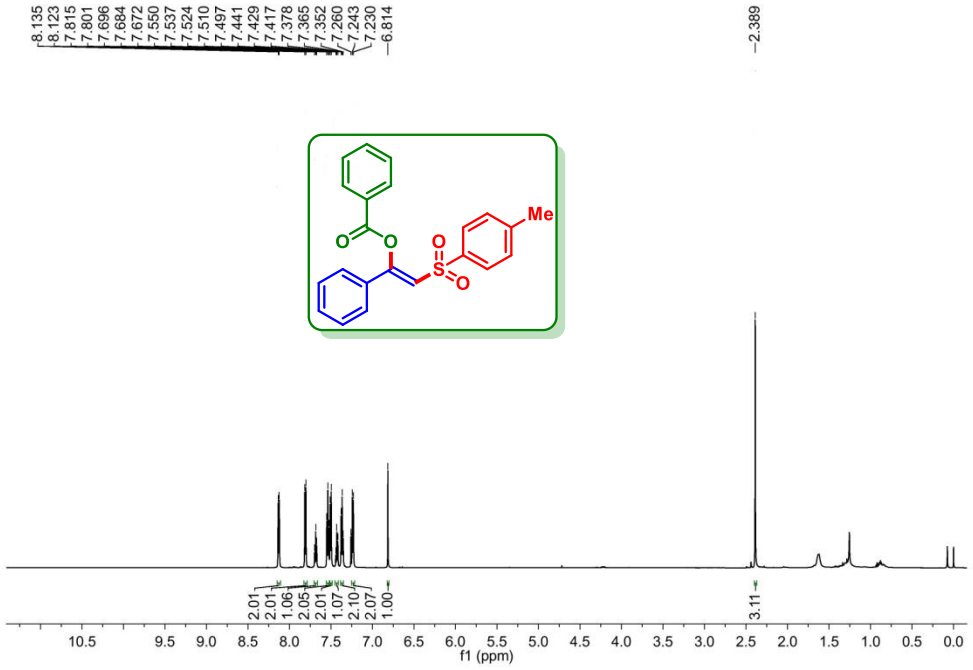

(Z)-1-Phenyl-2-tosylvinyl benzoate (1az): **^{13}C{^{1}H} NMR ($CDCl_3$, 150 MHz)**

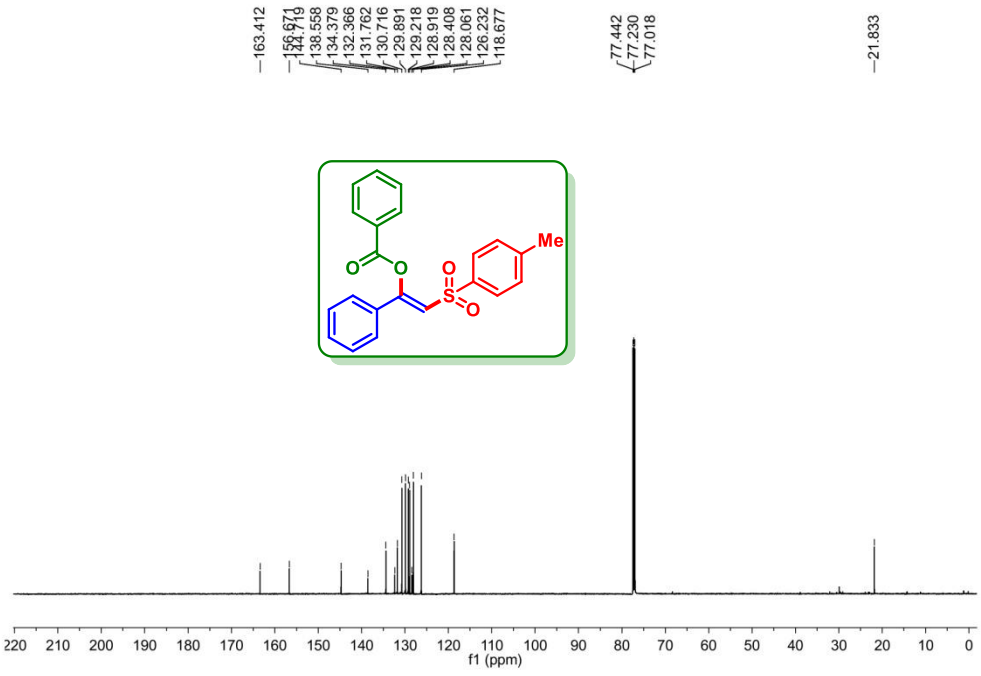

(Z)-1-Phenyl-2-tosylvinyl 4-methylbenzoate (1bz): **^{1}H NMR ($CDCl_3$, 400 MHz)**

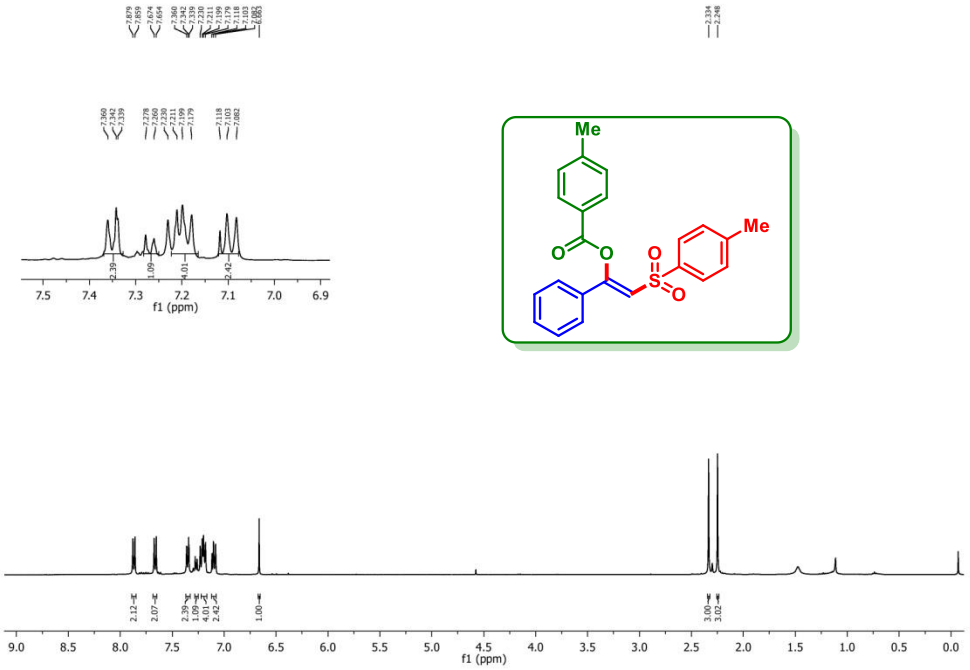

(Z)-1-Phenyl-2-tosylvinyl 4-methylbenzoate (1bz): **^{13}C{^{1}H} NMR ($CDCl_3$, 100 MHz)**

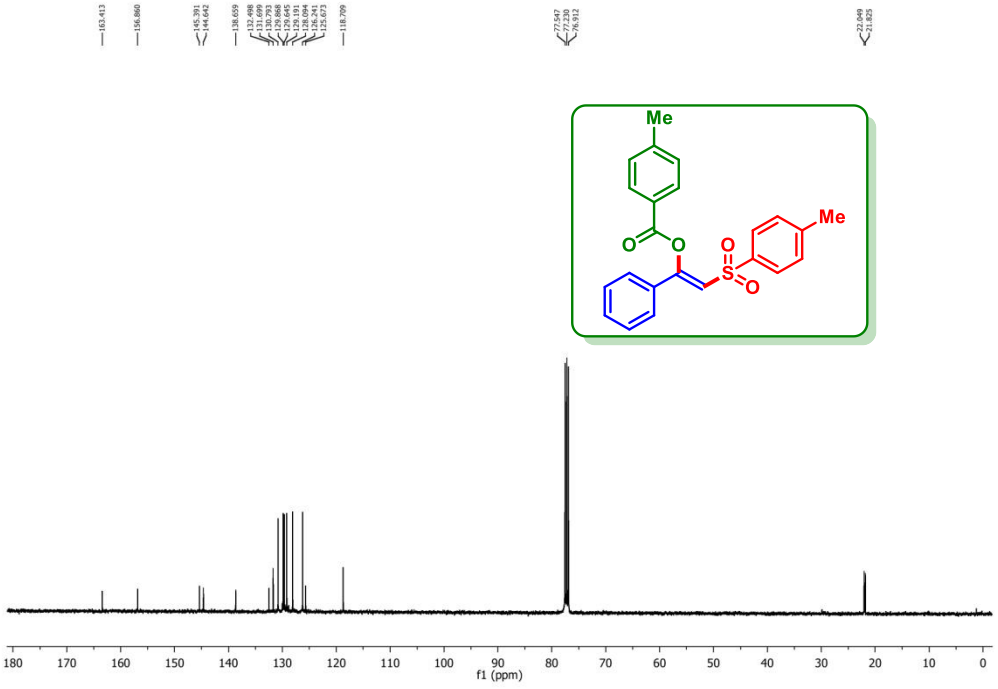

(Z)-1-Phenyl-2-tosylvinyl 4-chlorobenzoate (1dz): **^{1}H NMR ($CDCl_3$, 400 MHz)**

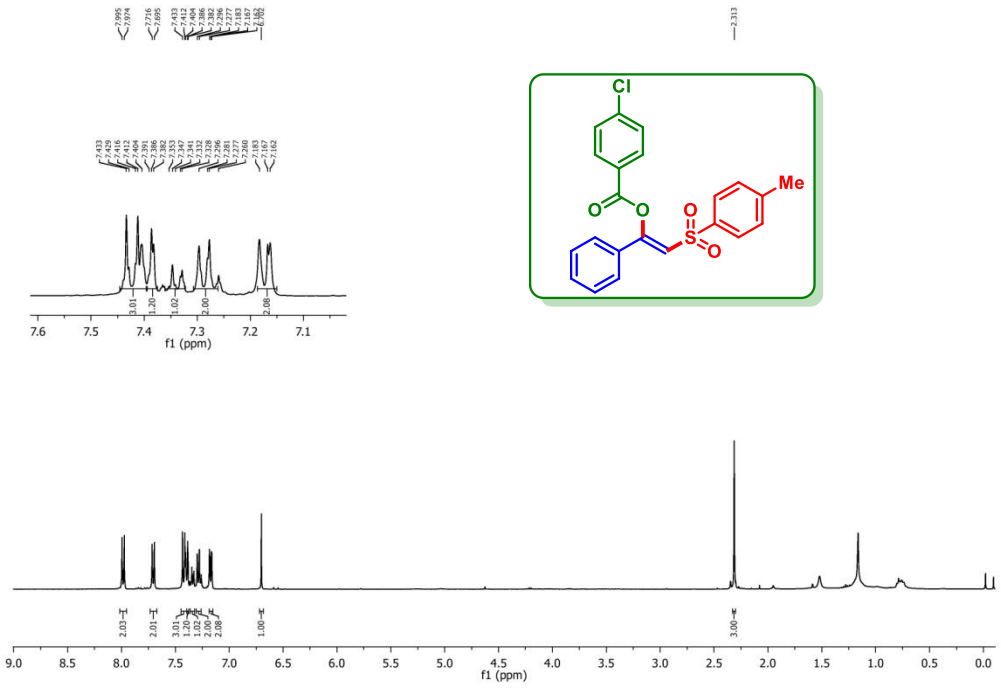

(Z)-1-Phenyl-2-tosylvinyl 4-chlorobenzoate (1dz): **^{13}C{^{1}H} NMR ($CDCl_3$, 100 MHz)**

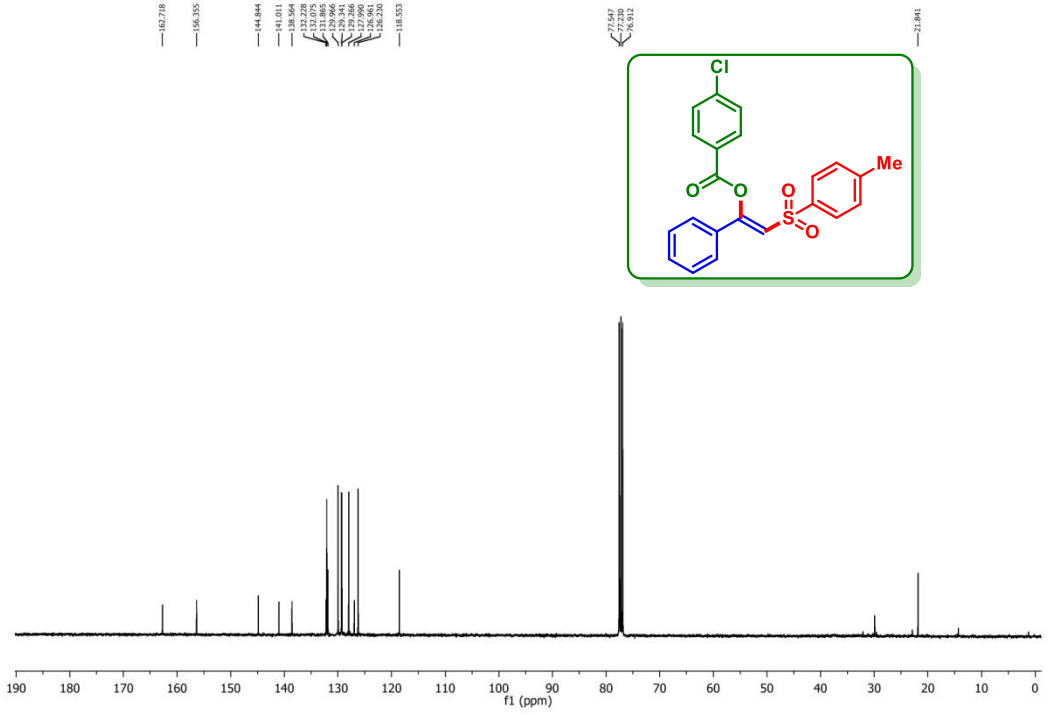

***(Z)-1-Phenyl-2-tosylvinyl stearate (1pz)*: ^{1}H NMR ($CDCl_3$, 400 MHz)**

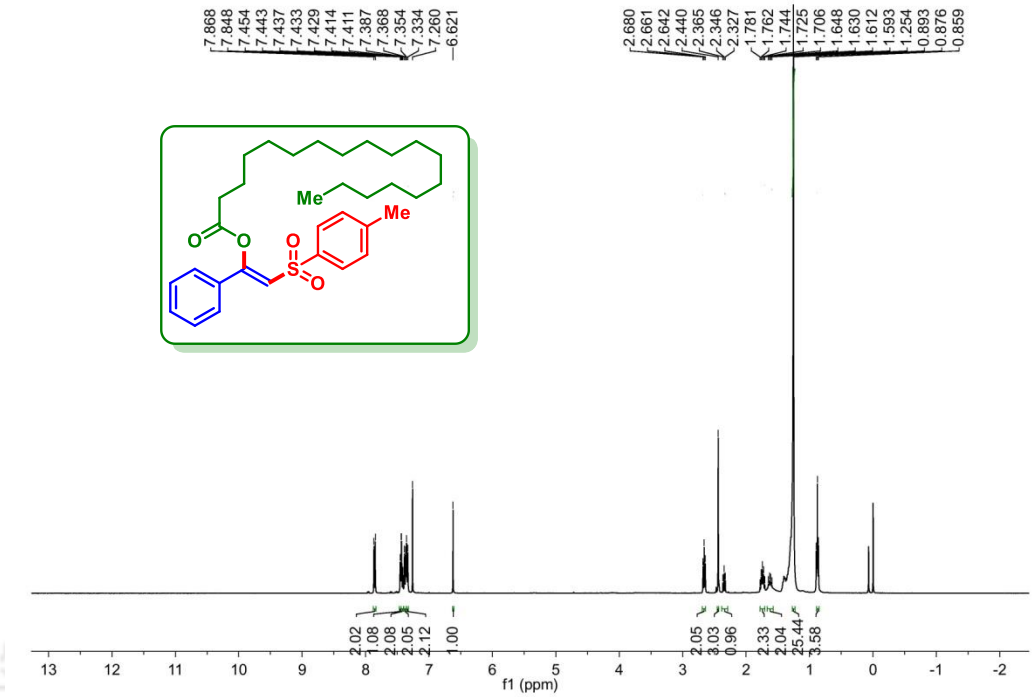

***(Z)-1-Phenyl-2-tosylvinyl stearate (1pz)*: ^{13}C{^{1}H} NMR ($CDCl_3$, 100 MHz)**

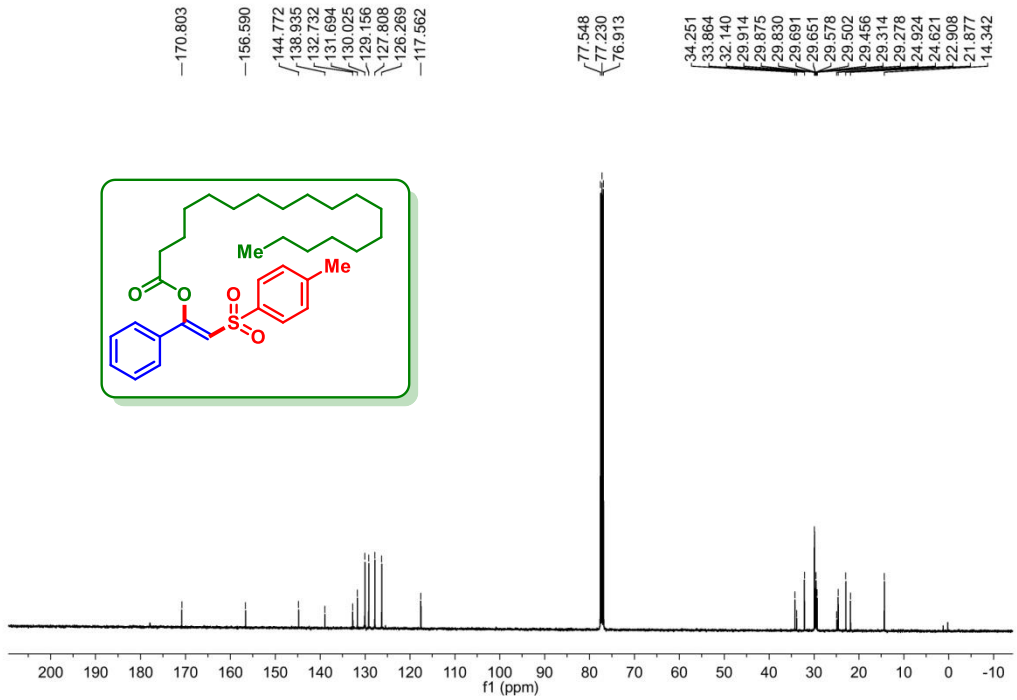

***(Z)-1-(tert-Butyl)-4-(1-thiocyanato-2-tosylvinyl)benzene* (*4vz*): ^{1}H NMR ($CDCl_3$, 500 MHz)**

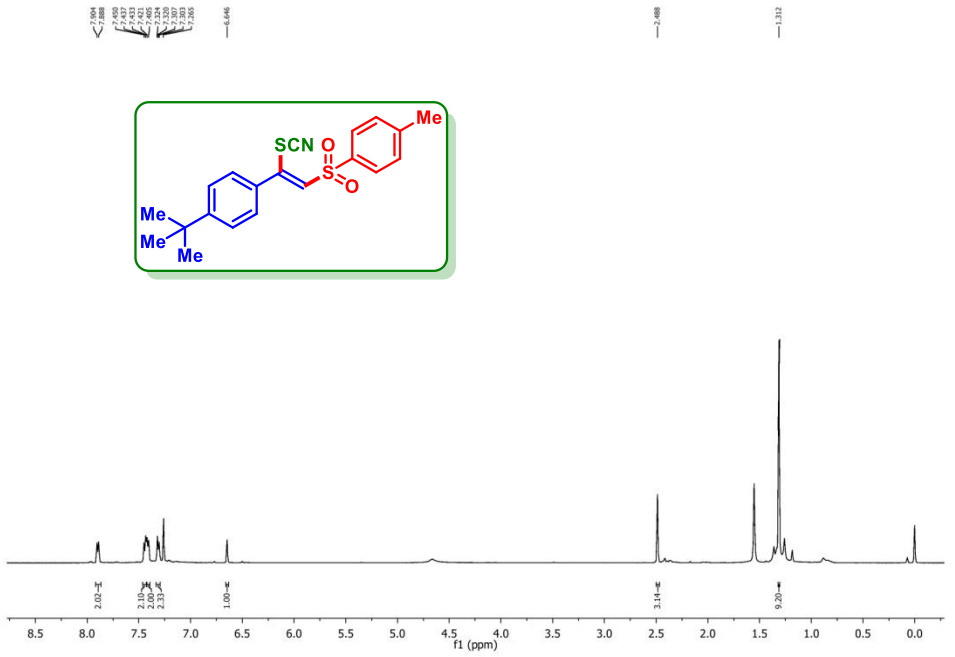

***(Z)-1-(tert-Butyl)-4-(1-thiocyanato-2-tosylvinyl)benzene* (*4vz*): ^{13}C{^{1}H} NMR ($CDCl_3$, 125 MHz)**

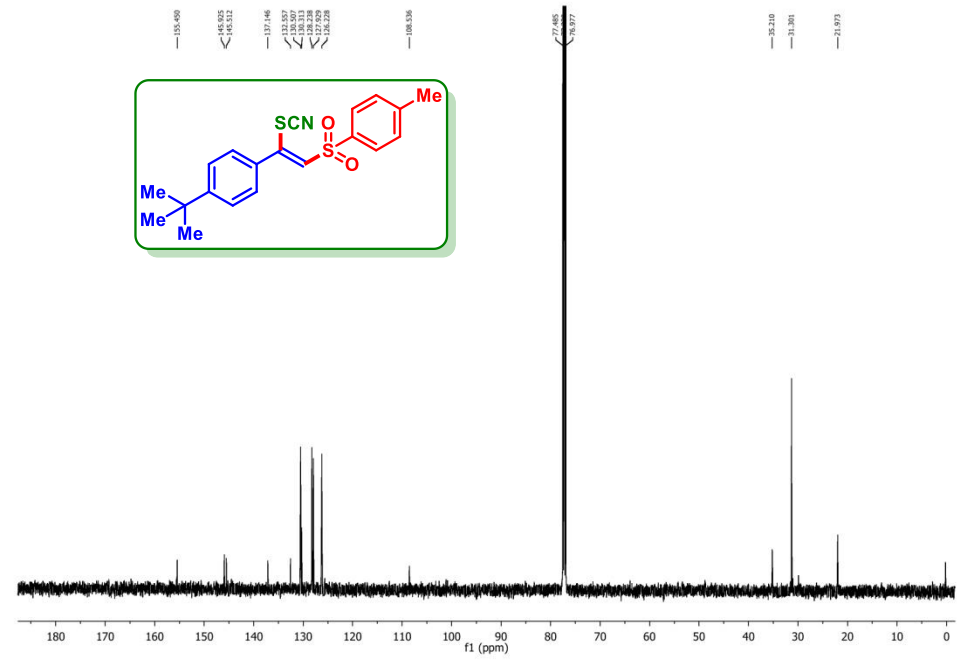

CHAPTER-III

Visible-Light-Mediated Synthesis of Thio Functionalized Pyrroles

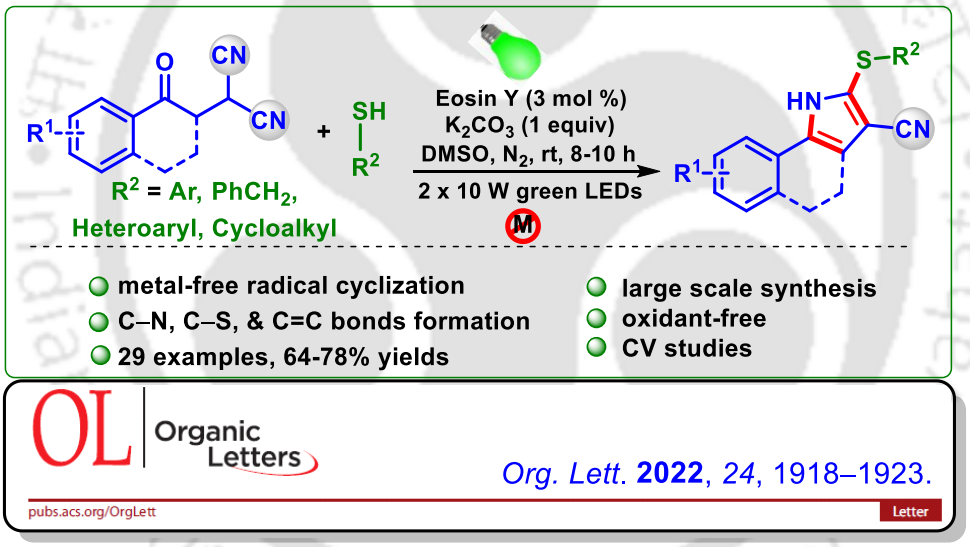

***Abstract:** An inimitable illustration of a green-light-induced synthesis of thio-functionalized pyrroles has been established using β-ketodinitriles and thiophenols as the reacting partners and eosin Y as the photocatalyst. Large-scale synthesis and some useful synthetic modifications of the thio-functionalized pyrroles are also demonstrated.*

CHAPTER III

Visible-Light-Mediated Synthesis of Thio Functionalized Pyrroles

III.1. Introduction:

Among various five-membered heterocyclic compounds, pyrroles are abundant in many natural products and pharmaceuticals, possessing biological activities such as antifungal, antiviral, antihyperlipidemic, and anticancer. In particular, atorvastatin (**I**), the cholesterol-lowering drug,[1a] tolmetin (**II**) the nonsteroidal anti-inflammatory drug (NSAIDs),[1b] sunitinib (**III**) the multitargeted antitumor, and pyrvinium (**IV**) used for the treatment of pinworm infestation all possess pyrrole unit (Figure III.1).

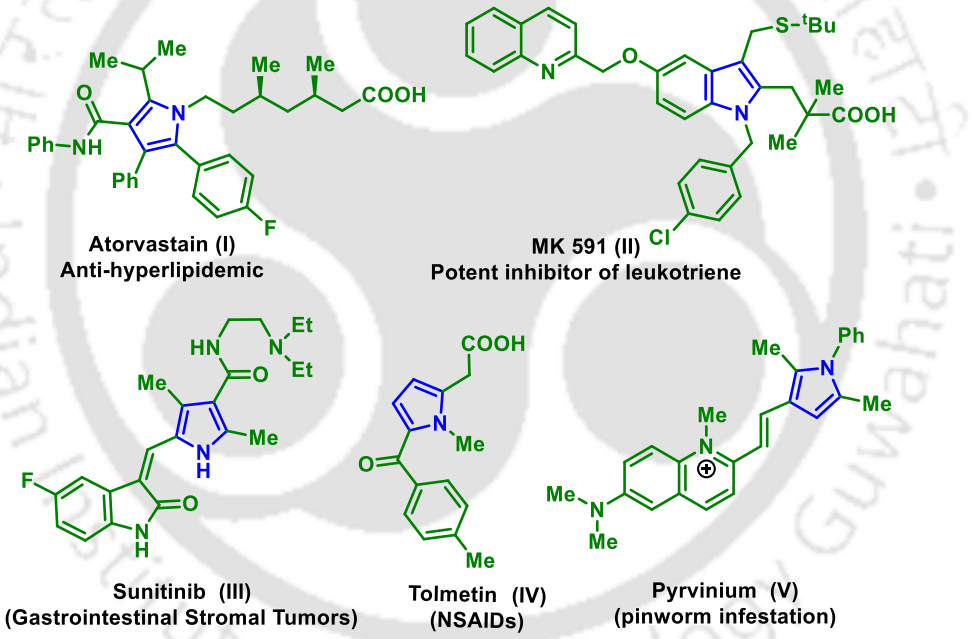

Figure III.1. *Bioactive compounds containing pyrrole unit.*

Owing to their diverse applications, the synthesis of substituted pyrroles has been an impressive area of research for the scientific community. Besides the conventional Paal−Knorr and Hantzsch synthesis, there are other well-established methodologies for the synthesis of such heterocycle.[2]

For instance, Wu and co-workers reported a Cu-catalyzed oxidative annulation for the synthesis of pyrrole-2-carbaldehyde from aryl methyl ketones, arylamines, and acetoacetate esters (Scheme III.1).[3]

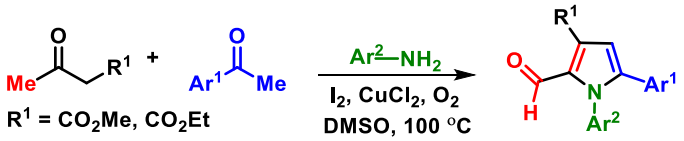

Scheme III.1. *Synthesis of pyrrole-2-carbaldehydes.*

In 2013 Kempe *et al*. reported an Ir-catalyzed synthesis of pyrrole using secondary alcohols and amino alcohols.[4] The protocol provides a wide range of functional groups on either of the coupling partners. Next, in 2014, Huang *et al*. reported an Au-catalyzed synthesis of pyrroles *via* intermolecular nitrene transfer from 2*H*-azirines to ynamides (Scheme III.2).[5]

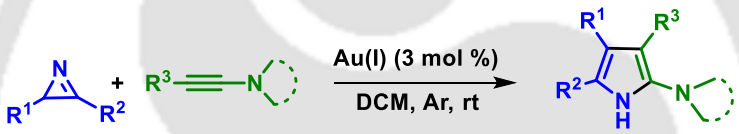

Scheme III.2. *Synthesis of pyrroles via intermolecular nitrene transfer from 2H-azirines to ynamides.*

In 2017 Kim and Oh *et al*. reported a Cu-catalyzed synthesis of substituted pyrrololactams by intermolecular alkyne-isocyanide click reactions which proceeds via ring expansion of spiro-2*H*-pyrroles (Scheme III.3).[6]

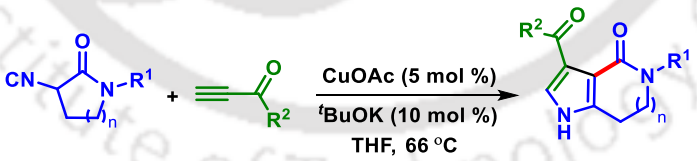

Scheme III.3. *Cu-catalyzed synthesis of substituted pyrrololactams.*

In the same year, Hein and coworkers reported a Cu-catalyzed synthesis of annulated aminopyrroles via heterocycloisomerization reaction (Scheme III.4).[7] The present protocol provides a diverse range of aminopyrroles in 36−93% isolated yields depending on the nature of the alkynyl substituent.

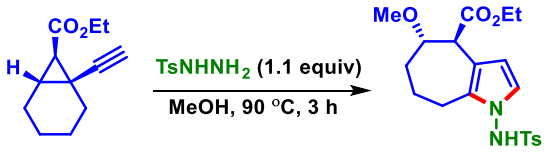

Scheme III.4. *Cu-catalyzed synthesis of annulated aminopyrroles via heterocycloisomerization.*

In 2019, Deng and coworkers reported an efficient method for the synthesis of pyrroles via a three-component annulation of amines, ketones, and nitrovinylarenes (Scheme III.5).[8]

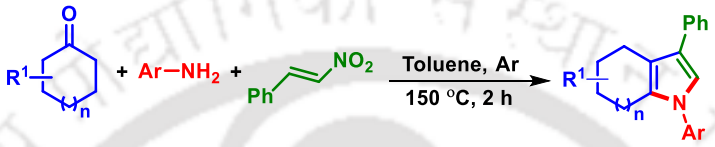

Scheme III.5. *Synthesis of pyrroles via a three-component annulation of amines, ketones, and nitrovinylarenes.*

Recently, Wan and co-workers reported the synthesis of NH-free pyrroles *via* Pd-catalyzed annulation of enaminones and alkenes (Scheme III.6).[9]

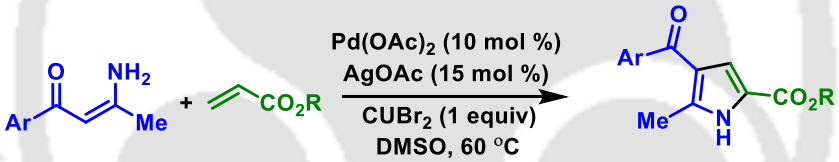

Scheme III.6. *Synthesis of NH-free pyrroles via Pd-catalyzed annulation of enaminones and alkenes.*

Although the above-mentioned transition-metal catalyzed protocols show high efficacy, the metal-free protocol can circumvent the toxicity issues of metal catalysis.[10] Recently, photocatalytic approaches have been gaining prominence due to operational simplicity, sustainability and safety. The synthesis of any targeted molecules under photocatalytic conditions has become an impressive area of research in modern organic chemistry.[11] In most photocatalytic strategy, visible light is employed as an energy source to promote single electron transfer (SET) for the construction of functionalized molecules, which otherwise require high temperature and transition metals catalysts.[12] Usually, the complexes of Ir, Ru, and organic dyes are employed for the excitation of organic molecules.[13] The demand for organic dyes as photocatalysts is increasing due to the advantages of nontoxicity, eco-compatibility, and cost-effectiveness over metal-based photocatalysts. Generally, eosin Y is

an excellent alternative to transition metal catalysts in several visible-light-driven organic transformations.[14] The radical cascade reactions are often triggered by suitably placed radical acceptors, *viz*. alkenes, alkynes, nitriles and isonitriles groups within the molecule. The use of nitrile as a radical acceptor in cascade reactions has been exploited for the construction of various heterocycles and carbocycles.[15]

III.2. Ideas Toward Nitrile-Triggered Access of *N*-Heterocycles

In 2019, Li *et al*. demonstrated an oxidative decarboxylative cascade cyclization of α-keto acids with 2-cyano-3-arylaniline-derived acrylamides. This cascade reaction provided a variety pyrido[4,3,2-*gh*]phenanthridines with a good functional group tolerance (Scheme III.7).[16]

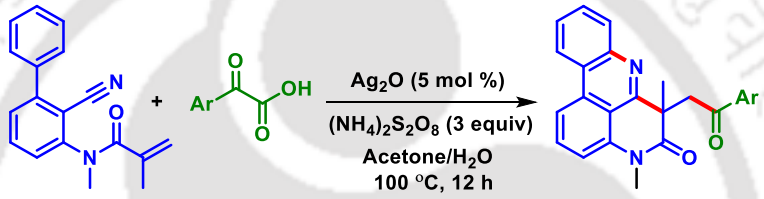

Scheme III.7. *Synthesis of pyrido[4,3,2-gh]phenanthridines.*

Recently, in 2022 Yu *et al*. demonstrated a persulfate-promoted synthesis of pyrrolo[1,2-*a*]indolediones via radical cyclization in the absence of any photosensitizer. In this method, aryl sulfonyl hydrazide and ammonium thiocyanate were used as the *S*-centered radical source (Scheme III.8).[17]

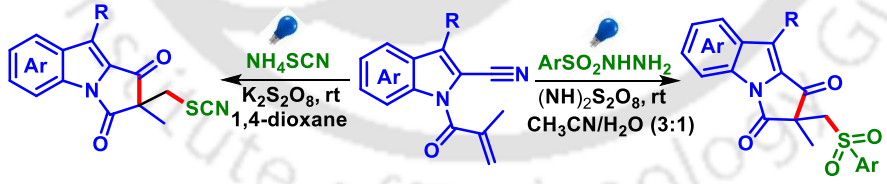

Scheme III.8. *Synthesis of pyrrolo[1,2-a]indolediones.*

Tang and co-workers in 2021, developed a photochemical phosphorylation of cyanoaromatics with the 1,6-enyne and provided a diverse range of phosphorylated amino phosphonates in good yields. The protocol utilized the P(O)−H compounds as the radical donors and CN-containing substrates as the radical acceptors (Scheme III.9).[18]

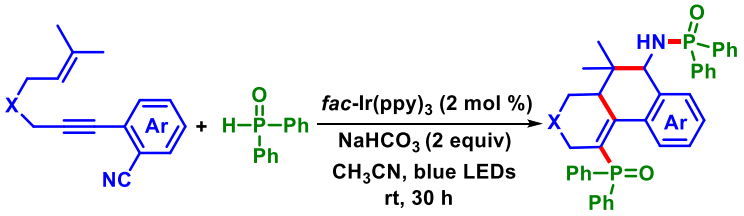

Scheme III.9. *Visible-light-mediated Synthesis of phosphorylated aminophosphonates.*

In 2017, Pan and coworkers developed an efficient photocatalytic oxidative/reductive cyclization reaction of *N*-cyanamide alkenes with aryl sulfinic acids or arylsulfonyl chlorides, which proceeds through C−S, C−C, and C−N bond formations. This photocatalytic strategy provided a wide variety of sulfonated quinazolinones (Scheme III.10).[19]

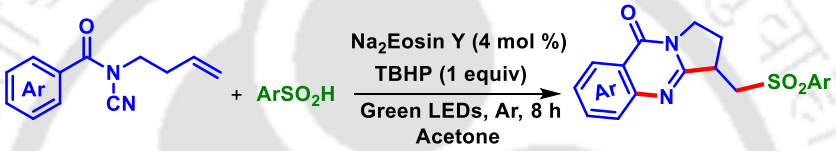

Scheme III.10. *Visible-light mediated synthesis of sulfonated quinazolinones.*

In 2018, Natarajan *et al.* developed a visible-light-induced synthesis of 2-substituted benzothiazoles using thiophenols and nitriles. This method provided a broad range of 2-aryl benzothiazoles in good yields (Scheme III.11).[20]

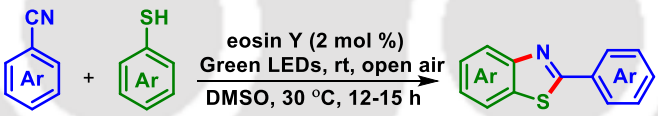

Scheme III.11. *Visible-light-mediated synthesis of 2-aryl benzothiazole.*

Previously, our group established a Pd-catalyzed nitrile-triggered protocol for the synthesis of 3-cyano pyrrole using boronic acid as the reacting partner under visible light irradiation. A diverse range of aryl boronic acid, *β*-ketodinitrile, and *γ*-ketodinitrile were well-tolerated in this protocol (Scheme III.12). [21]

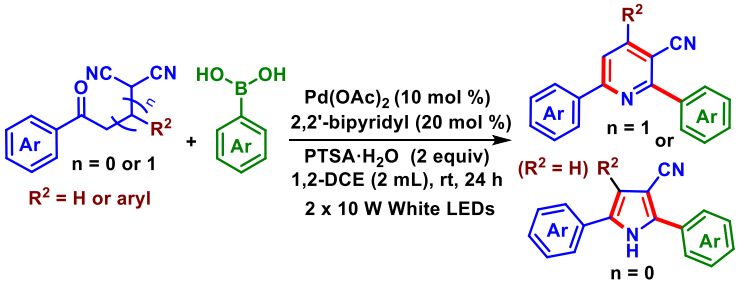

Scheme III.12. *Visible-light-mediated synthesis of 3-cyano pyrrole.*

Taking cues from the above-mentioned literature, we anticipated that a photo-induced thiyl radical addition might be possible with *β*-ketodinitriles as the radical acceptors leading to a pyrrole skeleton *via* the formation of nitrogen centre radical followed by an imine amine tautomerization and intramolecular nucleophilic addition of the amine to the ketone (Scheme III.13).[22] To confirm our hypothesis, CV measurements of benzene thiol (**a**) and *β*-ketodinitrile (**1**) was performed. The measured $E_{1/2\ oxd}$ of benzene thiol (+0.25 V *vs*. SCE) is less than the $E_{1/2\ oxd}$ of *β*-ketodinitriles (+0.95 V *vs*. SCE) which makes them ideal radical donors and acceptors respectively (Figure III.2).

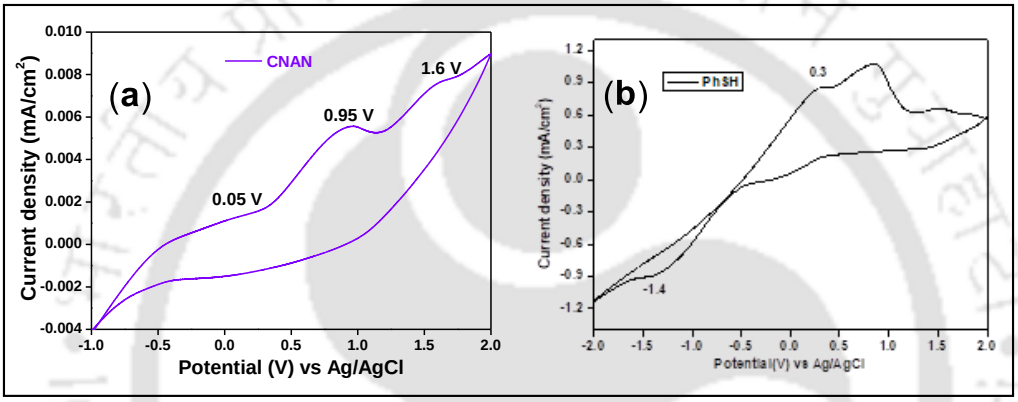

Figure III.2. *(a) CV graph of β-ketodinitrile (**1**). (b) CV graph of benzene thiol (**a**).*

III.3. Present Work

To realize this a preliminary reaction was carried out between 2-(2-oxo-2-phenylethyl)malononitrile (**1**, 1 equiv) and thiophenol (**a**, 2 equiv) in the presence of K_2CO_3 (1 equiv), eosin Y (3 mol %), in DMSO (1 mL) under the irradiation of 20 W (2 x 10) green LEDs under N_2 atmosphere. Gratifyingly, a new compound was obtained in 70% isolated yield along with the formation of thiophenol dimer. From the spectroscopic (^{1}H and ^{13}C NMR) analysis the product's structure was found to be thio-substituted pyrrole (**1a**) (Scheme III.14). Further, the X-ray crystallography analysis reconfirmed its structure to be 5-phenyl-2-(phenylthio)-1*H*-pyrrole-3-carbonitrile (**1a**) (Figure III.3).

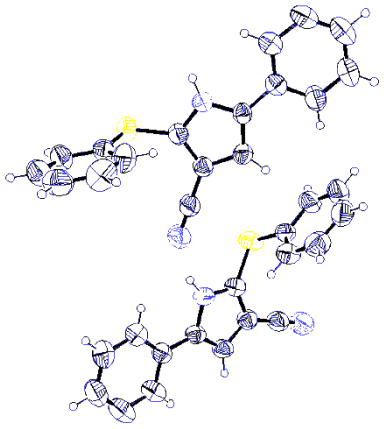

Figure III.3. *ORTEP diagram of 5-phenyl-2-(phenylthio)-1H-pyrrole-3-carbonitrile (**1a**) with 40% ellipsoid probability (CCDC 2118561).*

To the best of our knowledge, this is a unique report for the visible-light-mediated synthesis of thio-functionalized pyrroles using *β*-ketodinitrils and thiophenols as the reacting partners which have been demonstrated in Scheme III.13.[22]

III.3. Present Work

Scheme III.13. *Visible-light-mediated synthesis of thio-functionalized pyrroles.*

Optimization of the Reaction Conditions

Inspired by this photocatalytic approach, extensive optimization studies involving the selection of different catalytic systems, bases, and solvents was carried out. The use of organic dyes such as Rose Bengal, Rhodamine B, and Eosin B (Table III.1, entry 2–4) failed to improve the yield as compared to Eosin Y. Switching the catalytic system to $[Ru(bpy)_3](PF_6)_2$ and $[Ru(bpy)_3]Cl_2$ provided 43% and 58% yields respectively which are inferior to Eosin Y (Table III.1, entry 5 and 6).

Table III.1. Optimization of the reaction conditions[a,b]

entry	variation from optimal conditions[a]	yield (%)[b]
1.	**None**	**70**
2.	Rose Bengal instead Eosin Y	55
3.	Rhodamin B instead Eosin Y	52
4.	Eosin B instead Eosin Y	59
5	$[Ru(bpy)_3](PF_6)_2$ instead Eosin Y	43
6	$[Ru(bpy)_3]Cl_2$ instead Eosin Y	58
7	2 mol % Eosin Y	64
8	5 mol % Eosin Y	69
9	Na_2CO_3 instead of K_2CO_3	68
10	Cs_2CO_3instead of K_2CO_3	59
11	^tBuOK instead of K_2CO_3	55
12.	DMF instead of DMSO	62
13.	CH_3CN instead of DMSO	45
14.	EtOH instead of DMSO	25
15.	CH_3OH instead of DMSO	30
16.	1.5 equiv of K_2CO_3	65
17	1 equiv of thiol	45
18	2.5 equiv of thiol	69
19	2 x 10 W blue LEDs	62
20	2 x 10 W white LEDs	65
21	15 h instead 8-10 h	52
22	without Eosin Y	12
23	without base	Trace
24	reaction in dark	10

[a]Reaction condition: **1** (0.25 mmol), **a** (0.5 mmol), Eosin Y (3 mol %), K_2CO_3 (1 equiv), DMSO (1 mL), 10 h. [b]Isolated pure product. N.D not detected.

At 2 mol % eosin Y loading, 64% yield of the desired product (**1a**) was obtained (Table III.1, entry 7) whereas further increment (5 mol %) leads to an insignificant change in the yield of the product (Table III.1, entry 8). However, screening of other bases, such as

Na_2CO_3, Cs_2CO_3, and ^tBuOK, instead of K_2CO_3 did not improve the yield (Table III.1, entries 9-11). During solvent selection, DMSO was found to be the best as compared to other solvents such as DMF (62%), CH_3CN (45%), EtOH (25%), and CH_3OH (30%) tested (Table III.1, entries 12-15). Next, increasing the equivalence of base (1.5 equiv, 65%) had a detrimental effect, mostly leading to the formation of thiol dimers (Table III.1, entry 16). However, varying the equivalence of thiophenol from the standard condition (2 equiv.) failed to improve the yield (Table III.1. entries 17-18). Thus, the use of 2 equiv. of thiol was found to be optimal. The standard reaction was carried out using 2 x 10 W blue (430 nm) and white LEDs to study the effect of wavelength and intensity of light. LEDs of both wavelengths failed to improve the reaction yield beyond 65% (Table III.1, entries 19 and 20). Thus, the use of green light is found ideal for the excitation of eosin Y, since the emission spectra of eosin Y in DMSO (543 nm) is overlapping with the wavelength of the green light (513 nm) (Figure III.13). The reaction performed well in blue LED (62%) and white LED (65%). Further, an increase in the reaction time (Table III.1. entry 21) shows no significant improvement in the reaction yield. Control experiments revealed that eosin Y, base, and light source play a vital role in this transformation (Table III.1, entry 22-24). Eosin Y and light helps in the generation of thiyl radical whereas the base helps in the tautomerization and aromatization process to give the desired product. For all the reactions, proper aeration was maintained using a fan, preventing the surrounding temperature to increase, suggesting the photochemical nature of this protocol. After screening of several parameters, the optimal condition for this transformation was found to be the use of **1** (0.25 mmol), **a** (0.50 mmol, 2 equiv), K_2CO_3 (0.25 mmol, 2 equiv), eosin Y (3 mol %), in DMSO (1 mL) under 2 x 10 W green LEDs (Table III.1, entry 1).

Substrate Scope for Thio-functionalized Pyrroles

With the optimized reaction conditions in hand, this photochemical strategy was used for the synthesis of thio-functionalized pyrroles using various *β*-ketodinitriles (Scheme III.14). The *β*-ketodinitriles carrying electron-neutral (**1**), electron-donating groups such as *p*-Me (**2**), *p*-OMe (**3**), *p*-^{i}Pr (**4**), and electron-withdrawing substituents such as *p*-F (**5**), *p*-Cl (**6**), *p*-Br (**7**), and *p*-I (**8**) afforded their corresponding thio-functionalized pyrroles (**1a**, 70%), (**2a**, 72%), (**3a**, 77%), (**4a**, 75%), (**5a**, 69%), (**6a**, 72%), **(7a**, 70%), and (**8a**, 71%) in good yields. Apart from this, *β*-ketodinitriles originating from 2-acetonapthone (**9**), dioxolane ketone (**10**),

tetralone (**11**) cyclohexanone (**12**) and heteroaromatic ketones (**13** and **14**) were also reacted efficiently yielding the products (**9a**, 72%), (**10a**, 67%), (**11a**, 70%), (**12a**, 67%), (**13a**, 68%), and (**14a**, 69%) under the present photochemical conditions.

Scheme III.14. *Scope of thio-functionalized pyrroles with different β-ketodinitriles*[a-c]

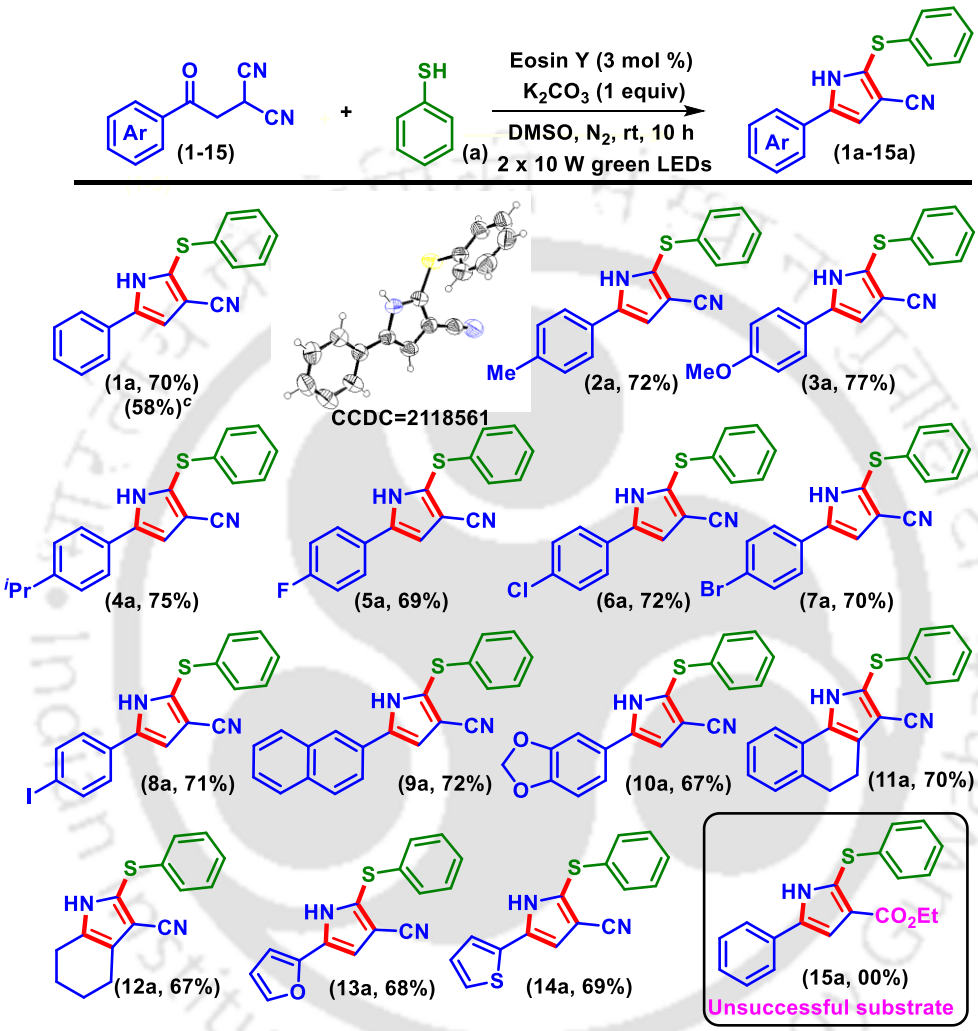

[a]Reaction conditions: **1-15** (0.25 mmol), **a** (0.5 mmol), K_2CO_3 (0.25 mmol), eosin Y (3 mol %), DMSO (1 mL), 2 x 10 W green LEDs, under N_2. [b]Isolated yield. [c]7 mmol scale.

To enhance the substrate scope, an ester containing substrate *viz.* ethyl 2-cyano-4-oxo-4-phenylbutanoate (**15**) was reacted under the standard condition. However, it failed to give the desired product (**15a**) even by altering the bases (NaOH, Cs_2CO_3). In all cases the starting material disappeared giving a multitude of products (at least 6-7 spots) non of which could be isolated and characterized. Only the disulphide adduct could be isolated. The synthetic utility was further demonstrated for a large-scale (7 mmol) synthesis giving the desired product **1a**

in 58% yield. Next, simple *β*-ketodinitrile (**1**) was reacted with various thiophenols (**b-m**) bearing electron-donating (EDGs) as well as electron-withdrawing (EWGs) groups and the results are summarized in Scheme 3.

Scheme III.15. *Scope of thio-functionalized pyrroles with different thiophenols*[a,b]

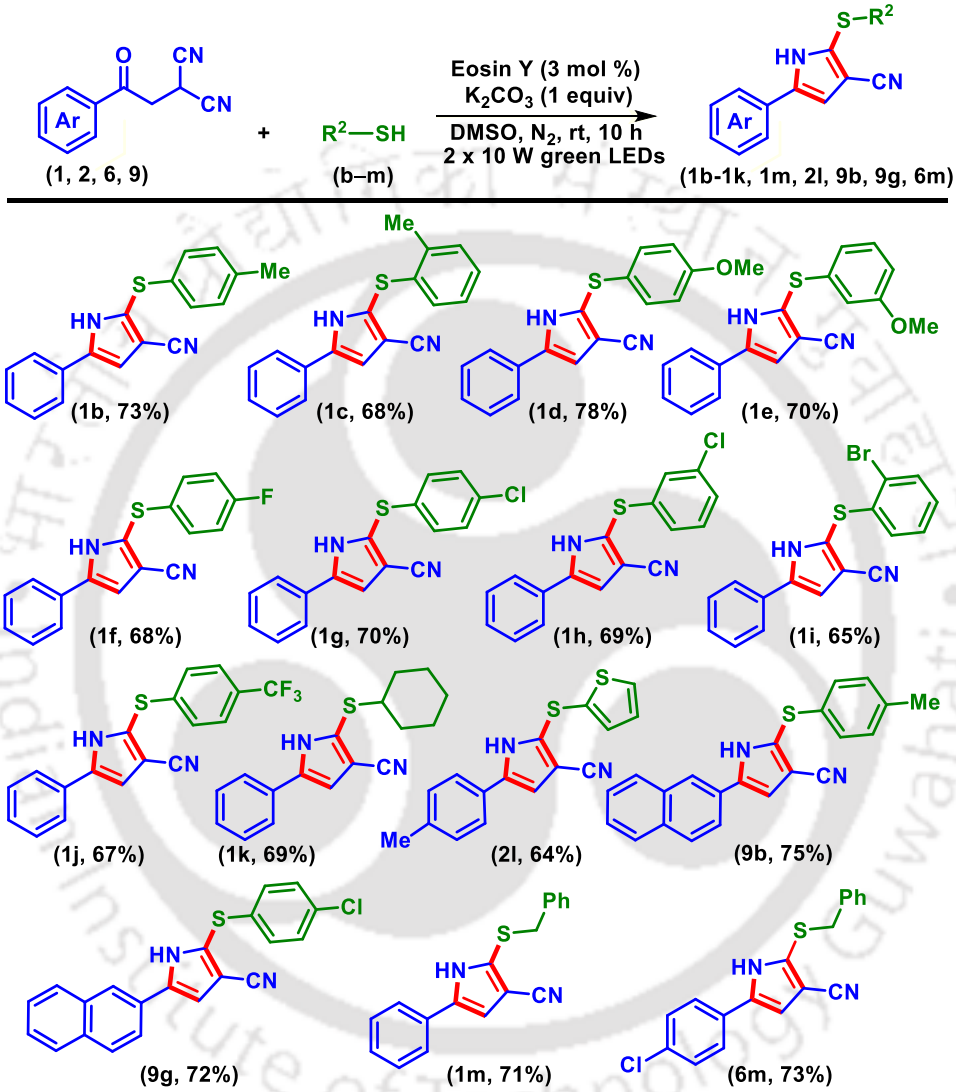

[a]Reaction conditions: **1**, **2**, **6**, **9** (0.25 mmol), **b-m** (0.5 mmol), K_2CO_3 (0.25 mmol), eosin Y (3 mol %), DMSO (1 mL), 2 x 10 W green LEDs, under N_2. [b]Isolated yield.

Thiophenols bearing EDGs such as *p*-Me (**b**), *o*-Me (**c**) *p*-OMe (**d**), *o*-OMe (**e**), and EWGs such as *p*-F (**f**), *p*-Cl (**g**), *m*-Cl (**h**) *o*-Br (**i**), *p*-CF_3 (**j**) were efficiently converted to their desired products {(**1b**, 73%), (**1c**, 68%), (**1d**, 78%)} and {(**1e**, 70%), (1**f** , 68%), (**1g**, 70%), (**1h**, 69%), (**1i**, 65%), (**1j**, 67%)} in good yields. Besides thiophenols, aliphatic thiol (**k**), and

heteroaromatic thiol (**l**) also underwent smooth reactions giving their desired products (**1k**, 69%), and (**2l**, 64%) under the present photochemical conditions. Thiophenols such as *p*-methyl thiophenol (**b**) and *p*-chloro thiophenol (**g**) reacted well with *β*-ketodinitriles obtained from 2-acetonapthone (**9**) giving their anticipated product **9b** and **9g** in 75% and 72% yields, respectively. Similarly, benzyl mercaptan (**m**) also reacted competently with *β*-ketodinitriles **1** and **6**, providing their respective thio-substituted pyrroles **1m** and **6m** in 71% and 73% yields (Scheme III.15).

After synthesizing a library of thio-functionalized pyrroles some control experiments were performed to understand the mechanism. The standard reaction under dark gave the desired product (**1a**) in 10% yield {Scheme III.16a (i)} and the yield remained unchanged even after prolonging the reaction time up to 48 h. This suggests the involvement of light in the present photochemical reaction. Similarly, in the absence of catalyst, the product (**1a**) was isolated in 12% yield, signifying its crucial role in the thiyl radical generation {Scheme III.16a (ii)}. In the absence of base, a trace amount of the product was obtained which suggests its involvement in some of the steps {Scheme III.16a (iii)}. To further understand the involvement of O_2 in the reaction another reaction was performed under an oxygen atmosphere in the absence of base. However, the reaction failed to give the desired product (**1a**) which indicates that oxygen has no positive involvement in this reaction {Scheme III.16a (iv)}. To confirm the involvement of the radical path, two independent reactions were performed, one in the presence of 2,6-di-*tert*-butyl-4-methyl phenol (BHT, 1 equiv) and the other in the presence of 1,1-diphenyl ethylene (1 equiv). In the case of BHT, <10% of the product (**1a**) was observed. The BHT adduct (**M**) with thiophenol (**a**) was detected by HRMS analysis of the reaction aliquot {Scheme III.16b (i)}. Similarly, in the presence of diphenyl ethylene <10% of the product (**1b**) and thiyl radical trapped adduct (**N**, 78%) {Scheme III.16b (ii)} was observed. The structure of the adduct **N** was confirmed by NMR (^{1}H) and HRMS analysis (Figure III.4 and III.5).

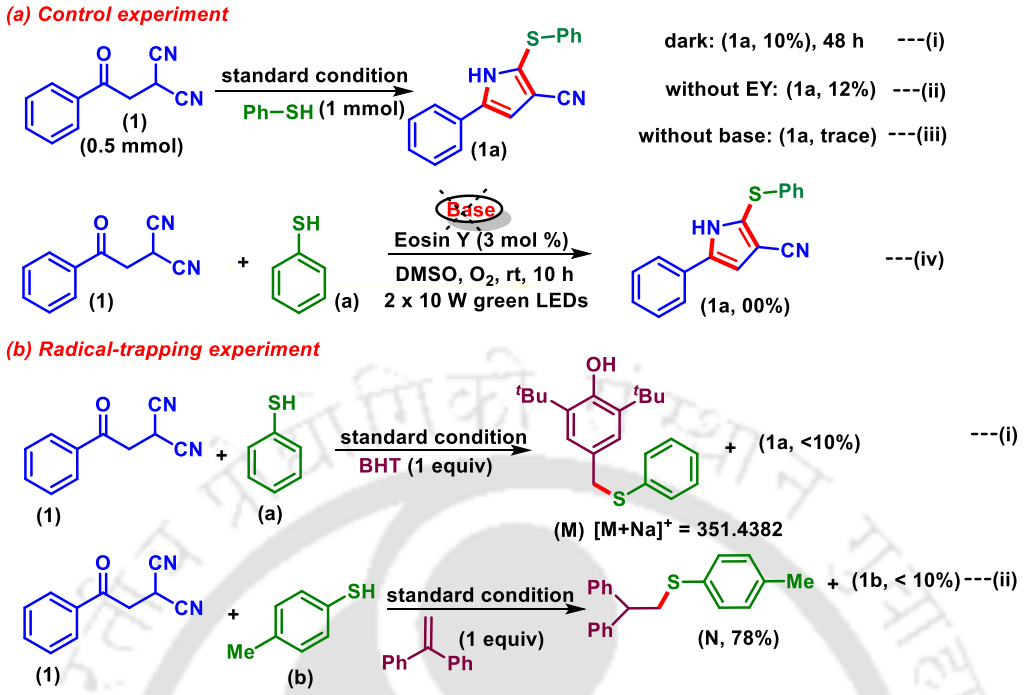

Scheme III.16. *Control experiments.*

^{1}H NMR and HRMS Spectra of Compound N

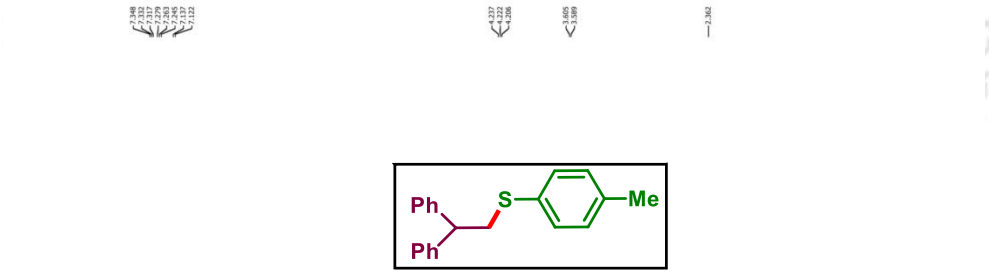

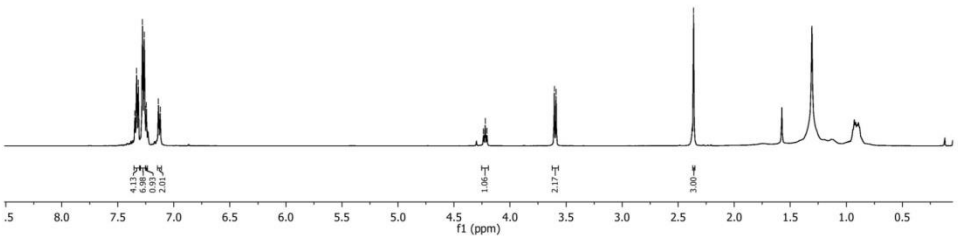

Figure III.4. *^{1}H NMR spectra of trapped Thiol (**b**) with 1,1-diphenyl ethylene.*

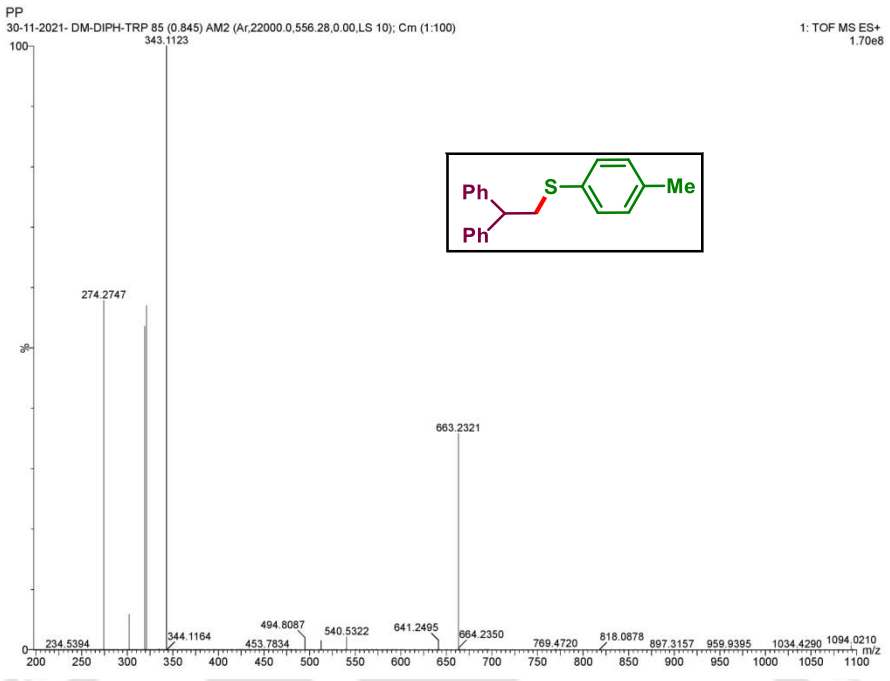

Figure III.5. *HRMS spectra of trapped thiol (**b**) with 1,1-diphenyl ethylene.*

Finally, an on-off experiment suggests that continuous irradiation of light is essential for the desired transformation (Figure III.6).[23] In this experiment, the reaction mixture was stirred and irradiated by 2 x 10 W green LEDs at room temperature under nitrogen atmosphere for 2.5 h, the corresponding product was isolated in 33% yield. Then the reaction mixture was continuously stirred in the dark for 2 h, the desired product was obtained in 35% yield. Furthermore, when the reaction mixture was stirred and irradiated by 2 x 10 W green LEDs at room temperature under nitrogen atmosphere for 3.5 h, the desired product was isolated in 64% yield. The above results indicated that continuously visible light irradiation is essential for promoting this transformation (Figure III.6, 7, 8, and 9). The NMR spectra were recorded taking nitromethane as the internal standard.

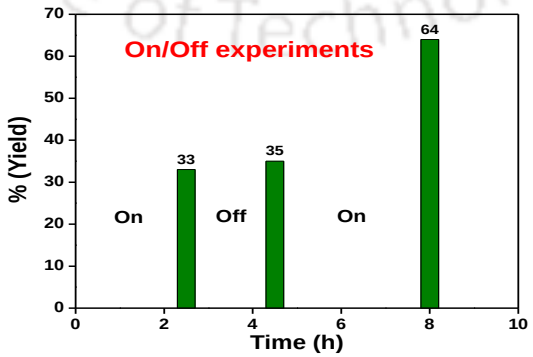

Figure III.6. *On-off experiments.*

Representative Spectra of On-off Experiments:

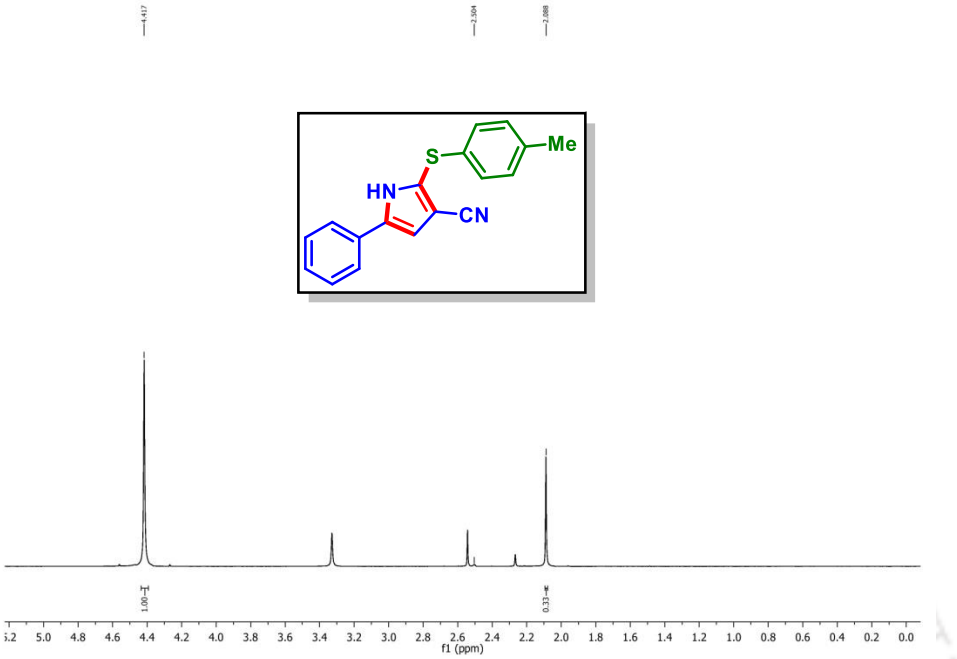

Figure III.7. *NMR spectra of On-off experiment (2.5 h light on).*

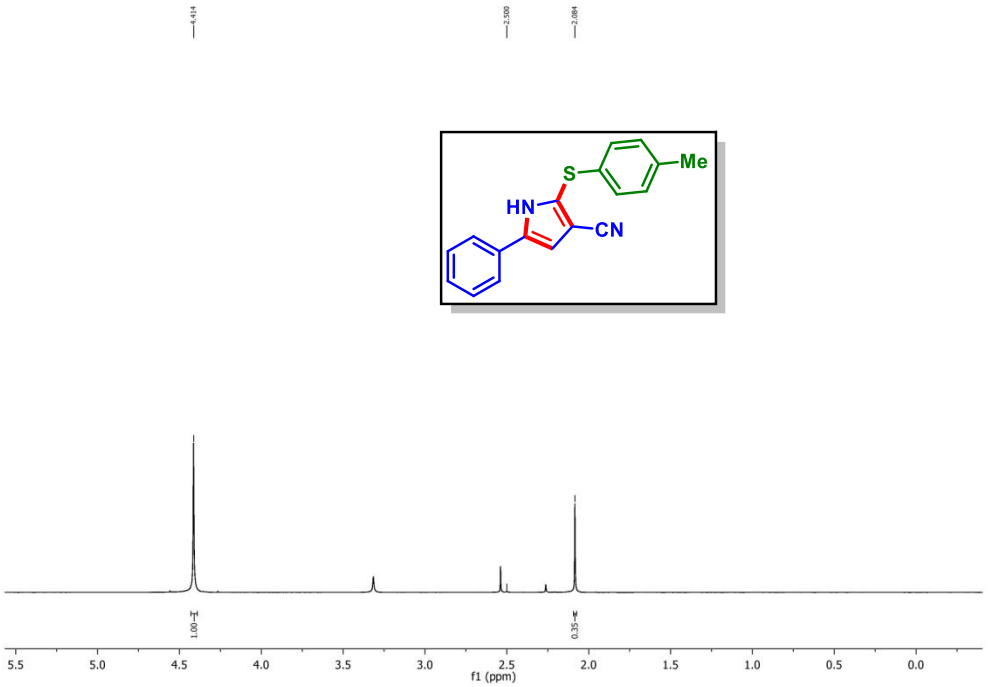

Figure III.8. *NMR spectra of On-off experiment (2 h light off).*

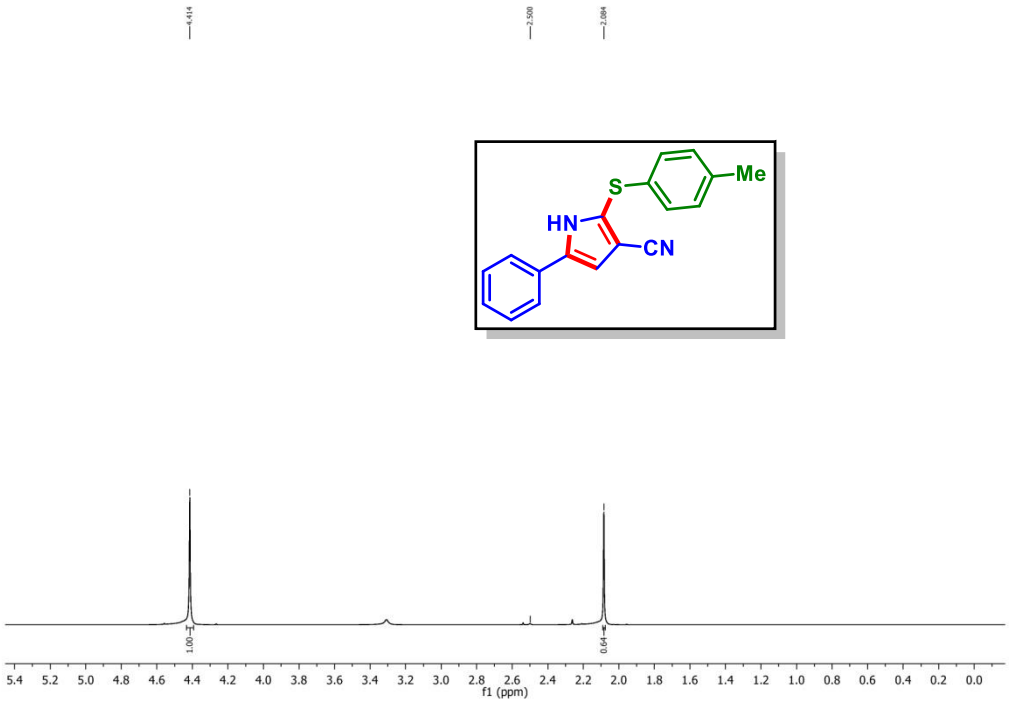

Figure III.9. *NMR spectra of On-off experiment (3.5 h light on).*

Next, a Stern−Volmer (SV) fluorescence quenching was performed using eosin Y as the probe and thiophenol (**a**) as a quencher.

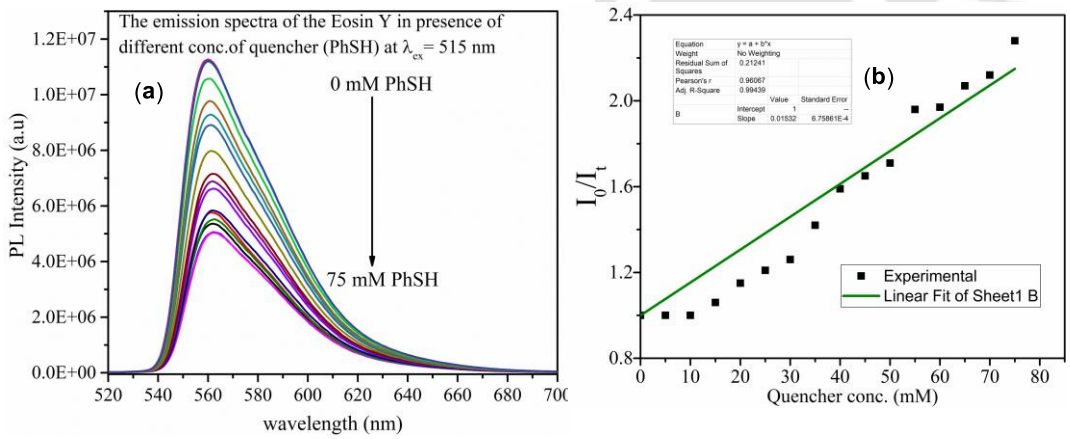

Figure III.10. *Stern-Volmer quenching experiments.*

At first, the excitation and emission spectra of eosin Y was recorded where a fluorescence maximum was obtained at 560 nm when excited at 515 nm (excitation maximum of eosin Y). The peak at 560 nm progressively decreases with increasing the quencher

thiophenol (**a**) concentration (5 →75 mM) (Figure III.10a). With these data, a Stern−Volmer graph was plotted using the equation $I_0/I_t = 1 + K_{SV}[Q]$. A linear quenching was observed (Figure III.10b). This suggests a facile electron transfer between eosin Y and thiophenol to generate a thiyl radical.[24] Further, CV experiments were carried out to confirm the exact role of eosin Y (as an oxidizing agent or a reducing agent). From the CV data, it is found that the oxidation potential of thiophenol ($E_{1/2\ ox}$ = +0.25 V *vs*. SCE) is lower than the oxidation potential of eosin Y ($E_{1/2\ ox}$ = +0.83 V *vs*. SCE for excited state of eosin Y). Similarly, the reduction potential of thiophenol (**a**) ($E_{1/2\ red}$ = -1.35 V *vs*. SCE) is lower than the reduction potential of eosin Y ($E_{1/2\ red}$ = -1.06 V *vs*. SCE for excited state of eosin Y). This indicates that thiophenols can be easily oxidized by the eosin Y and its role as an oxidizing agent for the facile generation of thiyl radical (Figure III.11a and III.11b).[25]

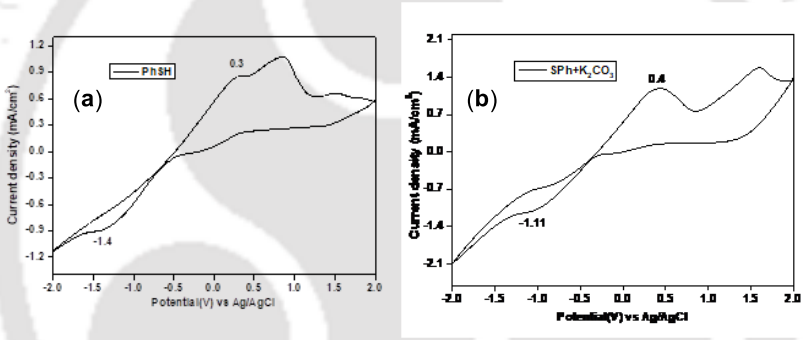

Figure III.11. *(a) CV graph of thiopheno. (b) CV graph of thiolate anion.*

Results obtained from the control experiments and literature reports, an acceptable reaction path is suggested in Scheme 5.[26] In the presence of green LEDs, eosin Y (EY) is photoexcited to EY^* which is reductively quenched by the thiophenol (**a**) to give (**a′**) and radical anion of eosin Y ($EY^{\cdot -}$). Next, the base abstracts a proton from the radical cation intermediate (**a′**) and generates a thiyl radical (**a′′**). The thiyl radical (**a′′**) adds to one of the nitrile groups of *β*-ketodinitrile (**1**) generating intermediate (**A**). Subsequently, intermediate **A** is reduced by $EY^{\cdot -}$ to an anionic intermediate (**B**), thereby completing the catalytic cycle. On protonation, the intermediate (**B**) generates an imine intermediate (**C**). The tautomerization of intermediate (**C**) to (**D**) followed by the attack of the amine nucleophile to the carbonyl group gives intermediate (**E**). Finally, the product (**1a**) is obtained *via* loss of a water molecule from intermediate (**E**) (Scheme III.17).

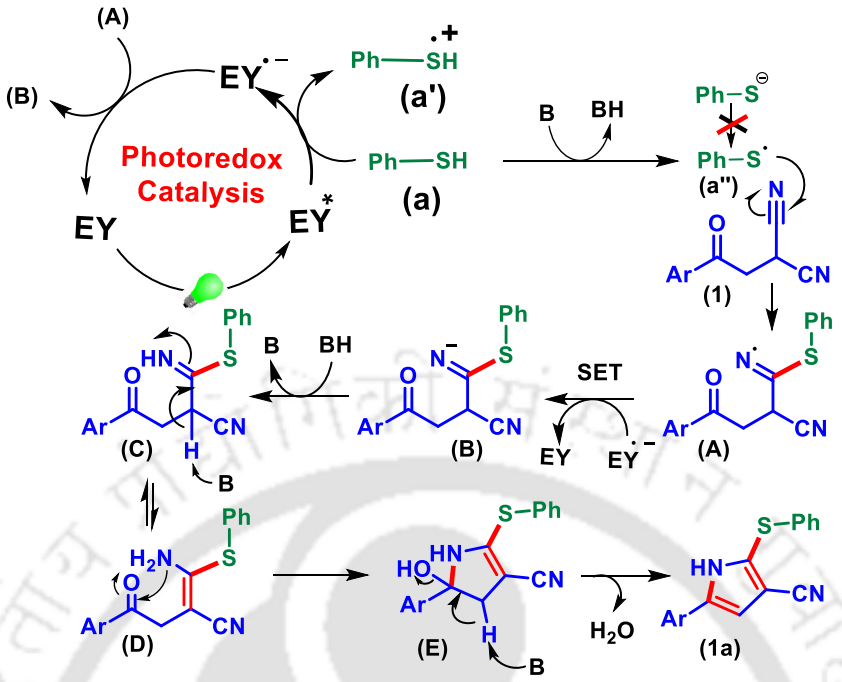

Scheme III.17. *A plausible mechanism for the formation of thio-functionalized pyrroles.*

To demonstrate the applicability of the present photochemical approach, the compound (**1a**) was subjected to some useful organic transformations (Scheme III.18). Treatment of **1a** with diphenyl acetylene resulted in the formation of the anuulated product (**P**) in 78 % yield (Scheme III.18).[27a] While, oxidation with *m*CPBA furnished 5-phenyl-2-(phenylsulfonyl)-1*H*-pyrrole-3-carbonitrile (**Q**) in 80% yield (Scheme III.18).[27b]

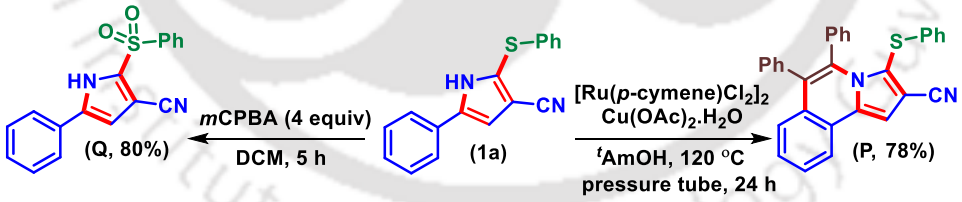

Scheme III.18. *Post-synthetic modification.*

In summary, a thio-triggered visible-light-mediated synthesis of thio-functionalized pyrrole is established using thiols, *β*-ketodinitriles and eosin Y as the photocatalyst. In this protocol, C-N, C-S, and C=C bonds are constructed simultaneously. This methodology is compatible to a range of substituents present in either of the coupling partners. The synthetic utility is demonstrated by a few useful transformations and scale up experiment. The mechanistic investigation reveals a photo-induced selective thiyl radical addition to one of the

nitrile groups of *β*-ketodinitriles followed by a nucleophilic attack and aromatization process to give the thio-functionalized pyrroles.

III.4. Experimental Section

III.4.1. General Information: All the reagents were commercial grade and purified according to the established procedures. All the reactions were carried out in oven-dried glassware. Highest commercial quality reagents were purchased and were used without further purification unless otherwise stated. Reactions were monitored by thin-layer chromatography (TLC) on a 0.25 mm silica gel plates ($60F_{254}$) visualized under UV illumination at 365 nm. Organic extracts were dried over anhydrous sodium sulfate (Na_2SO_4). Solvents were removed using a rotary evaporator under reduced pressure. Column chromatography was performed to purify the crude product on silica gel 60–120 mesh using a mixture of hexane and ethyl acetate as eluent. All the isolated compounds were characterized by ^{1}H, $^{13}C\{1H\}$ NMR, HRMS-spectrometric and IR spectroscopic techniques. NMR spectra for all the samples were recorded in deuterochloroform ($CDCl_3$). ^{1}H, $^{13}C\{1H\}$ were recorded in 600 (150) or 500 (125) or 400 (100) MHz spectrometer and were calibrated using tetramethylsilane or residual undeuterated solvent for ^{1}H NMR, deuterochloroform for ^{13}C NMR as an internal reference {$Si(CH_3)_4$: 0.00 ppm or $CHCl_3$: 7.260 ppm for ^{1}H NMR, 77.230 ppm for ^{13}C NMR}. ^{19}F NMR was calibrated without any internal standard in $CDCl_3$ in 400 MHz spectrometer. The chemical shifts are quoted in *δ* units, parts per million (ppm). ^{1}H NMR data is represented as follows: Chemical shift, multiplicity (s = singlet, d = doublet, t = triplet, q = quartet, q = quintet, m = multiplet, br = broad, dd = doublet of doublet, tt = triplet of triplet), integration and coupling constant(s) *J* in hertz (Hz). High-resolution mass spectra (HRMS) were recorded on a mass spectrometer using electrospray ionization-time of flight (ESI-TOF) reflection experiments. FT-IR spectra were recorded in KBr or neat and reported in the frequency of absorption (cm−1).

III.4.2. Crytallographic Description:

Sample Preparation:

The single crystal of compound **1a** was prepared by the slow evaporation method for which 10 mg of the compound (**1a**) was dissolved in 1 mL of DCM in a clean and dry 10 mL glass vial. MeOH (1 mL) was added to this solution slowly with a dropper. The mouth of the

glass vial was covered with a cap having a small hole and kept it for slow evaporation at room temperature. A single crystal of **1a** was obtained as a transparent white needle-like crystal after around 2-3 days.

Crystallographic Description of 5-Phenyl-2-(phenylthio)-1*H*-pyrrole-3-carbonitrile (1a):

$C_{17}H_{12}N_2S$, crystal dimensions 0.25 x 0.22 x 0.16 mm, M_r = 276.35, triclinic, space group P -1, a = 7.5884 (4), b = 13.3022 (7), c = 14.6150 (8) Å, α = 92.813 (2)°, β = 91.854 (2)°, γ = 97.475 (2)°, V = 1459.86 (14) Å^3, Z = 4, ρ_{calcd} = 1.257 mg/m^3, μ = 0.212 mm^{-1}, F(000)= 576.0, reflection collected / unique = 5163 / 3622, refinement method = full-matrix least-squares on F^2, final R indices [I> 2\s(I)]:R_1 = 0.0728, wR_2 = 0.1643, R indices (all data): R_1 = 0.0458, wR_2 = 0.1379, goodness of fit = 0.903. CCDC-2118561 for **5-phenyl-2-(phenylthio)-1*H*-pyrrole-3-carbonitrile (1a)** contains the supplementary crystallographic data for this paper. These data can be obtained free of charge from The Cambridge Crystallographic Data Centre via www.ccdc.cam.ac.uk/data_request/cif.

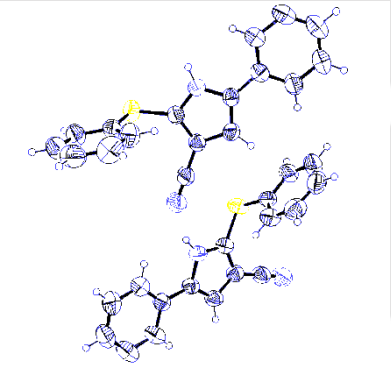

Figure III.12. *ORTEP diagram of 5-phenyl-2-(phenylthio)-1H-pyrrole-3-carbonitrile (**1a**) with 40% ellipsoid probability (CCDC 2118561).*

III.4.3. General Procedure for the Synthesis of 2-(2-Oxo-2- arylethyl)malononitriles (1−13).

2-(2-Oxo-2-arylethyl)malononitriles (**1**−**13**) are synthesized following slightly modified procedures.

To an oven-dried 100 mL round-bottom flask were added α-bromoacetophenone (1.97 g, 10.0 mmol) and malononitrile (0.66 g, 10.0 mmol); the reaction mixture was dissolved in EtOH (20 mL) and cooled in an ice bath. On the other hand, NaOH (0.4 g, 10.0 mmol) was dissolved in H_2O (20 mL), cooled in an ice bath, and added to the above reaction mixture

over a period of 5 min. After letting the reaction mixture stir for 30 min at 0 °C, H_2O (20 mL) was added, from which colourless residue appeared, which was filtered off and dried under air. Recrystallization of EtOH gave 2-(2-oxo-2-phenylethyl)malononitriles (**1**) as a white solid (1.39 g, yield 76%) (Scheme S1).

III.4.4. General Procedure for the Synthesis of 5-Phenyl-2-(phenylthio)-1*H*-pyrrole-3-carbonitrile (1a–13a) from 2-(2-Oxo-2-arylethyl)malononitriles (1−13) and Thiophenol (a)

To an oven-dried 10 mL borosilicate vial were added 2-(2-oxo-2-arylylethyl)malononitriles (**1**) (0.25 mmol, 46 mg), benzene thiol (**a**) (0.5 mmol, 55 mg), eosin Y (3 mol %, 5 mg), and K_2CO_3 (1 equiv, 34 mg) in 1 mL of DMSO and stirred at room temperature under N_2 atmosphere for 10 h, tentatively at a distance of ~6−8 cm from two 10 W green LED bulbs. After completion of the reaction (monitored by TLC analysis), the mixture was admixed with 25 mL of ethyl acetate followed by washing with a water (1 × 10 mL). The organic layer was dried over anhydrous Na_2SO_4, and the solvent was evaporated under reduced pressure. The crude residue thus obtained was purified by column chromatography over silica gel (60−120 mesh) using hexane and ethyl acetate (9:1) as an eluent to afford the 5-phenyl-2-(phenylthio)-1*H*-pyrrole-3-carbonitrile (**1a**) in 70% yield. The identity and purity of the product were confirmed by spectroscopic analysis (Scheme S2).

III.4.5. Radical-trapping Experiments:

To validate the radical nature of the reaction, two independent reactions were performed, one in the presence of 2,6-di-*tert*-butyl-4-methyl phenol (BHT, 1 equiv) and the other in the presence of 1,1-diphenyl ethylene (1 equiv).

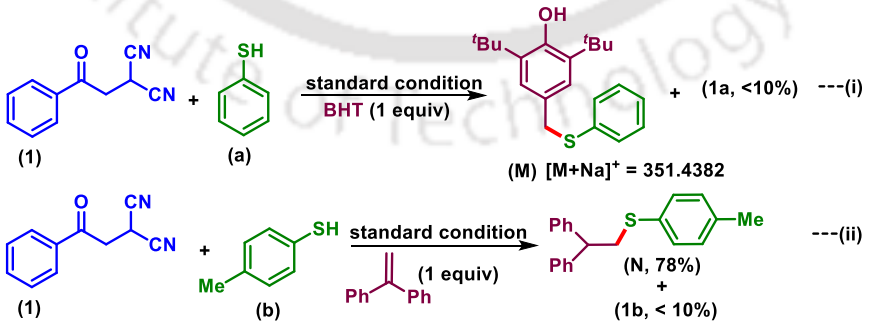

(i) To an oven-dried 10 mL borosilicate vial were added 2-(2-oxo-2-arylylethyl)malononitriles (1) (0.25 mmol, 45 mg), benzene thiol (a) (0.5 mmol, 55 mg), eosin Y (3 mol %, 4.0 mg), and K_2CO_3 (1 equiv, 34 mg) and BHT (1 equiv, 55 mg) in 1 mL of

DMSO and stirred at room temperature under N_2 atmosphere for 10 h tentatively at a distance of 6-8 cm from two 10 W green LEDs bulbs. Then the reaction was continued under N_2 atmosphere. It was found that for BHT, <10% of the product (**1a**) was observed. The BHT adduct (**M**) with thiophenol (**a**) was detected by HRMS analysis of the reaction aliquot {Scheme S4 (i)}.

(ii) To an oven-dried 10 mL borosilicate vial were added 2-(2-oxo-2-arylylethyl)malononitriles (**1**) (0.25 mmol, 45 mg), *p*-methyl benzene thiol (**b**) (0.5 mmol, 62 mg), eosin Y (3 mol %, 4.0 mg), and K_2CO_3 (1 equiv, 34 mg) and BHT (1 equiv, 55 mg) in 1 mL of DMSO and stirred at room temperature under N_2 atmosphere for 10 h tentatively at a distance of 6-8 cm from two 10 W green LEDs bulbs. It was found that in the presence of diphenyl ethylene <10% of the product (**1b**) and exclusive thiyl radical trapped adduct (**N**, 78%) was observed. The structure of the adduct (**N)** was confirmed by NMR as well as (^{1}H and ^{13}C) analysis {Scheme S4 (ii)}.

III.4.6. Reaction Performed in Dark:

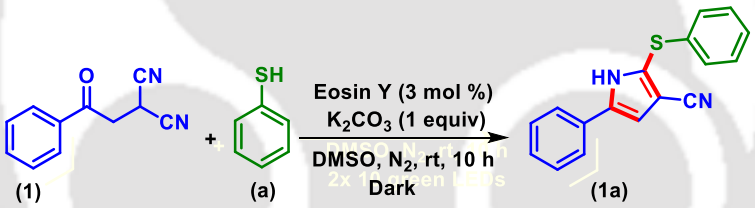

To an oven-dried 10 mL borosilicate vial were added 2-(2-oxo-2-phenylethyl)malononitriles (**1**) (0.25 mmol, 46 mg), benzene thiol (a) (0.5 mmol, 55 mg), eosin Y (3 mol %, 4 mg), and K_2CO_3 (1 equiv, 34 mg). The round bottom flask was then covered with an aluminium foil so that light cannot interact with the reaction mixture. Then the reaction mixture was kept in a vacuum then to the reaction mixture 1 mL of DMSO was added and stirred at room temperature under N_2 atmosphere for 10 h, tentatively at a distance of ~6−8 cm from two 10 W green LED bulbs. After completion of the reaction (monitored by TLC analysis), the mixture was admixed with 25 mL of ethyl acetate followed by washing with water (1 × 10 mL). The organic layer was dried over anhydrous Na_2SO_4, and the solvent was evaporated under reduced pressure. The crude residue thus obtained was purified by column chromatography over silica gel (60−120 mesh) using hexane and ethyl acetate (9:1) as

an eluent to afford the 5-phenyl-2-(phenylthio)-1*H*-pyrrole-3-carbonitrile (**1a**) in 10% yield. The identity and purity of the product were confirmed by spectroscopic analysis.

III.4.7. General Procedure for the Synthesis of 5,6-Diphenyl-3-(phenylthio)pyrrolo[2,1-a]isoquinoline-2-carbonitrile (P) from 5-Phenyl-2-(phenylthio)-1*H*-pyrrole-3-carbonitrile (1a) and Diphenyl Acetylene:

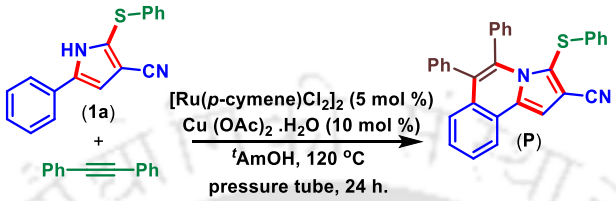

To an oven-dried pressure tube containing a magnetic bar was added 5-phenyl-2-(phenylthio)-1*H*-pyrrole-3-carbonitrile (**1a**) (45 mg, 0.25 mmol), diphenylacetylene (44 mg, 0.5 mmol), [Ru(p-cymene)Cl_2]$_2$ (7 mg, 0.0125 mmol), Cu $(OAc)_2.H_2O$ (4 mg, 0.05 mmol), and ^{t}AmOH. The reactions mixture was stirred in an oil bath preheated at 120 ^{o}C for 24 h. After completion of the reaction (monitored by TLC analysis), the reaction mixture was admixed with ethyl acetate (20 mL) and the organic layer was washed with water (1 x 5 mL). The organic layer was dried over anhydrous sodium sulfate (Na_2SO_4), and solvent was evaporated under reduced pressure. The crude product so obtained was purified over a column of silica gel using 5% ethyl acetate in hexane to give pure 5,6-diphenyl-3-(phenylthio)pyrrolo[2,1-a]isoquinoline-2-carbonitrile (**P**) in 78% yield. The identity and purity of the product was confirmed by spectroscopic analysis (Scheme S8).

III.4.8. General Procedure for the Synthesis of 5-Phenyl-2-(phenylsulfonyl)-1H-pyrrole-3-carbonitrile (Q) from 5-Phenyl-2-(phenylthio)-1*H*-pyrrole-3-carbonitrile (1a):

To a 10 mL round bottom flask was added 5-phenyl-2-(phenylthio)-1*H*-pyrrole-3-carbonitrile (**1a**) (45 mg, 0.25 mmol) and DCM. Then the reaction mixture was stirred under ice-cooled condition. Then to the reaction mixture mCPBA (172 mg, 1 mmol) was added pinch wise over a period of 5 minute. Then the reactions mixture was stirred at room temperature for about 5 h. After completion of the reaction (monitored by TLC analysis), the solvent was evaporated and the reaction mixture was admixed with ethyl acetate (20 mL) and the organic layer was washed with water (1 x 5 mL). The organic layer was dried over anhydrous sodium sulfate (Na_2SO_4), and the solvent was evaporated under reduced pressure.

The crude product so obtained was purified over a column of silica gel using 18% ethyl acetate in hexane to give pure 5-phenyl-2-(phenylsulfonyl)-1*H*-pyrrole-3-carbonitrile (**Q**) in 80% yield (Scheme S9). The identity and purity of the product was confirmed by spectroscopic analysis

III.4.9. UV−Visible Spectroscopy and Fluorescence Quenching Experiment (Stern−Volmer Studies).

UV-visible spectroscopy of reaction solution was recorded on a SHIMADZU UV3600 UV-visible spectrophotometer. The 0.01 M sample was prepared by mixing eosin Y in DMSO in a light path quartz UV cuvette. The UV-visible spectroscopy indicated that the maximum absorption wavelength of the reaction solution was found to be 543 nm. The absorption was collected and the results are listed in Figure S11.

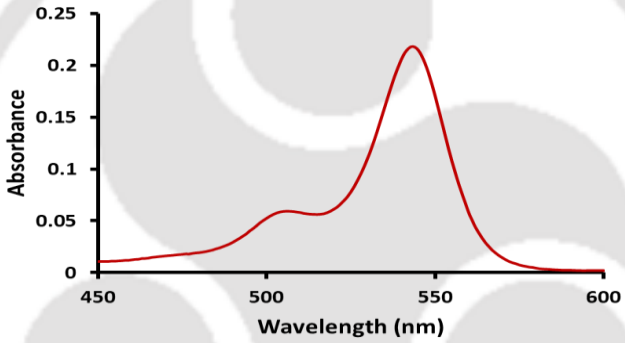

Figure III.13. UV-vis spectra of eosin Y in DMSO (0.01 M).

A 1 mM solution was prepared by mixing eosin Y in water by an appropriate dilution of 0.01 M stock solution and taken in a quartz UV cuvette of a 1 cm path length. The UV−visible spectroscopy showed λ_{max} of 515 nm (Figure 2a). For the fluorescence measurement, the sample was excited at 515 nm, and the emission was observed at 560 nm. For each fluorescence quenching experiment, a 5 μL (1 M) solution of benzene thiol (**a**) was added to eosin Y solution (1 mM) taken in a fluorescence cuvette, and fluorescence emission spectra were recorded after each addition (Figure S12). As evident from Figure S12, a decrease in emission intensity was observed after each addition of thiophenol (**a**) concentration (5−75 mM). This suggests that a facile electron transfer is possible between the catalyst and the quencher PhSH. This indicates that eosin Y might be helping in the generation of thiyl radical from the PhSH. With these data, the Stern−Volmer graph was

plotted using the equation I_0/I_t =1+ K_{SV} [Q], where I_0 and I_t are the integrated emission intensity in the absence and presence of quencher and K_{sv} is the quenching constant. A linear quenching was observed (Figure S13).

III.4.10. CV Experiments Performed to Determine the Redox Potentials.

Cyclic voltammetry (CV) was performed using a three-electrode cell configuration comprising a glassy carbon, a platinum wire, and Ag(s)/AgCl (0.01 M) as the working, auxiliary, and reference electrodes, respectively. Cyclic voltammetry experiment of PhSH and *β*-ketodinitrile (**1**) taken at a scan rate 100 mv/s. Experiment conditions: init E = 2.0 V, high E = 2.0 V, low E = −2.0 V, scan rate = 0.1 V/s, sample interval = 0.001 V, quiet time = 2s, sensitivity = 2e−4 A/ V]. The supporting electrolyte used was tetraethylammonium hexafluorophosphate (TEAHFP) $(C_2H_5)_4N(PF_6)$. Samples were prepared with a substrate concentration of 0.01 M in a 0.1 M TEAHFP in an acetonitrile electrolyte solution. From the result, it was found that the oxidation potential of thiophenol ($E_{1/2\ ox}$ = +0.25 V vs SCE) is lower than the oxidation potential of Eosin Y ($E_{1/2\ ox}$ = +0.83 V vs SCE for excited state of eosin Y). Similarly, the reduction potential of thiophenol (**a**) ($E_{1/2\ red}$ = -1.35 V vs SCE) is lower than the reduction potential value of Eosin Y ($E_{1/2\ red}$ = -1.06 V vs SCE for excited state of eosin Y (Figure S14). This indicates that thiophenols can be easily oxidized by the eosin Y which also confirms the role of eosin Y as an oxidizing agent and helps in the facile generation of the thiyl radical. The $E_{1/2\ Oxd}$ of *β*-ketodinitriles (**1**) is found to be + 0.95 V vs SCE (Figure S15).

III.5. References

[1] Atrovastatin: (a) Thompson, R. B. FASEB *J*. **2001**, *15*, 1671. Tolmetin: (b) Brogden, R. N.; Heel, R. C.; Speight, T. M.; Avery, G. S. Tolmetin *Drugs* **1978**, *15*, 429−450. Sunitinib (c) Le Tourneau, C.; Raymond, E.; Faivre, S.: Sunitinib: *Ther*. *Clin*. *Risk Manage*. **2007**, *3*, 341−348. Pyrvinium: (d) Cui, L.; Zhao, J.; Liu, J. *J*. *Med*. *Sci*. **2018**, *355*, 274−280.

[2] (a) Knorr, L. Synthesis of Pyrrole Derivatives. *Ber*. *Dtsch*. *Chem*. *Ges*. **1884**, *17*, 1635−1642. (b) Paal, C. *Ber*. *Dtsch*. *Chem*. *Ges*. **1885**, *18*, 367−371. (c) Hantzsch, *Ber*. *Dtsch*. *Chem*. *Ges*. **1890**, *23*, 1474−1476. (d) Luo, K.; Mao, S.; He, K.; Yu, X.; Pan, J.; Lin, J.; Shao, Z.; Jin, Y. *ACS Catal*. **2020**, *10*, 3733−3740. (e) Behera, B. K.; Sahu, A. K.; Devi, N. R.; Saikia, A. K. *J*. *Org*. *Chem*. **2021**, *86*, 12481−12493. (f) Andreou, D.; Essien, N. B.;

Pubill-Ulldemolins, C.; Terzidis, M. A.; Papadopoulos, A. N.; Kostakis, G. E.; Lykakis, I. N. *Org. Lett*. **2021**, *23*, 6685−6690.

[3] Wu, X.; Zhao, P.; Geng, X.; Wang, C.; Wu, Y-D.; Wu, A-X.. *Org*. *Lett*. **2018**, *20*, 688−691.

[4] Michlik, S.; Kempe, R.. *Nat. Chem*. **2013**, *5*, 140−144.

[5] Zhu, L.; Yu, Y.; Mao, Z.; Huang, X. *Org*. *Lett*. **2015**, *17*, 30−33.

[6] George, J.; Kim, H. Y.; Oh, K. *Org. Lett*. **2017**, *19*, 628–631.

[7] Wilkerson-Hill, S. M.; Yu, D.; Painter, P. P.; Fisher, E. L.; Tantillo, D. J.; Sarpong, R.; Hein. J. E. *J. Am. Chem. Soc*. **2017**, *139*, 10569−10577.

[8] Chen, J.; Chang, D.; Xiao, F.; Deng, G-J. *J. Org. Chem*. **2019**, *84*, 568−578.

[9] Fu, L.; Liu, Y.; Wan, J.-P. *Org*. *Lett*. **2021**, *23*, 4363−4367.

[10] (a) Kumar, A.; R.; Tadigoppula, N. *Green Chem*. **2017**, *19*, 5385. (b) Kayser, L. V.; Vollmer, M.; Welnhofer, M.; Krikcziokat, H.; Meerholz, K.; Arndtsen, B. A. *J*. *Am*. *Chem*. *Soc*. **2016**, *138*, 10516−10521. (c) Reddy, N. N. K.; Rawat, D.; Adimurthy, S. *J*. *Org*. *Chem*. **2018**, *83*, 9412−9421. (d) Teng, Q.-H.; Xu, Y.-L.; Liang, Y.; Wang, H.-S.; Wang, Y.-C.; Pan, Y-M. *Adv*. *Synth*. *Catal*. **2016**, *358*, 1897–1902. (e) Wu, X.; Li, K.; Wang, S.; Liu, C.; Lei, A. *Org*. *Lett*. **2016**, *18*, 56−59.

[11] (a) Sun, K.; Lv, Q.-Y.; Chen, X.-L.; Qua, L.-B.; Yu, B. *Green Chem*. **2021**, *23*, 232−248. (b) Zhou, Q.-Q.; Zou, Y.-Q.; Lu, L.-Q.; Xiao, W.-J. *Angew*. *Chem*. *Int*. *Ed*. **2019**, *58*, 1586–1604. (c) Masson, G.; König, B.; *Eur*. *J*. *Org*. *Chem*. **2020**, 1191–1192. (d) Giacomo E. M. Crisenza, Mazzarella, D.; Melchiorre, P. *J*. *Am*. *Chem*. *Soc*. **2020**, *142*, 5461−5476. (e) Liu, K.; Zou, M.; Lei, A. *J*. *Org*. *Chem*. **2016**, *81*, 7088−7092.

[12] (a) Pali, P.; Shukla, G.; Saha, P.; Singh, M. S. *Org*. *Lett*. **2021**, *23*, 3809−3813. (b) Chalotra, N.; Rizvi, M. A.; Shah, B. A. *Org*. *Lett*. **2019**, *21*, 4793–4797. (c) Skubi, K. L.; Blum, T. R.; Yoon, T. P. *Chem*. *Rev*. **2016**, *116*, 10035−10074. (d) Zhu, C.; Yue, H.; Chu, L.; Rueping, M. *Chem*. *Sci*. **2020**, *11*, 4051–4064.

[13] (a) Ppelliccia, S.; Alfano, A. I.; Luciano, P.; Novellino, E.; Massarotti, A.; Tron, G. C.; Ravelli, D.; Giustiniano, M. *J*. *Org*. *Chem*. **2020**, *85*, 1981−1990. (b) Shang, T.; Zhang, J.; Zhang, Y.; Zhang, F.; Li, X.-S.; Zhu, G. *Org*. *Lett*. **2020**, *22*, 3667−3672. (c) Wang, P.; Zhao Q.; Xiao, W.; Chen, J. *Green Synth. Catal*. **2020**, *1*, 42–51. (d) Xie, S.; Li, Y.; Liu,

P.; Sun, P.. *Org. Lett.* **2020**, *22*, 8774−8779. (e) Zhu, J.; Yang, W.-C.; Wang, X.-D.; Wu, L. *Adv. Synth. Catal.* **2018**, *360*, 386−400.

[14] (a) Bell, J. D.; Murphy, J. A. *Chem. Soc. Rev.* **2021**, *50*, 9540–9685. (b) Yan, D.-M.; Chen, J.-R.; Xiao, W. J. *Angew. Chem., Int. Ed.* **2019**, 58, 378 –380. (c) Xia, L.; Jin, M.; Jiao, Y.; Yu, S. *Org. Lett.* **2022**, *24*, 364−368. (d) Dahiya, A.; Das, B.; Sahoo, A. K.; Patel, B. K. *Adv. Synth.Catal.* **2022**, *364*, 966–973. (e) Wu, F.; Dong, W.; Fan, S.; Yuan, Y.; Liang, C.; Chen, A.; Yin, Z.; Zhang Z. *J. Org. Chem.* **2022**, *87*, 2, 1302–1312. (f) Rohokale, R. S.; Koenig, B.; Dhavale, D. D. *J. Org. Chem.* **2016**, *81*, 7121−7126. (g) Ansari, M. A.; Yadav, D.; Soni, S.; Srivastava, A.; Singh, M. S. *J. Org. Chem.* **2019**, *84*, 5404−5412.

[15] (a) Sun, K.; Lv, Q.-Y.; Lin, Y.-W.; Yu, B.; He, W.-M. *Org. Chem. Front.* **2021**, *8*, 445. (b) Qi, L.; Li, R.; Yao, X.; Zhen, Q.; Ye, P.; Shao, Y.; Chen, J. *J. Org. Chem.* **2020**, *85*, 1097−1108. (c) Qi, L.; Hu, K.; Yu, S.; Zhu, J.; Cheng, T.; Wang, X.; Chen, J.; Wu, H. *Org. Lett.* **2017**, *19*, 218−221. (d) Li, X.; Fang, X.; Zhuang, S.; Liu, P.; Sun, P. *Org. Lett.* **2017**, *19*, 3580−3583.

[16] Shang, J.-Q.; Wang, X.-X.; Xin, Y.; Li, Y.; Zhou, B.; Li, Y.-M. *Org. Biomol. Chem.* **2019**, *17*, 9447–9455.

[17] Huang, A.-X.; Zhu, H.-L.; Zeng, F.-L.; Chen, X.-L.; Huang, X.-Q.; Qu, L.-B.; Yu, B. *Org. Lett.* **2022**, *24*, 3014−3018.

[18] Shi, S.; Zheng, Z.; Zhang, Y.; Yang, Y.; Ma, D.; Gao, Y.; Liu, Y.; Tang, G.; Zhao, Y. *Org. Lett.* **2021**, *23*, 9348−9352.

[19] Qian, P.; Deng, Y.; Mei, H.; Han, J.; Zhou, J.; Pan, Y. *Org. Lett.* **2017**, *19*, 4798−4801.

[20] Natarajan, P.; Muskan, M.; Brar, N. K.; Kaur, J. J. *Org. Chem. Front.* **2018**, *5*, 1527−1531.

[21] Rakshit, A.; Kumar, P.; Alam, T.; Dhara, H.; Patel, B. K. *J. Org. Chem.* **2020**, *85*, 12482−12504.

[22] Sahoo, A. K.; Rakshit, A.; Dahiya, A.; Pan, A.; Patel, B. K. *Org. Lett.* **2022**, *24*, 1918−1923.

[23] (a) Lv, Y.; Luo, J.; Lin, M.; Yue, H.; Daia, B.; He, L. A *Org. Chem. Front.* **2021**, *8*, 5403–5409. (b) Gadde, K.; Mampuys, P.; Guidetti, A.; Ching, H. Y. V.; Herrebout, W. A.; Doorslaer, S. V.; Tehrani, K. A.; Maes, B. U. W. *ACS Catal.* **2020**, *10*, 8765−8779.

[24] (a) Roy, V. J.; Sen, P. P.; Roy, S. R. *J. Org. Chem.* **2021**, *86*, 16965−16976. (b) Sahoo, A. K.; Dahiya, A.; Das, B.; Behera, A.; Patel, B. K. *J. Org. Chem.* **2021**, *86*, 11968−11986. (c) Wang, W.; Huang, S.; Yan, S.; Sun, X.; Tung, C.-H.; Xu, Z. *Chin. J. Chem.* **2020**, *38*, 445–448. (d) Qi, J.; Wei, F.; Huang, S.; Tung, C.-H.; Xu, Z. *Angew. Chem., Int. Ed.* **2021**, *60*, 4561–4565.

[25] (a) Pavlishchuka, V. V.; Addison, A. W. *Inorg. Chim. Acta.* **2000**, *298*, 97−102. (b) Larsen, A. G.; Holm, A. H.; Roberson, M.; Daasbjerg, Kim. *J. Am. Chem. Soc.* **2001**, *123*, 1723–1729.

[26] (a) Liang, G.; Wang, J.-H.; Lei, T.; Cheng, Y.-Y.; Zhou, C.; Chen, Y.-J.; Ye, C.; Chen, B.; Tung, C.-H.; Wu, L.-Z. *Org. Lett.* **2021**, *23*, 8082−8087. (b) Zalesskiy, S. S.; Shlapakov, N. S.; Ananikov, V. P. *Chem. Sci.* **2016**, *7*, 6740–6745. (c) Rahaman, R.; Das, S.; Barman, P. *Green. Chem.* **2018**, *20*, 141–147. (d) Wei, W.; Bao, P.; Yue, H.; Liu, S.; Wang, L.; Li, Y.; Yang, D. *Org. Lett.* **2018**, *20*, 5291−5295. (e) Nair, A. M.; Kumar, S.; Volla, C. M. R. *Adv. Synth. Catal.* **2019**, *361*, 4983–4988. (f) Lynch, D. M.; Scanlan, E. M. *Molecules* **2020**, *25*, 3094.

[27] (a) Ackermann, L.; Wang, L.; Lygin, A. V. *Chem. Sci.* **2012**, *3*, 177–180. (b) Dar, A. A.; Enjamuri, N.; Shadab, Md.; Ali, N.; Khan, A. T. *ACS Comb. Sci.* **2015**, *17*, 671−681.

III.6. Spectral Data

***5-Phenyl-2-(phenylthio)-1H-pyrrole-3-carbonitrile* (*1a*):**

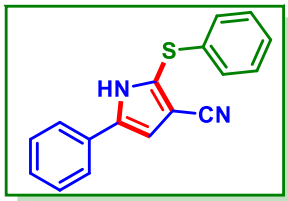

As a white solid (48 mg, 70% yield); mp 180-182 °C; purified over a column of silica gel (12% EtOAc in hexane); ^{1}H NMR ($CDCl_3$, 600 MHz): δ 9.21 (s, 1H), 7.49 (d, 2H, J = 7.2 Hz), 7.43 (t, 2H, J = 7.2 Hz), 7.35 (t, 1H, J = 7.2 Hz), 7.30 (q, 4H, J_1 = 15.0 Hz, J_2= 7.8 Hz), 7.24 (dd, 1H, J_1 =11.4 Hz, J_2 = 6 6 Hz), 6.78 (d, 1H, J = 2.4 Hz); ^{13}C{^{1}H} NMR ($CDCl_3$,150 MHz): δ 136.2, 135.3, 130.2, 129.6, 129.4, 128.7, 128.5, 127.4, 124.7, 115.7, 110.2, 103.2; IR (KBr, cm^{-1}): 3245, 2927, 2227, 1589, 1463, 1247, 1038;

HRMS (ESI/Q-TOF) (m/z): calcd for $C_{17}H_{12}N_2S$, $[M + H]^+$: 277.0794, found 277.0824.

***2-(Phenylthio)-5-(p-tolyl)-1H-pyrrole-3-carbonitrile* (*2a*):**

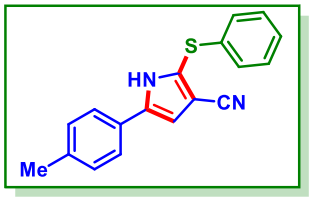

As a white solid (52 mg, 72% yield); mp 208-210 ^oC; purified over a column of silica gel (12% EtOAc in hexane); ^1H NMR ($CDCl_3$, 500 MHz): δ 8.86 (s, 1H), 7.34 (d, 2H, J = 8.0 Hz), 7.28 (d, 2H, J = 7.0 Hz), 7.25 (d, 2H, J = 6.5 Hz), 7.21 (d, 3H, J = 7.5 Hz), 6.72 (d, 1H, J = 3.0 Hz), 2.36 (s, 3H); $^{13}C\{^1H\}$ NMR ($CDCl_3$, 126 MHz): δ 138.6, 136.4, 135.5, 130.1, 129.7, 128.7, 127.5, 127.4, 126.8, 124.6, 115.6, 109.8, 103.5, 21.4.; IR (KBr, cm^{-1}): 3294, 3227, 2920, 2229, 1591, 1455, 1254, 1057; HRMS (ESI/Q-TOF) (m/z): calcd for $C_{18}H_{14}N_2S$ $[M + H]^+$: 291.0950, found 291.0952.

***5-(4-Methoxyphenyl)-2-(phenylthio)-1H-pyrrole-3-carbonitrile* (*3a*):**

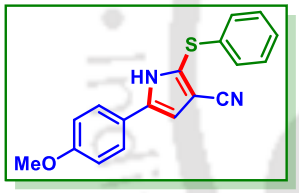

As a gummy (58 mg, 77% yield); purified over a column of silica gel (15% EtOAc in hexane); ^1H NMR ($CDCl_3$, 500 MHz): δ 8.84 (s, 1H), 7.34 (d, 2H, J = 9.0Hz), 7.26-7.23 (m, 2H), 7.28 – 7.21 (m, 2H), 7.17-7.15 (m, 1H), 6.89 (d, 2H, J = 9.0 Hz), 6.62 (d, 1H, J = 1.8 Hz), 3.83 (s, 3H); $^{13}C\{^1H\}$ NMR ($CDCl_3$, 126 MHz): δ 160.0, 136.4, 135.6, 129.7, 128.6, 127.4, 126.4, 126.2, 123.1, 115.7, 114.9, 109.4, 103.5, 55.6.; IR (KBr, cm^{-1}): 3245, 2928, 2852, 2228, 1589, 1475, 1038; HRMS (ESI/Q-TOF) (m/z): calcd for $C_{18}H_{14}N_2OS$, $[M + H]^+$: 307.090, found 307.0911.

***5-(4-Isopropylphenyl)-2-(phenylthio)-1H-pyrrole-3-carbonitrile* (4a):**

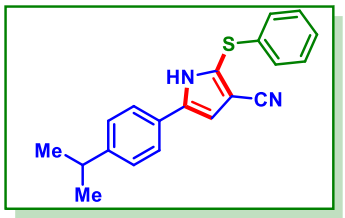

As a gummy (86 mg, 75% yield); Purification over a column of silica gel (10% EtOAc in hexane). ^1H NMR (500 MHz, DMSO-d_6): δ 12.83 (s, 1H), 7.68 (d, 2H, J = 8.2 Hz), 7.34 (t, 2H, J = 7.7 Hz), 7.28 (d, 2H, J = 8.2 Hz), 7.23 (t, 1H, J = 7.4 Hz), 7.17 (d, 2H, J = 7.5 Hz), 7.10 (d, 1H, J = 2.5 Hz), 2.88 (m, 1H), 1.20 (d, 6H, J = 6.9 Hz); $^{13}C\{^1H\}$ NMR (DMSO-d_6, 126

MHz): δ 148.2, 136.7, 136.2, 129.5, 127.9, 127.2, 126.8, 126.7, 126.6, 124.7, 115.7, 109.7, 101.9, 33.1, 23.7; IR (KBr, cm^{-1}): 3052, 2938, 2842, 2220, 1569, 1435, 1065; HRMS (ESI/Q-TOF) (m/z) calcd for $C_{20}H_{18}N_2S$ $[M + H]^+$ 319.1263, found 319.1283.

***5-(4-Fluorophenyl)-2-(phenylthio)-1H-pyrrole-3-carbonitrile* (*5a*):**

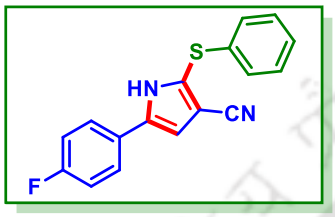

As a white solid (58 mg, 69% yield); mp 202-204 °C; purified over a column of silica gel (18% EtOAc in hexane); ^{1}H NMR ($CDCl_3$, 500 MHz): δ 9.04 (s, 1H), 7.42 – 7.39 (m, 2H), 7.24 (t, 4H, J = 4.5 Hz), 7.21 – 7.18 (m, 1H), 7.08 (t, 2H, J = 8.5 Hz), 6.67 (d, 1H, J = 3.0 Hz); $^{13}C\{^1H\}$ NMR ($CDCl_3$, 125 MHz): δ 163.8, 162.0, 135.2 (d, J = 70 Hz), 132.1, 129.7, 128.9, 127.6 (d, J = 49 Hz), 126.7 (d, J = 32 Hz), 125.3, 116.5 (d, J = 87.5 Hz), 115.5, 110.2, 103.3.; ^{19}F NMR ($CDCl_3$, 471 MHz): δ -112.57; IR (KBr, cm^{-1}): 3053, 2922, 2844, 2222, 1591, 1488, 1264, 1150, 1080; HRMS (ESI/Q-TOF) (m/z): calcd for $C_{17}H_{11}FN_2S$, $[M + H]^+$: 295.070, found 295.0704.

***5-(4-Chlorophenyl)-2-(phenylthio)-1H-pyrrole-3-carbonitrile* (*6a*):**

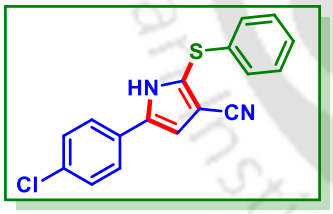

As a white solid (56 mg, 72% yield); mp 204-206 °C; purified over a column of silica gel (18% EtOAc in hexane); ^{1}H NMR ($CDCl_3$, 400 MHz): δ 9.20 (s, 1H), 7.38 – 7.28 (m, 5H), 7.23 (t, 3H, J = 4.0 Hz), 7.22 – 7.17 (m, 1H), 6.70 (d, 1H, J = 2.8 Hz); $^{13}C\{^1H\}$ NMR ($CDCl_3$, 125 MHz): δ 135.1, 135.06, 134.4, 129.7, 129.6, 129.0, 128.8, 128.1, 127.6, 126.0, 115.5, 110.6, 103.3; IR (KBr, cm^{-1}): 3059, 2989, 2920, 2229, 1581, 1494, 1264, 1092; HRMS (ESI/Q-TOF) (m/z): calcd for $C_{17}H_{11}ClN_2S$, $[M + H]^+$: 311.0404, found 311.0401.

***5-(4-Bromophenyl)-2-(phenylthio)-1H-pyrrole-3-carbonitrile* (*7a*):**

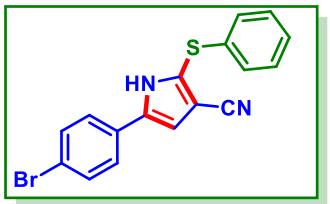

As a white solid (62 mg, 70% yield); mp 189-191 °C; purified over a column of silica gel (15% EtOAc in hexane); ^{1}H NMR ($CDCl_3$, 500 MHz): δ 9.11 (s, 1H), 7.50 (d, 2H, J = 8.5 Hz), 7.30 (d, 2H, J = 8.0 Hz), 7.24 (dd, 4H, J_1 = 8.5 Hz, J_2 = 6.5 Hz), 7.21-7.18 (m, 1H), 6.72. (d, 1H, J = 3.0 Hz); ^{13}C{^{1}H} NMR ($CDCl_3$,100 MHz): δ 135.1, 135.0, 132.6, 129.7, 129.2, 129.0, 128.2, 127.6, 126.2, 122.4, 115.5, 110.6, 103.3; IR (KBr, cm^{-1}): 3051, 2927, 2844, 2229, 1572, 1478, 1264, 1075; HRMS (ESI/Q-TOF) (m/z): calcd for $C_{17}H_{11}BrN_2S$, $[M + H]^+$: 354.9899, found 354.9934.

***5-(4-Iodophenyl)-2-(phenylthio)-1H-pyrrole-3-carbonitrile* (*8a*):**

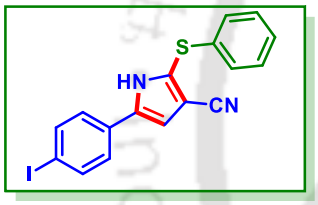

As a yellow solid (71 mg, 71% yield); mp 201-203 °C; Purification over a column of silica gel (12% EtOAc in hexane). ^{1}H NMR (DMSO-d_6, 500 MHz): δ 12.94 (s, 1H), 7.78 (d, 2H, J = 8.5 Hz), 7.56 (d, 2H, J = 8.5 Hz), 7.35 (dd, 2H, J_1 = 7.5, J_2 = 1.5 Hz), 7.24 (t, 1H, J = 7.5 Hz), 7.21– 7.18 (m, 3H). ^{13}C{^{1}H} NMR (DMSO-d_6, 126 MHz): δ 137.6, 135.9, 135.4, 129.7, 129.6, 127.0, 126.7, 126.6, 125.9, 115.5, 110.7, 102.0, 93.5; IR (KBr, cm^{-1}): 3059, 2937, 2834, 2209, 1522, 1458, 1235, 1025; HRMS (ESI/Q-TOF) (m/z): calcd for $C_{17}H_{11}IN_2S$, $[M + H]^+$: 402.9760, found 402.9764.

***5-(Naphthalen-2-yl)-2-(phenylthio)-1H-pyrrole-3-carbonitrile* (*9a*):**

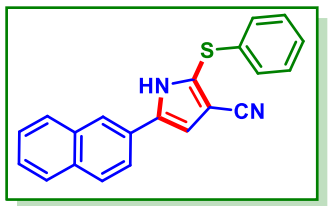

As a white solid (66 mg, 72% yield); mp 198-200 °C; purified over a column of silica gel (10% EtOAc in hexane); ^{1}H NMR ($CDCl_3$, 500 MHz): δ 9.45 (s, 1H), 7.82 (t, 2H, J = 10.5 Hz), 7.77 (t, 2H, J = 3.5 Hz), 7.52 (dd, 1H, J_1 = 9.0 Hz, J_2 = 1.5 Hz), 7.46 – 7.42 (m, 2H), 7.24-7.20 (m, 4H), 7.16 (t, 1H, J = 7.0 Hz), 6.78 (d, 1H, J = 2.5 Hz); ^{13}C{^{1}H} NMR ($CDCl_3$, 125 MHz): δ 138.0, 136.0, 133.6, 133.1, 131.3, 130.5, 129.8, 129.3, 128.9, 128.2,

128.0, 127.6, 127.2, 126.7, 123.1, 122.8, 115.8, 110.7, 102.8, 21.2.; IR (KBr, cm^{-1}): 3464, 3055, 2931, 2220, 1513, 1280, 1196, 1090; HRMS (ESI/Q-TOF) (m/z): calcd for $C_{21}H_{14}N_2S$, $[M + H]^+$: 327.0950, found 327.0954.

***5-(Benzo[d][1,3]dioxol-5-yl)-2-(phenylthio)-1H-pyrrole-3-carbonitrile* (*10a*):**

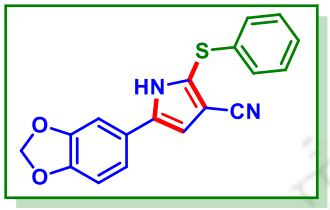

As a gummy (54 mg, 67% yield); purified over a column of silica gel (15% EtOAc in hexane); ^1H NMR (DMSO-d_6, 500 MHz): δ 12.72 (s, 1H), 7.36 (dd, 3H, J_1 = 7.0, J_2 = 5.0 Hz), 7.27 (dd, 1H, J_1 = 8.0, J_2 = 2.0 Hz), 7.23 (t, 1H, J = 7.5 Hz), 7.18 (t, 2H, J = 7.5 Hz), 7.06 (d, 1H, J = 3.0 Hz), 6.96 (d, 1H, J = 8.0 Hz), 6.05 (s, 2H). $^{13}C\{^1H\}$ NMR (DMSO-d_6, 126 MHz): δ 147.8, 146.9, 136.4, 136.2, 129.5, 126.9, 126.6, 124.5, 124.4, 118.6, 115.7, 109.5, 108.6, 105.3, 101.9, 101.2; IR (KBr, cm^{-1}): 3043, 2970, 2834, 2221, 1545, 1411, 1235, 1068; HRMS (ESI/Q-TOF) (m/z): calcd for $C_{18}H_{12}N_2O_2S$ $[M + NH_4]^+$: 344.1427, found 344.0509.

***2-(Phenylthio)-4,5-dihydro-1H-benzo[g]indole-3-carbonitrile* (*11a*):**

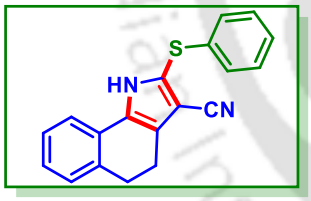

As a gummy (53 mg, 70% yield); purified over a column of silica gel (8% EtOAc in hexane); ^1H NMR (DMSO-d_6, 500 MHz): δ 12.89 (s, 1H), 7.63 (d, 1H, J = 7.5 Hz,), 7.36 (t, 2H, J = 7.5 Hz), 7.24 (t, 3H, J = 7.5 Hz), 7.20 (d, 2H, J = 7.5 Hz), 7.16 (t, 1H, J = 8.0 Hz), 2.93 (t, 2H, J = 7.5 Hz), 2.75 (t, 2H, J = 8.0 Hz).; $^{13}C\{^1H\}$ NMR (DMSO-d_6, 126 MHz): δ 136.3, 134.5, 131.9, 129.5, 128.4, 127.1, 126.9, 126.8, 126.7, 126.6, 123.8, 123.1, 120.7, 115.0, 99.9, 28.2, 19.9; IR (KBr, cm^{-1}): 3069, 2927, 2820, 2215, 1546, 1456, 1264, 1177, 1067; HRMS (ESI/Q-TOF) (m/z): calcd for $C_{19}H_{14}N_2S$, $[M + H]^+$: 303.0950 found 303.0951.

***5-(Furan-2-yl)-2-(phenylthio)-1H-pyrrole-3-carbonitrile* (*12a*):**

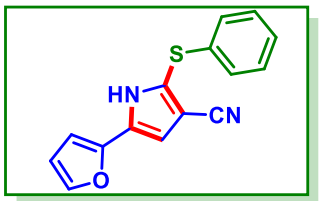

As a brown solid (45 mg, 68% yield); mp 188-190 ^oC; purified over a column of silica gel (18% EtOAc in hexane); ^1H NMR (DMSO-d_6, 500 MHz): δ 13.03 (s, 1H), 7.71 (d, 1H, J = 1.5 Hz),

7.36 (t, 2H, *J* = 7.5 Hz,), 7.24 (t, 1H, *J* = 7.0 Hz), 7.18 (t, 2H, *J* = 1.0 Hz), 6.92 (d, 1H, *J* = 2.5 Hz), 6.82 (d, 1H, *J* = 3.5 Hz), 6.58 (dd, 1H, J_1 = 3.0, J_2 = 1.5 Hz); $^{13}C\{^1H\}$ NMR (DMSO-d_6, 126 MHz): δ 145.4, 142.7, 135.9, 129.5, 128.2, 127.0, 126.7, 125.3, 115.4, 111.8, 108.9, 106.1, 101.7; IR (KBr, cm^{-1}): 3055, 2925, 2832, 2215, 1545, 1402, 1156, 1057; HRMS (ESI/Q-TOF) (m/z): calcd for $C_{15}H_{10}N_2OS$, $[M + H]^+$: 267.0587, found 267.0575.

***2-(Phenylthio)-5-(thiophen-2-yl)-1H-pyrrole-3-carbonitrile* (*13a*):**

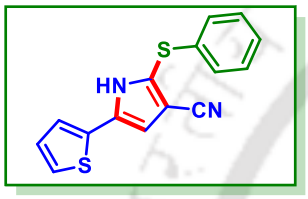

As a brown solid (48 mg, 69% yield); mp 195-197 ^oC; purified over a column of silica gel (18% EtOAc in hexane); ^1H NMR ($CDCl_3$, 500 MHz,): δ 9.42 (s, 1H), 7.25 (dd, 5H, J_1 = 9.5 Hz, J_2 = 4.0 Hz), 7.21-7.18 (m, 1H), 7.15 (d, 1H, *J* = 3.0 Hz), 7.01 (t, 1H, *J* = 4.5 Hz), 6.60 (d, 1H, *J* = 2.5 Hz); $^{13}C\{^1H\}$ NMR ($CDCl_3$, 125 MHz): δ135.1, 133.0, 130.7, 129.6, 128.9, 128.1, 127.5, 127.47, 125.2, 123.8, 115.6, 110.4, 102.8.; IR (KBr, cm^{-1}): 3069, 2944, 2210, 1546, 1489, 1210, 1148, 1085; HRMS (ESI/Q-TOF) (m/z): calcd for $C_{15}H_{10}N_2S_2$, $[M + H]^+$: 283.0358, found 283.0368.

***5-Phenyl-2-(p-tolylthio)-1H-pyrrole-3-carbonitrile* (*1b*):**

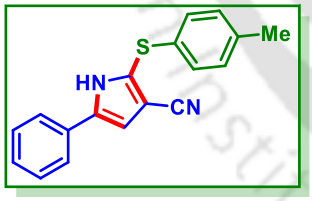

As a white solid (53 mg, 68% yield); mp201-203 ^oC; purified over a column of silica gel (12% EtOAc in hexane); ^1H NMR ($CDCl_3$, 400 MHz): δ 9.03 (s, 1H), 7.41 (d, 2H, *J* = 7.6 Hz), 7.36 (t, 2H, *J* = 7.2 Hz), 7.29 (d, 1H, *J* = 6.8 Hz), 7.20 (t, 2H, J = 9.6 Hz), 7.06 (d, 2H, *J* = 7.6 Hz), 6.69 (d, 1H, *J* = 2.0 Hz), 2.26 (s, 3H); $^{13}C\{^1H\}$ NMR ($CDCl_3$, 100 MHz): δ 137.9, 135.9, 131.3, 130.4, 130.3, 129.7, 129.4, 128.6, 128.4, 124.7, 115.8, 110.2, 102.6, 21.2; IR (KBr, cm^{-1}): 3294, 2920, 2857, 2229, 1591, 1455, 1264, 1051; HRMS (ESI/Q-TOF) (m/z): calcd for $C_{18}H_{14}N_2S$, $[M + H]^+$: 291.0950, found 291.0980.

***5-Phenyl-2-(o-tolylthio)-1H-pyrrole-3-carbonitrile* (*1c*):**

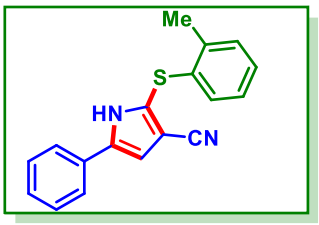

As a white solid (49 mg, 68% yield); mp 202-204 °C; purified over a column of silica gel (12% EtOAc in hexane); ^{1}H NMR ($CDCl_3$, 500 MHz): δ 9.05 (s, 1H), 7.45 (d, 2H, J = 7.5 Hz,), 7.41 (t, 2H, J = 7.5 Hz), 7.32 (t, 1H, J = 7.0 Hz), 7.18 (d, 1H, J = 7.0 Hz,), 7.15 (dd, 1H, J_1 = 7.5 Hz, J_2 = 1.5 Hz,), 7.12-7.08 (m, 1H), 7.01 (dd, 1H, J_1 = 7.5Hz, J_2 = 0.5 Hz,), 6.75 (d, 1H, J = 2.5 Hz,), 2.45 (s, 3H); ^{13}C{^{1}H} NMR ($CDCl_3$, 125 MHz): δ 137.1, 136.2, 134.4, 130.9, 130.3, 129.4, 128.8, 128.5, 127.5, 127.3, 127.2, 124.7, 115.6, 110.2, 103.0, 20.4; IR (KBr, cm^{-1}): 3259, 2926, 2850, 2224, 1519, 1228, 1049; HRMS (ESI/Q-TOF) (m/z): calcd for $C_{18}H_{17}N_3S$, $[M + NH_4]^+$: 308.1216, found 308.1240.

***2-((4-Methoxyphenyl)thio)-5-phenyl-1H-pyrrole-3-carbonitrile* (*1d*):**

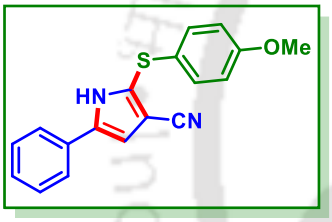

As a brown solid (58 mg, 78% yield); mp 102-104 °C; purified over a column of silica gel (15% EtOAc in hexane); ^{1}H NMR ($CDCl_3$, 500 MHz): δ 9.12 (s, 1H), 7.44 (t, 2H, J = 8.5 Hz), 7.39 (dd, 2H, J_1 = 10.0 Hz, J_2 = 7.5Hz), 7.37 (t, 1H, J = 3.0 Hz), 7.30 (t, 1H, J = 7.5 Hz), 6.83 (d, 2H, J = 9.0 Hz), 6.70 (d, 1H, J = 3.0 Hz), 3.77 (s, 3H); ^{13}C{^{1}H} NMR ($CDCl_3$, 125 MHz): δ 160.0, 135.6, 132.8, 130.4, 130.0, 129.4, 129.0, 128.3, 124.7, 123.1, 115.3, 110.1, 101.6, 55.6; IR (KBr, cm^{-1}): 3066, 2945, 2847, 1740, 1610, 1235, 1062; HRMS (ESI/Q-TOF) (m/z): calcd for $C_{23}H_{20}O_4S$, $[M + NH_4]^+$: 410.1421, found 410.1420.

***2-((3-Methoxyphenyl)thio)-5-phenyl-1H-pyrrole-3-carbonitrile* (*1e*):**

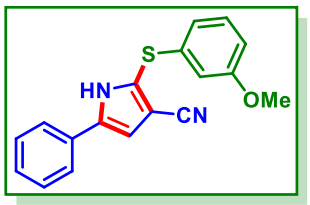

As a brown solid (53 mg, 70% yield); mp 198-200 °C; purified over a column of silica gel (18% EtOAc in hexane); ^{1}H NMR ($CDCl_3$, 500 MHz): δ 9.50 (s, 1H), 7.47 (d, 2H, J = 7.5 Hz), 7.40 (t, 2H, J = 7.5 Hz), 7.31 (t, 1H, J = 8.0 Hz), 7.17 (t, 1H, J = 8.0 Hz), 6.81 (d, 1H, J = 8.0 Hz), 6.78 (t, 1H, J = 2.5 Hz), 6.73 (d, 1H, J = 2.5 Hz), 3.74 (s, 3H); ^{13}C{^{1}H} NMR ($CDCl_3$, 125 MHz): δ 160.4, 136.7, 136.4, 130.4, 130.3, 129.4, 128.4,

127.1, 124.7, 120.8, 115.7, 114.1, 113.0, 110.2, 103.2, 55.5; IR (KBr, cm^{-1}): 3249, 2920, 2834, 2210, 1555, 1415, 1149, 1089; HRMS (ESI/Q-TOF) (m/z): calcd for $C_{18}H_{14}N_2OS$, $[M + H]^+$: 307.090, found 307.0934.

***2-((4-Fluorophenyl)thio)-5-phenyl-1H-pyrrole-3-carbonitrile* (*1f*):**

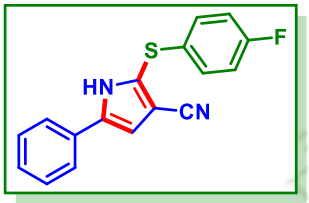

As a white solid (50 mg, 68% yield); mp 206-208 °C; purified over a column of silica gel (18% EtOAc in hexane); ^1H NMR ($CDCl_3$, 500 MHz): δ 9.23 (s, 1H), 7.48 (d, 2H, J = 6.0 Hz), 7.41 (s, 2H), 7.32 (s, 3H), 6.97 (t, 2H, J = 7.5 Hz), 6.73 (s, 1H); $^{13}C\{^1H\}$ NMR ($CDCl_3$, 125 MHz): δ 136.5, 133.8 (d, J = 75.2 Hz), 130.1, 129.9 (d, J = 80 Hz), 129.6, 129.5, 128.7, 127.2, 126.6, 124.8, 115.4, 110.5, 103.7; ^{19}F NMR ($CDCl_3$, 471 MHz): δ –113.6; IR (KBr, cm^{-1}): 3045, 2915, 2825, 2210, 1546, 1406, 1234, 1145, 1063; MS (ESI/Q-TOF) (m/z): calcd for $C_{17}H_{11}FN_2S$, $[M + H]^+$: 295.070, found 295.0704.

***2-((4-Chlorophenyl)thio)-5-phenyl-1H-pyrrole-3-carbonitrile* (*1g*):**

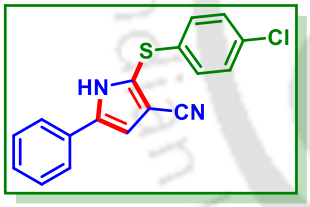

As a white solid (54 mg, 70% yield); mp 199-201 °C; purified over a column of silica gel (18% EtOAc in hexane); ^1H NMR ($CDCl_3$, 500 MHz): δ 9.18 (s, 1H), 7.40 – 7.35 (m, 4H), 7.30 – 7.28 (m, 1H), 7.26 (t, 3H, J = 5.5 Hz), 7.24-7.20 (m, 1H), 6.73 (d, 1H, J = 3.0 Hz); $^{13}C\{^1H\}$ NMR ($CDCl_3$, 125 MHz): δ 163.7, 161.2, 136.3, 131.7, 131.66, 129.4, 128.5, 128.1, 124.8, 116.9, 116.5, 110.2, 102.7; IR (KBr, cm^{-1}): 3266, 2947, 2839, 2215, 1541, 1405, 1242, 1167, 1065; HRMS (ESI/Q-TOF) (m/z): calcd for $C_{17}H_{11}ClN_2S$, $[M + H]^+$: 311.0404, found 311.0401.

***2-((3-Chlorophenyl)thio)-5-phenyl-1H-pyrrole-3-carbonitrile* (*1h*):**

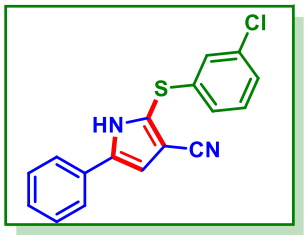

As a white solid (53 mg, 69% yield); mp 203-205 °C; purified over a column of silica gel (18% EtOAc in hexane); ^1H NMR ($CDCl_3$, 400 MHz): δ 9.32 (s, 1H), 7.49 (d, 2H, J = 7.4 Hz), 7.42 (t, 2H, J = 7.6 Hz), 7.34 (t, 1H, J = 7.2 Hz), 7.19 (d, 2H, J = 7.2 Hz), 7.09-7.07 (m, 1H), 6.78 (d, 1H, J = 2.8 Hz); $^{13}C\{^1H\}$ NMR

($CDCl_3$, 100 MHz): δ 137.6, 136.8, 135.5, 130.6, 130.1, 129.5, 128.7, 127.9, 127.5, 126.2, 125.7, 124.8, 115.4, 110.5, 104.1; IR (KBr, cm^{-1}): 3240, 2812, 2211, 1557, 1401, 1146, 1076; HRMS (ESI/Q-TOF) (m/z): calcd for $C_{17}H_{11}ClN_2S$, $[M + H]^+$ 311.0404, found 311.0434.

***2-((2-Bromophenyl)thio)-5-phenyl-1H-pyrrole-3-carbonitrile* (*1i*):**

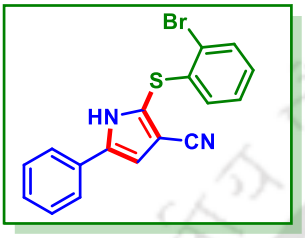

As a white solid (57 mg, 65% yield); mp 197-199 °C; purified over a column of silica gel (15% EtOAc in hexane); ^1H NMR ($CDCl_3$, 500 MHz): δ 9.01 (s, 1H), 7.51 (d, 3H, J = 8.0 Hz), 7.42 (dd, 3H, J_1 = 18.5 Hz, J_2 = 8.0Hz), 7.25 (d, 2H, J = 6.0 Hz), 7.18(t, 1H, J = 8.0 Hz), 6.80 (d, 1H, J = 7.5 Hz); $^{13}C\{^1H\}$ NMR ($CDCl_3$, 125 MHz): δ 136.4, 133.5, 133.1, 129.5, 128.8, 128.78, 128.6, 128.4, 128.3, 128.2, 127.2, 124.8, 115.1, 110.6, 104.7; IR (KBr, cm^{-1}): 3058, 2922, 2829, 2204, 1556, 1422, 1227, 1148, 1071; HRMS (ESI/Q-TOF) (m/z): calcd for $C_{17}H_{14}BrN_3S$, $[M + NH_4]^+$: 372.0165, found 372.0198.

***5-Phenyl-2-((4-(trifluoromethyl)phenyl)thio)-1H-pyrrole-3-carbonitrile* (*1j*):**

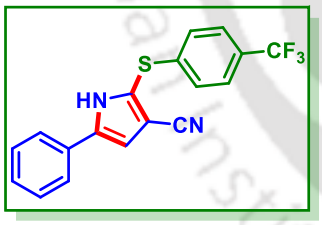

As a white solid (58 mg, 67% yield); mp 208-210 °C; purified over a column of silica gel (15% EtOAc in hexane); ^1H NMR ($CDCl_3$, 500 MHz): δ 9.60 (s, 1H), 7.46 – 7.43 (m, 5H), 7.35 (t, 2H, J = 7.5 Hz), 7.28 (d, 1H, J = 7.5 Hz,), 7.19 (d, 1H, J = 4.0 Hz,), 6.76 (d, 1H, J = 1.9 Hz); $^{13}C\{^1H\}$ NMR ($CDCl_3$, 125 MHz): δ 141.0, 137.1, 130.0, 129.5, 128.8, 127.3, 126.5 (q, J_1 = 29 Hz, J_2 = 14.5 Hz), 125.1, 124.9, 124.6, 123.0, 115.1, 110.7, 104.7; ^{19}F NMR ($CDCl_3$, 471 MHz): δ –62.6; IR (KBr, cm^{-1}): 3263, 2919, 2853, 2208, 1448, 1242, 1127, 1037; HRMS (ESI/Q-TOF) (m/z): calcd for $C_{18}H_{11}F_3N_2S$, $[M + H]^+$: 345.0668, found 345.0710.

***2-(Cyclohexylthio)-5-phenyl-1H-pyrrole-3-carbonitrile* (*1k*):**

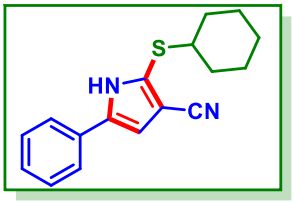

As a gummy (48 mg, 69% yield); purified over a column of silica gel (5% EtOAc in hexane); ^{1}H NMR ($CDCl_3$, 500 MHz): δ 8.97 (s, 1H), 7.47 (d, 2H, J = 8.0 Hz,), 7.42 (t, 2H, J = 7.5 Hz), 7.32 (t, 1H, J = 7.0 Hz), 6.72 (d, 1H, J = 3.0 Hz), 3.08-3.02 (m, 1H), 2.38 (dd, 2H, J_1 = 12.5 Hz, J_2 = 2.5 Hz), 1.80-1.77 (m, 2H), 1.75 (t, 1H, J = 2.5 Hz), 1.31-1.18 (m, 5H); ^{13}C{^{1}H} NMR ($CDCl_3$, 150 MHz): δ 135.2, 130.5, 129.4, 129.0, 128.3, 124.6, 116.4, 110.1, 103.2, 49.9, 33.9, 26.2, 25.6; IR (KBr, cm^{-1}): 3063, 2959, 2229, 1537, 1420, 1197, 1019, HRMS (ESI/Q-TOF) (m/z): calcd for $C_{17}H_{18}N_2S$, $[M + H]^+$: 283.1263, found 283.1267.

***2-(Thiophen-2-ylthio)-5-(p-tolyl)-1H-pyrrole-3-carbonitrile* (*2l*):**

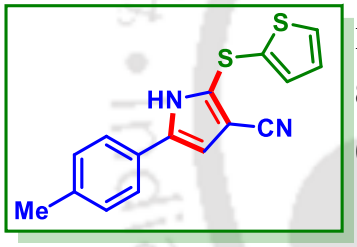

As a white solid (110 mg, 52% yield); mp 195-197 ^{o}C; ^{1}H NMR (DMSO-d_6, 500 MHz): δ 12.38 (s, 1H), 7.58 (d, 2H, J = 8.0 Hz), 7.26 (t, 2H, J = 6.5 Hz), 7.21 (d, 2H, J = 7.5 Hz), 7.18 (d, 2H, J = 7.0 Hz), 6.85 (d, 1H, J = 2.5 Hz), 2.30 (s, 3H); ^{13}C {^{1}H} NMR (DMSO-d_6, 125 MHz): δ 137.0, 136.8, 135.4, 129.3, 128.7, 128.3, 127.7, 127.2, 124.4, 115.9, 108.7, 100.1, 20.7; IR (KBr, cm^{-1}): 3025, 2924, 2215, 1547, 1410, 1225, 1145, 1048; HRMS (ESI/Q-TOF) (m/z): calcd. for $C_{16}H_{12}N_2S_2$, $[M + H]^+$: 297.0515, found 297.0543.

***5-(Naphthalen-2-yl)-2-(p-tolylthio)-1H-pyrrole-3-carbonitrile* (*9b*):**

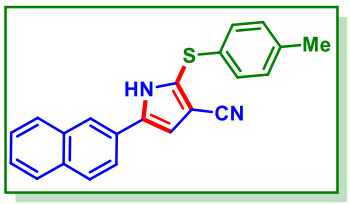

As a white solid (64 mg, 75% yield); mp 190-192 ^{o}C; purified over a column of silica gel (12% EtOAc in hexane); ^{1}H NMR ($CDCl_3$, 500 MHz): δ 9.01 (s, 1H), 7.78 (d, 2H, J = 8.0 Hz), 7.74 (d, 2H, J = 9.0 Hz), 7.47 (dd, 1H, J_1 = 8.5 Hz, J_2 = 1.5 Hz), 7.43 – 7.38 (m, 2H), 7.18 (t, 2H, J = 3.0Hz), 7.03 (d, 2H, J = 8.0 Hz), 6.76 (d, 1H, J = 2.5 Hz), 2.22 (s, 3H).; ^{13}C{^{1}H} NMR ($CDCl_3$, 125 MHz): δ 138.0, 136.0, 133.6, 133.1, 131.3, 130.5, 129.8,

129.3, 128.9, 128.2, 128.0, 127.6, 127.2, 126.7, 123.1, 122.8, 115.8, 110.7, 102.8, 21.2.; IR (KBr, cm^{-1}): 3464, 3055, 2931, 2209, 1513, 1430, 1280, 1196, 1090; HRMS (ESI/Q-TOF) (m/z): calcd for $C_{22}H_{16}N_2S$, $[M + H]^+$: 341.1107, found 341.1116.

***2-((4-Chlorophenyl)thio)-5-(naphthalen-2-yl)-1H-pyrrole-3-carbonitrile* (*9g*):**

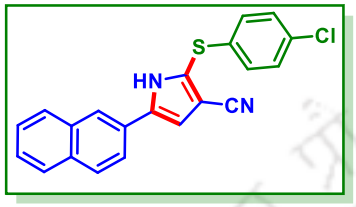

As a white solid (65 mg, 72% yield); mp 194-196 °C; purified over a column of silica gel (15% EtOAc in hexane); ^{1}H NMR (DMSO-d_6, 500 MHz): δ 13.08 (s, 1H), 8.32 (s, 1H), 7.97 (d, 1H, J = 8.5 Hz), 7.90 (q, 3H, J_1 = 12.5Hz, J_2 = 6.0 Hz), 7.55-7.49 (m, 2H), 7.43 (d, 2H, J = 8.5 Hz), 7.32 (s, 1H), 7.23 (d, 2H, J = 8.5 Hz); ^{13}C{^{1}H} NMR (DMSO-d_6, 125 MHz): δ 136.6, 135.1, 133.0, 132.3, 131.4, 129.5, 128.7, 128.5, 127.8, 127.6, 127.5, 126.8, 126.3, 125.1, 123.0, 122.9, 115.5, 110.9, 102.1.; IR (KBr, cm^{-1}): 3055, 2925, 2210, 1519, 1409, 1238, 1147, 1052; HRMS (ESI/Q-TOF) (m/z): calcd for $C_{21}H_{13}ClN_2S$, $[M + H]^+$: 361.0561, found 361.0564.

***2-(Benzylthio)-5-phenyl-1H-pyrrole-3-carbonitrile* (*1m*):**

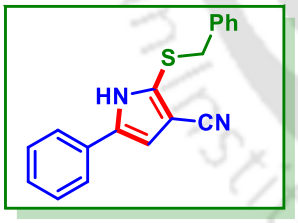

As a gummy (51 mg, 71% yield) ; purified over a column of silica gel (10% EtOAc in hexane); ^{1}H NMR ($CDCl_3$, 500 MHz): δ 8.45 (s, 1H), 7.32 (t, 2H, J = 7.5 Hz), 7.22 (q, 6H, J_1 = 10.5 Hz, J_2 = 6.5 Hz), 7.13 (t, 2H, J = 1.5 Hz), 6.62 (d, 1H, J =, 3.0 Hz), 3.97 (s, 2H) ; ^{13}C{^{1}H} NMR ($CDCl_3$, 125 MHz): δ 137.9, 135.3, 130.4, 129.3, 129.2, 129.0, 128.9, 128.2, 127.9, 124.5, 115.9, 109.9, 102.4, 42.1.; IR (KBr, cm^{-1}): 3066, 2920, 2872, 2212, 1521, 1149, 1080; HRMS (ESI/Q-TOF) (m/z): calcd for $C_{18}H_{14}N_2S$, $[M + H]^+$: 291.0950, found 291.0958.

***2-(Benzylthio)-5-(4-chlorophenyl)-1H-pyrrole-3-carbonitrile* (*6m*):**

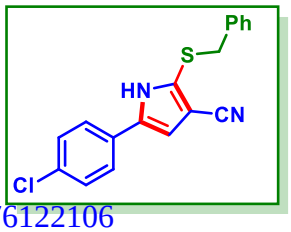

As a gummy (59 mg, 73% yield); purified over a column of silica gel (10% EtOAc in hexane); ^{1}H NMR (DMSO-d_6, 500 MHz): δ 12.51 (s, 1H), 7.71 (d, 2H, J = 8.5 Hz), 7.47 (d, 2H, J =

8.5 Hz), 7.26 – 7.16 (m, 3H), 7.18 (t, 2H, *J* = 1.5 Hz), 6.97 (d, 1H, *J* = 2.5 Hz), 4.15 (s, 2H); $^{13}C\{^{1}H\}$ NMR (DMSO-d_6, 125 MHz): δ 137.0, 134.0, 131.8, 129.3 129.2, 128.8, 128.7, 128.3, 127.2, 126.1, 115.7, 109.9, 100.3, 40.5.; IR (KBr, cm^{-1}): 3060, 2907, 2852, 2211, 1557, 1423, 1149, 1047; HRMS (ESI/Q-TOF) (m/z): calcd for $C_{18}H_{16}ClN_3S$, $[M + NH_4]^+$: 342.0826, found 342.0865.

***5,6-Diphenyl-3-(phenylthio)pyrrolo[2,1-a]isoquinoline-2-carbonitrile* (*P*):**

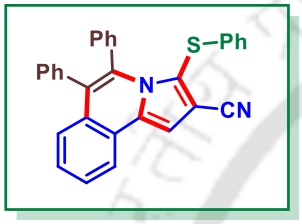

As a white solid (89 mg, 78% yield, mp 212–214 °C); Purification over a column of silica gel (5% EtOAc in hexane). ^{1}H NMR ($CDCl_3$, 500 MHz): δ 8.19 (d, 1H, *J* = 8.0 Hz), 7.58 (q, 2H, J_1 = 15.0Hz, J_2 = 7.5 Hz), 7.38 (t, 1H, *J* = 8.0 Hz), 7.18 – 7.11 (m, 5H), 7.09 (t, 2H, *J* = 7.0 Hz), 7.04 (t, 3H, *J* = 8.5 Hz), 6.98 (t, 2H, *J* = 7.5 Hz), 6.91 (d, 2H, *J* = 7.5 Hz), 6.51 (d, 2H, *J* = 7.5 Hz).; $^{13}C\{^{1}H\}$ NMR ($CDCl_3$, 125 MHz): δ 138.6, 136.0, 135.3, 135.2, 133.6, 131.2, 131.1, 131.0, 129.0, 128.9, 128.5, 128.4, 128.0, 127.9, 127.7, 127.3, 127.1, 125.9, 125.7, 124.4, 122.4, 121.0, 115.8, 109.7, 104.7; IR (KBr, cm^{-1}): 3058, 2962, 2924, 2852, 2224, 1628, 1591, 1511, 1488, 1426, 1295, 1231, 1051, 889, 792, 768, 722, 698; HRMS (ESI/Q-TOF) (m/z) calcd for $C_{31}H_{20}N_2S$ $[M + H]^+$ 453.1420, found 453.1411.

***5-Phenyl-2-(phenylsulfonyl)-1H-pyrrole-3-carbonitrile* (*Q*):**

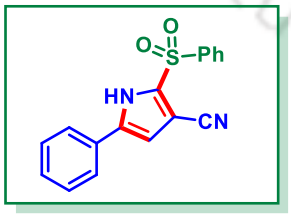

As a yellow solid (62 mg, 80% yield, mp 179–181 °C); Purification over a column of silica gel (18% EtOAc in hexane). ^{1}H NMR ($CDCl_3$, 500 MHz): δ 10.98 (s, 1H), 8.13 (d, 2H, *J* = 8.0 Hz,), 7.62 (t, 1H, *J* = 7.5 Hz), 7.58-7.53 (m, 4H), 7.39 (t, 2H, *J* = 7.5 Hz), 7.34 (t, 1H, *J* = 7.5 Hz), 6.78 (s, 1H).; $^{13}C\{^{1}H\}$ NMR ($CDCl_3$, 125 MHz): δ 169.5, 140.5, 137.9, 134.4, 129.9, 129.4, 129.0, 128.4, 127.7, 125.7, 113.4, 112.3, 99.5; IR (KBr, cm^{-1}): 3061, 2959, 2925, 2852, 2217, 1511, 1423, 1155, 1045,

725; HRMS (ESI/Q-TOF) (m/z) calcd for $C_{17}H_{12}N_2O_2S$ $[M + H]^+$ 309.0692; found 309.0700.

II.7. Representative Spectra

2-(Phenylthio)-5-(p-tolyl)-1H-pyrrole-3-carbonitrile (2a): ^{1}H NMR ($CDCl_3$, 500 MHz)

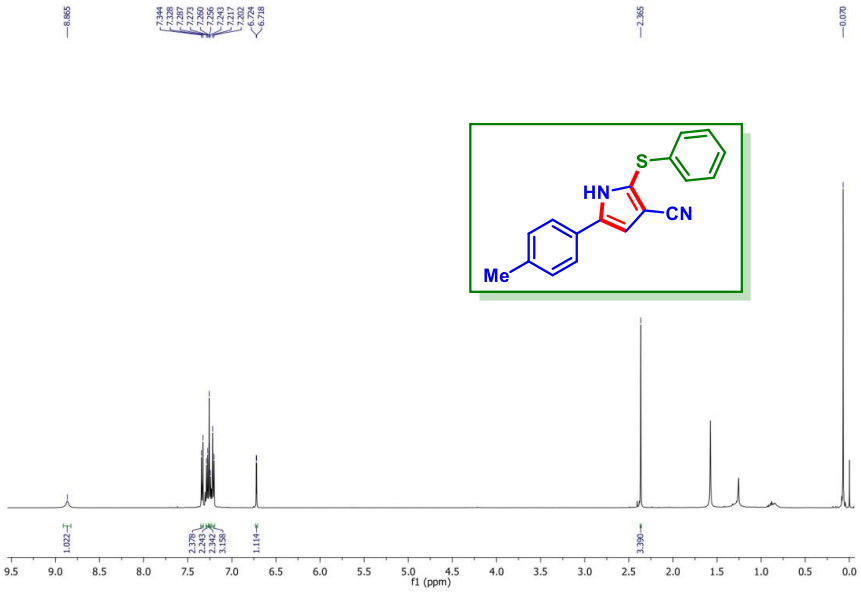

2-(Phenylthio)-5-(p-tolyl)-1H-pyrrole-3-carbonitrile (2a): $^{13}C\{^{1}H\}$ NMR ($CDCl_3$, 126 MHz)

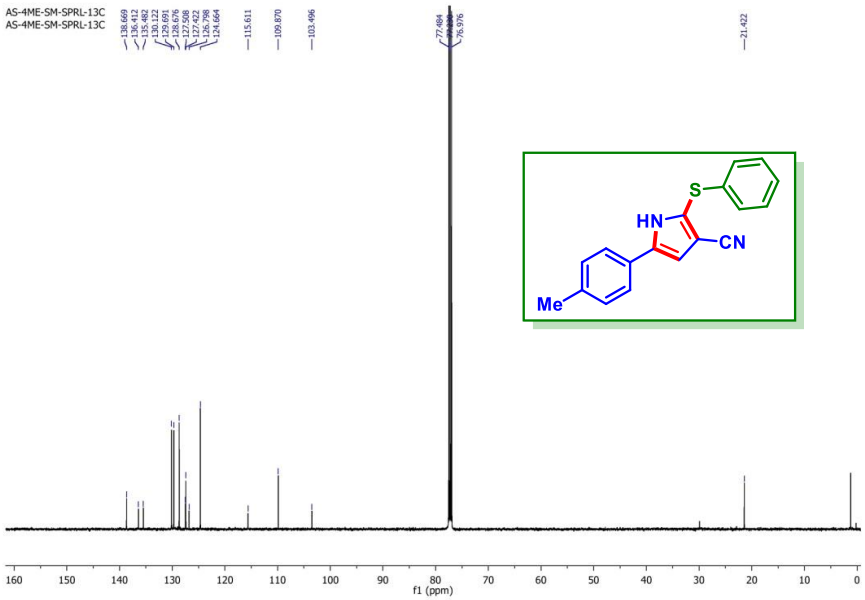

5-(4-Chlorophenyl)-2-(phenylthio)-1H-pyrrole-3-carbonitrile (6a): ^{1}H NMR ($CDCl_3$, 400 MHz)

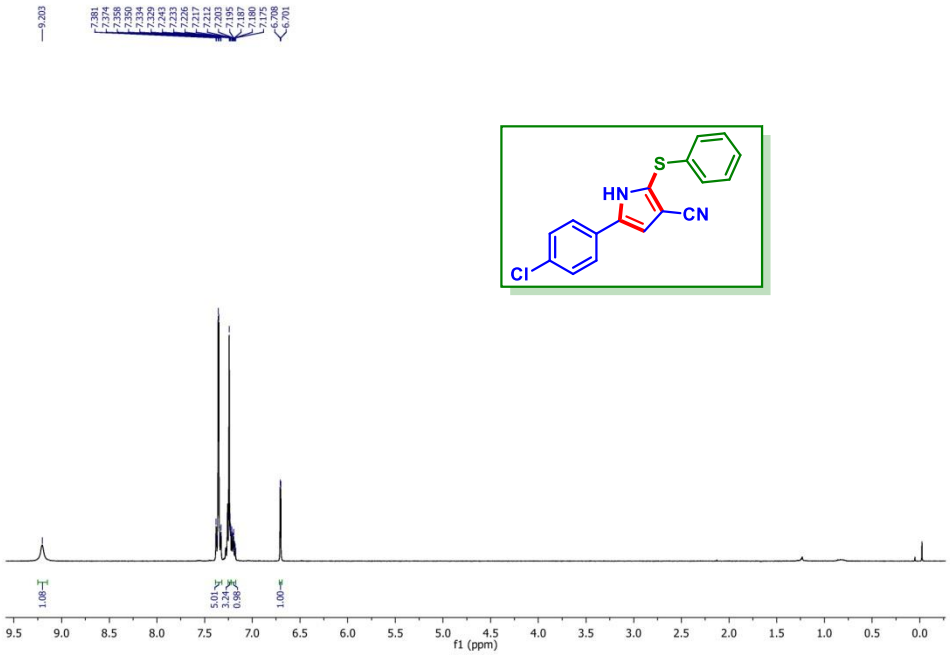

5-(4-Chlorophenyl)-2-(phenylthio)-1H-pyrrole-3-carbonitrile (6a): $^{13}C\{^{1}H\}$ NMR ($CDCl_3$, 126 MHz)

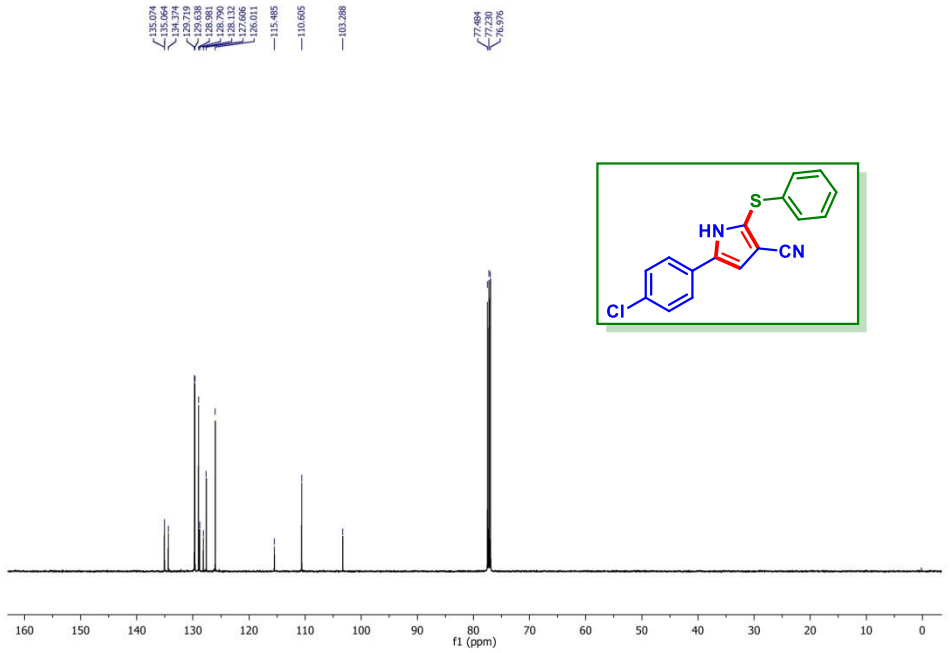

2-(Phenylthio)-4,5-dihydro-1H-benzo[g]indole-3-carbonitrile (11a): ^{1}H NMR (DMSO-d_6, 500 MHz)

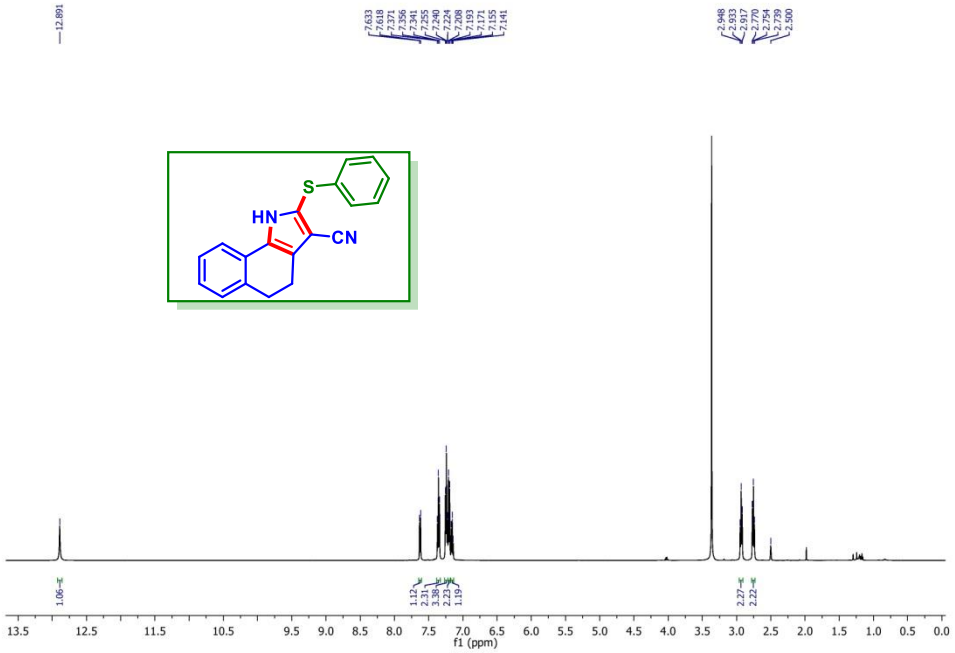

2-(Phenylthio)-4,5-dihydro-1H-benzo[g]indole-3-carbonitrile (11a): $^{13}C\{^{1}H\}$ NMR (DMSO-d_6, 125 MHz)

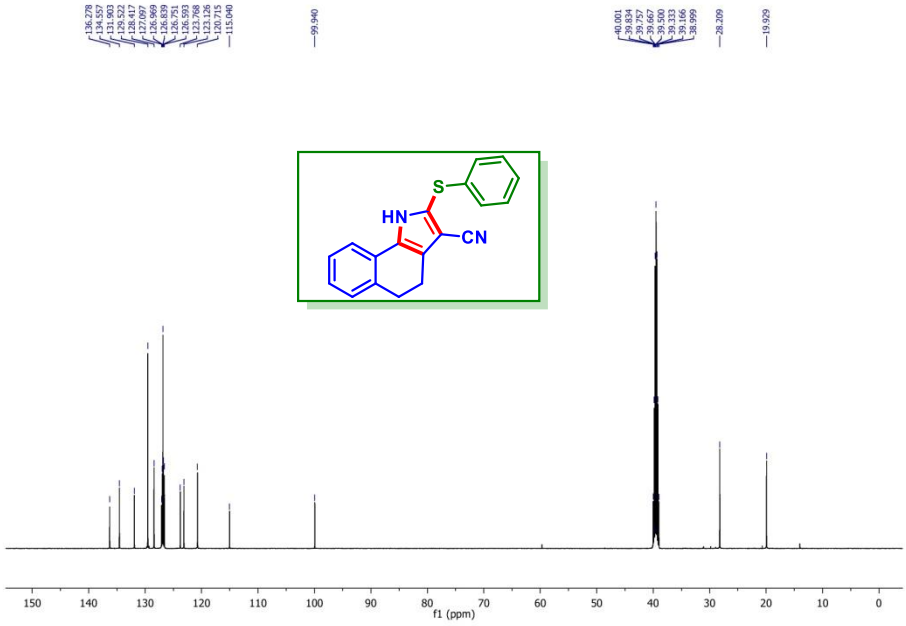

2-((4-Methoxyphenyl)thio)-5-phenyl-1H-pyrrole-3-carbonitrile (1d): ^{1}H NMR ($CDCl_3$, 500 MHz)

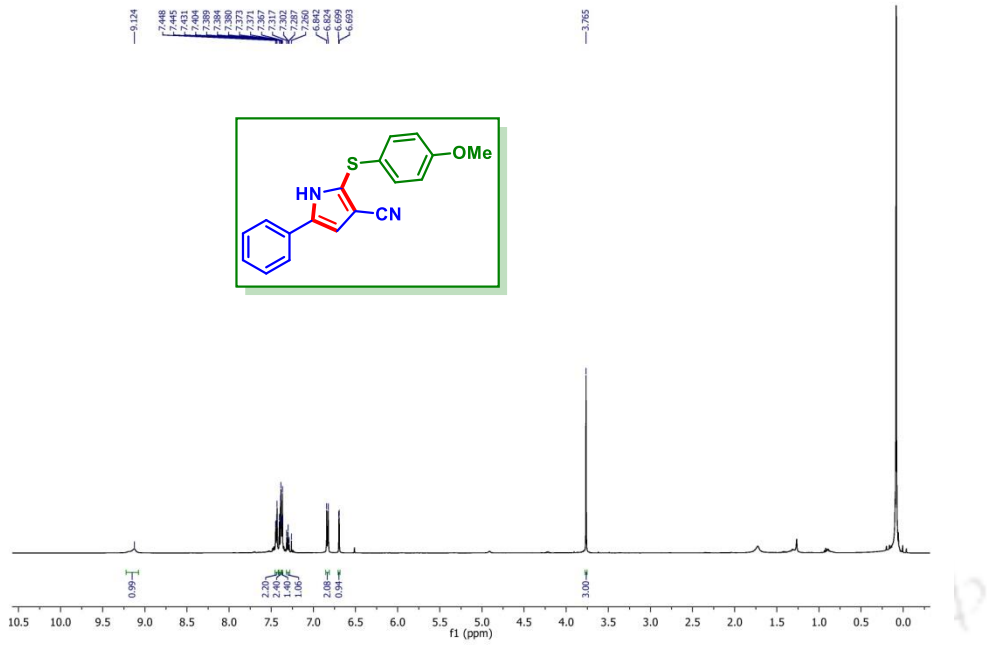

2-((4-Methoxyphenyl)thio)-5-phenyl-1H-pyrrole-3-carbonitrile (1d): $^{13}C\{^{1}H\}$ NMR ($CDCl_3$, 125 MHz)

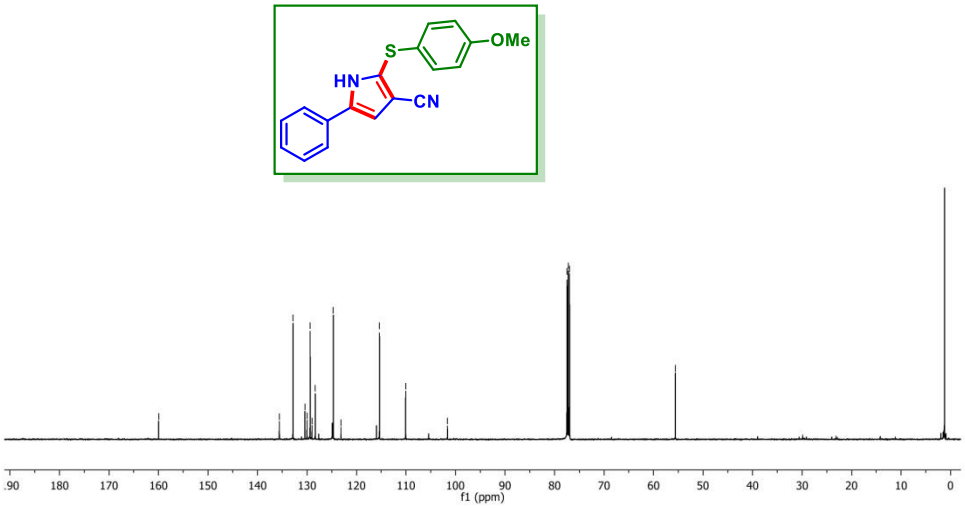

2-((4-Chlorophenyl)thio)-5-phenyl-1H-pyrrole-3-carbonitrile (1g): ^{1}H NMR ($CDCl_3$, 500 MHz)

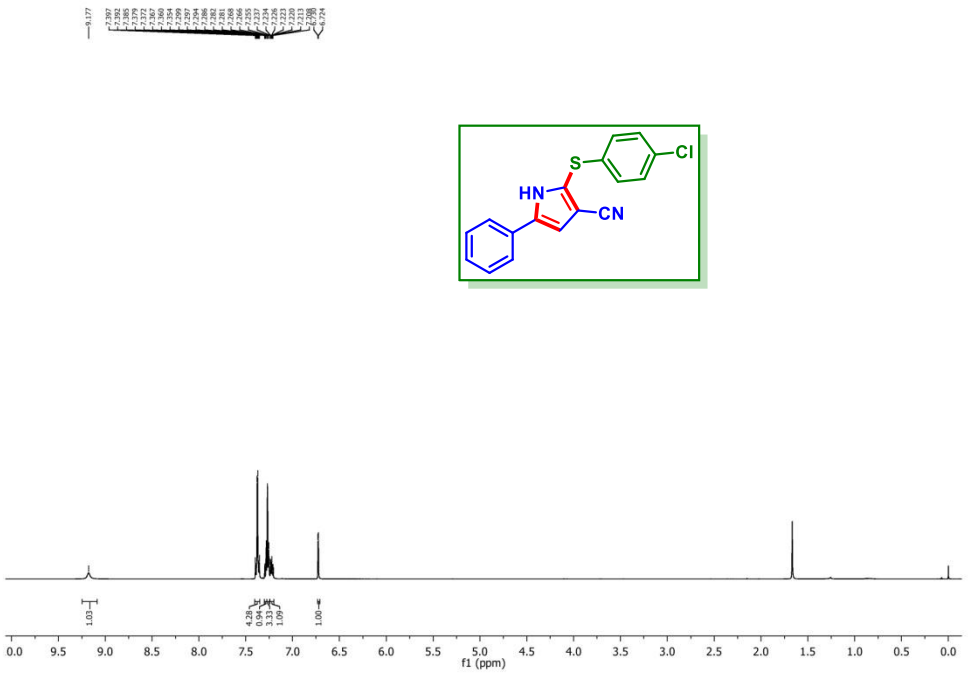

2-((4-Chlorophenyl)thio)-5-phenyl-1H-pyrrole-3-carbonitrile (1g): $^{13}C\{^{1}H\}$ NMR ($CDCl_3$, 125 MHz)

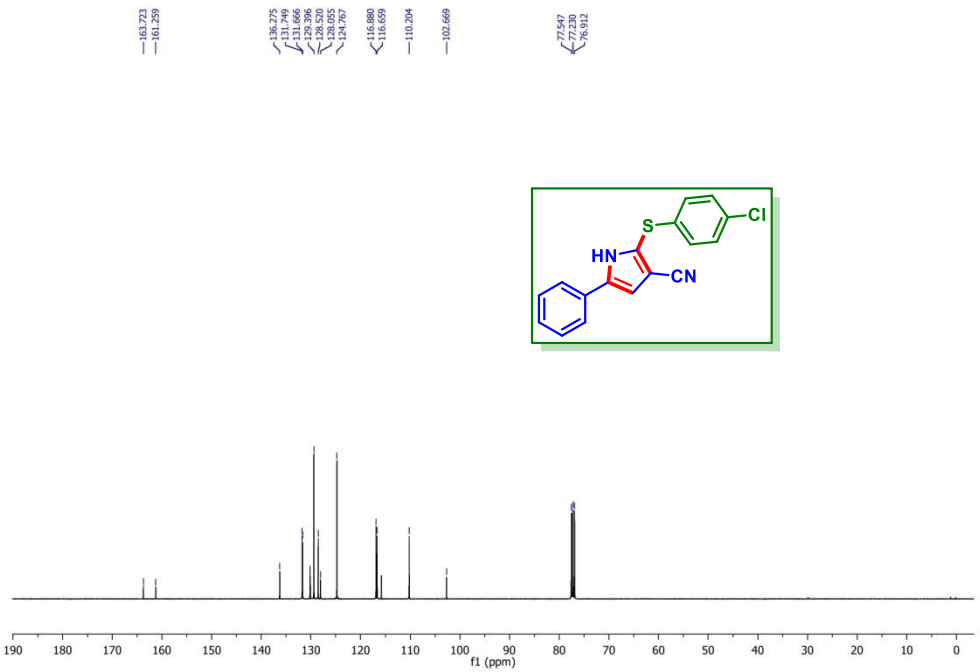

2-(Benzylthio)-5-phenyl-1H-pyrrole-3-carbonitrile (1m): ^{1}H NMR ($CDCl_3$, 500 MHz)

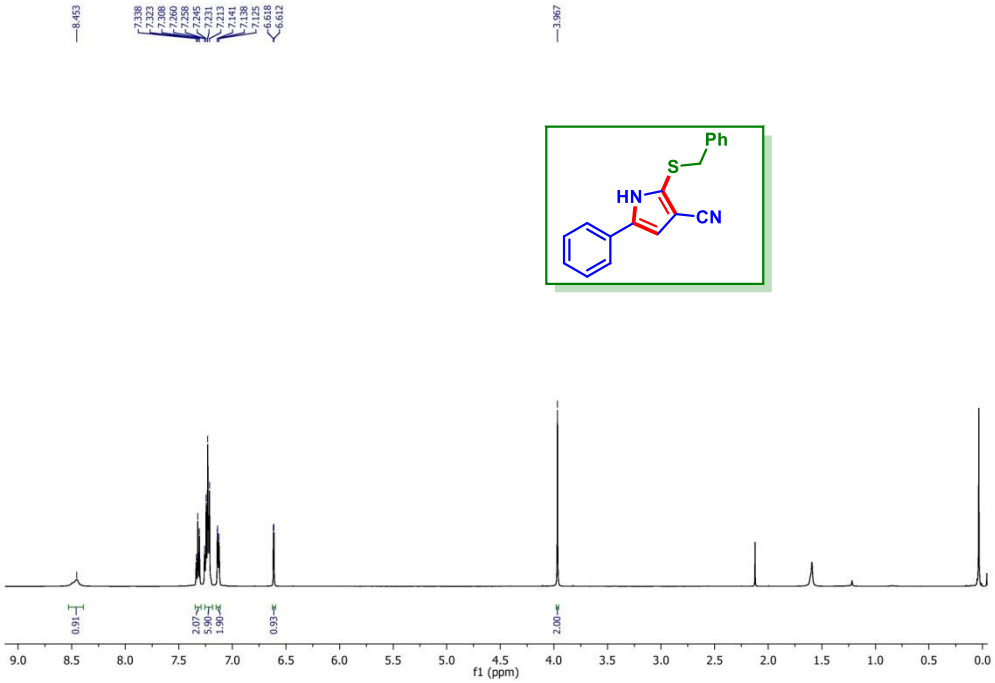

2-(Benzylthio)-5-phenyl-1H-pyrrole-3-carbonitrile (1m): $^{13}C\{^{1}H\}$ NMR ($CDCl_3$, 125 MHz)

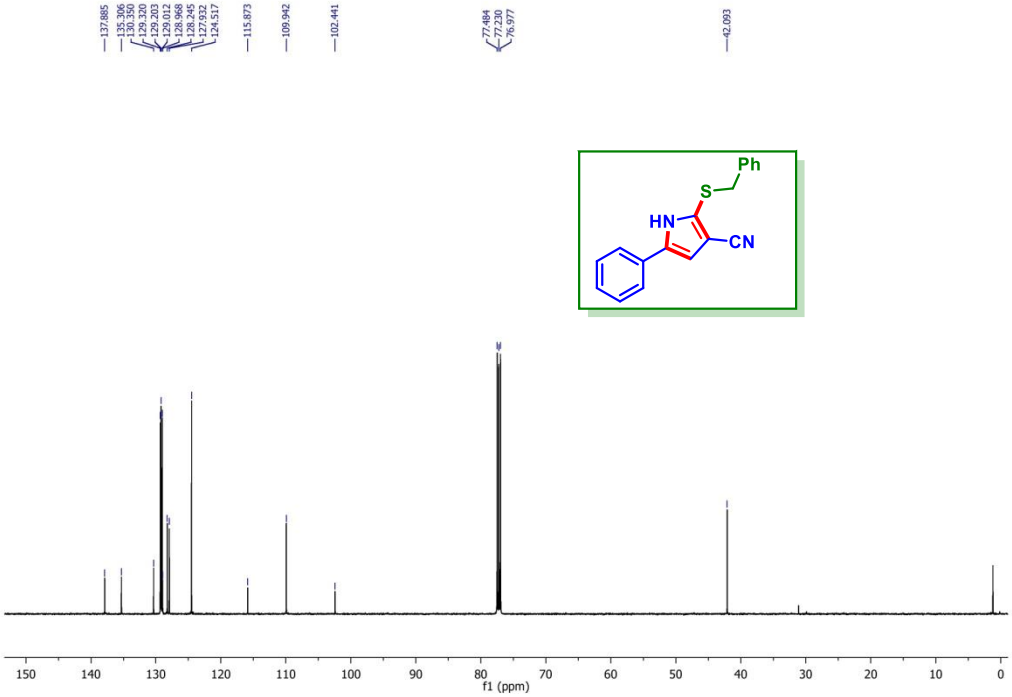

CHAPTER-IV

Visible/Solar-Light-Driven Thiyl-Radical-Triggered Synthesis of Multi-Substituted Pyridines

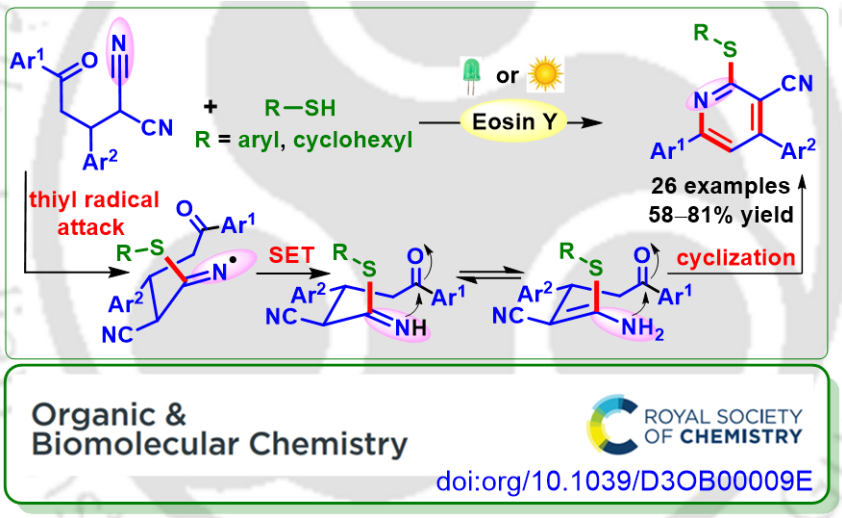

Abstract: *A light-triggered synthesis of thio-functionalized pyridines is demonstrated using γ-ketodinitriles, thiols, and eosin Y as the photocatalyst. The reaction proceeds via the selective attack at one of the cyano groups by an in situ generated thiyl radical. The reaction also proceeds with nearly equal efficiency using direct sunlight. Large-scale synthesis and a few useful synthetic transformations of the substituted pyridines are also performed.*

भारतीय प्रौद्योगिकी संस्थान गुवाहाटी
Indian Institute of Technology Guwahati

CHAPTER IV

Visible/Solar-Light-Driven Thiyl-Radical-Triggered Synthesis of Multi-Substituted Pyridines

IV.1. Introduction:

The photochemical transformations by harnessing visible light have grabbed significant attention due to their sustainability, unique reactivity, and operational simplicity.[1] Besides the use of LEDs as a source of visible light efforts have been made on utilizing renewable sources of energy such as sunlight in photochemical reactions.[17a] Usually, a photochemical reaction is triggered by visible light in combination with a suitable photocatalyst (organic dyes or transition-metal complexes) facilitating the SET process for the construction of various organic frameworks which otherwise require thermal conditions.[2] Though the transition-metal complexes are better for the excitation of organic molecules, the employment of organic dyes has also been useful in many photochemical transformations. In particular, eosin Y has become a competitor to metal catalysts in various reactions due to its cost-effectiveness.[3] Owing to the prevalence of pyridine frameworks in various natural products, and pharmaceuticals, they have found applications in the fields of biology, medicinal sciences, and advanced materials, etc.[4] Moreover, pyridine-containing compounds are used in cancer therapy,[5a] asymmetric catalysis,[5b] and supramolecular chemistry.[5c] For instance, two well-known drugs Aciphex (**I**),[6a] and Nexium (esomeprazole) (**II**)[6b] used for the treatment of duodenal ulcers, and acid reflux both contain pyridine backbones (Figure IV.1). There are other pyridine-bearing drugs such as Amrinone D (inocor) (**III**), and Etoricoxib E (arcoxia) (**IV**) used for the treatment of acute heart failure and arthritis.[6c,d] Avandia (rosiglitazone A) (**V**), and Actos (pioglitazone B) (**VI**) which are used as an antidiabetic drug also contain pyridine backbone,[6e,f] and are used as anticancer drug. Further, the thio-functionalized pyridines (**XI**) and (**XII**) are reported to show antimicrobial activity (Figure. IV.1).[7] Considering the multi-faceted applications of substituted pyridines, synthetic chemists are vying for alternative methods to synthesize pyridine core. There are well-established classical methods such as Hantzsch,[8a] and Kröhnke[8b] pyridine synthesis and several others.[9] The past years have reported few transition-metal catalyzed [4 + 2] hetero Diels-Alder reactions of 1-

azadienes with alkynes under thermal conditions.[10a-c] Recently, [2+2+2] cycloadditions of alkynes with nitriles under metal or metal-free catalysis are reported.[10d-g] Besides these, there are methods that employ nitriles to synthesize nitrogenous heterocycles.[11a-d] Previously, the McQuade group reported a few methods for the synthesis of multi-substituted pyridines employing alkylidene malononitriles.[11e-g]

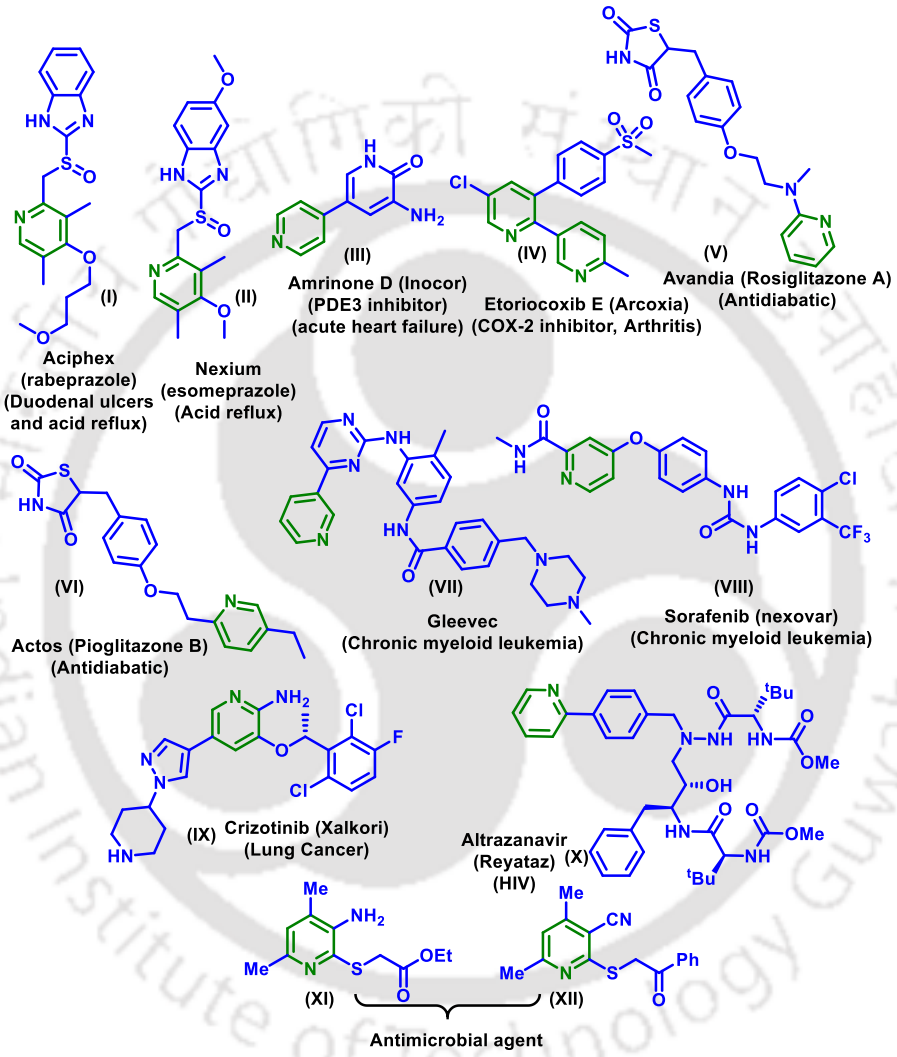

Figure IV.1. *Bioactive compounds containing pyridine unit.*

Further, the Gao and Tang group reported visible-light-induced phosphorylation with the 1,6-enyne moiety for the diverse and selective synthesis of phosphorylated polyheterocycles leading to phosphorylated aminophosphonates, iminophosphonates, and ketones.[11h] Recently, the Chen and Yu group in 2022, employed 1-acryloyl-2-cyanoindoles as the precursors to

synthesize various sulfonated/thiocyanated pyrrolo[1,2-*a*]indolediones under visible-light irradiation.[11i]

IV.2. Ideas Toward Synthesis of Functionalized Pyridines

The Chen group in 2020, introduced a nickel(II)-catalyzed synthesis of pyrroles and pyridines *via* coupling of ketonitrile with aryl boronic acid (Scheme IV.1).[12a]

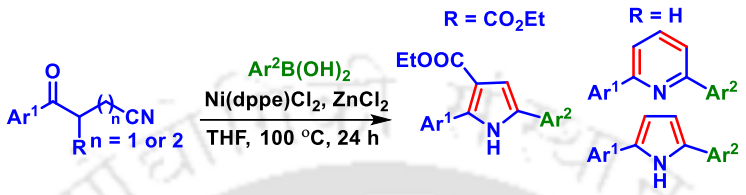

Scheme IV.1. *Synthesis of pyrrole-2-carbaldehydes.*

In 2019, Ji *et al*. reported a cascade cyclization of 3-isocyano-[1,1′-biphenyl]-2-carbonitriles with aryl boronic acids to synthesize pyrrolopyridines under Mn(III) catalysis (Scheme IV.2).[12b]

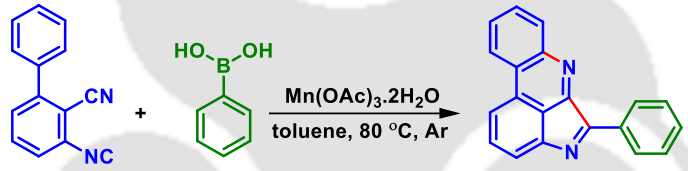

Scheme IV.2. *Mn(III) catalyzed synthesis of* pyrrolopyridines.

Previously, Zhang and Yu group reported visible-light-mediated vinyl isocyanide insertions with Umemoto's reagent and electron-deficient bromides using Ir(III) (Scheme IV.3).[12c]

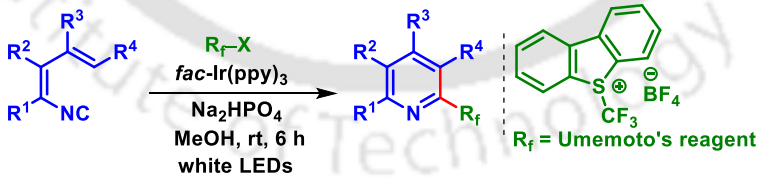

Scheme IV.3. *Visible-light-mediated synthesis of functionalized pyridines.*

Though the above-mentioned methodologies are well-established and have utilized transition metal for the synthesis of pyridine frameworks, a metal-free approach is always desirable.[13]

In 2015, McQuade *et al*. demonstrated an efficient method for the synthesis of halogenated pyridines using alkylidenemalononitrile. The formation of alkylidenemalononitrile involves the formation of an oxocarbonium salt. Substoichiometric addition of acetic acid improved the yield of enamines thereby enabling the formation of halogenated pyridines in good yields (Scheme IV.4).[11e]

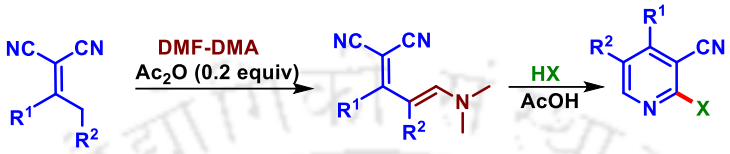

Scheme IV.4. *Synthesis of* functionalized pyridine *from alkylidenemalononitrile.*

An intramolecular radical-triggered heterocycles synthesis possesses radical acceptors such as alkene, alkyne, nitrile, and isonitrile with appropriately placed radical precursors. In this context, nitrile has turned out to be an excellent radical acceptor to access various carbocycles, and heterocycles.[14] Basically a transition metal is required to activate the nitrile through coordination with the *N*-atom or the π-electrons of the C≡N triple bond making it a good acceptor for the nucleophilic/radical attack, followed by cyclization to access nitrogenous heterocycles.[15] However, a metal-free photocatalytic approach employing nitrile as a radical acceptor would be interesting to generate poly-substituted pyridines. Previously, our group reported a nitrile-triggered synthesis of thio-substituted pyrroles with β-ketodinitriles as an acceptor and thiophenol as the radical donor (Scheme IV.5).[16a]

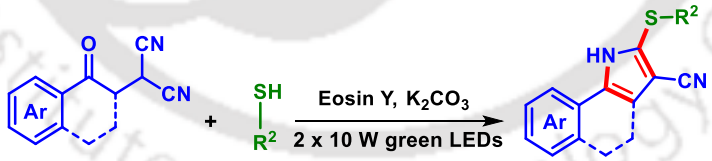

Scheme IV.5. *Synthesis of thio-functionalized pyrroles.*

Our interest in nitrile-based precursors,[15a,b,16a] we hypothesized that a reaction is feasible with γ-ketodinitriles as the radical acceptors. To confirm our hypothesis, CV of γ-ketodinitrile (**1**) and thiophenol (**a**) were measured. The estimated $E_{1/2oxd}$ of benzene thiol (+0.25 V vs the SCE) is lower compared to $E_{1/2oxd}$ of γ-ketodinitriles (+2.13 V, +0.38 V vs the SCE), enabling them as suitable radical donor and acceptor pairs (Figure IV.2). Our interest in nitrile-based

precursors,[15a,b,16a] we hypothesized that a reaction is feasible with γ-ketodinitriles as the radical acceptors.

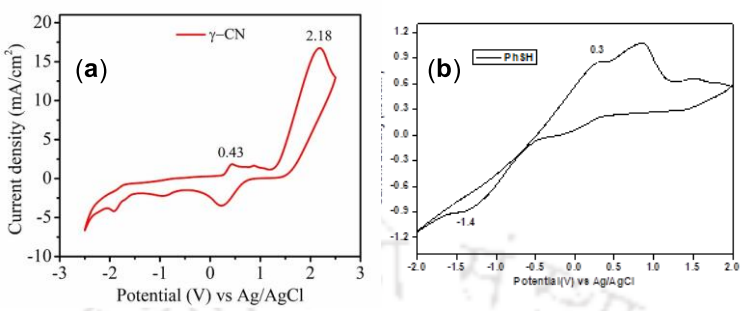

Figure IV.2. *(a) CV graph of β-ketodinitrile (**1**). (b) CV graph of benzene thiol(**a**).*

IV.3. Present Work

To verify our hypothesis, a preliminary reaction was carried out between 2-(3-oxo-1,3-diphenylpropyl)malononitrile (**1**, 1 equiv) and thiophenol (**a**, 2 equiv) in the presence of eosin Y (3 mol %) and K_2CO_3 (1 equiv) in DMSO (1 mL) under the irradiation of 20 W (2 x 10 W) green LEDs (wavelength-523 nm and flux-39 mW/cm^2) in N_2 atmosphere for 8 h. A new compound was obtained in 55% isolated yield along with the formation of diphenyl disulfide. From the spectroscopic (^{1}H and ^{13}C{^{1}H} NMR) analyses, the structure of the product was found to be 4,6-diphenyl-2-(phenylthio)nicotinonitrile (**1a**). Further, X-ray crystallography analysis of one of its analogs (**1f**) validates its structure (Figure IV.3).

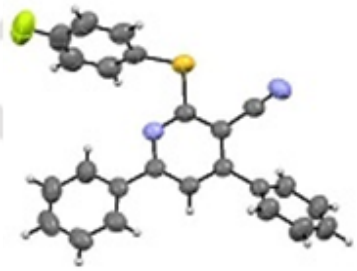

Figure IV.3. *ORTEP diagram of 4,6-diphenyl-2-(phenylthio)nicotinonitrile (**1f**) with 40% ellipsoid probability (CCDC 2201897).*

To the best of our knowledge, this is a unique report for the visible-light-mediated synthesis of thio-functionalized pyridines using γ-ketodinitrils and thiophenols as the reacting partners which has been demonstrated in Scheme IV.6.[16f]

IV.3. Present Work

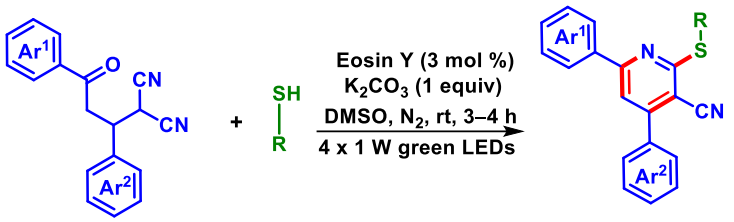

Scheme IV.6. *Visible-light-mediated synthesis of thio-functionalized pyridines.*

Optimization of the Reaction Conditions

Inspired by the present photocatalytic approach, further screening involving the choice of different catalytic systems, bases, light sources, and solvents was carried out.

Table IV.1. Optimization of the reaction conditions[a,b]

entry	variation from optimal conditions[a]	yield (%)[b]
1.	**None**	**78**
2.	$[Ru(bpy)_3]Cl_2$ instead Eosin Y	68
3	$[Ru(bpy)_3](PF_6)_2$ instead Eosin Y	60
4	Eosin B instead of Eosin Y	62
5	Rose Bengal instead of Eosin Y	57
6	Rhodamin B instead Eosin Y	58
7	2 mol % Eosin Y	67
8	5 mol % Eosin Y	75
9	Na_2CO_3 instead of K_2CO_3	65
10	Cs_2CO_3 instead of K_2CO_3	59
11	KOH instead of K_2CO_3	55
12	Et_3N instead of K_2CO_3	70
13	DBU instead of K_2CO_3	52
14	DMF instead of DMSO	58
15	CH_3CN instead of DMSO	42
16	EtOH instead of DMSO	15
17	CH_3OH instead of DMSO	20

18	1 equiv of thiol	52
19	2.5 equiv of thiol	72
20	4 x 1 W blue LEDs	65
21	4 x 1 W white LEDs	70
22	2 x 10 W green LEDs	68
23	8 h instead 2–3 h	45
24	Sunlight	65
25	without Eosin Y	10
26	without base	trace
27	reaction in dark	10
28	Reaction at 60 ^{o}C without eosin Y	00
[a]Reaction condition: **1** (0.25 mmol), **a** (0.5 mmol), Eosin Y (3 mol %), K_2CO_3 (1 equiv), DMSO (1 mL), 3 h. [b]Isolated pure product.		

The employment of transition metal complexes such as $[Ru(bpy)_3]Cl_2$, and $[Ru(bpy)_3](PF_6)_2$ provided 68% and 60% yields respectively which are inferior to Eosin Y (Table IV.1, entries 2 and 3). The use of other organic dyes such as Eosin B, Rose Bengal, and Rhodamine B, (Table IV.1, entries 4-6) were unable to improve the yield as compared to eosin Y. At 2 mol % eosin Y loading, 67% yield of the desired product (**1a**) was obtained (Table IV.1, entry 7) while increasing the catalyst loading to 5 mol % did not improve the yield significantly (Table IV.1, entry 8). Screening of other bases, such as Na_2CO_3, Cs_2CO_3, KOH, and Et_3N, instead of K_2CO_3 did not improve the yield (Table IV.1, entries 9-12). Further, the use of one of the organic bases, DBU failed to improve the yield (Table IV.1, entry 13). During solvent selection, DMSO was found to be the best as compared to other solvents such as DMF (58%), CH_3CN (42%), EtOH (15%), and CH_3OH (20%) tested (Table IV.1, entries 14-17). However, varying the equivalence of thiophenol from the standard condition failed to improve the yield (Table IV.1, entries 18 and 19). Thus, the use of 2 equivalent of thiol was found to be optimal. The standard reaction when carried out using 4 x 1 W blue (430 nm) and white LEDs were unable to improve the reaction yield beyond 70% (Table IV.1, entries 20 and 21). Thus, the use of green light is found to be the best option for the excitation of eosin Y, since both the absorption (543 nm) and emission (560 nm) spectra

of eosin Y in DMSO coincide with the wavelength of the green light (523 nm).[16a] Next, the use of 2 x 10 W green LEDs (bulb) did not prove to be much beneficial as compared to the use of 4 x 1 W green LEDs (523 nm) having a measured flux of 39 mW/cm^2 (Table IV.1, entry 22). Further, an increase in the reaction time shows no significant improvement in the reaction yield (45%) (Table IV.1, entry 23). The use of a natural energy source (sunlight) was able to excite the catalyst and gave the desired product in slightly less yield as compared to the use of 4 x 1 W green LEDs (Table IV.1, entry 24). Control experiments revealed that eosin Y, base, and light source are indispensable for this protocol (Table IV.1, entries 25-27). However, the formation of 10% of the product in the absence of catalyst eosin Y may be due to the possible competitive anionic pathway which is suppressed in the presence of eosin Y via the SET process. To see whether the desired product is formed under the thermal condition, the reaction of (**1**) with thiophenol (**a**) was carried out at 60 ^{o}C. The reaction failed to give the desired thio-functionalized pyridines and decomposed to its corresponding chalcones and form diphenyldisulfide (Table IV.1, entry 28). After screening several parameters such as different catalytic systems, bases, light sources, and solvents the optimal conditions for this transformation were found to be the combination of 2-(3-oxo-1,3-diphenylpropyl)malononitrile (**1**, 0.25 mmol), benzenethiol (**a**, 0.50 mmol, 2 equiv), K_2CO_3 (0.25 mmol, 1 equiv), and eosin Y (3 mol %) in DMSO (1 mL) under four 1 W green LEDs (Table IV.1, entry 1).

With the optimized conditions, the present protocol was then implemented for the construction of multi-substituted pyridines using a variety of *γ*-ketodinitriles (Scheme IV.7). The *γ*-ketodinitrile carrying both unsubstituted phenyl rings (**1**) reacted with benzenethiol (**a**) giving the substituted pyridine (**1a**) in 78% yield. The *γ*-ketodinitriles having electron-donating substituents such as *p*-Me (**2**), *p*-OMe (**3**), and electron-withdrawing substituents such as *p*-F (**4**), *p*-Cl (**5**) on the aroyl ring provided their corresponding poly-functionalized pyridines (**2a**, 75%), (**3a**, 78%), (**4a**, 71%), and (**5a**, 74%) in good yields. Similarly, the variation of substituents (EDGs or EWGs) on the *a*-phenyl ring of the malononitrile also underwent smooth reactions with (**a**) giving products (**6a**, 74%), (**7a**, 76%), (**8a**, 69%), (**9a**, 71%), and (**10a**, 71%) respectively. Besides this, heteroaromatic *γ*-ketodinitriles (**11** and **12**) reacted efficiently giving poly-substituted pyridines (**11a**, 72%; and **12a**, 69%). In addition to this, *γ*-ketodinitriles containing 1-naphthyl ring instead of a phenyl ring (**13**) and 2-naphthyl

and 1-naphthyl ring on either side (**14**), also gave the desired products (**13a**, 79%, and **14a**, 81%).

Scheme IV.7. *Scope of multi-functionalized pyridines with different γ-ketodinitriles*[a,b,c]

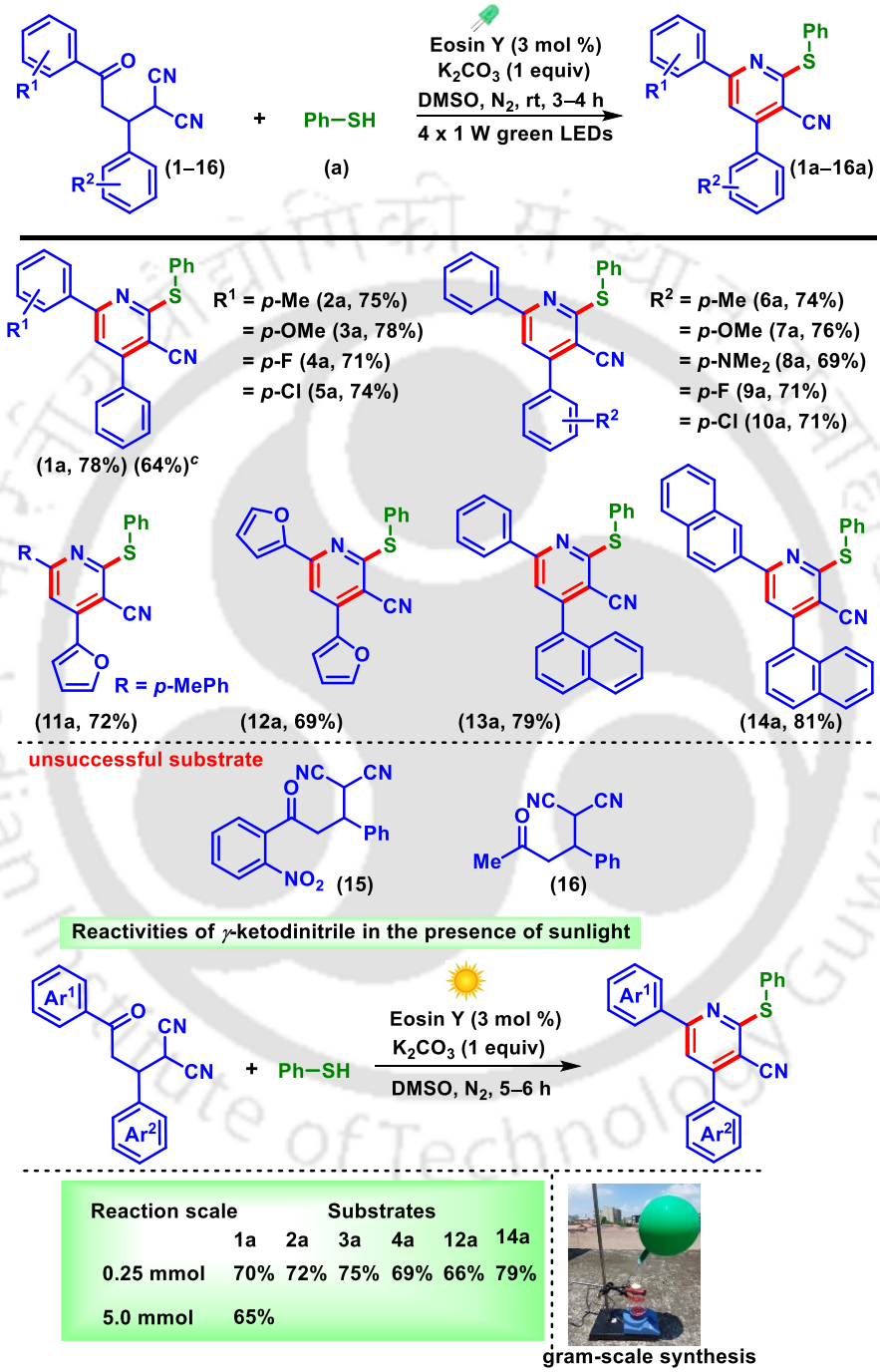

[a]Reaction conditions: **1-16** (0.25 mmol), **a** (0.5 mmol), K_2CO_3 (0.25 mmol), eosin Y (3 mol %), DMSO (1 mL), four 1 W green LEDs, under N_2 for 3-4 h. [b]Isolated yield. [c]5 mmol scale.

However, γ-ketodinitrile having strong electron withdrawing group *o*-NO_2 (**15**) on the γ-aryl ring of the γ-ketodinitrile and methyl group (**16**) instead of the γ-aryl ring of the γ-ketodinitrile failed to react. The failure of the electron-withdrawing substrate (**15**) may be due to both steric and electronic factors and for (**16**) due to the lesser reactivity of the alkyl group containing substrate. The applicability of the protocol was further implemented to a gram-scale (5 mmol) synthesis, giving the product **1a** in 64% yield. The use of LEDs as an energy source for visible light have been frequently used in various photochemical reactions but the use of direct sunlight in photochemical reactions makes the protocol more sustainable. The sunlight is the combination of all possible wavelengths of light, where blue light accounts for 25%. So instead of a specialized reaction setup whether the reaction can be carried out under the sunlight.[17a] To check the compatibility of the reaction, γ-ketodinitriles **1**, **2**, **3**, **4**, **12** and **14** having EDGs and EWGs were reacted with thiophenol (**a**) under the direct sunlight for 5 h. It was observed that all the substrates provided their corresponding pyridines (**1a**, 70%), (**2a**, 72%), (**3a**, 75%), (**4a**, 69%), (**12a**, 66%), (**14a**, 79%) in good yields under the irradiation of the direct sunlight. The efficiency of the sunlight-mediated reaction was also demonstrated through a large-scale synthesis (5 mmol) yielding the pyridine **1a** in 65% yield.

Next, γ-ketodinitrile (**1**) was reacted with various thiophenols (**b**–**k**) having electron-donating groups (EDGs) and electron-withdrawing groups (EWGs) as shown in Scheme IV.8. Thiophenols having EDGs such as *p*-Me (**b**), *o*-Me (**c**), *p*-OMe (**d**), *m*-OMe (**e**), and EWGs such as *p*-F (**f**), *p*-Cl (**g**), *m*-Cl (**h**), *o*-Br (**i**), and *p*-CF_3 (**j**) were reacted efficiently to give their respective products (**1b**, 73%); (**1c**, 67%); (**1d**, 74%); (**1e**, 69%); (**1f**, 72%); (**1g**, 69%); (**1h**, 59%); (**1i**, 58%); and (**1j**, 59%), in good yields. Further, polyaromatic thiol such as 2-napthyl thiol underwent a smooth reaction, and yielded the corresponding thio-functionalized pyridine **1k** in 72% yield. Besides aromatic thiols, heteroaromatic thiol such as thiophene 2-thiol (**l**), and aliphatic thiols such as cyclohexane thiol (**m**) reacted to give the desired pyridine, **1l** in 75%, and **1m** in 56% yield. Further, to see whether this methodology is compatible with acyclic alkyl thiols, γ-ketodinitrile (**1**) was reacted with ethyl thiol (**n**), propyl thiol (**o**), butyl thiol (**p**), *tert*-butyl thiol (**q**) under the present photochemical conditions. All the alkyl thiols failed to give any clean products, which is due to the inability of alkyl thiols to form corresponding thiyl radicals. However, on prolonging the reaction time, the γ-ketodinitrile (**1**)

started decomposing giving a hydrogenated chalcone (**1′**) and the corresponding disulphides.[16d]

Scheme IV.8. *Scope of multi-functionalized pyridines with different thiophenols.*[a,b]

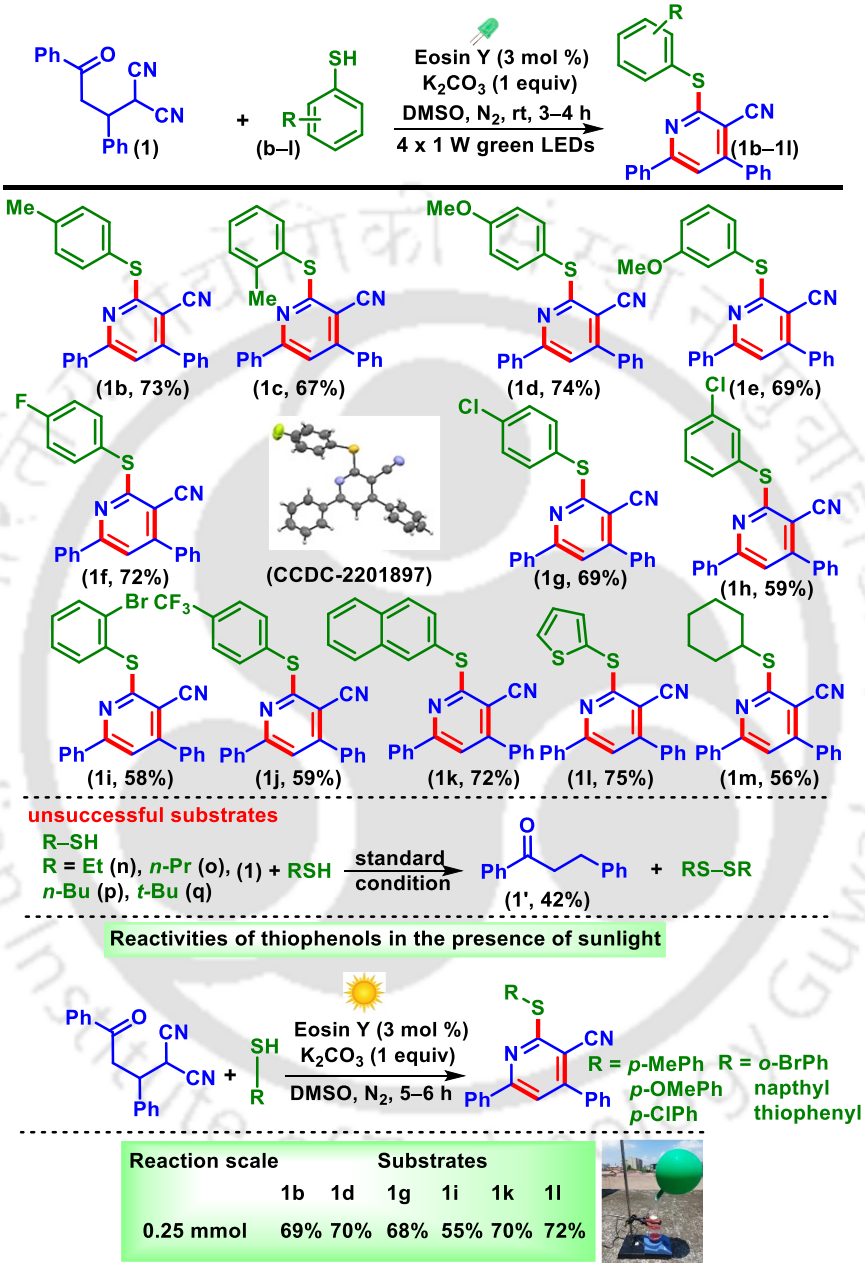

[a]Reaction conditions: **1** (0.25 mmol), **b-k** (0.5 mmol), K_2CO_3 (0.25 mmol), eosin Y (3 mol %), DMSO (1 mL), four 1 W green LEDs, under N_2 for 3-4 h. [b]Isolated yield.

After synthesizing a variety of poly-substituted pyridines, we also successfully performed the reactions under sunlight for a few thiophenols (**b**, **d**, **g, I, k, l**). The reaction proceeded well with thiophenols having different substituents. The *γ*-ketodinitrile **1**, when reacted with

thiophenols **b**, **d**, **g**, **i**, **k**, **l** and in the presence of sunlight for 5 h gave their corresponding products **1b**, **1d**, **1g**, **1i**, **1k**, and **1l** in 69%, 70%, 68%, 55%, 70%, and 72% yields.[17b] Hence it is concluded that sunlight can excite the catalyst eosin Y and shows almost equal efficacy compared to the use of green LEDs. Next, some control experiments were carried out to decipher the mechanistic hypothesis. When the reaction was performed in dark, the product (**1a**) obtained in 10% yield [Scheme IV.9a (i)] and the yield remain unaltered upon prolonging the reaction to 24 h. This confirms the crucial role of light in initiating the reaction.

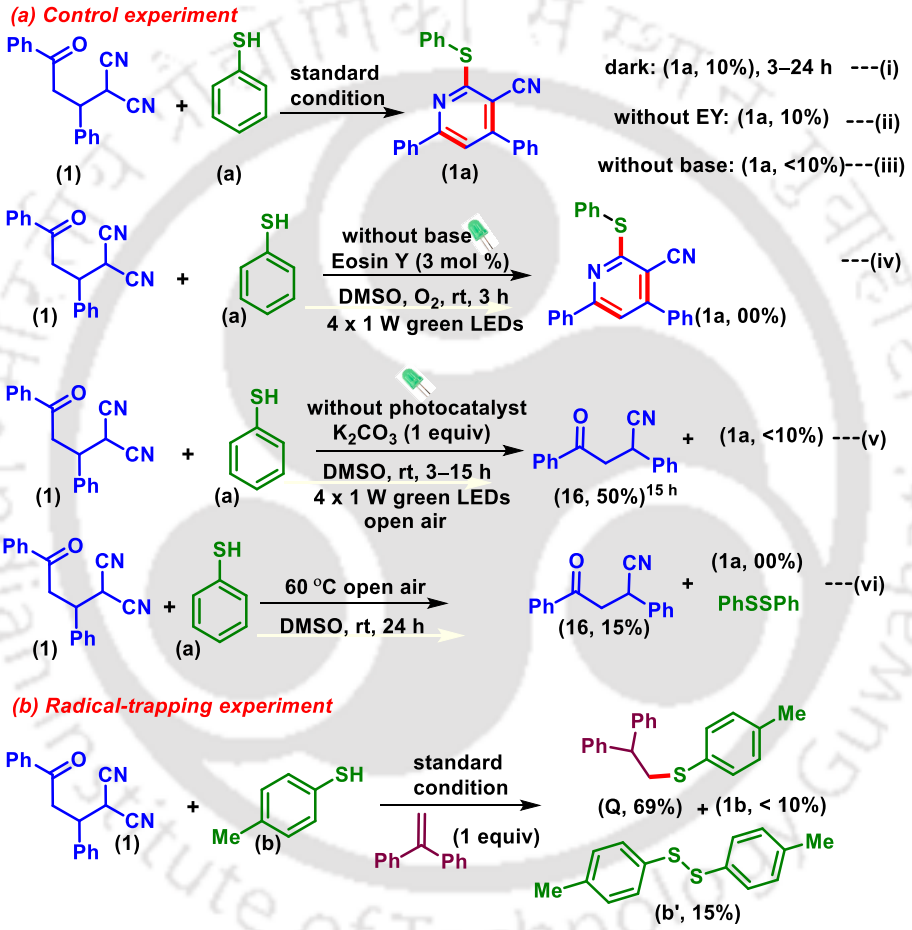

Scheme IV.9. *Control experiments.*

Further, the omission of catalyst, from the reaction provided only 10% of the product (**1a**) suggesting its role in the formation of the thiyl radical [Scheme IV.9a (ii)]. Omission of the base resulted in a trace amount of the product (<10%) [Scheme IV.9a (iii)]. These experiments reveal that photocatalyst, light, and base are indispensable for this protocol. To see whether O_2 in the form of superoxide helps in the generation of thiyl radical a reaction was carried out in the absence of a base under an oxygen atmosphere.[16b] However, no desired

product (**1a**) was obtained confirming the non-involvement of oxygen [Scheme IV.9a (iv)]. Further, the reaction in the absence of photosensitizer under aerobic conditions resulted in a trace amount (<10%) of the product (**1a**) along with the formation of diphenyldisulfide and a decyanated product, 4-oxo-2,4-diphenylbutanenitrile (**16**) [Scheme IV.9a (v)]. To ascertain the role of oxygen if any in the generation of thiyl radical a reaction was perfomed at 60 ^{o}C in the absence of base under an air atmosphere. This condition gave no desired product and most of the γ-ketodinitrile (**1**) remained unconsumed along with the formation of substantial amount of diphenyldisulfide and a trace amount of decyanated product (**16**) [Scheme IV.9a (vi)].[16d,e] The formation of decyanated product (**16**) from a dicyano substrate (**1**) under a basic and aerobic medium is reported.[16d] Further, it was observed that the use of 1,1-diphenyl ethylene as a radical scavenger resulted in a lower yield (<10%) of the product (**1b**) along with the trapped adduct (**Q**, 69%) and dimer (**b'**) of the corresponding thiol. This supports the intermediacy of thiyl radical (Scheme IV.9b). The structure of the adduct **Q** was confirmed by NMR (^{1}H and ^{13}C{^{1}H}) and HRMS analyses (Figure IV.9, 10, and 11 respectively). Finally, an on-off experiment has been performed to show that a continuous supply of light is necessary (Figure IV.4).[16,18]

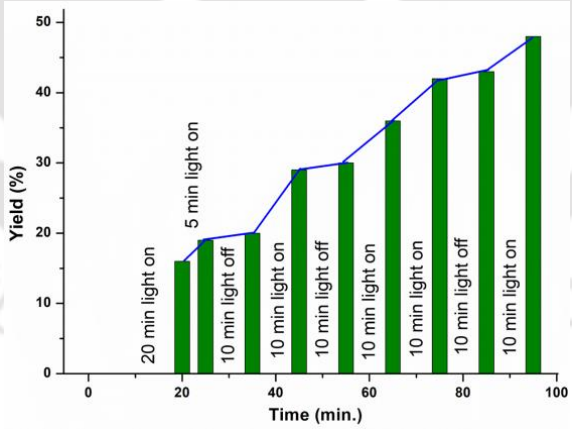

Figure IV.4. *Stair type graph for on-off experiment.*

From the Stern−Volmer (SV) fluorescence quenching experiment, which employed eosin Y as the probe and thiophenol (**a**) as a quencher, suggests a smooth electron transfer between thiophenol and eosin Y.[16a] For further confirmation a fluorescence quenching experiment was performed taking eosin Y as the probe and thiolate anion (thiol + base) as quencher. It was observed that no uniform decrease in the fluorescence maxima intensity was observed upon successive addition of the quencher thiolate anion even at higher concentration. However, a uniform quenching pattern was observed with a lower concentration of thiophenol as quencher. This suggests that there is a smooth electron transfer between the probe eosin Y and thiophenols compared to thiolate anion [Figure IV.5. (i) and (ii)].

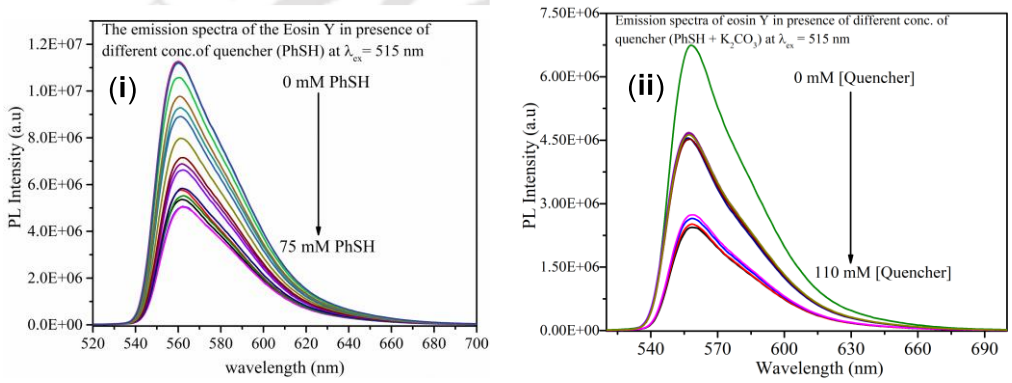

Figure IV.5. *(i) Fluorescence quenching of eosin Y with thiophenols as quencher. (ii) Fluorescence quenching of eosin Y with thiolate anion (thiophenols + base) as quencher.*

To further confirm, whether the generation of thiyl-radical is directly from the thiophenols or from the thiolate anion CV measurements were done.

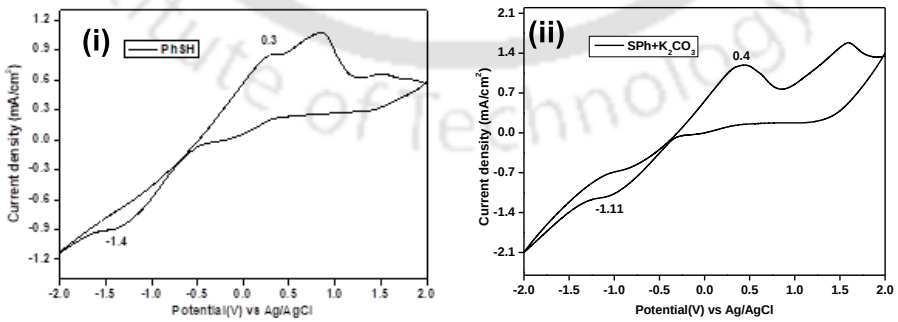

Figure IV.6. *(i) CV graph of benzene thiol. (ii) CV graph of benzene thiol (**a**) in the presence of base.*

The CV measurements, revealed that the oxidation potential of thiophenol ($E_{1/2ox}$ = +0.25 V vs SCE) is lower than the oxidation potential of eosin Y ($E_{1/2ox}$ = +0.83 V vs SCE for excited state of eosin Y). This enables the oxidation of thiophenol by the eosin Y and facilitates the formation of thiyl radical (Figure IV.6). However, the possible formation of thiyl-radical from the thiolate anion can not be completely ruled out. As evident from the CV value the thiolate anion ($E_{1/2\ ox}$ = +0.35 V vs SCE) has a higher tendency to gain electron than PhSH ($E_{1/2ox}$ = +0.25 V vs SCE) or PhSH preferably lose an electron than the thiolate anion. When comparing these values with the oxidation potential of eosin Y ($E_{1/2\ ox}$ = +0.83 V vs SCE for the excited state of eosin Y), it is clear that EY* will better oxidize PhSH rather than the thiolate anion. [Figure IV.6 (i) and (ii)] (Figure IV.6).[16a]

Based on control experiments and literature reports, a mechanistic path is suggested in Scheme IV.10.[16,19]

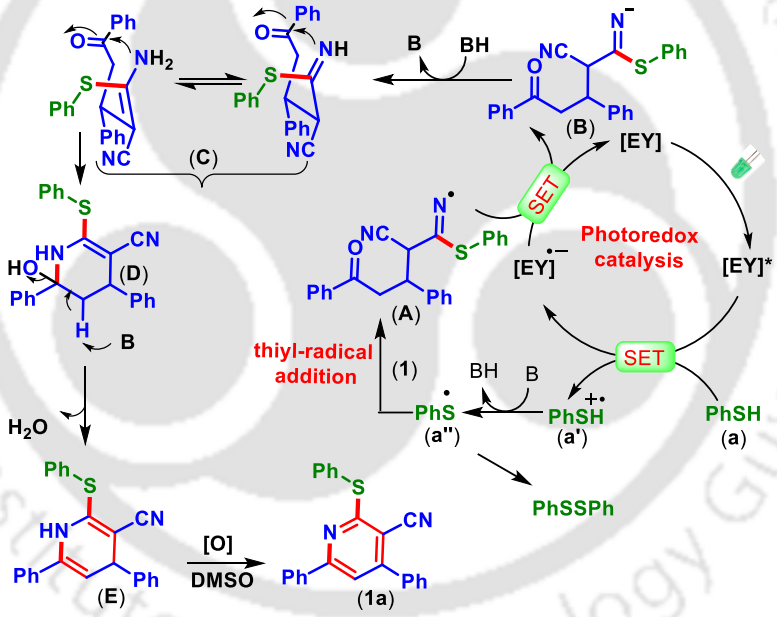

Scheme IV.10. *Plausible mechanism.*

Initially, green LEDs, excited the eosin Y (EY) to EY*, which oxidizes the thiophenol (**a**) to a radical cation (**a**′). Next, the thiyl radical (**a**″) is obtained *via* deprotonation from the radical cation (**a**′). The thiyl radical (**a**″) undergoes addition to one of the nitrile groups of *γ*-ketodinitrile (**1**), generating intermediate **A**. Subsequently, (**A)** is converted to an anionic intermediate (**B**) *via* a reductive quenching. The intermediate (**B**) upon protonation generates an imine intermediate (**C**) (detected by HRMS analysis of reaction mixture, Figure S19) The nucleophilic attack of imine (**C**) to the carbonyl group provided the intermediate **D**. Finally,

the loss of a water molecule from the intermediate **D** gives intermediate **E** (detected by HRMS analysis of the reaction mixture), which upon tautomerization followed by oxidative aromatization produces pyridine **1a** (Scheme IV.10 and Figure IV.17).

To illustrate the utility of the present photochemical approach, pyridine (**1a**) was employed for some synthetic transformations (Scheme IV.11). Oxidation of (**1a**) with mCPBA provided the sulfonylated pyridine (**1aa**) in 75% yield.[20] Further, **1a** was subjected to annulation using diphenyl acetylene which provided the C-H, N annulated product **1ab** in 68% yield.[21] Base hydrolysis of (**1a**) gave 4,6-diphenyl-2-(phenylthio)nicotinamide (**1ac**) in 78% yield which is an analog of nicotinamide (a form of vitamin B_3) used for the treatment of pellagra.[22a,b]

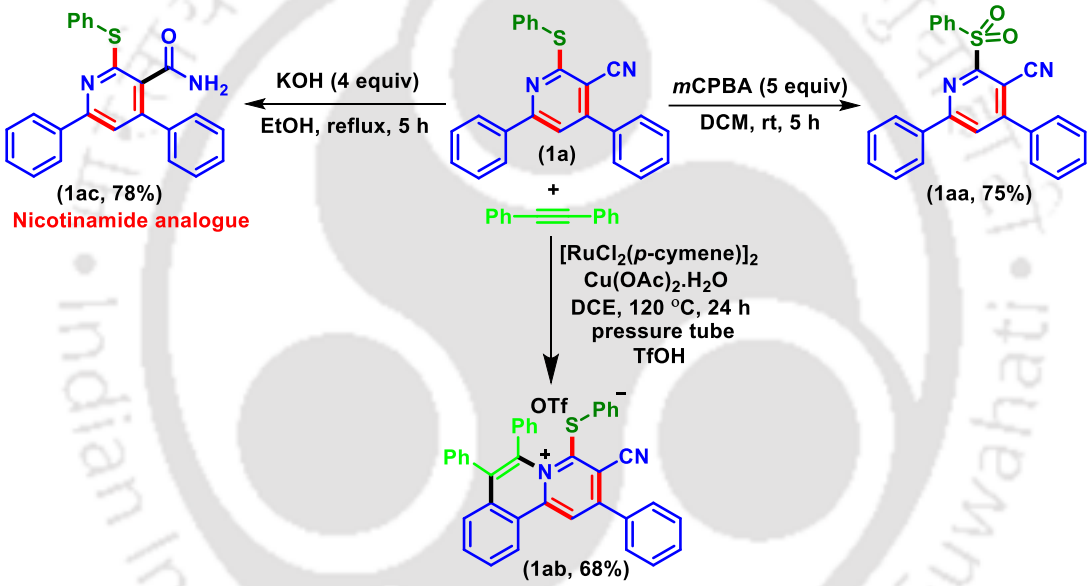

Scheme IV.11. *Post-synthetic transformation.*

In summary, a thiyl radical-triggered synthesis of multi-substituted pyridines is demonstrated using γ-ketodinitriles, thiols, in the presence of eosin Y under metal-free conditions. This protocol simultaneously constructs C–N, C–S, and C=C bonds. This methodology can tolerate different substituents in both coupling partners. A few post-translational modifications and a scale-up reaction are illustrated to show the practical utility of the present protocol. The reaction also underwent flawlessly employing sunlight as a sustainable energy source.

IV.4. Experimental Section

IV.4.1. General information: All the reagents were commercial grade and purified according to the established procedures. All the reactions were carried out in oven-dried glassware. The highest commercial quality reagents were purchased and were used without further purification unless otherwise stated. Reactions were monitored by thin-layer chromatography (TLC) on a 0.25 mm silica gel plates ($60F_{254}$) visualized under UV illumination at 365 nm. Organic extracts were dried over anhydrous sodium sulfate (Na_2SO_4). Solvents were removed using a rotary evaporator under reduced pressure. Column chromatography was performed to purify the crude product on silica gel 60-120 mesh using a mixture of hexane and ethyl acetate as eluent. All the isolated compounds were characterized by ^1H, $^{13}C\{1H\}$ NMR, HRMS-spectrometric and IR spectroscopic techniques. NMR spectra for all the samples were recorded in deuterochloroform ($CDCl_3$). ^1H, $^{13}C\{1H\}$ were recorded in 600 (150) or 500 (125) or 400 (100) MHz spectrometer and were calibrated using tetramethylsilane or residual undeuterated solvent for ^1H NMR, deuterochloroform for ^{13}C NMR as an internal reference {$Si(CH_3)_4$: 0.00 ppm or $CHCl_3$: 7.260 ppm for ^1H NMR, 77.230 ppm for $^{13}C\{^1H\}$ NMR}. ^{19}F NMR was calibrated without any internal standard in $CDCl_3$ in 400 MHz spectrometers. The chemical shifts are quoted in δ units, parts per million (ppm). ^1H NMR data is represented as follows: Chemical shift, multiplicity (s = singlet, d = doublet, t = triplet, q = quartet, m = multiplet, br = broad, dd = doublet of doublets), integration and coupling constant(s) *J* in hertz (Hz). High-resolution mass spectra (HRMS) were recorded on a mass spectrometer using electrospray ionization-time of flight (ESI-TOF) reflection experiments. FT-IR spectra were recorded in KBr or neat and reported in the frequency of absorption (cm^{-1}).

IV.4.2. Crystallographic Information:

(A) Sample Preparation:

The single crystal of compound **1f** was prepared by the slow evaporation method for which 10 mg of the compound (**1f**) was dissolved in 1 mL of DCM in a clean and dry 10 mL glass vial. MeOH (0.5 mL) was added to this solution slowly with a dropper. The mouth of the glass vial was covered with a cap having a small hole and kept it for slow evaporation at

room temperature. Transparent white needle-like single crystals of **1f** was obtained after 2–3 days.

(B) Crystallographic Description of 2-(4-Fluorophenyl)thio)-4,6-diphenylnicotinonitrile (1f):

Diffraction data were collected at 292 K with MoKα radiation (λ = 0.71073 Å) using a Bruker Nonius SMART APEX CCD diffractometer equipped with graphite monochromator and Apex CD camera. The SMART software was used for data collection and for indexing the reflections and determining the unit cell parameters. Data reduction and cell refinement were performed using SAINT[1,2] software and the space groups of these crystals were determined from systematic absences by XPREP and further justified by the refinement results. The structures were solved by direct methods and refined by full-matrix least-squares calculations using SHELXTL-97[3] software. All the non-H atoms were refined in the anisotropic approximation against F^2 of all reflections.

1. G. M. Sheldrick, SADABS, 1996, based on the method described in: R. H. Blessing, *Acta Crystallogr.* 1995, **A51**, 33–38.
2. SMART and SAINT, Siemens Analytical X-ray Instruments Inc., Madison, WI, 1996.
3. G. M. Sheldrick, *Acta Crystallogr.*, 2008, **A64**, 112–122.

$C_{24}H_{15}FN_2S$, crystal dimensions 0.35 x 0.31 x 0.29 mm, M_r = 382.44, monoclinic, space group P 21/c, a = 13.2258 (5), b = 8.0745 (3), c = 19.2139 (8) Å, α = 90°, β = 109.317 (1)°, γ = 90°, V = 1936.37 (13) Å^3, Z = 4, ρ_{calcd} = 1.312 g/cm^3, μ = 0.188 mm^{-1}, F(000)= 792.0, reflection collected / unique = 32809 / 3414, refinement method = full-matrix least-squares on F^2, final R indices [I> 2\s(I)]:R_1 = 0.0407, wR_2 = 0.0973, R indices (all data): R_1 = 0.0601, wR_2 = 0.1182, goodness of fit = 1.037. CCDC-2201897 for 2-((4-fluorophenyl)thio)-4,6-diphenylnicotinonitrile **(1f)** contains the supplementary crystallographic data for this paper. These data can be obtained free of charge from The Cambridge Crystallographic Data Centre via www.ccdc.cam.ac.uk/data_request/cif.

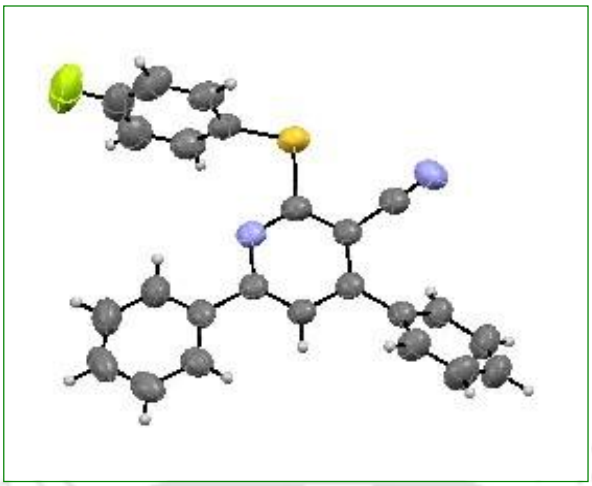

Figure IV.8. *ORTEP diagram of 2-((4-fluorophenyl)thio)-4,6-diphenylnicotinonitrile (**1f**) with 40% ellipsoid probability (CCDC 2201897).*

IV.4.3. General Procedure for the Synthesis of 2-(3-oxo-1,3-diphenylpropyl)malononitrile (1–16):

Compounds **1**–**16** were synthesized as per the following the method described in S. Lin, Y. Wei and F. Liang. *Chem. Commun.*, 2012, **48**, 9879.

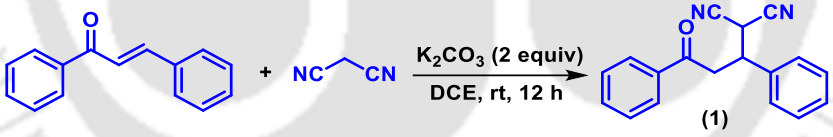

Compounds (1−14) were synthesized by a slight modification of the literature procedure. To an oven-dried 50 mL round-bottom flask were added chalcone, 1,3-diphenyl-2-propen-1-one (1.04 g, 5.0 mmol.), malononitrile (0.66 g, 10.0 mmol), K_2CO_3 (1.38 g, 10.0 mmol), and DCE (5 mL). The reaction mixture was stirred at room temperature for 12 h. Then, the reaction mixture was admixed with ethyl acetate (30 mL) and the organic layer was washed with water (10 mL). The organic layer was dried over anhydrous Na_2SO_4, and the solvent was evaporated under reduced pressure. The crude product so obtained was purified over a column of silica gel (hexane/ethyl acetate, 9:1) to give pure 2-(3-Oxo-1,3-diphenylpropyl)malononitrile (**1**) (1.30 g, 95%).

IV.4.4. General Procedure for the Synthesis of 4,6-diphenyl-2-(phenylthio)nicotinonitrile (1a) from 2-(3-oxo-1,3-diphenylpropyl)malononitrile (1) and Thiophenol (a):

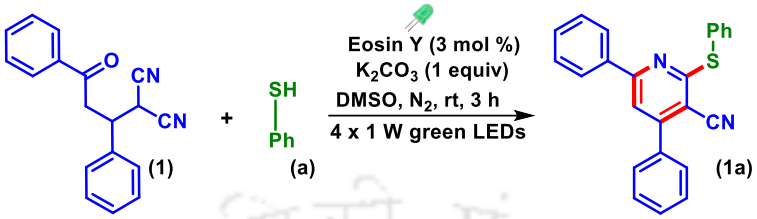

To an oven-dried 10 mL borosilicate vial were added 2-(3-oxo-1,3-diphenylpropyl)malononitrile (**1**) (0.25 mmol, 68 mg), eosin Y (3 mol%, 5 mg), and K_2CO_3 (1 equiv, 34 mg). Then to the reaction mixture benzene thiol (**a**) (0.5 mmol, 55 mg) in 1 mL of DMSO was added and stirred at room temperature under N_2 atmosphere for 3 h, tentatively at a distance of ~1–2 cm from four 1 W green LEDs. After completion of the reaction (monitored by TLC analysis), the mixture was diluted with water (10 mL) followed by extraction with ethyl acetate (20 mL). The organic layer was dried over anhydrous Na_2SO_4, and the solvent was evaporated under reduced pressure. The crude residue thus obtained was purified by column chromatography over silica gel (60−120 mesh) using hexane and ethyl acetate (98:2) as an eluent to afford the 4,6-diphenyl-2-(phenylthio)nicotinonitrile (**1a**) in 78% yield. The identity and purity of the product were confirmed by spectroscopic analysis (Scheme S2).

IV.4.5. General Procedure for 5 mmol Scale Reaction for the Synthesis of 4,6-Diphenyl-2-(phenylthio)nicotinonitrile (1a):

To an oven-dried 50 mL borosilicate round bottom flask, were added 2-(3-oxo-1,3-diphenylpropyl)malononitrile (**1**) (5 mmol, 1.37 g), eosin Y (3 mol %, 0.135 g), and K_2CO_3 (1 equiv, 0.966 g). Then to the reaction mixture benzene thiol (**a**) (10.0 mmol, 1.10 g) in 2 mL of DMSO was added and stirred at room temperature under N_2 atmosphere for 3 h, tentatively at a distance of ~1–2 cm from four 1 W green LEDs. After completion of the reaction (monitored by TLC analysis), the reaction mixture was admixed with ethyl acetate (50 mL) and the organic layer was washed with ice-cooled water (20 mL). The organic layer was dried over anhydrous Na_2SO_4, and the solvent was evaporated under reduced pressure. The crude residue thus obtained was purified by column chromatography over silica gel

(60–120 mesh) using hexane and ethyl acetate (98:2) as eluent to afford the 4,6-diphenyl-2-(phenylthio)nicotinonitrile (**1a**) in 64% yield. The identity and purity of the product was confirmed by spectroscopic analysis.

IV.4.6. General Procedure for the Synthesis of 4,6-Diphenyl-2-(phenylthio)nicotinonitrile (1a) in the Presence of Sunlight:

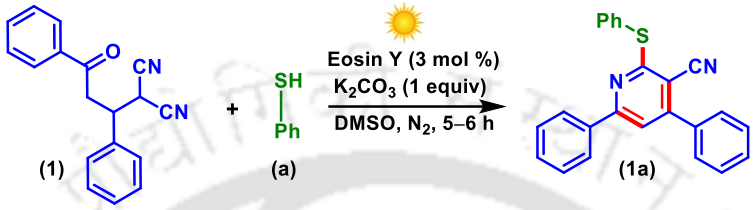

To an oven-dried 25 mL borosilicate round bottom flask, was added 2-(3-oxo-1,3-diphenylpropyl)malononitrile (**1**) (0.25 mmol, 68 mg), eosin Y (3 mol %, 5 mg), and K_2CO_3 (1 equiv, 34 mg). Then to the reaction mixture benzene thiol (**a**) (0.5 mmol, 55 mg), in 1 mL DMSO was added and stirred at room temperature under N_2 atmosphere for 5–6 h, with the surrounding temperature 30–35 ^oC. After completion of the reaction (monitored by TLC analysis), the reaction mixture was admixed with ethylacetate (20 mL) and the organic layer was washed with water (10 mL). The organic layer was dried over anhydrous Na_2SO_4, and the solvent was evaporated under reduced pressure. The crude residue thus obtained was purified by column chromatography over silica gel (60-120 mesh) using hexane and ethyl acetate (98:2) as eluent to afford the 4,6-diphenyl-2-(phenylthio)nicotinonitrile (**1a**) in 70% yield. The identity and purity of the product was confirmed by spectroscopic analysis.

Light Information and Reaction Set-up:

Luxeon star 4 x 1 W green LEDs were used as a light source for this light promoted reaction without using any filter. The measured wavelength is 523 nm with measured flux of 39 mW/cm^2, and borosilicate glass vial was used as a reaction vessel. Distance from the light source to the irradiation vessel ~1–2 cm. Regular fan was used for proper aeration to maintain the temperature 28–30 ^{o}C (Figure IV.7).

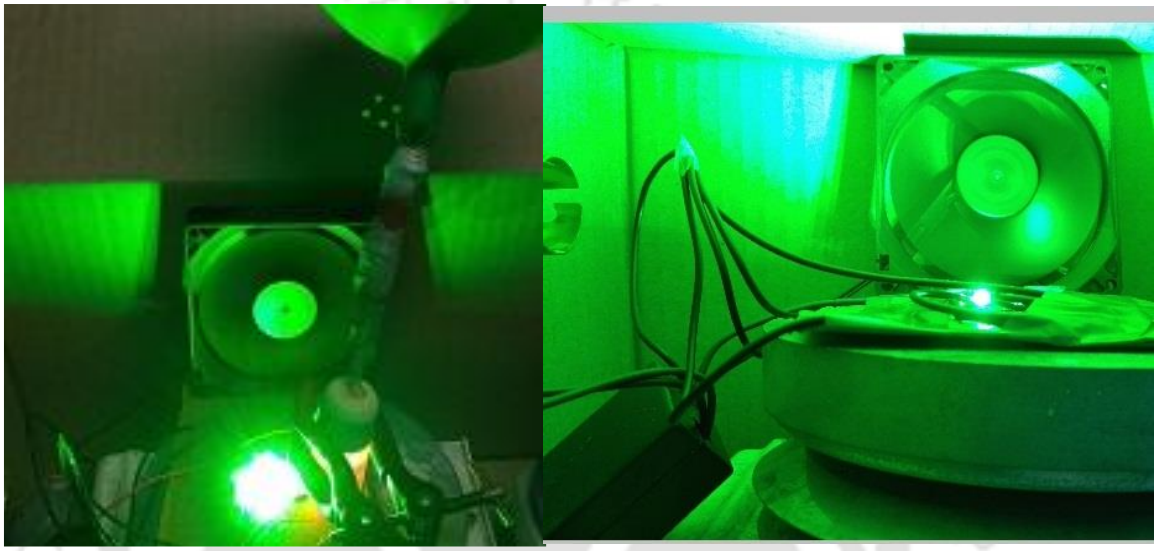

Figure IV.7. *Photochemical reaction set-up (outside & inside view).*

IV.4.7. Post Synthetic Applications:

(A) General Procedure for the Synthesis of 4,6-diphenyl-2-(phenylsulfonyl)nicotinonitrile (1aa) from 4,6-diphenyl-2-(phenylthio)nicotinonitrile (1a):

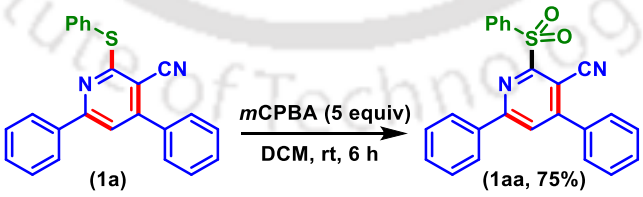

To a 10 mL round bottom flask was added 4,6-diphenyl-2-(phenylthio)nicotinonitrile (**1a**) (91 mg, 0.25 mmol) and DCM. Then the reaction mixture was stirred under ice-cooled condition. Then to the reaction mixture mCPBA (215 mg, 1.25 mmol) was added pinch wise over a period of 5 minute. Then the reactions mixture was stirred at room temperature for 6 h.

After completion of the reaction (monitored by TLC analysis), the solvent was evaporated and the reaction mixture was admixed with ethyl acetate (15 mL) and the organic layer was washed with saturated bicarbonate solution (5 mL). The organic layer was dried over anhydrous sodium sulfate (Na_2SO_4), and the solvent was evaporated under reduced pressure. The crude product so obtained was purified over a column of silica gel using 8% ethyl acetate in hexane to give pure 4,6-diphenyl-2-(phenylsulfonyl)nicotinonitrile (**1aa**) in 75% yield. The identity and purity of the product was confirmed by spectroscopic analysis.

(B) General Procedure for the Synthesis of 3-cyano-2,6,7-triphenyl-4-(phenylthio)pyrido[2,1-*a*]isoquinolin-5-ium (1ab) from 4,6-diphenyl-2-(phenylthio)nicotinonitrile (1a) and Diphenyl Acetylene.

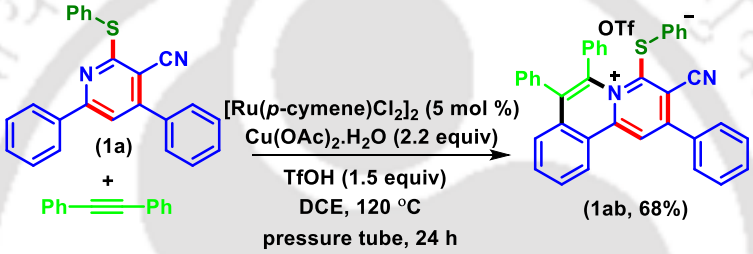

To an oven-dried pressure tube containing a magnetic bar was added 4,6-diphenyl-2-(phenylthio)nicotinonitrile (1a) (0.20 mmol, 72 mg), diphenylacetylene (0.024 mmol, 43 mg), [Ru(*p*-cymene)Cl_2]$_2$ (0.01 mmol, 6 mg), Cu(OAc)$_2$.H_2O (0.44 mmol, 84 mg), TfOH (0.30 mmol, 45mg) and DCE (2 mL). The reactions mixture was stirred in an oil bath preheated at 120 ^oC for 24 h. After completion of the reaction (monitored by TLC analysis), the reaction mixture was admixed with ethyl acetate (20 mL) and the organic layer was washed with saturated sodium bicarbonate solution (10 mL). The organic layer was dried over anhydrous sodium sulfate (Na_2SO_4), and solvent was evaporated under reduced pressure. The crude product so obtained was purified over a column of silica gel using 2% methanol in DCM to give pure 3-cyano-2,6,7-triphenyl-4-(phenylthio)pyrido[2,1-*a*]isoquinolin-5-ium (**1ab**) in 68% yield. The identity and purity of the product was confirmed by spectroscopic analysis.

(C) General Procedure for the Synthesis Of 4,6-diphenyl-2-(phenylthio)nicotinamide (1ac) from 4,6-diphenyl-2-(phenylthio)nicotinonitrile (1a):

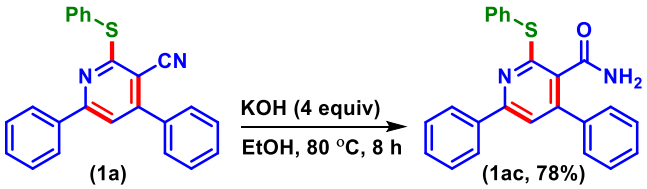

To a oven-dried round bottom flask was added 4,6-diphenyl-2-(phenylthio)nicotinonitrile (**1a**) (0.20 mmol, 72 mg), KOH (0.8 mmol, 44 mg), and ethanol (2 mL). Then the reaction mixture was stirred under ice-cooled condition for 8 h. After completion of the reaction (monitored by TLC analysis), the solvent was evaporated and the reaction mixture was admixed with ethyl acetate (20 mL) and the organic layer was washed with water (10 mL). The organic layer was dried over anhydrous sodium sulfate (Na_2SO_4), and the solvent was evaporated under reduced pressure. The crude product so obtained was purified over a column of silica gel using 20% ethyl acetate in hexane to give pure 4,6-diphenyl-2-(phenylthio)nicotinamide (**1ac**) in 78% yield. The identity and purity of the product was confirmed by spectroscopic analyses.

IV.4.8. Mechanistic Investigations:

Radical-trapping Experiments:

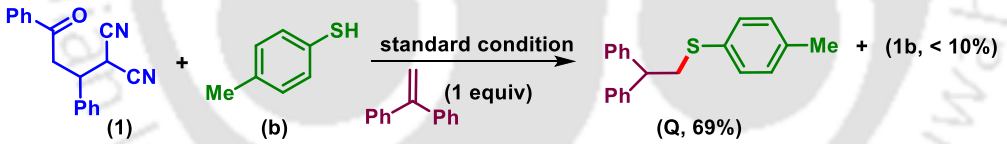

(i) To an oven-dried 10 mL borosilicate vial was added 2-(3-oxo-1,3-diphenylpropyl)malononitrile (**1**) (0.25 mmol, 68 mg), *p*-methyl benzene thiol (**b**) (0.5 mmol, 62 mg), eosin Y (3 mol%, 5 mg), and K_2CO_3 (1 equiv., 34 mg). Then 1,1-diphenyl ethylene (1 equiv, 45 mg) in 1 mL of DMSO was added and stirred at room temperature under N_2 atmosphere for 3 h tentatively at a distance of ~1–2 cm from four 1 W green LEDs. It was found that in the presence of diphenyl ethylene <10% of the product (**1b**) and exclusive thiyl radical trapped adduct (**Q**, 69%) was observed. The structure of the adduct (**Q**) was confirmed by HRMS (Figure IV.9), ^{1}H NMR (Figure IV.10), and ^{13}C{^{1}H} (Figure IV.11) analyses.

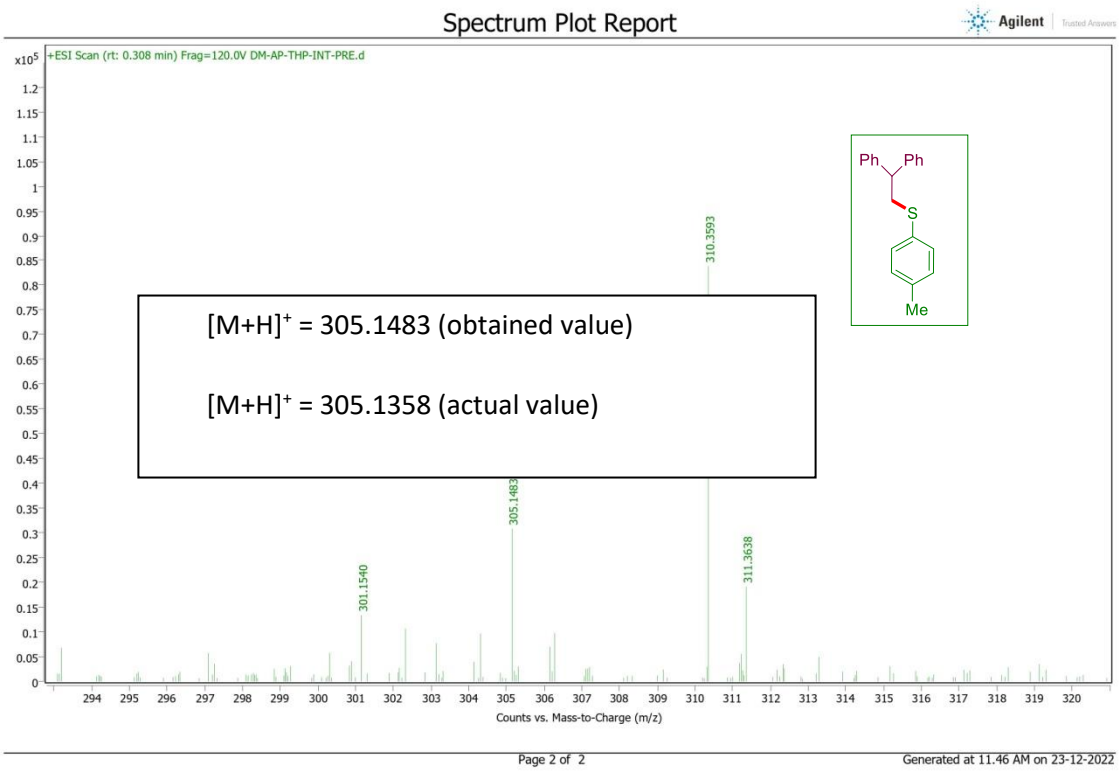

Figure IV.9. *HRMS spectra of thiyl-radical trapped adduct (**Q**).*

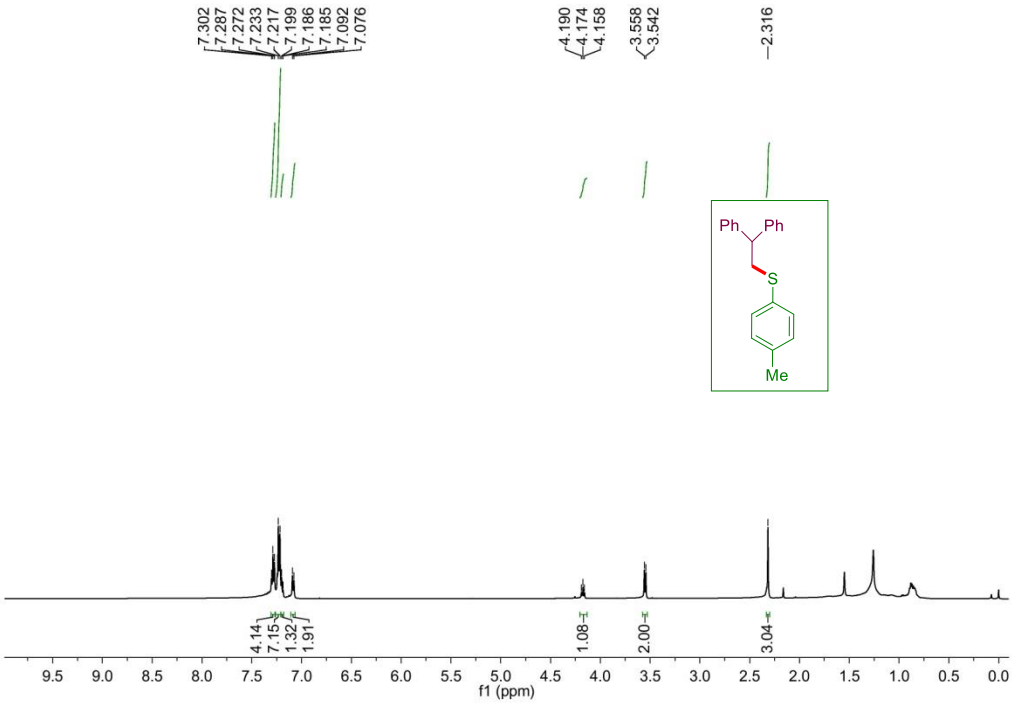

Figure IV.10. *^{1}HNMR spectra of thiyl-radical trapped adduct (Q).*

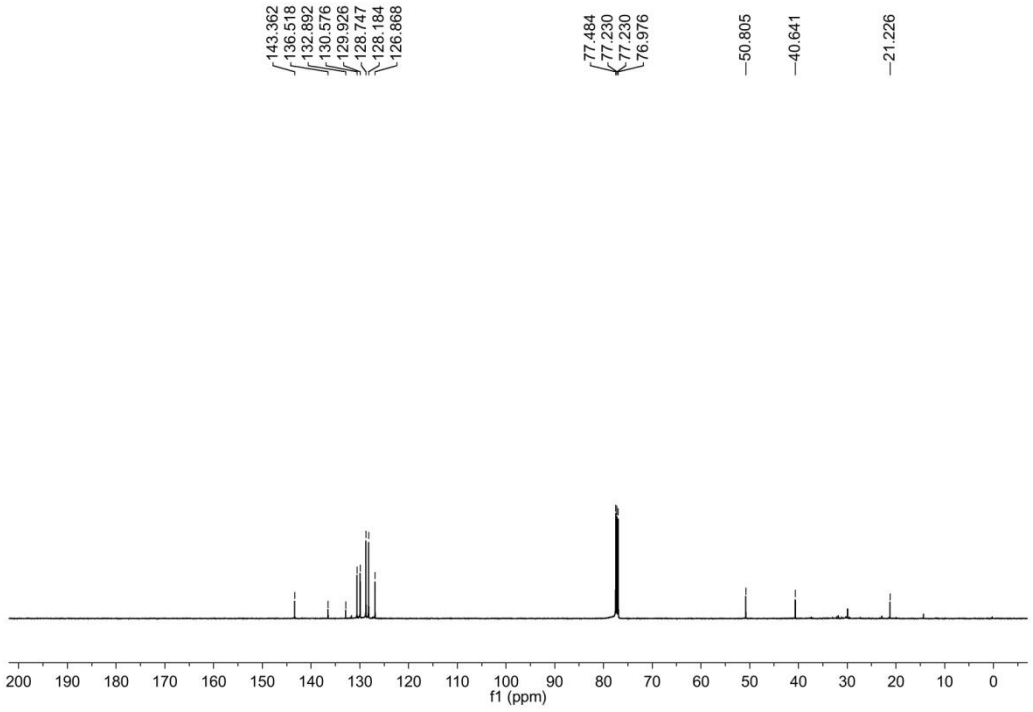

Figure IV.11. *$^{13}C\{1H\}$ NMR spectra of thiyl-radical trapped adduct (Q).*

Control Experiments

(I) In the Absence of Light:

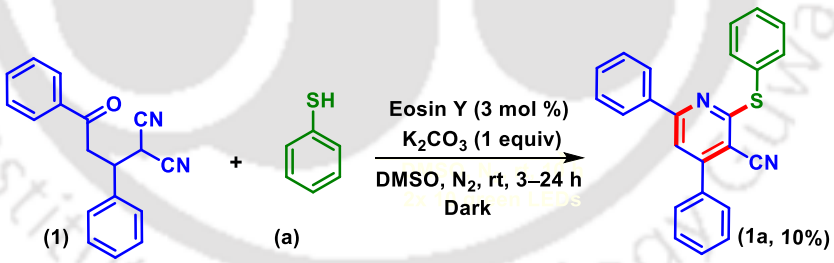

To an oven-dried 10 mL borosilicate vial was added 2-(3-oxo-1,3-diphenylpropyl)malononitrile (**1**) (0.25 mmol, 68 mg), eosin Y (3 mol%, 5 mg), and K_2CO_3 (1 equiv., 34 mg). Then benzene thiol (**a**) (0.5 mmol, 55 mg), in 1 mL of DMSO was added and then covered with an aluminium foil so that light cannot interact with the reaction mixture. Then the reaction mixture stirred at room temperature under N_2 atmosphere for 3 h. It was observed that around 10% of **1a** was formed (monitored by TLC analysis). Then the reaction was continued for 24 h to check the further progress. After completion of the reaction, the reaction mixture was admixed with ethyl acetate (20 mL) and the organic layer was washed

with ice-cooled water (10 mL). The organic layer was dried over anhydrous Na_2SO_4, and the solvent was evaporated under reduced pressure. The crude residue thus obtained was purified by column chromatography over silica gel (60−120 mesh) using hexane and ethyl acetate (98:2) as an eluent to afford the 4,6-diphenyl-2-(phenylthio)nicotinonitrile (**1a**) in 10% yield. The identity and purity of the product were confirmed by spectroscopic analysis.

(II) In the Absence of Catalyst:

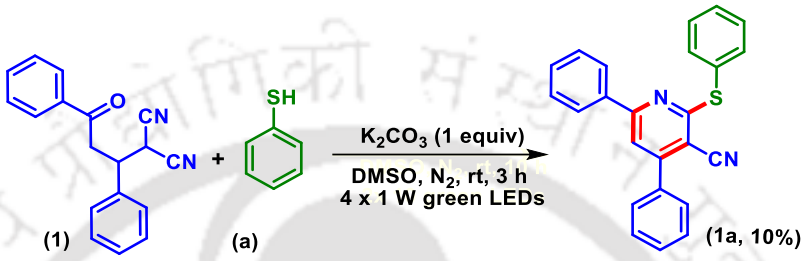

To an oven-dried 10 mL borosilicate vial were added 2-(3-oxo-1,3-diphenylpropyl)malononitrile (**1**) (0.25 mmol, 68 mg), and K_2CO_3 (1 equiv, 34 mg). Then benzene thiol (**a**) (0.5 mmol, 55 mg) in 1 mL of DMSO was added and stirred at room temperature under N_2 atmosphere for 3 h, tentatively at a distance of ~1−2 cm from four 1 W green LEDs. After completion of the reaction (monitored by TLC analysis), the reaction mixture was admixed with ethyl acetate (20 mL) and the organic layer is washed with ice-cooled water (10 mL). The organic layer was dried over anhydrous Na_2SO_4, and the solvent was evaporated under reduced pressure. The crude residue thus obtained was purified by column chromatography over silica gel (60−120 mesh) using hexane and ethyl acetate (98:2) as an eluent to afford the 4,6-diphenyl-2-(phenylthio)nicotinonitrile (**1a**) in 10% yield suggesting the crucial role of catalyst in the generation of thiyl radical. The identity and purity of the product were confirmed by spectroscopic analysis.

(III) Reaction in the Absence of Base

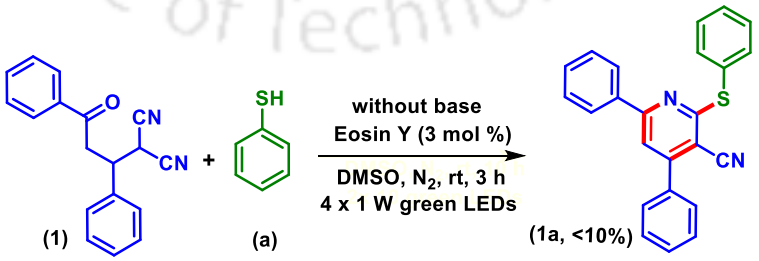

To an oven-dried 10 mL borosilicate vial was added 2-(3-oxo-1,3-diphenylpropyl)malononitrile (**1**) (0.25 mmol, 68 mg), and eosin Y (3 mol%, 5 mg). Then benzene thiol (**a**) (0.5 mmol, 55 mg) in 1 mL of DMSO was added and stirred at room

temperature under N_2 atmosphere for 10 h, tentatively at a distance of ~1−2 cm from four 1 W green LEDs. It was found that a trace amount (<10%) of the product (**1a**) was obtained (as monitored by TLC) suggesting the necessity of the base in the present protocol.

(IV) Reaction in the Absence of Base and in the Presence of Oxygen

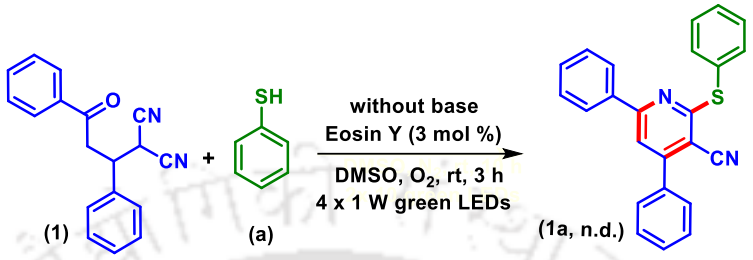

To an oven-dried 10 mL borosilicate vial was added 2-(3-oxo-1,3-diphenylpropyl)malononitrile (**1**) (0.25 mmol, 68 mg), and eosin Y (3 mol%, 5 mg). Then benzene thiol (**a**) (0.5 mmol, 55 mg), in 1 mL of DMSO was added and stirred at room temperature under O_2 atmosphere for 3 h, tentatively at a distance of ~1−2 cm from four 1 W green LEDs. It was found that no desired product (**1a**) was obtained (as monitored by TLC) suggesting the silence of oxygen in the present protocol.

(V) Reaction in the Absence of Photosensitizer in Open Air

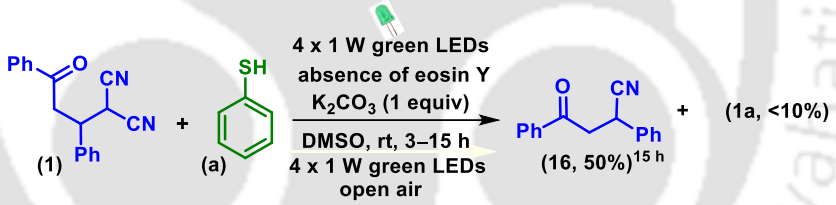

To an oven-dried 10 mL borosilicate vial were added 2-(3-oxo-1,3-diphenylpropyl)malononitrile (**1**) (0.25 mmol, 68 mg), and K_2CO_3 (1 equiv, 34 mg). Then benzene thiol (**a**) (0.5 mmol, 55 mg) in 1 mL of DMSO was added and stirred at room temperature under open air for 3 h, tentatively at a distance of ~1−2 cm from four 1 W green LEDs. It was observed that the desired product **1a** was obtained in <10% yield, while to see the further conversion the reaction was continued for 15 h and it was observed that (**1**) consumed completely and a new spot was formed. After completion of the reaction (monitored by TLC analysis), the reaction mixture was admixed with ethyl acetate (20 mL) and the organic layer is washed with ice-cooled water (10 mL). The organic layer was dried over anhydrous Na_2SO_4, and the solvent was evaporated under reduced pressure. The crude residue thus obtained was purified by column chromatography over silica gel (60−120 mesh) using hexane and ethyl acetate (98:2) as an eluent to afford the 4,6-diphenyl-2-

(phenylthio)nicotinonitrile (**1a**) in <10% yield and 4-oxo-2,4-diphenylbutanenitrile (16), in 50% yield. The identity of the product was confirmed by ^{1}HNMR analysis (Figure IV.12).

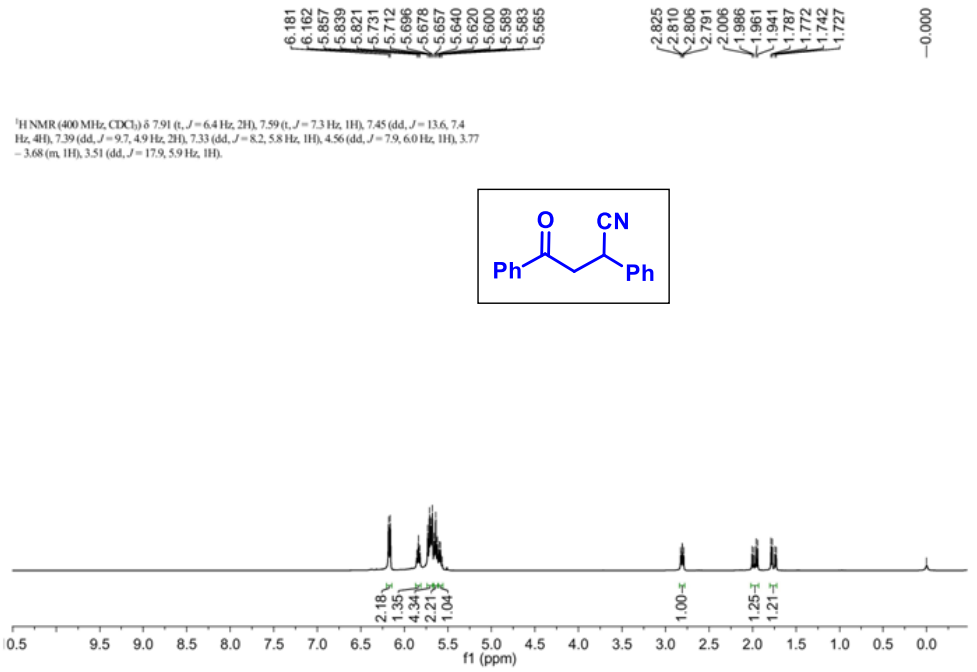

Figure IV.12. *^{1}H NMR spectra of (**16**).*

(VI) Reaction under Thermal Condition in the Absence of Base and Eosin Y in Open Air

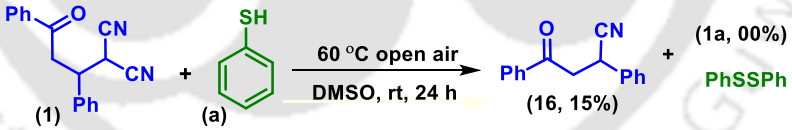

To an oven-dried 10 mL round bottom flask were added 2-(3-oxo-1,3-diphenylpropyl)malononitrile (**1**) (0.25 mmol, 68 mg), benzene thiol (**a**) (0.5 mmol, 55 mg) in 1 mL of DMSO was added and stirred at 60 °C under open air for 24 h. After completion of the reaction (monitored by TLC analysis), the reaction mixture was admixed with ethyl acetate (20 mL) and the organic layer is washed with ice-cooled water (10 mL). The organic layer was dried over anhydrous Na_2SO_4, and the solvent was evaporated under reduced pressure. The crude residue thus obtained was purified by column chromatography over silica gel (60−120 mesh) using hexane and ethyl acetate (98:2) as an eluent to afford the 4-oxo-2,4-diphenylbutanenitrile (**16**), in 15% yield. The identity of the product was confirmed by

^{1}HNMR analysis. No trace of the desired product 4,6-diphenyl-2-(phenylthio)nicotinonitrile (**1a**) was obtained.

On-off Experiments

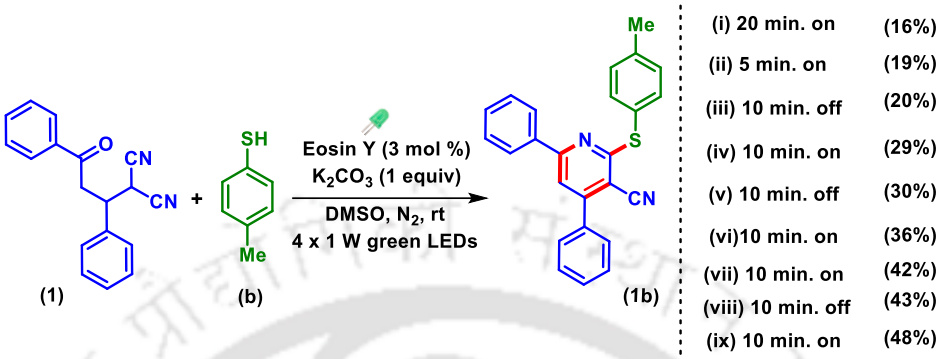

The reaction mixture was stirred and irradiated by 4 x 1 W green LEDs at room temperature under a nitrogen atmosphere for 20 minutes, and the corresponding product (**1b**) was isolated in 16% yield. Then the reaction mixture was continuously stirred for further 5 minutes and the desired product (**1b**) was obtained in 19% yield. When the reaction mixture was continued under dark for another 10 min the desired product (**1b**) was obtained in 20% yield. Furthermore, when the reaction mixture was stirred and irradiated by 4 x 1 W green LEDs at room temperature under a nitrogen atmosphere for 10 minutes, the desired product (**1b**) was isolated in 29% yield. This procedure was repeated at regular time intervals and the above results indicated that continuous visible light irradiation is essential for promoting this transformation (Figure IV.4). The NMR spectra were recorded taking nitromethane as the internal standard $CDCl_3$ as the solvent (Figure IV.13–16).

Representative Spectra for On-off Experiments

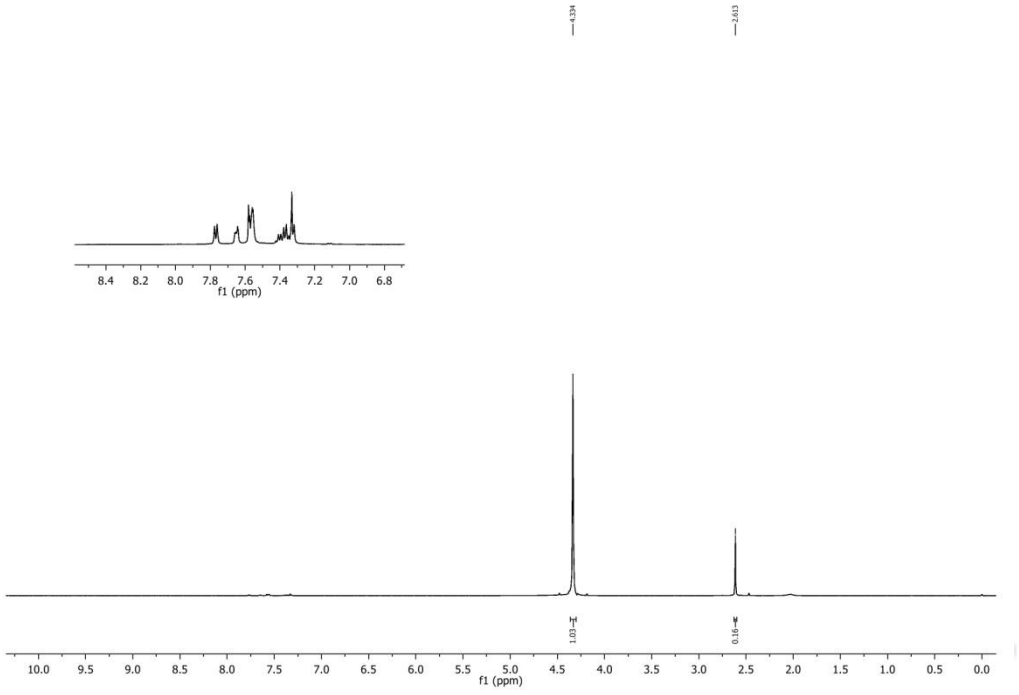

Figure IV.13. *^{1}H NMR spectra of the on-off experiment (20 min. light on).*

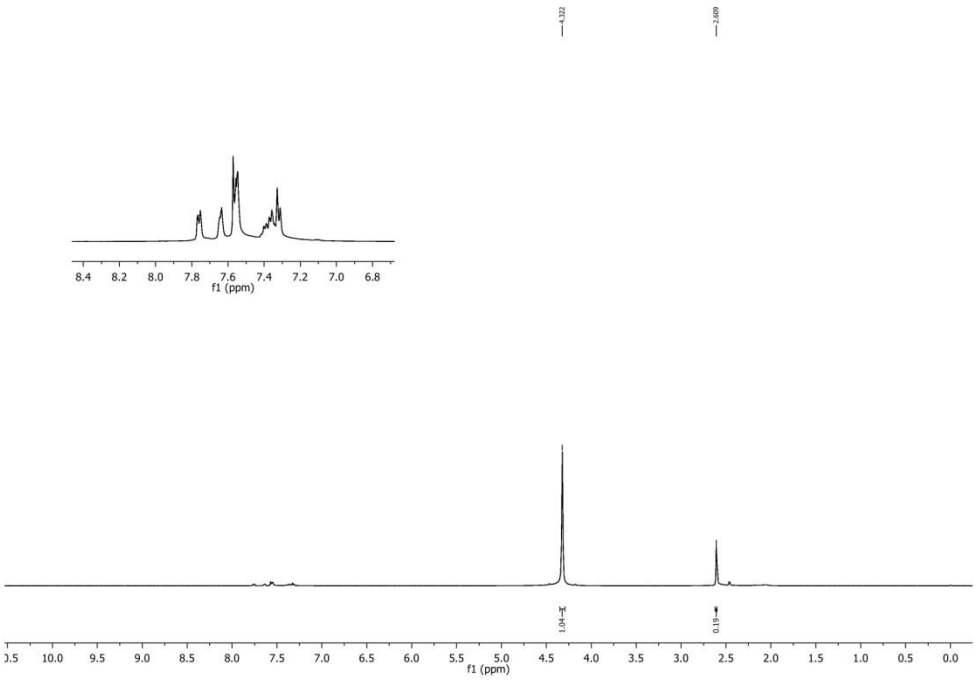

Figure IV.14. *^{1}H NMR spectra of the on-off experiment (further 5 min. light on).*

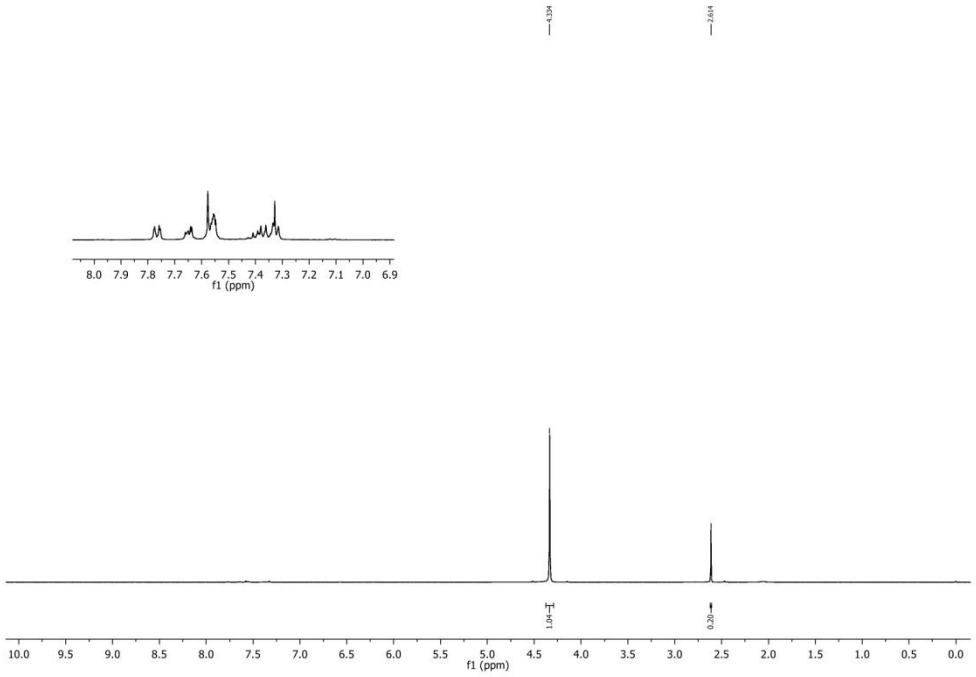

Figure IV.15. *^{1}H NMR spectra of the on-off experiment (further 10 min. light off).*

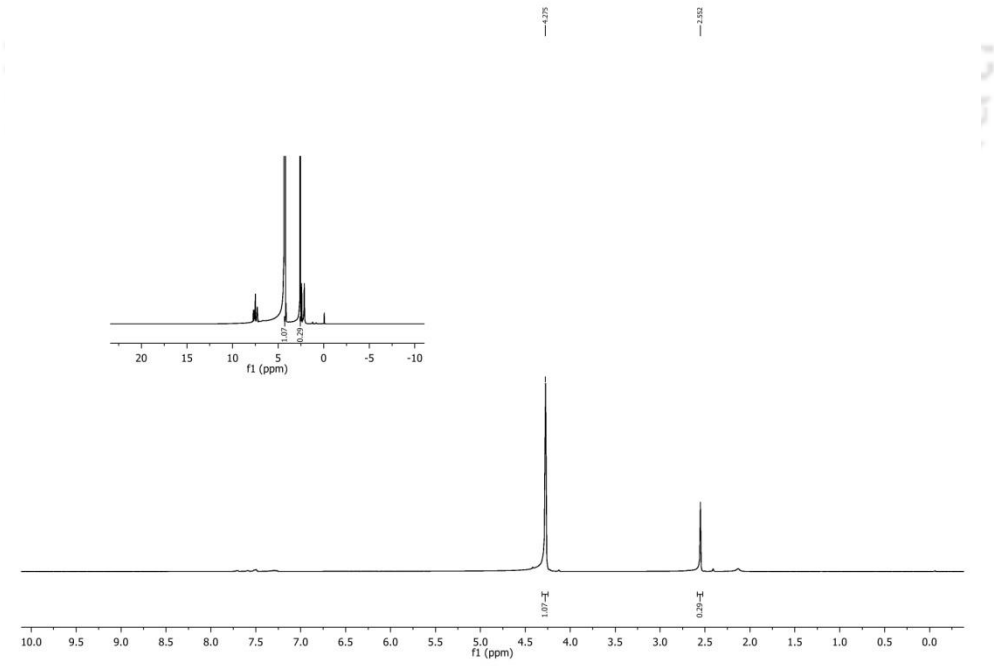

Figure IV.16. *^{1}H NMR spectra of the on-off experiment (further 10 min. light on).*

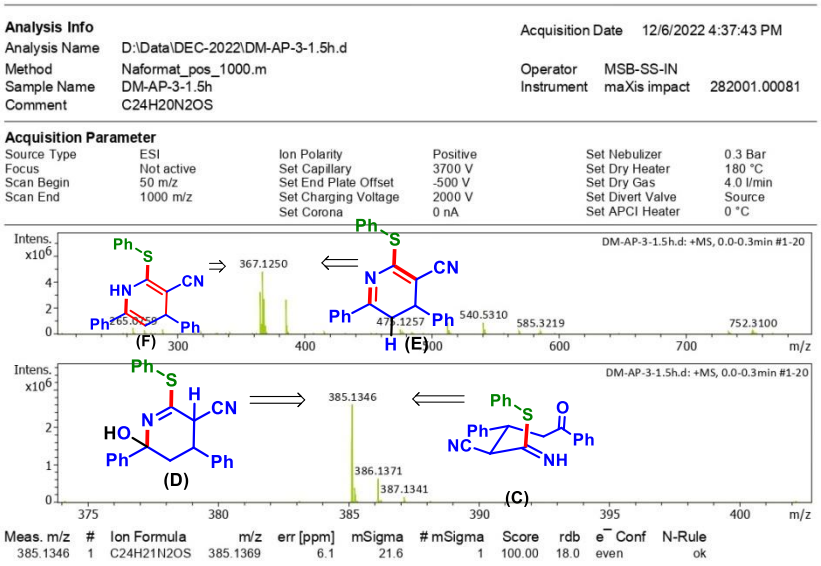

Figure IV.17. *HRMS spectrum after 1.5 h.*

IV.4.9. SV Experiments:

A 1 mM solution was prepared by mixing eosin Y in water by an appropriate dilution of 0.01 M stock solution and taken in a quartz UV cuvette of a 1 cm path length. The UV−visible spectroscopy showed λmax of 515 nm. For the fluorescence measurement, the sample was excited at 515 nm, and the emission was observed at 560 nm. For each fluorescence quenching experiment, a 5 μL (1 M) solution of benzene thiol (a) was added to eosin Y solution (1 mM) taken in a fluorescence cuvette, and fluorescence emission spectra were recorded after each addition (Figure IV.5). As evident from Figure S6, a decrease in emission intensity was observed after each addition of thiophenol (a) concentration (5−75 mM). This suggests that a facile electron transfer is possible between the catalyst and the quencher PhSH. This indicates that eosin Y might be helping in the generation of thiyl radical from the PhSH. With these data, the Stern−Volmer graph was plotted using the equation I0/It =1+ KSV [Q], where I0 and It are the integrated emission intensity in the absence and presence of quencher and Ksv is the quenching constant. A linear quenching was observed.

IV.4.10. CV Experiments:

(A) CV Experiments Performed to Determine the Redox Potentials.

Cyclic voltammetry (CV) was performed using a three-electrode cell configuration comprising a glassy carbon, a platinum wire, and Ag(s)/AgCl (0.01 M) as the working, auxiliary, and reference electrodes, respectively. Cyclic voltammetry experiment of PhSH and *β*-ketodinitrile (**1**) taken at a scan rate 100 mv/s. Experiment conditions: init E = 2.0 V, high E = 2.0 V, low E = −2.0 V, scan rate = 0.1 V/s, sample interval = 0.001 V, quiet time = 2s, sensitivity = 2e−4 A/ V]. The supporting electrolyte used was tetraethylammonium hexafluorophosphate (TEAHFP) $(C_2H_5)_4N(PF_6)$. Samples were prepared with a substrate concentration of 0.01 M in a 0.1 M TEAHFP in an acetonitrile electrolyte solution. From the result, it was found that the oxidation potential of thiophenol ($E_{1/2\ ox}$ = +0.25 V vs SCE) is lower than the oxidation potential of Eosin Y ($E_{1/2\ ox}$ = +0.83 V vs SCE for excited state of eosin Y). Similarly, the reduction potential of thiophenol (**a**) ($E_{1/2\ red}$ = -1.35 V vs SCE) is lower than the reduction potential value of Eosin Y ($E_{1/2\ red}$ = -1.06 V vs SCE for excited state of eosin Y This indicates that thiophenols can be easily oxidized by the eosin Y which also confirms the role of eosin Y as an oxidizing agent and helps in the facile generation of the thiyl radical. Further, the CV value of thiolate anion ($E_{1/2\ ox}$ = +0.35 V *vs*. SCE) shows that it has a stronger tendency to gain electron than PhSH ($E_{1/2\ ox}$ = +0.25 V *vs*. SCE) or PhSH has a better tendency to lose electron than thiolate anion (Fig. S6). While comparing these values with the oxidation potential of eosin Y ($E_{1/2\ ox}$ = +0.83 V *vs*. SCE for excited state of eosin Y) it is clear that EY* will preferably accept an electron from PhSH rather than from the thiyl anion.[1] The $E_{1/2\ Oxd}$ of *γ*-ketodinitriles (**1**) is found to be 0.38 V + 2.13 V & vs SCE (Figure. IV.2, and 6).

IV.5. References

[1] (a) Sun, K.; Lv, Q.-Y.; Chen, X.-L.; Qua, L-B.; Yu, B. *Green Chem*. **2021**, *23*, 232–248. (b) Zhou, Q.-Q.; Zou, Y.-Q.; Lu, L.-Q.; Xiao, W.-J. *Angew*. *Chem., Int*. *Ed*. **2019**, *58*, 1586–1604. (c) Masson, G.; König, B. *Eur*. *J*. *Org*. *Chem*. **2020**, 1191-1192. (d) Crisenza, G. E. M.; Mazzarella, D.; Melchiorre, P. *J*. *Am*. *Chem*. *Soc*. **2020**, *142*, 5461–5476. (e) McCarver, S. J.; Qiao, J. X.; Carpenter, J.; Borzilleri, R. M.; Poss, M. A.; Eastgate, M. D.; Miller, M. M.; MacMillan, D. W. C. *Angew*. *Chem*., *Int*. *Ed*. **2017**, *56*,

728–732. (f) Srivastava, V.; Singh, P. K.; Tivaria S.; Singh, P. P. *Org. Chem. Front.* **2022**, *9*, 1485–1507. (g) Pokhriyal, A. Karki, B. S.; Kant, R.; Rastogi, N. *J. Org. Chem.* **2021**, *86*, 4661–4670. (h) Xiao, Q.; Tong, Q.-X.; Zhong, J.-J. *Molecules.* **2022**, *27*, 619. (i) Altaf, A. A.; Shahzad, A.; Gul, Z.; Rasool, N.; Badshah, A.; Lal B.; Khan, E. *Journal of Drug Design and Medicinal Chemistry*. **2015**, *1*, 1–11.

[2] (a) Chalotra, N.; Rizvi, M. A.; Shah, B. A. *Org. Lett.* **2019**, *21*, 4793–4797. (b) Skubi, K. L.; Blum T. R.; Yoon, T. P. *Chem. Rev.* **2016**, *116*, 10035–10074. (c) Zhu, C.; Yue, H.; Chu L.; Rueping, M. *Chem. Sci.* **2020**, *11*, 4051–4064. (d) Liang, X.-A.; Niu, L.; Wang, S.; Liu J.; Lei, A. *Org. Lett.* **2019**, *21*, 2441–2444. (e) Saha, A.; Guin, S.; Ali, W.; Bhattacharya, T.; Sasmal, S.; Goswami, N.; Prakash, G.; Sinha, S. K.; Chandrashekar, H. B.; Panda, S.; Anjana S. S.; Maiti, D. *J. Am. Chem. Soc.* **2022**, *144*, 1929–1940. (f) Kumar, J.; Ahmad, A.; Rizvi, M. A.; Ganie, M. A.; Khajuria, C.; Shah, B. A. *Org. Lett.* **2020**, *22*, 5661–5665.

[3] (a) Bell J. D.; Murphy, J. A. *Chem. Soc. Rev.* **2021**, *50*, 9540–9685. (b) Yan, D.-M.; Chen, J.-R.; Xiao, W. J. *Angew. Chem., Int. Ed.* **2019**, *58*, 378–380. (c) Xia, L.; Jin, M.; Jiao, Y.; Yu, S. *Org. Lett.* **2022**, *24*, 364–368. (d) Dahiya, A.; Das, B.; Sahoo A. K.; Patel, B. K. *Adv. Synth. Catal.* **2022**, *364*, 966–973. (e) Wu, F.; Dong, W.; Fan, S.; Yuan, Y.; Liang, C.; Chen, A.; Yin, Z.; Zhang, Z. *J. Org. Chem.* **2022**, *87*, 1302−1312. (f) Rohokale, R. S.; Koenig, B.; Dhavale, D. D. *J. Org. Chem.* **2016**, *81*, 7121–7126. (g) Sahoo, A. K.; Dahiya, A.; Das, B.; Behera, A.; Patel, B. K. *J. Org. Chem.* **2021**, *86*, 11968–11986. (h) Roy V. J.; Sen, P. P.; Roy, S. R. *J. Org. Chem.* **2021**, *86*, 16965–16976.

[4] (a) Eicher, T.; Hauptmann S.; Speicher, A. The Chemistry of Heterocycles, 2nd ed. Wiley-VCH Verlag GmbH & Co. Weinheim, **2003**. (b) Allais, C.; Grassot, J.-M.; Rodriguez, J.; Constantieux, T. *Chem. Rev.* **2014**, *114*, 10829–10868. (c) Hill, M. D. *Chem. Eur. J.* **2010**, *16*, 12052−12062. (d) Stolar, M.; Baumgartner, T. *Chem. Commun.* **2018**, *54*, 3311–3322.

[5] (a) Han H.; Hurley, L. H.; *Trends Pharmacol. Sci.* **2000**, *21*, 136–142 (b) Chelucci, G.; *Chem. Soc. Rev.* **2006**, *35*, 1230–1243. (c) Constable, E. C.; Housecroft, C. E.; Neuburger, M.; Phillips, D.; Raithby, P. R.; Schofield, E.; Sparr, E.; Tocher, D. A.; Zehnder M.; Zimmermann, Y. *J. Chem. Soc. Dalton Trans.* **2000**, *13*, 2219–2228.

[6] (a) Baldwin, C. M.; Keam, S. J.; *Drugs* **2009**, *69*, 1373–1401. (b) Boushra, A. F.; Elsayed, A. M.; Ibrahim, N. A.; Abdelwahed, M. K.; Ahmed, E. I. A. *Mol*. *Biol*. *Rep*. **2019**, *46*, 4843–4860. (c) Charrier, J.-D.; Miller, A.; Kay, D. P.; Brenchley, G.; Twin, H. C.; Collier, P. N.; Ramaya, S.; Keily, S. B.; Durrant, S. J.; Knegtel, R. M. A.; Tanner, A. J.; Brown, K.; Curnock, A. P.; Jimenez, J.-M. *J. Med*. *Chem*. **2011**, *54*, 2341–2350. (d) Croom K. F.; Siddiqui, M. A. A.; *Drugs* **2009**, *69*, 1513–1532. (e) Liu, J.; Huang, Z.; Ma, W.; Peng, S.; Li, Y.; Miranda, K. M.; Tian J.; Zhang, Y. *Eur*. *J*. *Med*. *Chem*. **2019**, *162*, 650–665. (f) Mosure, S. A.; Shang, J.; Eberhardt, J.; Brust, R.; Zheng, J.; Griffin, P. R.; Forli S.; Kojetin, D. J. *J*. *Med*. *Chem*. **2019**, *62*, 2008–2023.

[7] (a) Takami, A.; Ohtake, S.; Morishita, E.; Terasaki, Y.; Fukushima, T.; Kurokawa, T.; Sugimori, N.; Matono, S.; Ohata, K.; Saito, C.; Yamaguchi, M.; Hosokawa, K.; Yamazaki, H.; Kondo Y.; Nakao, S. *Int*. *J*. *Hematol* **2012**, *96*, 357–363. (b) Chen, F.; Fang, Y.; Zhao, R.; Le, J.; Zhang, B.; Huang, R.; Chen Z.; Shao, J. *Eur*. *J*. *Med*. *Chem*. **2019**, *179*, 916–936. (c) Frampton, J. E. *Drugs* **2013**, *73*, 2031–2051. (d) Croom, K. F.; Dhillon S.; Keam, S. J. *Drugs* **2012**, *69*, 1107–1140.

[8] (a) Hantzsch, A. *Ber*. *Dtsch*. *Chem*. *Ges*. **1881**, *14*, 1637–1638. (b) Kröhnke, F. *Synthesis* **1976**, 1–24.

[9] (a) Nie, B.; Wu, W.; Ren, Q.; Wang, Z.; Zhang, J.; Zhang, Y.; Jiang, H. *Org*. *Lett*. **2020**, *22*, 7786–7790. (b) Rammal, F.; Gao, D.; Boujnah, S.; Gaumont, A. C.; Hussein, A. A.; Lakhdar, S. *Org*. *Lett*. **2020**, *22*, 7671–7675. (c) Hardegger, L. A.; Habegger J.; Donohoe, T. J. *Org*. *Lett*. **2015**, *17*, 3222–3225.(d) Sujatha, C.; Bhatt, C. S.; Ravva, M. K.; Suresh, A. K.; Namitharan, K. *Org*. *Lett*. **2018**, *20*, 3241–3244. (e) Bai, D.; Wang, X.; Zheng G.; Li, X. *Angew*. *Chem*., *Int*. *Ed*. **2018**, *57*, 6633–6637.(f) Heravi, M. R. P.; Soufi, A. *Chin. Chem. Lett*. **2015,** *26*, 263–266.

[10] (a) Neely, J. M.; Rovis, T. *Org*. *Chem*. *Front*. **2014**, *1*, 1010–1015. (b) Boger, D. L.; *Chem*. *Rev*. **1986**, *86*, 781–793. (c) Wu, J.; Xu, W.; Yu Z.-X.; Wang, J. *J*. *Am*. *Chem*. *Soc*. **2015**, *137*, 9489–9496. (d) Kumar, P.; Prescher S.; Louie, J. A. *Angew*. *Chem*., *Int*. *Ed*. **2011**, *50*, 10694–10698. (e) Onodera, G.; Shimizu, Y.; Kimura, J.; Kobayashi, J.; Ebihara, Y.; Kondo, K.; Sakata K.; Takeuchi, R. *J*. *Am*. *Chem*. *Soc*. **2012**, *134*, 10515–10531. (f)

Ye, F.; Haddad, M. *Org*. *Lett*. **2017**, *19*, 1104−1107. (g) Xie, L.-G.; Shaaban, S.; Chen, X. Maulide, N. *Angew*. *Chem*., *Int*. *Ed*. **2016**, *55*, 12864−12867.

[11] (a) Rakshit, A.; Dhara, H. N.; Alam, T.; Dahiya, A.; Patel, B. K. *J*. *Org*. *Chem*. **2021**, *86*, 17504−17510. (b) Rakshit, A.; Dhara, H. N.; Sahoo, A. K.; Alam T.; Patel, B. K. *Org*. *Lett*. **2022**, *24*, 3741−3746. (c) Natarajan, P.; Muskan, M.; Brar N. K.; Kaur, J. J. *Org*. *Chem*. *Front*. **2018**, *5*, 1527−1531. (d) Zhang, Y.; Sun, K.; Lv, Q.; Chen, X.; Qu L.; Yu, B. *Chin*. *Chem*. *Lett*. **2019**, *30*, 1361–1368. (e) Longstreet, A. R.; Campbell, B. S.; Gupton B. F.; McQuade, D. T. *Org*. *Lett*. **2013**, *20*, 5298–5301. (f) Longstreet, A. R.; Rivalti D.; McQuade, D. T. *J*. *Org*. *Chem*. **2015**, *80*, 8583−8596. (g) de Souza, J. M.; Abdiaj, I.; Chen, J.; Hanson, K.; de Oliveira K. T.; McQuade, D. T. *Org*. *Biomol*. *Chem*. **2021**, ***19***, 1991–1999. (h) Shi, S.; Zheng, Z.; Zhang, Y.; Yang, Y.; Ma, D.; Gao, Y.; Liu, Y. Tang, G.; Zhao, Y. *Org*. *Lett*. **2021**, *23*, 9348−9352. (i) Huang, A.-X.; Zhu, H.-L.; Zeng, F.-L.; Chen, X.-L.; Huang, X.-Q.; Qu, L.-B.; Yu, B. *Org*. *Lett*. **2022**, *24*, 3014−3018.

[12] (a) Zhen, Q.; Li, R.; Qi, L.; Hu, K.; Yao, X.; Shao, Y.; Chen, J. *Org*. *Chem*. *Front*. **2020**, *7*, 286–291. (b) Xu, P.; Zhu, Y.-M.; Wang, F.; Wang, S.-Y.; Ji, S.-J. *Org*. *Lett*. **2019**, *21*, 683–686. (c) Tong, K.; Zheng, T.; Zhang, Y.; Yu, S. *Adv*. *Synth*. *Catal*. **2015**, *357*, 3681−3686.

[13] (a) Song, Z.; Huang, X.; Yi, W.; Zhang, W. *Org*. *Lett*. **2016**, *18*, 5640−5643. (b) Dong, J.; Bao, L.; Hu, Z.; Ma, S.; Zhou, X.; Hao, M.; Li, N.; Xu, X. *Org*. *Lett*. **2018**, *20*, 1244−1247. (c) Allais, C.; Grassot, J.-M.; Rodriguez, J.; Constantieux, T. *Chem*. *Rev*. **2014**, *114*, 10829−10868. (d) Wan, J.-P.; Jing, Y.; Hu C.; Sheng, S. *J*. *Org*. *Chem*. **2016**, *81*, 6826−6831.

[14] (a) Sun, K.; Lv, Q.-Y.; Lin, Y.-W.; Yu B.; He, W.-M. *Org*. *Chem*. *Front*. **2021**, *8*, 445−465. (b) Li, X.; Fang, X.; Zhuang, S.; Liu, P.; Sun, P. *Org*. *Lett*. **2017**, *19*, 3580−3583.

[15] (a) Dhara, H. N.; Rakshit, A.; Alam T.; Patel, B. K. *Org*. *Biomol*. *Chem*. **2022**, *20*, 4243−4277. (b) Rakshit, A.; Sau, P.; Ghosh S.; Patel, B. K. *Adv*. *Synth*. *Catal*. **2019**, *361*, 3824−3836. (c) Zuo, H.-D.; Ji, X.-S.; Guo, C.; Hao, S.-J.; Tu W.-J.; Jiang, B. *Org*. Chem. *Front*. **2021**, *8*, 1496−1502.

[16] (a) Sahoo, A. K.; Rakshit, A.; Dahiya, A.; Pan A.; Patel, B. K. *Org*. *Lett*. **2022**, *24*, 1918−1923. (b) Natarajan, P.; Manjeet, M.; Muskan, M.; Brar N. K.; Kaur, J. J. *Org*.

Chem. *Front*. **2018**, *5*, 1527–1531. (c) Xing, Z.; Yang, M.; Sun, H.; Wang, Z.; Chen, P.; Liu, L.; Wang, X.; Xie X.; She, X. *Green Chem*. **2018**, *20*, 5117–5122. (d) Lin, S.; Wei Y.; Liang, F. *Chem*. *Commun*. **2012**, *48*, 9879–9881. (e) McCourt R. O.; Scanlan, E. M. *Chem*. *Eur*. *J*. **2020**, *26*, 15804–15810. (f) Sahoo, A. K.; Rakshit, A.; Pan A.; Dhara, H. N. Patel, B. K. DOI: 10.1039/D3OB09E.

[17] (a) Liu, Y.; Wang, B.; Qiao, X.; Tung C.-H.; Wang, Y. *ACS Catal*. **2017**, *7*, 4093–4099. (b) Su, Y.; Zhang L.; Jiao, N. *Org*. *Lett*. **2011**, *13*, 2168–2171.

[18] (a) Lv, Y.; Luo, J.; Lin, M.; Yue, H.; Daia B.; He, L. A. *Org*. *Chem*. *Front*. **2021**, *8*, 5403–5409. (b) Gadde, K.; Mampuys, P.; Guidetti, A.; Ching, H. Y. V.; Herrebout, W. A.; Doorslaer, S. V.; Tehrani K. A.; Maes, B. U. W. *ACS*. *Catal*. **2020**, *10*, 8765–8779.

[19] (a) Pavlishchuka, V. V.; Addison, A. W.; *Inorg*. *Chim*. *Acta*. **2000**, *298*, 97–102. (b) Larsen, A. G.; Holm, A. H.; Roberson M.; Daasbjerg, K. *J*. *Am*. *Chem*. *Soc*. **2001**, *123*, 1723–1729. (c) Zalesskiy, S. S.; Shlapakov, N. S.; Ananikov, V. P. *Chem*. *Sci*. **2016**, ***7***, 6740–6745. (d) Wei, W.; Bao, P.; Yue, H.; Liu, S.; Wang, L.; Li, Y.; Yang, D. *Org*. *Lett*. **2018**, *20*, 5291–5295. (e) Rahaman, R.; Das S.; Barman, P. *Green. Chem*. **2018**, *20*, 141–147. (f) Liang, G.; Wang, J.-H.; Lei, T.; Cheng, Y.-Y.; Zhou, C.; Chen, Y.-J.; Ye, C. Chen, B.; Tung C-H.; Wu, L-Z. *Org*. *Lett*. **2021**, *23*, 8082–8087. (g) Nair, A. M.; Kumar S.; Volla, C. M. R. *Adv*. *Synth*. *Catal*. **2019**, *361*, 4983–4988. (h) Lynch, D. M.; Scanlan, E. M. *Molecules* **2020**, *25*, 3094–3133.

[20] Dar, A. A.; Enjamuri, N.; Shadab, Md.; Ali N.; Khan, A. T. *ACS Comb*. *Sci*. **2015**, *17*, 671–681.

[21] Ghosh, S.; Pal, S.; Rajamanickam, S.; Shome, R.; Mohanta, P. R.; Ghosh S. S.; Patel, B. K. *ACS Omega.* **2019**, *4*, 5565–5577.

[22] (a) Hall J. H.; Gisler, M. A.; *J*. *Org*. *Chem*. **1976**, *41*, 3769–3770. (b) Alport, A. C.; Edin, M. D.; Cairo, P. G. M. D.; Cairo, G. H. M. B. *The Lancet* **1938**, *24*, 1460–1463.

IV.6. Spectral Data

***4,6-Diphenyl-2-(phenylthio)nicotinonitrile* (*1a*):**

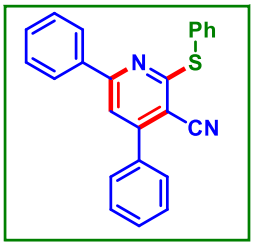

As a white solid (71 mg, 78% yield); mp 170–172 °C; purified over a column of silica gel $R_f = 0.2$, (2% EtOAc in hexane); ^{1}H NMR ($CDCl_3$, 500 MHz) δ 7.75 (d, 2H, J = 7.0 Hz), 7.30 (t, 2H, J = 5.0 Hz), 7.65 (d, 2H, J = 6.0 Hz), 7.56 (d, 4H, J = 7.5 Hz), 7.51 (d, 3H, J = 5.0 Hz), 7.40 (t, 1H, J = 7.0 Hz). 7.35 (t, 2H, J = 7.5 Hz); ^{13}C{^{1}H} NMR ($CDCl_3$, 125 MHz): δ 164.3, 158.4, 155.0, 137.0, 136.4, 136.2, 130.7, 130.2, 129.6, 129.3, 129.2, 129.0, 128.9, 128.6, 127.4, 116.1, 116.0, 103.3; IR (KBr, cm^{-1}): 3044, 2925, 2216, 1434, 1247, 1038; HRMS (ESI/Q-TOF) (m/z): calcd for $C_{24}H_{17}N_2S$, $[M + H]^+$: 365.1107, found 365.1107.

***4-Phenyl-2-(phenylthio)-6-(p-tolyl)nicotinonitrile* (*2a*):**

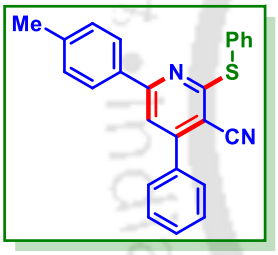

As a white solid $R_f = 0.2$, (71 mg, 75% yield); mp 198–200 °C; purified over a column of silica gel (2% EtOAc in hexane); ^{1}H NMR ($CDCl_3$, 500 MHz): δ 7.69 (t, 2H, J = 5.0 Hz), 7.64 (d, 4H, J = 8.0 Hz), 7.54 (d, 3H, J = 6.0 Hz), 7.52–7.47 (m, 4H), 7.16 (d, 2H, J = 8.0 Hz), 2.36 (s, 3H); ^{13}C{^{1}H} NMR ($CDCl_3$, 125 MHz): δ 164.1, 158.5, 154.8, 141.2, 136. 5, 136.2, 134.3, 130.2, 129.7, 129.6, 129.3, 129.2, 129.0, 128.6, 127.3, 116.1, 115.8, 102.9, 21.5; IR (KBr, cm^{-1}): 3075, 2912, 2219, 1435, 1234, 1057; HRMS (ESI/Q-TOF) (m/z): calcd for $C_{25}H_{19}N_2S$ $[M + H]^+$: 379.1263, found 379.1257.

***6-(4-Methoxyphenyl)-4-phenyl-2-(phenylthio)nicotinonitrile* (*3a*):**

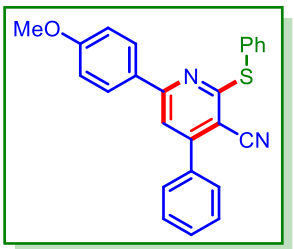

As a white solid (77 mg, 78% yield); mp 188-190 °C; $R_f = 0.2$, purified over a column of silica gel, (2% EtOAc in hexane); ^{1}H NMR ($CDCl_3$, 500 MHz): δ 7.69 (d, 4H, J = 9.0 Hz), 7.63 (t, 2H, J = 2.0 Hz), 7.56–7.48 (m, 6H), 7.48 (s, 1H), 6.85 (d, 2H, J = 8.5 Hz), 3.82 (s, 3H); ^{13}C{^{1}H} NMR ($CDCl_3$, 125 MHz): δ 164.0, 161.9, 158.1, 154.6, 136.6, 136.2, 130.1, 129.5, 129.3, 129.2, 129.1, 129.0, 128.6, 128.5, 116.2, 115.2, 114.3, 102.3, 55.5; IR (KBr, cm^{-1}): 3025,

2828, 2218, 1455, 1035; HRMS (ESI/Q-TOF) (m/z): calcd for $C_{25}H_{19}N_2OS$, $[M + H]^+$: 395.1213, found 395.1218.

***6-(4-Fluorophenyl)-4-phenyl-2-(phenylthio)nicotinonitrile* (*4a*):**

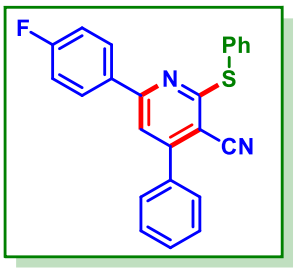

As a white solid (68 mg, 71% yield); mp 215–217 °C; $R_f = 0.2$, purified over a column of silica gel (2% EtOAc in hexane); ^{1}H NMR ($CDCl_3$, 500 MHz): δ 7.72 (t, 2H, J = 7.5 Hz), 7.68 (d, 2H, J = 7.5 Hz), 7.63 (d, 2H, J = 5.0 Hz), 7.55 (d, 3H, J = 5.5 Hz), 7.50 (d, 4H, J = 8.0 HZ), 7.02 (t, 2H, J = 8.5 Hz); ^{13}C{^{1}H} NMR ($CDCl_3$, 100 MHz): δ 164.5 (d, J = 249.8 Hz), 164.47, 157.3, 155.0, 136.3, 133.2 (d, J = 3.3 Hz), 130.3, 129.7, 129.4, 129.3, 128. 9, 128.6, 127.8, 127.4, 116.0 (d, J = 21.3 Hz), 115.9, 115.7, 103.2; ^{19}F NMR ($CDCl_3$, 471 MHz) δ –110.3; IR (KBr, cm^{-1}): 3063, 2912, 2824, 2212, 1468, 1264, 1080; HRMS (ESI/Q-TOF) (m/z): calcd for $C_{24}H_{16}FN_2S$, $[M + H]^+$: 383.1013, found 383.1019.

***6-(4-Chlorophenyl)-4-phenyl-2-(phenylthio)nicotinonitrile (5a)*:**

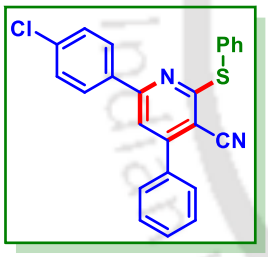

As a white solid (74 mg, 74% yield); mp 196-198 °C $R_f = 0.2$, Purification over a column of silica gel (2% EtOAc in hexane). ^{1}H NMR ($CDCl_3$, 500 MHz): δ 7.75 (d, 2H, J = 7.0 Hz), 7.70 (dd, 2H, J_1 = 6.5 Hz, J_2 = 1.5 Hz), 7.65 (dd, 2H, J_1 = 8.0 Hz, J_2 = 2.5 Hz), 7.55 (t, 3H, J = 7.5 Hz), 7.51–7.48 (m, 3H), 7.43 (t, 1H, J = 7.0 Hz), 7.35 (t, 2H J = 7.3 Hz); ^{13}C{^{1}H} NMR ($CDCl_3$, 125 MHz): δ 164.3, 158.4, 154. 9, 137.0, 136.4, 136.2, 130.7, 130.2, 129.6, 129.3, 129.2, 129.0, 128.9, 128.6, 127.4, 116.1, 116.0, 103.3; IR (KBr, cm^{-1}): 3062, 2928, 2822, 2221, 1469, 1065; HRMS (ESI/Q-TOF) (m/z) calcd for $C_{24}H_{16}ClN_2S$ $[M + H]^+$ 399.0717, found 399.0716.

***6-Phenyl-2-(phenylthio)-4-(p-tolyl)nicotinonitrile* (*6a*):**

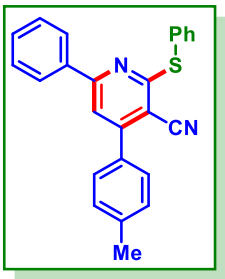

As a white solid (70 mg, 74% yield); mp 196–198 °C; $R_f = 0.2$, purified over a column of silica gel (2% EtOAc in hexane); ^{1}H NMR ($CDCl_3$, 500 MHz): δ 7.75 (d, 2H, J = 7.5 Hz), 7.71–7.69 (m, 2H), 7.56 (d, 3H, J = 8.0 Hz), 7.51–7.49 (m, 3H), 7.40 (t, 1H, J = 7.0 Hz), 7.35 (t, 4H, J = 7.0 Hz), 2.46 (s, 3H); ^{13}C{^{1}H} NMR ($CDCl_3$, 125

MHz): δ 164.1, 158.3, 154.9, 140.5, 137.1, 136.2, 133.5, 130.6, 129.9, 129.6, 129.3, 129.0, 128.9, 128.5, 127.3, 116.1, 116.0, 103.2, 21.5; IR (KBr, cm^{-1}): 3069, 2979, 2219, 1494, 1092; HRMS (ESI/Q-TOF) (m/z): calcd for $C_{25}H_{19}N_2S$, $[M + H]^+$: 379.1263, found 379.1257.

***4-(4-Methoxyphenyl)-6-phenyl-2-(phenylthio)nicotinonitrile* (*7a*):**

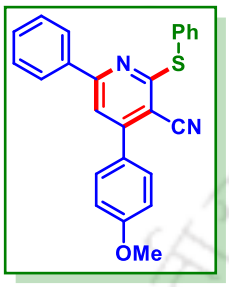

As a white solid (75 mg, 76% yield); mp 189–191 °C; $R_f = 0.2$, purified over a column of silica gel (2% EtOAc in hexane); ^1H NMR ($CDCl_3$, 500 MHz): δ 7.74 (d, 2H, J = 7.0 Hz), 7.69 (dd, 2H, J_1 = 6.5 Hz, J_2 = 2.0 Hz), 7.62 (d, 2H, J = 9.0 Hz), 7.53 (s, 1H), 7.50 (dd, 3H, J_1 = 5.0 Hz, J_2 = 1.8 Hz), 7.38 (d, 1H, J = 7.0 Hz), 7.34 (t, 2H, J = 8.0 Hz), 7.06 (d, 2H, J = 8.5 Hz), 3.89 (s, 3H); $^{13}C\{^1H\}$ NMR ($CDCl_3$, 125 MHz): δ 164.0, 161.9, 158.1, 154.6, 136.6, 136.2, 130.1, 129.6, 129.5, 129.3, 129.2, 129.1, 129.0, 128.5, 116.1, 115.2, 114.3, 102.4, 55.6; IR (KBr, cm^{-1}): 3061, 2937, 2844, 2229, 1468, 1075; HRMS (ESI/Q-TOF) (m/z): calcd for $C_{25}H_{19}N_2OS$, $[M + H]^+$: 395.1213, found 395.1219.

***4-(4-(Dimethylamino)phenyl)-6-phenyl-2-(phenylthio)nicotinonitrile* (*8a*):**

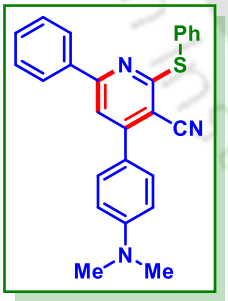

As a brownish gummy (70 mg, 69% yield); $R_f = 0.2$, purified over a column of silica gel (2% EtOAc in hexane); ^1H NMR ($CDCl_3$, 500 MHz): δ 7.74 (d, 2H, J = 6.5 Hz), 7.69 (dd, 2H, J_1 = 5.5 Hz, J_2 = 2.5 Hz), 7.62 (d, 2H, J = 9.0 Hz), 7.53 (s, 1H), 7.49-7.48 (m, 3H), 7.39–7.32 (m, 3H), 6.82 (d, 2H, J = 9.0 Hz), 3.05 (s, 6H); $^{13}C\{^1H\}$ NMR ($CDCl_3$, 125 MHz): δ 164.1, 157.9, 154.8, 151.7, 137.4, 136.1, 130.4, 129.8, 129.4, 129.3, 129.2, 128.9, 127.3, 123.2, 116.9, 115.5, 112.2, 102.4, 40.4; IR (KBr, cm^{-1}): 3053, 2961, 2844, 2220, 1411, 1068; HRMS (ESI/Q-TOF) (m/z): calcd for $C_{26}H_{22}N_3S$ $[M + H]^+$: 408.1529, found 408.1533.

***4-(4-Fluorophenyl)-6-phenyl-2-(phenylthio)nicotinonitrile* (*9a*):**

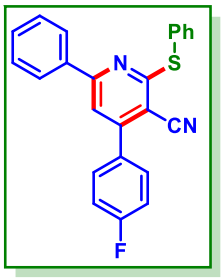

As a yellow solid (68 mg, 71% yield); mp 216–218 °C; R_f = 0.2, Purification over a column of silica gel (2% EtOAc in hexane). ^{1}H NMR ($CDCl_3$, 500 MHz): δ 7.76 (d, 2H, J = 7.5 Hz), 7.72 (dd, 2H, J_1 = 6.5 Hz, J_2 = 1.5 Hz), 7.68–7.65 (m, 2H), 7.55–7.52 (m, 4H), 7.43 (t, 1H, J = 7.5 Hz), 7.38 (t, 2H, J = 7.5 Hz), 7.29 (d, 2H, J = 8.0 Hz); ^{13}C{^{1}H} NMR ($CDCl_3$, 125 MHz): δ 164.5, 164.1 (d, J = 249.5 Hz), 158.5, 154.9, 153.8, 136.9, 136.2, 130.8, 130.7 (d, J = 8.5 Hz), 129.7, 129.4, 129.3, 129.0, 127.7, 127.4, 116.5 (d, J = 21.7 Hz), 116.0, 103.2; ^{19}F NMR ($CDCl_3$, 471 MHz) δ –110.3 IR (KBr, cm^{-1}): 3069, 2927, 2834, 2205, 1458, 1235, 1025; HRMS (ESI/Q-TOF) (m/z): calcd for $C_{24}H_{16}FN_2S$, [M + H]$^+$: 383.1013, found 383.1019.

***4-(4-Chlorophenyl)-6-phenyl-2-(phenylthio)nicotinonitrile* (*10a*):**

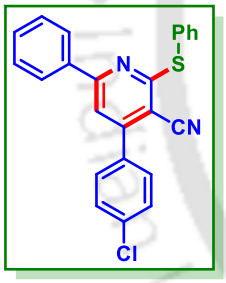

As a white solid (71 mg, 71% yield); mp 195–197 °C; R_f = 0.2, purified over a column of silica gel (2% EtOAc in hexane); ^{1}H NMR ($CDCl_3$, 500 MHz): δ 7.73 (d, 2H, J = 7.5 Hz), 7.68 (d, 2H, J = 6.0 Hz), 7.58 (d, 2H, J = 8.5 Hz), 7.52 (t, 6H, J = 11.5 Hz), 7.40 (t, 1H, J = 7.5 Hz), 7.35 (d, 2H, J = 7.5 Hz); ^{13}C{^{1}H} NMR ($CDCl_3$, 125 MHz): δ 164.6, 158.6, 153.6, 136.9, 136.7, 136.3, 134.8, 130.9, 130.0, 129.7, 129.6, 129.4, 129.0, 128.9, 127.7, 127.4, 115.8, 103.1; IR (KBr, cm^{-1}): 3064, 3045, 2841, 2219, 1146, 1090; HRMS (ESI/Q-TOF) (m/z): calcd for $C_{24}H_{16}ClN_2S$, [M + H]$^+$: 399.0717, found 399.0712

***4-(Furan-2-yl)-2-(phenylthio)-6-(p-tolyl)nicotinonitrile* (*11a*):**

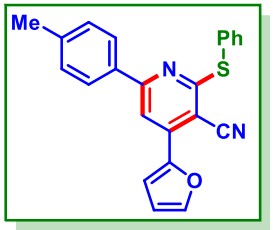

As a white solid (67 mg, 72% yield); mp 134–136 °C; R_f = 0.2, purified over a column of silica gel (2% EtOAc in hexane); ^{1}H NMR ($CDCl_3$, 500 MHz): δ 7.89 (s, 1H), 7.66 (d, 4H, J = 9.0 Hz), 7.62 (t, 2H, J = 4.5 Hz), 7.48 (d, 3H, J = 6.5 Hz), 7.15 (d, 2H, J = 8.0 Hz), 6.64 (d, 1H, J = 1.5 Hz), 2.36 (s, 3H); ^{13}C{^{1}H} NMR ($CDCl_3$, 125 MHz): δ 164.4, 158.5, 148.3, 144.9, 141.3, 141.1, 136.2, 134.3,

129.7, 129.5, 129.2, 129.0, 127.3, 116.7, 114.3, 113.1, 110.6, 97.4, 21.5; IR (KBr, cm^{-1}): 3059, 2945, 2810, 2210, 1545, 1254, 1175, 1065; HRMS (ESI/Q-TOF) (m/z): calcd for $C_{23}H_{17}N_2OS$, $[M + H]^+$: 369.1056 found 369.1060.

***4,6-Di(furan-2-yl)-2-(phenylthio)nicotinonitrile* (*12a*):**

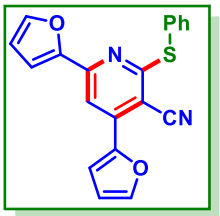

As a white solid (60 mg, 69% yield); mp 136–138 °C; $R_f = 0.2$, purified over a column of silica gel (2% EtOAc in hexane); ^1H NMR ($CDCl_3$, 500 MHz): δ 7.80 (s, 1H), 7.65–7.62 (m, 3H), 7.61 (d, 1H, J = 3.5 Hz), 7.51 (s, 1H), 7.48 (dd, 3H, J_1 = 5.0 Hz, J_2 = 1.5 Hz), 6.63 (dd, 1H, J_1 = 3.5 Hz, J_2 = 2.0 Hz,), 6.58 (d, 1H, J = 3.0 Hz,), 6.44 (dd, 1H, J_1 = 3.5 Hz, J_2 = 2.0 Hz); $^{13}C\{^1H\}$ NMR ($CDCl_3$, 125 MHz): δ 164.6, 152.7, 150.5, 148.2, 145.2, 145.0, 141.4, 136.1, 129.6, 129.2, 128.8, 116.6, 114.5, 113.1, 112.8, 112.6, 109.1, 97.0; IR (KBr, cm^{-1}): 3069, 2937, 2824, 2215, 1576, 1177, 1067; HRMS (ESI/Q-TOF) (m/z): calcd for $C_{20}H_{13}N_2O_2S$, $[M + H]^+$: 345.0692 found 345.0698.

***4-(Naphthalen-1-yl)-6-phenyl-2-(phenylthio)nicotinonitrile* (*13a*):**

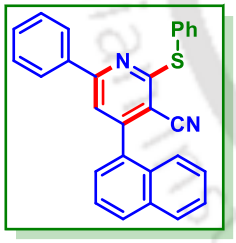

As a white solid (83 mg, 79% yield); mp 210–212 °C; $R_f = 0.2$, purified over a column of silica gel (2% EtOAc in hexane); ^1H NMR ($CDCl_3$, 500 MHz): δ 8.04 (d, 1H, J = 8.0 Hz), 8.00 (d, 1H, J = 8.5 Hz), 7.81–7.75 (m, 4H), 7.70 (d, 1H, J = 8.5 Hz), 7.64 (t, 2H, J = 6.5 Hz), 7.60–7.52 (m, 6H), 7.42 (t, 1H, J = 7.5 Hz), 7.37 (t, 2H, J = 7.4 Hz); $^{13}C\{^1H\}$ NMR ($CDCl_3$, 125 MHz): δ 163.8, 157.9, 154.3, 136.8, 136.2, 134.0, 133.8, 130.7, 130.70, 130.2, 129.7, 129.3, 128.9, 128.86, 128.7, 127.4, 127.3, 127.2, 126.6, 125.3, 124.8, 117.7, 115.3, 105.5; IR (KBr, cm^{-1}): 3059, 2917, 2840, 2219, 1556, 1067; HRMS (ESI/Q-TOF) (m/z): calcd for $C_{28}H_{19}N_2S$, $[M + H]^+$: 415.1263, found 415.1266.

***4-(Naphthalen-1-yl)-6-(naphthalen-2-yl)-2-(phenylthio)nicotinonitrile* (*14a*):**

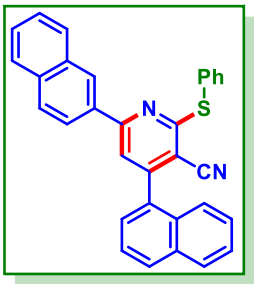

As a white solid (94 mg, 81% yield); mp 178–180 °C; R_f = 0.2, purified over a column of silica gel (2% EtOAc in hexane); ^{1}H NMR ($CDCl_3$, 500 MHz): δ 8.27 (s, 1H), 8.04 (d, 1H, *J* = 8.0 Hz), 8.00 (d, 1H, *J* = 8.0 Hz), 7.84 (q, 3H, *J* = 7.5 Hz), 7.82 (t, 2H, *J* = 4.0 Hz), 7.78 (t, 2H, *J* = 7.5 Hz), 7.73 (d, 1H, *J* = 8.0 Hz), 7.65 (t, 3H, *J* = 7.5 Hz), 7.63 (d, 1H, *J* = 2.0 Hz), 7.60 (t, 2H, *J* = 9.5 Hz), 7.56 (d, 1H, *J* = 8.0 Hz), 7.53–7.49 (m, 2H); ^{13}C{^{1}H} NMR ($CDCl_3$, 125 MHz): δ 164.0, 157.7, 154.4, 136.5, 134.5, 134.1, 134.0, 133.9, 133.3, 130.8, 130.3, 129.8, 129.4, 129.1, 128.9, 128.8, 128.6, 128.0, 127.8, 127.6, 127.3, 127.28, 126.7, 126.69, 125.4, 124.9, 123.9, 117.7, 115.4, 105.4; IR (KBr, cm^{-1}): 3069, 2954, 2210, 1546, 1479, 1085; HRMS (ESI/Q-TOF) (m/z): calcd for $C_{32}H_{21}N_2S$, $[M + H]^+$: 465.1420, found 465.1418.

***4,6-Diphenyl-2-(p-tolylthio)nicotinonitrile* (*1b*):**

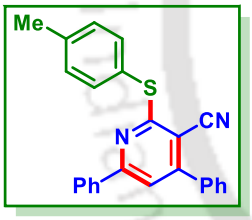

As a white solid (69 mg, 73% yield); mp197–199 °C; R_f = 0.2, purified over a column of silica gel (2% EtOAc in hexane); ^{1}H NMR ($CDCl_3$, 500 MHz): δ 7.78 (d, 2H, *J* = 7.5 Hz), 7.68 (d, 2H, *J* = 7.5 Hz), 7.63 (d, 2H, *J* = 5.0 Hz), 7.55 (d, 3H, *J* = 5.5 Hz), 7.50 (d, 4H, *J* = 8.0 Hz), 7.02 (t, 2H, *J* = 8.5 Hz), 2.47 (s, 3H); ^{13}C{^{1}H} NMR ($CDCl_3$, 125 MHz): δ 164.6, 158.4, 154.9, 145.1, 139.9, 137.1, 136.5, 136.1, 133.0, 130.1 129.2, 129.0, 128.6, 127.4, 125.3, 122.3, 116.1, 103.2, 21.6; IR (KBr, cm^{-1}): 3084, 2910, 2867, 2219, 1264, 1051; HRMS (ESI/Q-TOF) (m/z): calcd for $C_{25}H_{19}N_2S$, $[M + H]^+$: 379.1263, found 379.1268.

***4,6-Diphenyl-2-(o-tolylthio)nicotinonitrile* (*1c*):**

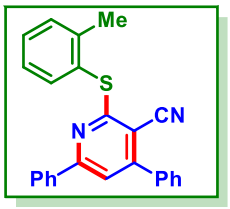

As a white solid (63 mg, 67% yield); mp 196–198 °C; R_f = 0.2, purified over a column of silica gel (2% EtOAc in hexane); ^{1}H NMR ($CDCl_3$, 500 MHz): δ 7.70 (q, 5H, *J* = 8.0 Hz), 7.57 (d, 4H, *J* = 6.5 Hz), 7.47 (t, 2H, *J* = 7.5 Hz), 7.39 (d, 1H, *J* = 6.5 Hz), 7.34 (q, 3H, J

= 8.0 Hz), 2.49 (s, 3H); $^{13}C\{^{1}H\}$ NMR ($CDCl_3$, 125 MHz): δ 163.9, 158.2, 154.7, 143.8, 137.2, 136.8, 136.4, 130.7, 130.6, 130.3, 130.2, 129.1, 128.9, 128.5, 128.3, 127.2, 126.8, 116.1, 115.6, 103.1, 21.1; IR (KBr, cm^{-1}): 3049, 2926, 2854, 2229, 1049; HRMS (ESI/Q-TOF) (m/z): calcd for $C_{25}H_{19}N_2S$, $[M + H]^+$: 379.1263, found 379.1257.

***2-((4-Methoxyphenyl)thio)-4,6-diphenylnicotinonitrile* (*1d*):**

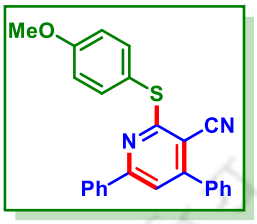

As a white solid (73 mg, 74% yield); mp 200–202 °C; R_f = 0.2, purified over a column of silica gel (2% EtOAc in hexane); ^{1}H NMR ($CDCl_3$, 500 MHz): δ 7.78 (d, 2H, J = 7.0 Hz), 7.64 (d, 2H, J = 8.5 Hz), 7.61 (d, 2H, J = 8.5 Hz), 7.55 (d, 4H, J = 4.5 Hz), 7.41–7.34 (m, 3H), 7.04 (d, 2H, J = 8.5 Hz), 3.90 (s, 3H); $^{13}C\{^{1}H\}$ NMR ($CDCl_3$, 125 MHz): δ 165.0, 161.1, 158.4, 154.8, 137.9, 137.1, 136.5, 130.7, 130.2, 129.2, 128.9, 128.6, 127.4, 119.4, 116.1, 116.0, 114.9, 103.0, 55.7; IR (KBr, cm^{-1}): 3056, 2965, 2827, 2211, 1062; HRMS (ESI/Q-TOF) (m/z): calcd for $C_{25}H_{19}N_2OS$, $[M + H]^+$: 395.1213, found 395.1218.

***2-((3-Methoxyphenyl)thio)-4,6-diphenylnicotinonitrile* (*1e*):**

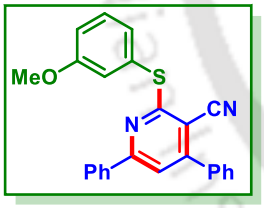

As a brown solid (68 mg, 69% yield); mp 194–196 °C; R_f = 0.2, purified over a column of silica gel (2% EtOAc in hexane); ^{1}H NMR ($CDCl_3$, 500 MHz): δ 7.80 (d, 2H, J = 7.0 Hz), 7.65 (dd, 2H, J_1 = 8.0 Hz, J_2 = 2.0 Hz), 7.57 (s, 1H), 7.55 (t, 2H, J = 6.0 Hz), 7.42–7.35 (m, 5H), 7.30–7.26 (m, 2H), 7.06 (dd, 1H, J_1 = 8.5 Hz, J_2 = 2.5 Hz), 3.84 (s, 3H); $^{13}C\{^{1}H\}$ NMR ($CDCl_3$, 125 MHz): δ 164.0, 160.1, 158.5, 154.9, 137.0, 136.4, 130.8, 130.3, 130.0, 129.8, 129.2, 129.0, 128.6, 128.3, 127.4, 120.9, 116.2, 116.0, 115.96, 103.4, 55.7; IR (KBr, cm^{-1}): 3059, 2910, 2834, 2210, 1089; HRMS (ESI/Q-TOF) (m/z): calcd for $C_{25}H_{19}N_2OS$, $[M + H]^+$: 395.1213, found 395.1220.

***2-((4-Fluorophenyl)thio)-4,6-diphenylnicotinonitrile* (*1f*):**

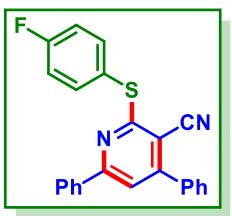

As a white solid (69 mg, 72% yield); mp 216–218 °C; R_f = 0.2, purified over a column of silica gel (2% EtOAc in hexane); ^{1}H NMR ($CDCl_3$, 500 MHz): δ 7.75 (d, 2H, J = 7.0 Hz), 7.68 (d, 1H, J

= 5.5 Hz), 7.66–7.63 (m, 3H), 7.56–7.54 (m, 4H), 7.43–7.36 (m, 3H), 7.21 (t, 2H, *J* = 9.0 Hz).; $^{13}C\{^{1}H\}$ NMR ($CDCl_3$, 125 MHz): δ 164.0, 163.9 (d, *J* = 248 Hz), 162.9, 158.5, 154.9, 138.4 (d, *J* = 8.5 Hz), 136.9, 136.3, 130.8, 130.3, 129.3, 129.0, 128.6, 127.3, 116.6, 116.4 (d *J* = 18.3 Hz), 115.9, 103.2; ^{19}F NMR ($CDCl_3$, 471 MHz) δ –111.0; IR (KBr, cm^{-1}): 3055, 2935, 2845, 2215, 1476, 1063; MS (ESI/Q-TOF) (m/z): calcd for $C_{24}H_{16}FN_2S$, $[M + H]^+$: 383.1013, found 383.1020.

***2-((4-Chlorophenyl)thio)-4,6-diphenylnicotinonitrile* (*1g*):**

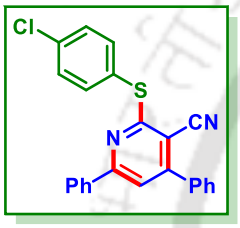

As a white solid (68 mg, 69% yield); mp 194–196 °C; R_f = 0.2, purified over a column of silica gel (18% EtOAc in hexane); ^{1}H NMR ($CDCl_3$, 500 MHz): δ 7.76 (d, 2H, *J* = 7.5 Hz), 7.64 (dd, 4H, J_1 = 10.5 HZ, J_2 = 3.0 HZ), 7.56 (t, 4H, *J* = 8.0 Hz), 7.48 (d, 2H, *J* = 8.5 Hz), 7.44–7.37 (m, 3H); $^{13}C\{^{1}H\}$ NMR ($CDCl_3$, 125 MHz): δ 163.6, 158.6, 155.0, 145.1, 137.4, 133.0, 130.9, 130.3, 129.5, 129.3, 129.1, 128.8, 128.6, 127.3, 122.3, 116.4, 115.8, 103.4; IR (KBr, cm^{-1}): 3066, 2947, 2849, 2219, 1167, 1065; HRMS (ESI/Q-TOF) (m/z): calcd for $C_{24}H_{16}ClN_2S$, $[M + H]^+$: 399.0717, found 399.0716.

***2-((3-Chlorophenyl)thio)-5-phenyl-1H-pyrrole-3-carbonitrile* (*1h*):**

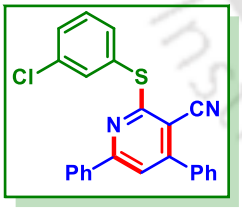

As a white solid (58 mg, 59% yield); mp 199–201 °C; R_f–0.2, purified over a column of silica gel (2% EtOAc in hexane); ^{1}H NMR ($CDCl_3$, 500 MHz): δ 7.80 (d, 2H, *J* = 7.0 Hz), 7.76 (s, 1H), 7.64 (dd, 2H, J_1 = 7.5 Hz, J_2 = 2.5 Hz), 7.60 (s, 1H), 7.56 (t, 4H, *J* = 8.0 Hz), 7.49 (d, 1H, *J* = 8.5 Hz), 7.44–7.37 (m, 4H); $^{13}C\{^{1}H\}$ NMR ($CDCl_3$, 125 MHz): δ 163.1, 158.6, 155.1, 136.9, 136.3, 135.9, 134.7, 133.9, 130.9, 130.7, 130.4, 130.3, 129.8, 129.3, 129.1, 128.6, 127.4, 116.6, 115.8, 103.5; IR (KBr, cm^{-1}): 3064, 2812, 2211, 1547, 1401, 1146, 1076; HRMS (ESI/Q-TOF) (m/z): calcd for $C_{24}H_{16}ClN_2S$, $[M + H]^+$ 399.0717, found 399.0712.

***2-((2-Bromophenyl)thio)-4,6-diphenylnicotinonitrile* (*1i*):**

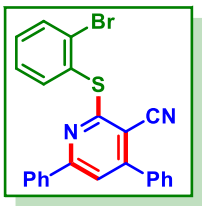

As a white solid (64 mg, 58% yield); mp 165–167 °C; R_f = 0.2, purified over a column of silica gel (2% EtOAc in hexane); ^{1}H NMR ($CDCl_3$, 500 MHz): δ 7.82 (d, 1H, J = 8.0 Hz), 7.78 (dd, 1H, J_1 = 7.5 Hz, J_2 = 1.0 Hz), 7.71 (d, 2H, J = 7.5 Hz), 7.66 (t, 2H, J = 5.5 Hz), 7.56 (t, 4H, J = 7.5 Hz), 7.43 (t, 1H, J = 6.5 Hz), 7.39 (d, 2H, J = 6.5 Hz), 7.37–7.33 (m, 2H); ^{13}C{^{1}H} NMR ($CDCl_3$, 125 MHz): δ 162.9, 158.5, 154.9, 138.3, 137.0, 136.3, 133.7, 131.6, 131.4, 130.8, 130.7, 130.3, 129.2, 129.0, 128.6, 128.2, 127.4, 116.3, 115.9, 103.4; IR (KBr, cm^{-1}): 3068, 2932, 2849, 2205, 1148, 1071; HRMS (ESI/Q-TOF) (m/z): calcd for $C_{24}H_{16}BrN_2S$, $[M + H]^+$: 443.0212, found 443.0215.

***4,6-Diphenyl-2-((4-(trifluoromethyl)phenyl)thio)nicotinonitrile* (*1j*):**

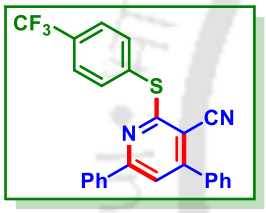

As a white solid (64 mg, 59% yield); mp 218–220 °C; R_f = 0.2, purified over a column of silica gel (2% EtOAc in hexane); ^{1}H NMR ($CDCl_3$, 500 MHz): δ 7.82 (d, 2H, J = 8.0 Hz), 7.76 (d, 2H, J = 8.0 Hz), 7.69 (d, 2H, J = 7.5 Hz), 7.65 (t, 2H, J = 3.5 Hz), 7.60 (s, 1H), 7.56 (d, 3H, J = 5.0 Hz), 7.41 (d, 1H, J = 7.0 Hz), 7.36 (t, 2H, J = 7.5 Hz); ^{13}C{^{1}H} NMR ($CDCl_3$, 125 MHz): δ 163.0, 158.6, 155.1, 136.7, 136.2, 133.9, 131.7, 131.5, 131.0, 130.4, 129.3, 129.0, 128.6, 127.3, 126.1 (q, J = 3.6 Hz), 116.6, 115.7, 103.7; ^{19}F NMR ($CDCl_3$, 471 MHz): δ –62.8; IR (KBr, cm^{-1}): 3053, 2919, 2853, 2208, 1448, 1037; HRMS (ESI/Q-TOF) (m/z): calcd for $C_{25}H_{16}F_3N_2S$, $[M + H]^+$: 433.0981, found 433.0984.

***2-(Naphthalen-2-ylthio)-4,6-diphenylnicotinonitrile* (*1k*):**

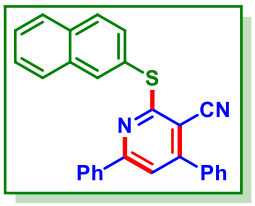

As a white solid (71 mg, 72% yield); mp 225–227 °C; R_f = 0.2, purified over a column of silica gel (2% EtOAc in hexane); ^{1}H NMR ($CDCl_3$, 400 MHz): δ 8.22 (s, 1H), 7.93 (t, 2H, J = 8.4 Hz), 7.88 (d, 1H, J = 7.8 Hz), 7.72–7.70 (m, 2H), 7.67–7.63 (m, 3H), 7.58–7.56 (m, 6H), 7.31 (t, 1H, J = 7.2 Hz), 7.23 (t, 2H, J = 8.0 Hz); ^{13}C{^{1}H} NMR ($CDCl_3$, 100 MHz): δ 164.2, 158.5, 154.9, 136.9, 136.4, 135.4, 133.9, 133.6, 132.6, 130.7, 130.3, 129.3, 128.9, 128.6, 128.2,

128.0, 127.4, 127.3, 126.7, 126.3, 116.3, 116.0, 103.4; IR (KBr, cm^{-1}): 3053, 2919, 2853, 2208, 1448, 1037; HRMS (ESI/Q-TOF) (m/z): calcd for $C_{28}H_{19}N_2S$, $[M + H]^+$: 415.1263, found 415.1263.

***4,6-Diphenyl-2-(thiophen-2-ylthio)nicotinonitrile* (*1l*):**

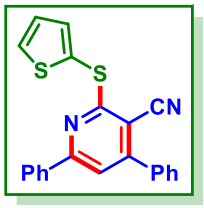

As a white solid (69 mg, 75% yield); mp 220–222 °C; $R_f = 0.2$, purified over a column of silica gel (2% EtOAc in hexane); ^1H NMR ($CDCl_3$, 500 MHz): δ 7.83 (d, 2H, J = 7.0 Hz), 7.69 (dd, 1H, J_1 = 5.5 Hz, J_2 = 1.0 Hz), 7.64-7.62 (m, 2H), 7.59 (s, 1H), 7.55 (dd, 3H, J_1 = 5.0 Hz, J_2 = 2.0 Hz), 7.43–7.37 (m, 4H), 7.21 (q, 1H, J = 3.5 Hz); $^{13}C\{^1H\}$ NMR ($CDCl_3$, 125 MHz): δ 164.0, 158.9, 154.9, 137.6, 136.9, 136.3, 132.9, 130.8, 130.3, 129.3, 129.0, 128.6, 128.0, 127.5, 125.9, 116.6, 115.7, 103.0; IR (KBr, cm^{-1}): 3053, 2919, 2853, 2208, 1448, 1037; HRMS (ESI/Q-TOF) (m/z): calcd for $C_{22}H_{15}N_2S_2$, $[M + H]^+$: 371.0671, found 371.0671.

***2-(Cyclohexylthio)-4,6-diphenylnicotinonitrile* (1m):**

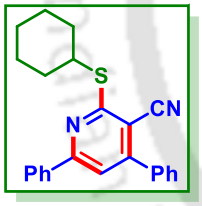

As a brown gummy (52 mg, 56% yield); $R_f = 0.2$, purified over a column of silica gel (2% EtOAc in hexane); ^1H NMR ($CDCl_3$, 500 MHz): δ 8.02 (dd, 1H, J_1 = 8.0 Hz, J_2 = 2.4 Hz), 7.87 (d, 1H, J = 7.6 Hz), 7.55–7.53 (m, 1H), 7.48–7.42 (m, 4H), 7.38 (t, 1H, J = 8.0 Hz), 7.23 (t, 1H, J = 7.2 Hz), 7.18 (d, 2H, J = 1.6 Hz), 3.23 (t, 1H, J = 7.6 Hz), 3.00 (t, 1H, J = 8.0 Hz), 2.15–2.12 (m, 1H), 1.81–1.77 (m, 1H), 1.63–1.57 (m, 1H), 1.54–1.43 (m, 5H), 1.37–1.26 (m, 1H); $^{13}C\{^1H\}$ NMR ($CDCl_3$, 125 MHz): δ 164.4, 158.3, 154.5, 141.3, 136.9, 133.1, 130.5, 128.5, 128.4, 128.1, 127.3, 126.1, 115.3, 103.7, 44.0, 40.5, 32.9, 25.8; IR (KBr, cm^{-1}): 3053, 2969, 2224, 1197, 1019, HRMS (ESI/Q-TOF) (m/z): calcd for $C_{24}H_{23}N_2S$, $[M + H]^+$: 371.1576, found 371.1574.

***1,3-Diphenylpropan-1-one* (*1'*):**

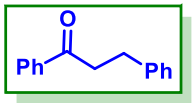

As a colorless gummy (22 mg, 42% yield); $R_f = 0.25$, purified over a column of silica gel (1% EtOAc in hexane); ^1H NMR ($CDCl_3$, 400 MHz): δ 8.03 (d, 2H, J = 7.6 Hz), 7.62 (t, 1H, J = 7.2

Hz), 7.52 (d, 2H, *J* = 7.6 Hz), 7.37 (t, 2H, *J* = 7.6 Hz), 7.33 (d, 2H, *J* = 6.0 Hz), 7.29 (d, 1H, *J* = 7.2 Hz), 3.37 (t, 2H, *J* = 7.2 Hz), 3.15 (t, 2H, *J* = 8.0 Hz); $^{13}C\{^{1}H\}$ NMR ($CDCl_3$, 100 MHz): δ 199.4, 141.5, 137.1, 132.2, 128.8, 128.7, 128.6, 128.2, 126.3, 40.6, 30.3; IR (KBr, cm^{-1}): 3053, 2919, 2853, 1705, 1448, 1037; HRMS (ESI/Q-TOF) (m/z): calcd for $C_{15}H_{15}O$, $[M + H]^+$: 211.1117, found 211.1110.

4,6-Diphenyl-2-(phenylsulfonyl)nicotinonitrile (***1aa***):

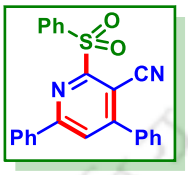

As a white solid (74 mg, 75% yield); mp 200–204 °C; R_f = 0.3, purified over a column of silica gel (8% EtOAc in hexane); ^{1}H NMR ($CDCl_3$, 500 MHz): δ 8.96 (s, 1H), 8.00 (d, 2H, *J* = 8.5 Hz), 7.82 (s, 1H), 7.65 (d, 2H, *J* = 7.5 Hz), 7.55 (d, 3H, *J* = 6.0 Hz), 7.47 (d, 2H, *J* = 7.5 Hz), 7.37 (d, 5H, *J* = 8.5 Hz); ^{13}C NMR ($CDCl_3$, 125 MHz,): δ 159.8, 154.2, 153.1, 140.9, 136.1, 135.5, 133.8, 132.9, 130.4, 129.7, 129.69, 129.4, 128.5, 128.3, 128.2, 120.0, 117.3, 106.7; IR (KBr, cm^{-1}): 3045, 2924, 2211, 1145, 1045; HRMS (ESI/Q-TOF) (m/z): calcd. for $C_{24}H_{17}N_2O_2S$, $[M + H]^+$: 397.1005, found 397.1020.

3-Cyano-2,6,7-triphenyl-4-(phenylthio)pyrido[2,1-a]isoquinolin-5-ium (***1ab***):

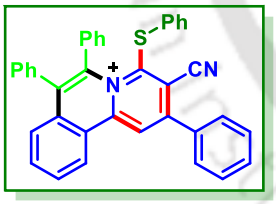

As a white solid (92 mg, 68% yield); mp 192–194 °C; R_f = 0.3, purified over a column of silica gel (2% methanol in DCM); ^{1}H NMR ($CDCl_3$, 500 MHz): δ 9.09 (s, 1H), 8.89 (d, 1H, *J* = 8.5 Hz), 8.84 (s, 1H), 8.29 (s, 1H), 7.99 (t, 1H, *J* = 8.0 Hz), 7.92 (t, 1H, *J* = 8.0 Hz), 7.81 (t, 2H, *J* = 3.5 Hz), 7.66 (d, 1H, *J* = 8.0 Hz), 7.56 (dd, 3H, J_1 = 4.5 Hz, J_2 = 1.5 Hz), 7.48 (d, 2H, *J* = 6.5 Hz), 7.43 (q, 4H, *J* = 6.0 Hz), 7.32 (d, 4H, *J* = 4.0 Hz), 7.26 (s, 1H), 7.21 (t, 2H, *J* = 3.0 Hz); $^{13}C\{^{1}H\}$ NMR ($CDCl_3$, 125 MHz): δ 166.2, 151.5, 143.1, 138.7, 136.9, 135.7, 135.3, 134.5, 134.0, 133.1, 131.4, 131.2, 131.0, 130.9, 130.3, 130.2, 130.0, 129.5, 129.1, 128.8, 128.7, 128.3, 125.5, 124.5, 123.1, 119.3; IR (KBr, cm^{-1}): 3054, 2931, 2205, 1196, 1090; HRMS (ESI/Q-TOF) (m/z): calcd for $C_{38}H_{26}N_2S$, $[M + H]^+$: 542.1811, found 542.1816.

***4,6-Diphenyl-2-(phenylthio)nicotinamide* (*1ac*):**

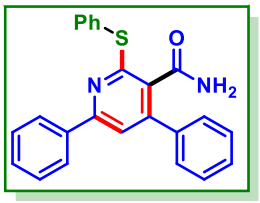

As a white solid (75 mg, 78% yield); mp 238–240 °C; $R_f = 0.25$, purified over a column of silica gel (20% EtOAc in hexane); ^{1}H NMR ($CDCl_3$ + DMSO-d_6, 500 MHz): δ 8.84 (s, 1H), 7.98 (d, 2H, J = 7.5 Hz), 7.66 (s, 1H), 7.48 (d, 2H, J = 7.5 Hz), 7.44–7.37 (m, 8H), 6.65 (d, 2H, J = 27.0 Hz), 2.87 (s, 2H); ^{13}C{^{1}H} NMR ($CDCl_3$ + DMSO-d_6, 125 MHz): δ 169.1, 157.9, 149.0, 148.9, 148.92, 148.8, 147.9, 138.0, 137.6, 129.1, 129.0, 128.5, 128.4, 128.3, 128.0, 127.6, 126.6, 120.7; IR (KBr, cm^{-1}): 3071, 2956, 2817, 1649, 1147, 1052; HRMS (ESI/Q-TOF) (m/z): calcd for $C_{24}H_{19}N_2OS$, $[M + H]^+$: 383.1213, found 383.1220.

IV.7. Representative Spectra

4,6-Diphenyl-2-(phenylthio)nicotinonitrile (1a) : ^{1}H NMR ($CDCl_3$, 500 MHz)

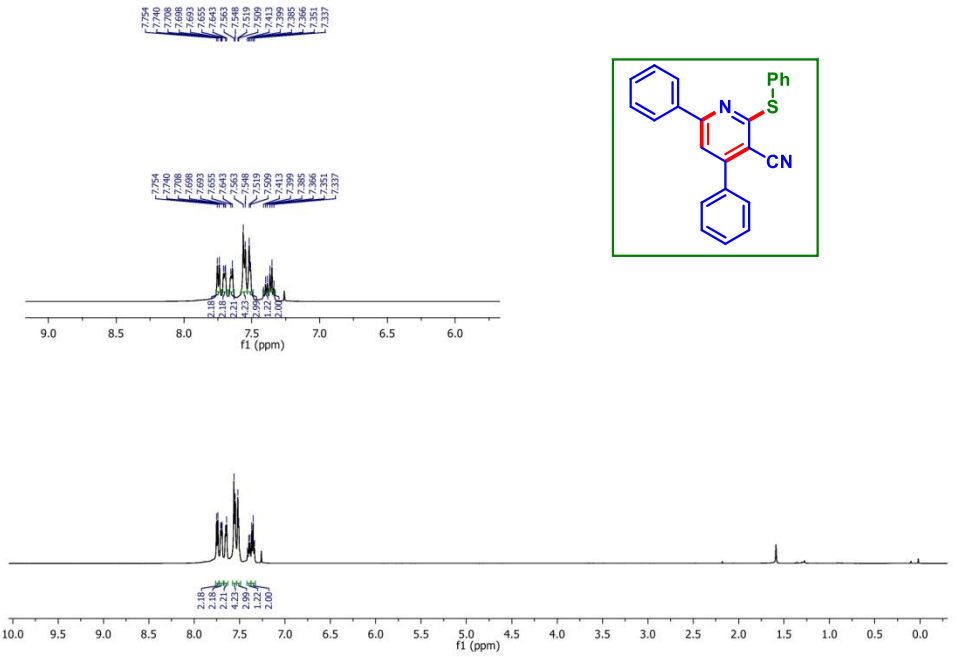

4,6-Diphenyl-2-(phenylthio)nicotinonitrile (1a): $^{13}C\{^{1}H\}$ NMR ($CDCl_3$, 125 MHz)

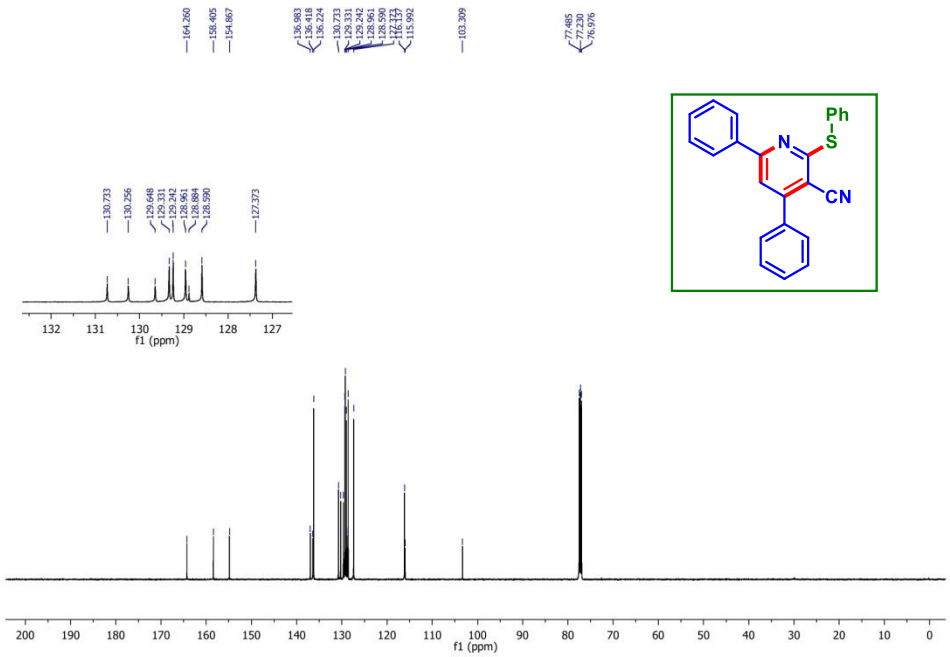

***4-(Naphthalen-1-yl)-6-(naphthalen-2-yl)-2-(phenylthio)nicotinonitrile* (*14a*): ^{1}H NMR ($CDCl_3$, 500 MHz)**

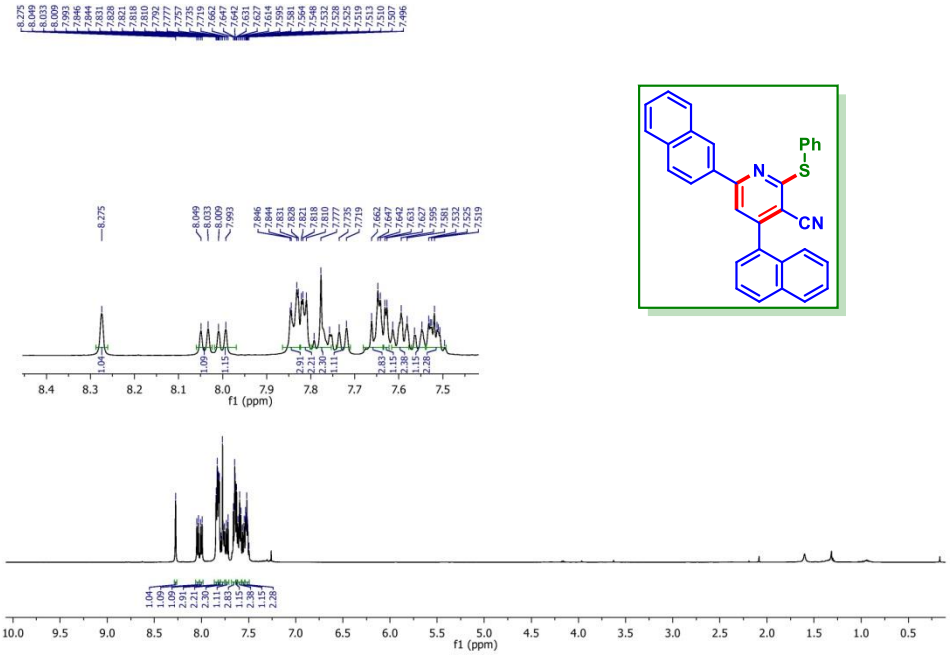

***4-(Naphthalen-1-yl)-6-(naphthalen-2-yl)-2-(phenylthio)nicotinonitrile* (*14a*): $^{13}C\{^{1}H\}$ NMR ($CDCl_3$, 125 MHz)**

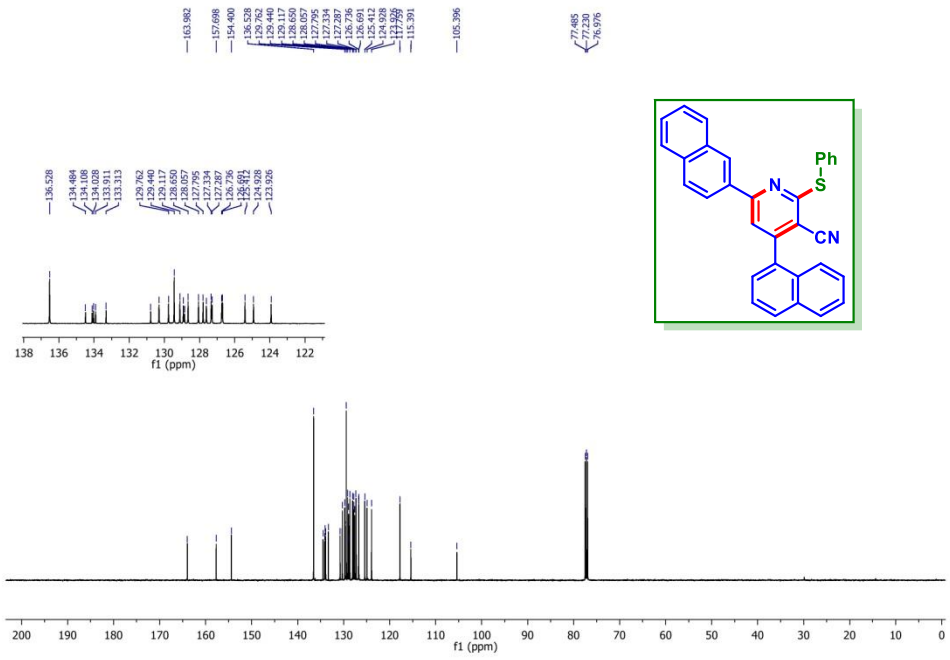

4,6-Di(furan-2-yl)-2-(phenylthio)nicotinonitrile (12a): ^{1}H NMR (CDCl$_3$, 500 MHz)

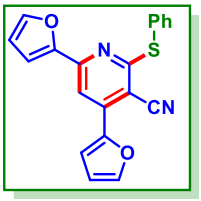

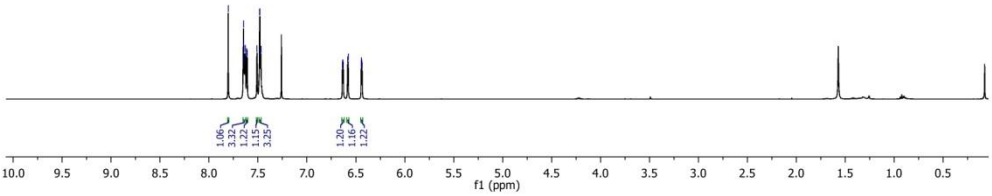

4,6-Di(furan-2-yl)-2-(phenylthio)nicotinonitrile (12a): ^{13}C{^{1}H} NMR (CDCl$_3$, 125 MHz)

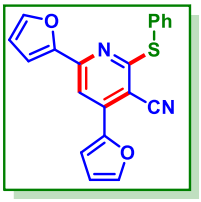

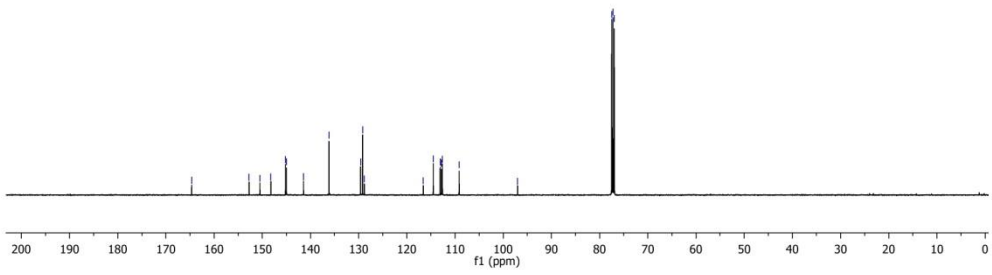

4,6-Diphenyl-2-(p-tolylthio)nicotinonitrile (1b): ^{1}H NMR ($CDCl_3$, 500 MHz)

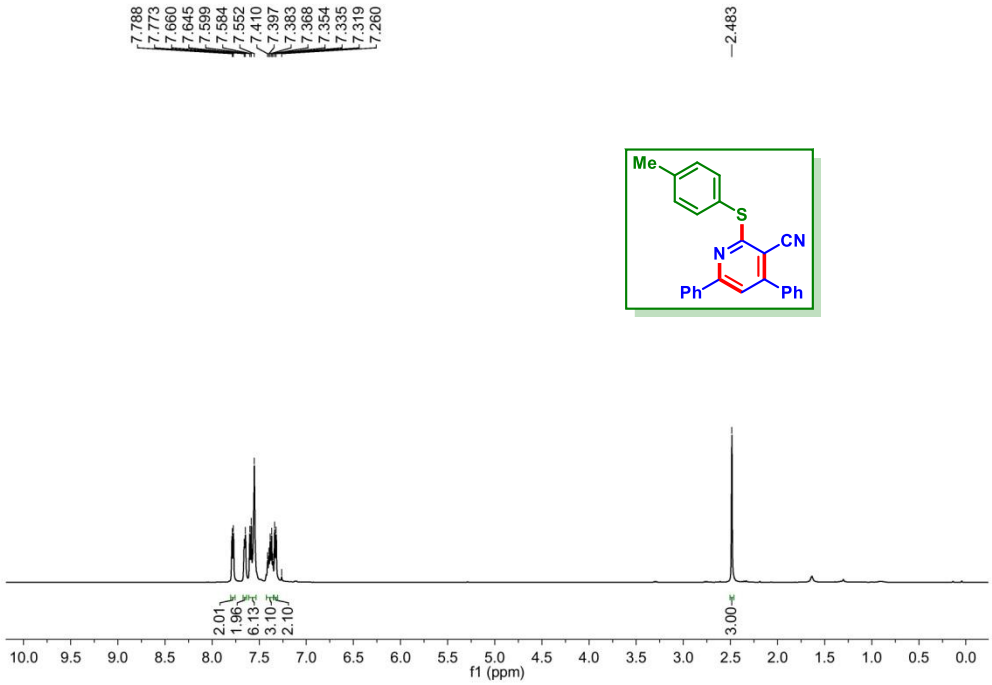

4,6-Diphenyl-2-(p-tolylthio)nicotinonitrile (1b): $^{13}C\{^{1}H\}$ NMR ($CDCl_3$, 125 MHz)

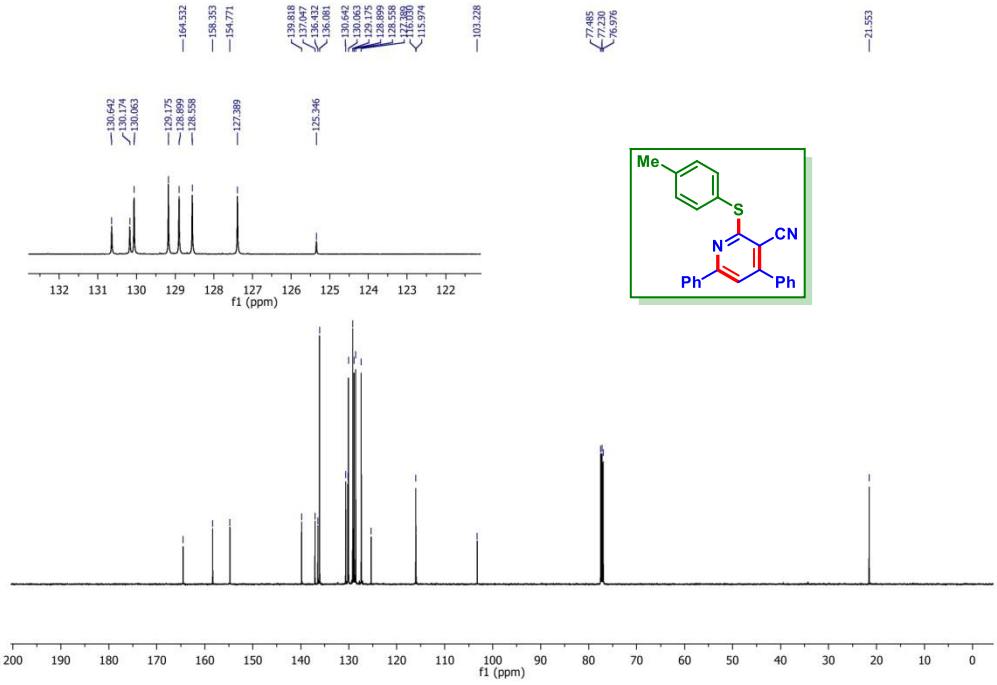

4,6-Diphenyl-2-(thiophen-2-ylthio)nicotinonitrile (1l): ^{1}H NMR (CDCl$_3$, 500 MHz)

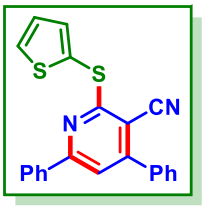

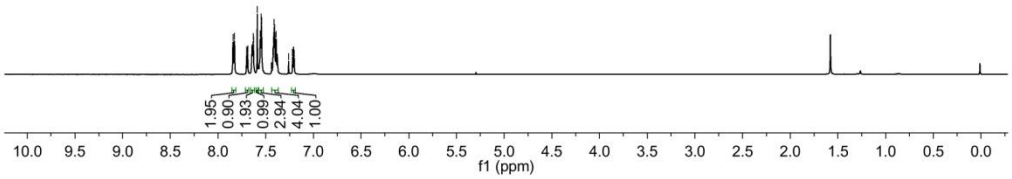

4,6-Diphenyl-2-(thiophen-2-ylthio)nicotinonitrile (1l): ^{13}C{^{1}H} NMR (CDCl$_3$, 125 MHz)

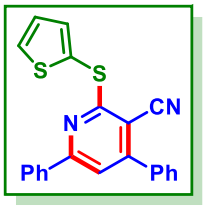

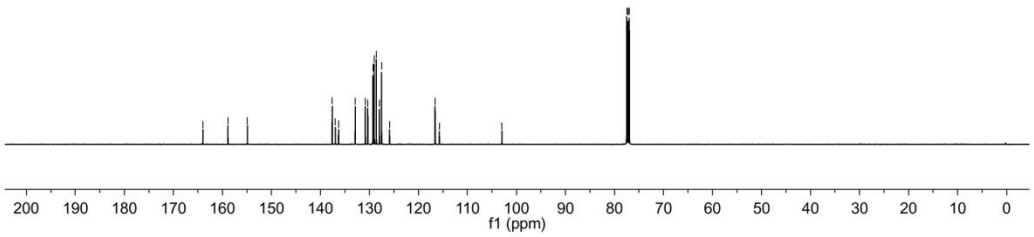

List of Publications

1. Behera, A.; Sau, P.; **Sahoo, A. K**.; Patel, B. K. *J. Org. Chem*. **2018**, *83*, 11218-11231.
2. Behera, A.; Rakshit, A.; **Sahoo, A. K**.; Patel, B. K. *Eur. J. Org. Chem*. **2019**, 1154–1165.
3. **Sahoo, A. K**.; Dahiya, A.; Das, B.; Behera, A.; Patel, B. K. *J. Org. Chem.* **2021**, *86*, 11968–11986.
4. Dahiya, A.; Das, B.; **Sahoo, A. K**.; Patel, B. K. *Adv. Synth.Catal*. **2022**,*364*, 966–973.
5. **Sahoo, A. K**.; Rakshit, A.; Dahiya, A.; Pan, A.; Patel, B. K. *Org. Lett*. **2022**, *24*, 1918–1923.
6. Rakshit, A.; Dhara, H. N.; **Sahoo, A. K**.; Alam, T.; Patel, B. K. *Org. Lett*. **2022**, *24*, 3741−3746.
7. Dam, B.; **Sahoo, A. K**. Patel, B. K. *Green Chem.* **2022**, *24*, 7122−7130.
8. Das, B. Dahiya, A.; **Sahoo, A. K**. Patel, B. K. *J. Org. Chem*. **2022**, *87*, 13383−13388.
9. Dhara, H. N.; Rakshit, A.; Alam, T.; **Sahoo, A. K**. Patel, B. K. *Org. Lett*. **2023**, *25*, 471−476.
10. Sahoo, A. K.; Rakshit, A.; Pan, A.; Dhara, H. N.; Patel, B. K. *Org. Biomol. Chem*. **2023** DOI: 10.1039/D3OB09E.

Reviewes

1. Dahiya, A.; **Sahoo, A. K**.; Alam, T.; Patel, B. K. *Chem. Asian. J*. **2019**, *14*, 4454–4492.

2 **Sahoo, A. K**.; Dahiya, A.; Rakshit, A.; Patel, B. K. *Syn Open*. **2021**, *5*, 232–251.

3 Dahiya, A.; **Sahoo, A. K**. Chakraborty, N. Das, B.; Patel, B. K. *Org. Biomol. Chem*. **2022**, *20*, 2137–2137.

4 Rakshit, A.; Dhara, H. N.; **Sahoo, A. K**.; Patel, B. K. *Chem Asian J*. **2022**, *17*.

Book Chapters

1. Development in Wastewater Treatment Research and Processes Innovative Microbe-Based Applications for Removal of Chemicals and Metals in Wastewater Treatment Plants. *Biological methods for textile dyes removal from wastewaters*, **Ashish Kumar Sahoo**, Anjali Dahiya and Bhisma K. Patel. ISBN: 978-0-323-85657-7.

2 Conventional Liquid Biofuels, *Bubul Das*, ***Ashish Kumar Sahoo***, *Anjali Dahiya and Bhisma K. Patel*. ISBN: 978-981-16-8094-6.